UNIVERSITY OF CAMERINO

School of Advanced Studies

PhD course: Life and Health Sciences

Curriculum: Nutrition, food and health

Title of the thesis:

Molecular insights into inflammation: the role of diet-derived compounds, aging and cardiovascular disease.

PhD Student

Chiara Rucci

Coordinator of the PhD course

Prof. Attilio Fabretti

Supervisors

Prof. Rosita Gabbianelli

Prof. Laura Bordoni

2025/2026

TABLE OF CONTENTS

1. General Introduction

1.1 Overview on inflammation as biological process

Inflammation is a complex and highly regulated biological response of the body to harmful stimuli, whether of exogenous or endogenous origin. It is characterized by the activation of the immune system primarily aimed at eliminating the insult and restoring the homeostasis [1].

Common inflammatory triggers include pathogens, toxic compounds and damaged cells, all of which can trigger either acute and/or chronic inflammatory responses [2]. Acute inflammation represents a protective process that acts against injuries and promote tissue repair. However, when the inflammatory response fails to resolve or becomes dysregulated, acute inflammation can evolve into a chronic inflammatory state [3]. Prolonged local inflammation can result in loss of cellular function, tissue damage, and disruption of organ homeostasis [2].

When chronic inflammation becomes systemic, it triggers continuous activation of immune and metabolic pathways associated with oxidative stress, mitochondrial disfunction and altered cellular signaling affecting multiple organs and apparatuses [4]. Among the organs involved in chronic inflammation progression, the gut plays a crucial role acting both as a target and as a modulator of inflammation. Its dysfunction induces immune activation perpetuating systemic inflammation throughout a bidirectional crosstalk [5]. Similarly, the cardiovascular system is affected by inflammation. Systemic and local inflammation have a key role in the development of cardiovascular disease (CVD). Indeed, inflammatory biomarkers have been shown to predict CVD onset [6]. In turn, endothelial damage characterizing cardiometabolic diseases promotes vascular low-grade inflammation contributing to fueling the systemic response of the immune system [6].

This scenario is typical of the aging state, during which inflammaging, the persistent low-grade inflammation associated with aging, triggers the development of age-related diseases whose prevalence is exponentially increasing worldwide.

1.2 Molecular mechanisms of inflammation

Inflammatory process starts with tissue damage, triggering a cascade of signals that recruit leukocytes to the affected site. Activated leukocytes release molecules that amplify the inflammatory response [7]. Even though the specific inflammatory mechanism depends on the nature of the harmful agent, all inflammatory processes converge on a common innate immune response, initiated by the recognition of the harmful stimulus throughout pattern recognition receptors (PRRs) expressed on the cell surface of immune and non-immune cells such as dendritic cells, macrophages, monocytes, neutrophils, endothelial and epithelial cells. PRRs can be grouped into several families including Toll-like receptors (TLRs), C-type lecithin receptors (CLRs), retinoic acid- inducible receptor RIG-I (RLRs) and NOD-like receptors (NLRs) [7].

PRRs can recognize microbial structures known as pathogen associated molecular patterns (PAMPs) or endogenous signals, activated by tissue damage, known as damaged associated molecular patterns (DAMPs). Except for some NLRs, the binding between PRRs and PAMPs or DAMPs activate a process of signal transduction that induce the transcription of genes encoding for pro-inflammatory molecules [7].

Key intracellular signal transduction pathways include the Nuclear Factor kappa B (NF-κB), mitogen-activated protein kinase (MAPK), Janus kinase - activator of transcription (JAK/STAT), and activation of interferon regulatory factors (IRF) pathways [7]. The activation of these pathways induces the release of inflammatory mediators (cytokines, chemokines, free radicals, histamine ecc) which are key component of the innate immune response aimed at eliminating the harmful stimulus. Among them, cytokines and chemokines play a crucial role in the inflammation event. The most important cytokines involved in the inflammatory process are Tumor necrosis factor (TNF-a), interleukin 1B (IL-1b), and interleukin 6 (IL-6) which regulate endothelial activation, leukocyte recruitment and the production of acute phase proteins [7]. At this point the harmful agent is eliminated, and tissue repair mechanisms are activated to restore homeostasis.

Failure of resolution phase or persistence of the harmful stimuli leads to the transition from acute to chronic inflammation which, if not resolved, can became systemic [7].

In particular, in chronic inflammatory states, leukocytes such as neutrophils, monocytes and macrophages persist at site of inflammation continuously producing harmful molecules which damage tissues. The inflammatory signaling cascade becomes self-sustained, with pro-inflammatory cytokines circulating systemically.

1.3 Inflammation as a crossroad between aging, gut health and cardiovascular disease

Aging is defined as the time-related irreversible process leading to the progressive deterioration of the physiological functions of the body [8]. The biological mechanisms underlying aging are interconnected throughout six pillars (stem cell regeneration, metabolism, proteostatis, macromolecular damage, stress response and epigenetics) which converge on inflammation [9]. Dysfunction in one or more of these pillars fuel low grade chronic sterile inflammatory state (Figure 1) [9].

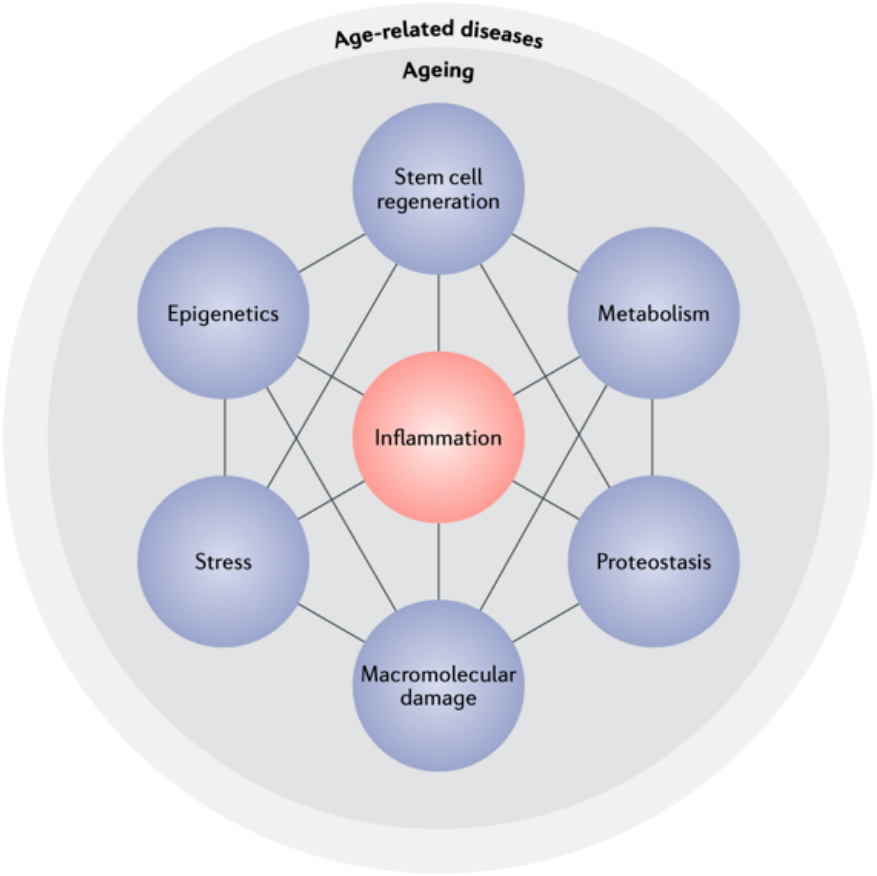

Figure 1: The seven pillars of aging: stem cell regeneration, metabolism, proteostasis, macromolecular damage, stress response and epigenetics [9].

At cellular level aging is established throughout mechanisms including cellular senescence, impairment of mitophagy and autophagy mechanisms, mitochondrial dysfunction, activation of the inflammasome and dysregulation of ubiquitin proteasome system [9]. Cellular senescence is a process which induces a gradual impairment of cellular proliferation and differentiation caused by telomer shortening, genomic instability and epigenetic alterations. Senescent cells exited the cell cycle being unable to divide, however they remain metabolically active acquiring a peculiar senescent associated secretory phenotype (SASP) characterized by the production of inflammatory cytokines, chemokines, grow factors and proteases [9]. Interestingly, the SASP not only has a local paracrine effect which alters the composition of extracellular matrix and propagates the senescent phenotype, but it sustains systemic inflammaging [10]. Indeed, aging is associated with immune dysregulation leading to high blood levels of pro-inflammatory mediators and reduced capacity to trigger an adequate inflammatory response to restore the homoeostasis [11]. Furthermore, the accumulation of DAMPs originated by mitochondrial breakdown, microbiota or persistent infections typical of aging further amplify this pro-inflammatory environment [12]. All these processes fuel systemic low-grade inflammation which is associated with the majority of age-related diseases. Notably, aging is considered one of the stronger risk factors for neurodegenerative diseases, metabolic disorders and cardiometabolic pathologies, whose prevalence has exponentially increased in the last decades [8].

The gastrointestinal tract is the largest interface between the internal body and the external environment [5]. It continuously interacts with external no-self factors throughout food intake and microbial exposure, and it simultaneously communicate with the internal physiological networks, playing a central role in maintaining the homeostasis. In particular, the intestinal epithelial barrier has a crucial role for gut health since it directly interplays with gut microbiota and immune cells orchestrating a dynamic crosstalk that shapes immune responses to antigens maintaining the balance between tolerance and immune activation [13]. However, the gut barrier is a dynamic

structure influenced by several factors: activity of intercellular connections, composition of intestinal microbiota, hormone, diet and enteric nervous system [5]. The integrity of the intestinal epithelium is fundamental for gut and overall health, and it depends on tight junction functionality, protein complexes which inhibit paracellular permeability avoiding the translocation of harmful molecules from the gut lumen into the internal environment [5]. Impairment of the integrity of the barrier and its dysfunction leads to unregulated passage of harmful molecules, bacterial components and products of bacterial metabolism. This process involves the activation of innate immune pathways, which recognize microbial-derived molecules like lipopolysaccharides (LPS) triggering the production of pro-inflammatory cytokines, contributing to both local and systemic low-grade inflammation [5]. This condition is known as the "leaky gut syndrome" and it can be caused by dysbiosis, aging, bacterial infections, oxidative stress, alcohol and chronic allergens exposure as well as by systemic inflammation itself [5]. Thus, chronic low-grade inflammation, along with additional environmental and metabolic stressors, is a key factor in the development of gut dysfunction, which in turn enhances inflammatory signaling (Figure 2) [14]. This bidirectional crosstalk establishes a self-perpetuating cycle that exacerbate the impairment of the immune response typical of the aging process.

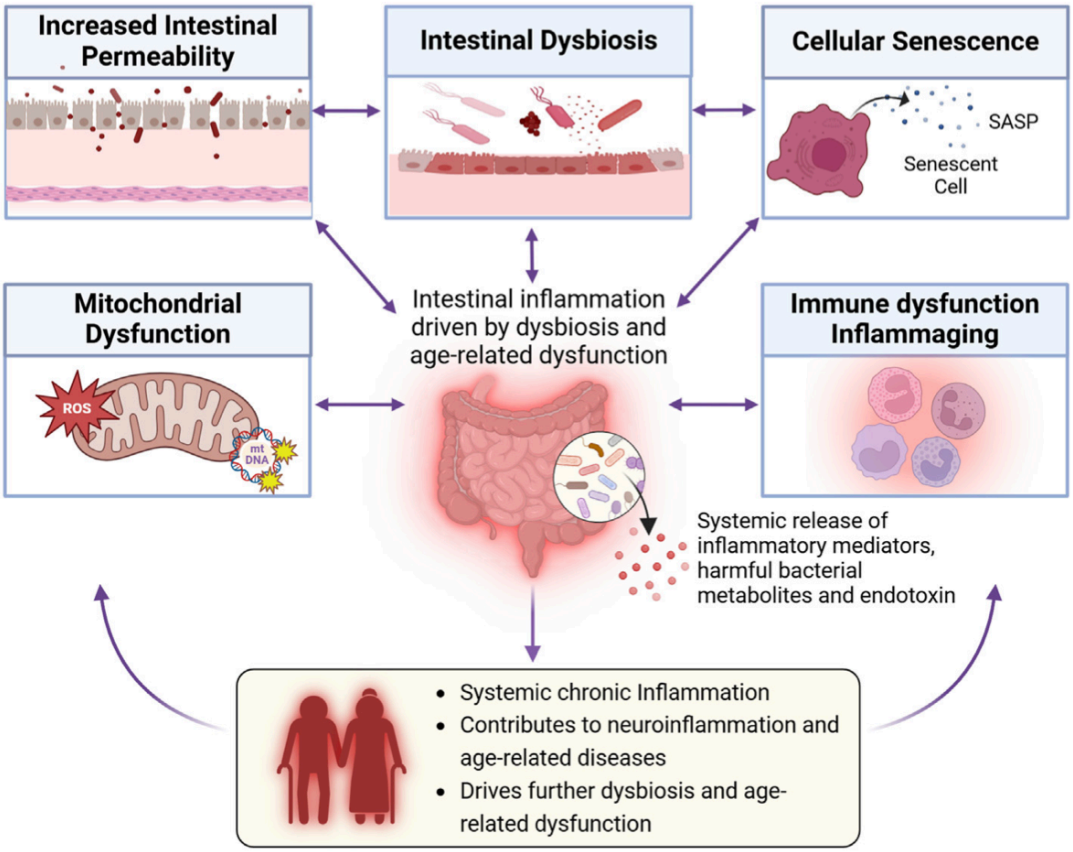

Figure 2: The crosstalk between intestinal permeability, age-related dysbiosis and all hallmarks of aging [14].

Inflammaging has been linked to the development of atherosclerosis and CVD. In fact, damage occurring during inflammation trigger the development of atherosclerotic plaques in the vascular endothelium while atherosclerosis itself contributes to the generation of DAMPs sustaining the inflammation [12]. Thus, the mechanisms by which inflammaging impacts the CVD development are several. In brief, the dysregulation of the immune system, the mitochondrial disfunction, the oxidative stress and the epigenetic changes occurring during aging fuel inflammation that triggers the development of atherosclerosis, endothelial dysfunctions, vascular stiffness and coagulation changes, characteristic of CVD [15].

1.4 Molecular regulation of health: epigenome, transcriptome and mitochondria. Role in inflammation and aging.

At cellular level, the maintaining of health depends on a complex network of molecular mechanisms among which the regulation of the epigenome, transcriptome and the mitochondrial homeostasis play a crucial role. The epigenome includes all the biochemical modification of the DNA and histones that play a role in regulating gene expression without affecting the DNA sequence [16]. These epigenetic mechanisms mainly include DNA methylation, post-translation histone modifications and non-coding-RNAs regulation [16]. All these processes affect chromatin accessibility and transcriptional activity. Among epigenetic modifications, DNA methylation is one of the most studied. It consists in the addition or removal of a methyl group by DNA methyl transferases enzymes (DNMTs) and ten eleven translocation enzymes (TETs) in the DNA sequence [17]. DNMTs use SAM (S-adenosylmethionine) as a methyl group donor to catalyze the methylation of cytosines at CpG dinucleotides while TETs mediate the demethylation of 5-methylcitosine [16]. The DNA methylation on specific regions of the genome has been demonstrated to affect gene expression: hypermethylation in the promoter regions has been suggested to be associated with gene silencing while hypomethylation can lead to gene activation. Thus, DNA methylation is one of the cellular mechanisms regulating the transcriptome, which includes all the RNA molecules expressed in a cell in a precise moment. In turn, the transcriptome affects cellular functions being the first step in shaping cellular response. Indeed, activation or repression of gene expression regulates the production or inhibition of specific proteins, together with other regulatory mechanisms acting at translational and post-translational levels.

Among cellular functions, mitochondrial activity is a key factor to maintain tissues homeostasis. Indeed, beyond the primary energetic function, mitochondria play a crucial role in signal transduction, reactive oxygen species signaling, iron/calcium buffering, regulation of cell death and steroid hormone biosynthesis [18], [19]. Dysregulation of mitochondrial functions leads to the occurrence of several diseases such as CVD, metabolic diseases and neurodegenerative disorders.

The interplay between the epigenome, the transcriptome and mitochondrial activity is well established. Epigenetic modifications regulate gene expression, while the enzymes responsible for epigenetic marks apposition have been suggested to use mitochondrial metabolites as substrates or cofactors, thus requiring proper mitochondrial function for the maintenance of epigenetics landscape [20]. In particular, it has been hypothesized that mitochondrial DNA (mtDNA) influences the epigenome regulating the production of epigenome-modifying metabolites originated by tricarboxylic acid cycle (TCA) and oxidative phosphorylation (OXPHOS) [21]. Among them methionine, SAM (promotes methylation), S-adenosylhomocysteine (SAH, inhibits methylation), alpha-ketoglutarate (aKG, promotes DNA demethylation), acetyl CoA (promotes histone acetylation), and NAD+ (promotes histone deacetylation) are the best known [21].

In turn, nuclear DNA plays a key role in regulating mitochondrial function since nuclear encoded genes are responsible for mtDNA replication and transcription [21]. Thus, nuclear DNA and mtDNA communicate throughout an anterograde (nucleus to mitochondria) and retrograde (mitochondria to nucleus) mechanism maintaining the integrity and functionality of both genomes and the overall cellular homeostasis.

In this contest, inflammation and aging perturb the system affecting epigenetic landscape, gene expression and mitochondrial functionality.

It is well known that during aging epigenetic changes accumulate. Several epigenetic mechanisms have been suggested to regulate senescence pathways: alteration in DNA methylation, abnormal post-translation histone modifications, dysregulated chromatin remodelling and dysfuction of non-coding RNAs [22].

Among this, DNA methylation is a key determinant of the aging phenotype, characterized by a global genomic hypomethylation and hypermethylation in specific sites. This epigenetic change can silence genes involved in immune response, anti-inflammatory processes or DNA repair and activate senescence associated genes [22], [23], [24]. However, the model where age-related DNA methylation changes exert a biological effect via gene expression changes is still under debate since, in some cellular models, the correlation between gene expression and DNA methylation changes was weak [23]. The association between aging and DNA methylation has led

to the development of epigenetic clocks. Steve Horvat discovered 393 tissues independent CpGs sites whose methylation level can predict the age of the donor [23]. In parallel to epigenetic alterations, mitochondrial dysfunction is another key process occurring during aging.

Indeed, mitochondria act as the core to link inflammation oxidative stress and aging (Fig 3) [25].

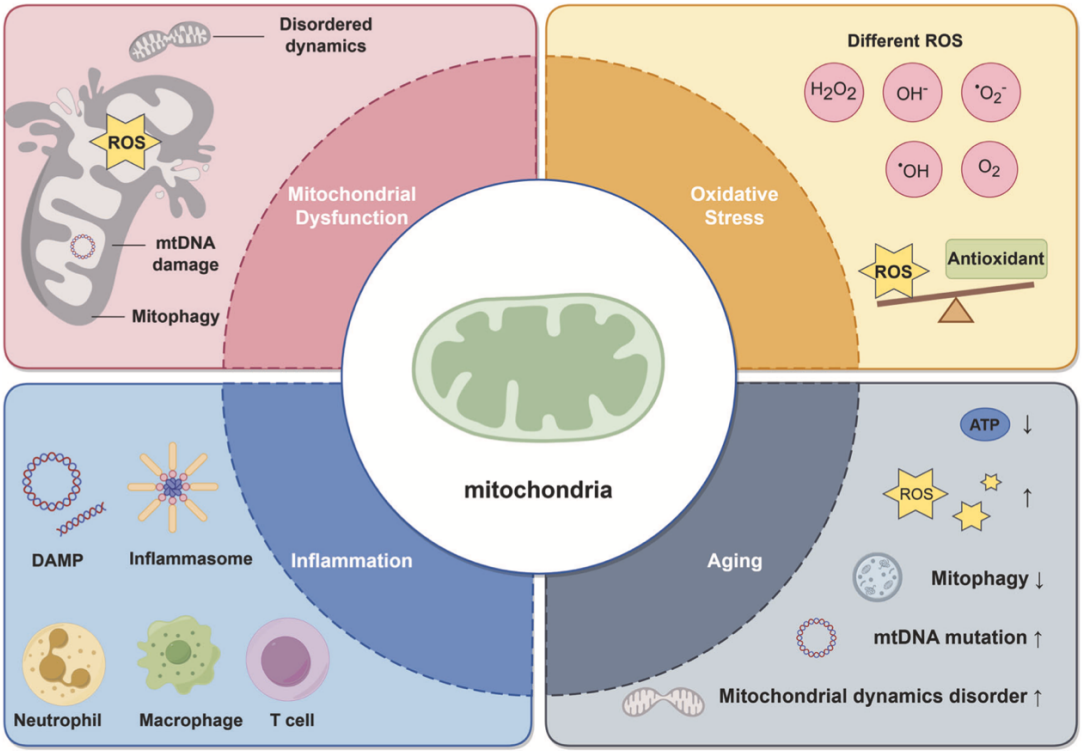

Figure 3: Mitochondria as a link between oxidative stress, inflammation and aging[25] .

In turn, mitochondrial dysfunction itself is one of the markers of inflammaging, leading to reduced energy metabolism, ROS overproduction and mtDNA damage. Interestingly, high levels of reactive oxygen species have been suggested to activate NLRP3 which is one of the key mediators of inflammatory response [18]. However, mitochondria have been suggested to trigger inflammation also through the release of their constituents [25]. It is well-known that mitochondria are the evolutionary remnants of Alphaproteobacteria, thus some of their components can be recognized by

the immune system activating an inflammatory response [26]. In particular, mtDNA has been suggested to act as a DAMP once released in the extracellular milleu or in the circulation, triggering inflammation.
The impairment of epigenetic regulation and mitochondrial dysfunction is typical of the inflammaging process leading to occurrence of the age-related diseases whose prevalence is exponentially increasing.

1.5 Nutrigenomic effect of dietary compounds: microbiota metabolites and phytochemicals. Focus on inflammation.

Nutrigenomics is defined as the science that studies the relationship between nutrition and gene expression [27], [28]. This discipline combines epigenetics, transcriptomics, proteomics, metabolomics and other approaches to study the precise effect of nutrient at the molecular level [27], [28]. Indeed, food not only provides nutrients necessary for life, but it also contains bioactive molecules able to modulate metabolic pathways contributing to the maintenance of health [29].
In particular, dietary factors have been suggested to modulate chronic low-grade inflammation which is involved in the development of various multifactorial and lifestyle-related diseases.[30], [31]. Indeed, consumption of a balanced healthy diet, rich in fruit and vegetables, is associated with reduction lower risk of age-related diseases and it has been proposed to decelerate the aging process [14]. Beyond providing the adequate amount of macro and micronutrients, a healthy diet ensures an adequate intake of dietary fibers, which promotes the maintenance of a balanced gut microbiota composition, essential for overall health and well-being [32].
Gut microbiota eubiosis is important to maintain intestinal and systemic health since gut microorganisms can produce beneficial or harmful molecules depending on the diet and on the composition of the microbiota itself. These microbiota metabolites can exert local and systemic effects influencing intestinal epithelium functionality but also distant organs functions [33]. The mechanisms of action of all the microbiota metabolites have not been completely elucidated yet, thus their potential effect on gene expression or epigenetic marks is a promising area for further investigations. Gut microbiota metabolites can be divided into three families: metabolites directly

produced from diet by microbiota such as SCFAs, metabolites that are produced by the host and modified by the microbiota such as secondary bile acids and metabolites that are produced de novo (Table 1) [33].

Groups	Typical metabolites	Typical targets	Specific functions
Short-chain fatty acids	Acetate, propionate, butyrate, hexanoate, isovalerate, isobutyrate, 2-methylpropionate, valerate	Directly act on GPR41, GPR43, GPR109A, GPR81, GPR91, HDAC1 and HDAC3	Regulation of gut microbiota composition, gut barrier integrity, appetite, energy homeostasis, gut hormone production, circadian clocks; inhibit proinflammatory cytokines; stimulate water and sodium absorption; modulate systemic immune response
Bile acids	Cholate, hyocholate, deoxycholate, taurohyocholate, ursodeoxycholate, taurocholate, tauro-α-muricholate, glycocholate, hyodeoxycholate, tauro-β-muricholate, lithocholate, taurodeoxylcholate	Directly act on FXR, VDR, PXR/SXR, constitutive androstane receptor (CAR), TGR5, sphingosine 1-phosphate receptor 2 (S1PR2), formyl-peptide receptor (FPR), muscarinic acetylcholine receptor (mAChR)	Facilitate lipid and vitamin absorption; regulation of gut microbiota composition, gut hormones, intestinal immunity, intestinal electrolyte and fluid balance, gut motility, lipid homeostasis, glucose homeostasis, amino acid homeostasis, circadian clocks; influence neurotransmission and physiology
Gases	H_2S, H_2, CO_2, CH_4, NO	NO targets soluble guanylate cyclase, H_2S cause conformational changes of target proteins by sulfhydration	CH_4 slows gut motility; H_2S regulates gut inflammation, motility, epithelial secretion and susceptibility to infections; NO mediates gastric mucosal protection and regulate mucosal blood flow
Tryptophan and indole derivatives	Indole-3-lactic acid, indole acetic acid, indole-3-acetamide, indole pyruvic acid, indoxyl sulfuric acid, indole, serotonin	Directly targeting on AhR and PXR	Influence the gut microbial spore formation, drug resistance, biofilm formation, and virulence; regulate intestinal barrier functions, gut hormone secretion, gut motility, systemic immune response
Choline metabolites	TMA, methylamine, dimethylglycine, dimethylamine,	Direct target unknown, but can activate NF-κB, protein kinase C (PKC), NLRP3 inflammasome	Inhibits bile acid synthesis; promote inflammation, thrombosis; affects myocardial hypertrophy and fibrosis; exacerbates mitochondrial dysfunction
Vitamins	Vitamin B2, Vitamin B3, Vitamin B5, Vitamin B6, Vitamin B9, Vitamin B12, vitamin K	Vitamin receptors	Involved in cellular metabolism; modulate immune function and cell proliferation; supply vitamins for hosts
Neurotransmitters	Dopamine, catecholamines, 5-HT, and GABA	Adrenergic receptors, 5-HT receptors, GABA receptors	Regulate gut motility, memory and stress responses, immune function of nervous system
Lipids	Conjugated fatty acids, cholesterol, phosphatidylcholines, triglycerides, LPS	LPS targets directly on TLR4	LPS triggers systemic inflammation; conjugated fatty acids regulate hyperinsulinemia, immune system, lipoprotein profiles; cholesterol acts as material bases for bile acid synthesis.
Others	Ethanol; triphosadenine; lantibiotic such as ruminococcin A and cytolysin; microcin such as microcin B17; organic acids such as benzoate and hippurate; polyamines such as cadaverine, and spermidine	Triphosadenine activate P2X and P2Y receptors	Enhance or damage gut barrier; regulate intestinal or systemic immune response; act as antibiotics to modulate gut microbiota composition; supply the nutrients; be toxic to host cells

Table 1: Most common microbiota metabolites and their role in health and disease [33].

Dysbiosis has a pivotal role in altering the production of bacterial metabolites: changes in microbiota composition directly affect the quantity and diversity of metabolites generated [33]. Thus, diet plays a key role in regulating health: it shapes the microbiota composition and modulate its metabolites production, thereby affecting gut health. The impairment of this interconnected system leads to the disruption of the intestinal barrier which contribute to fuel systemic inflammation [14] .

Moreover, dietary factors may contribute directly to the control of chronic low-grade inflammation. For example, fruit and vegetables have been suggested to contain several bioactive molecules exerting their anti-inflammatory effect throughout a nutrigenomic mechanism [29]. The most known plant derived bioactive compounds having epigenetic effects are: sulforaphane, green tea catechins, ellagic acid (EA), genistein, curcumin, indole-3-carbinol (I3C), resveratrol (RVT), diallyl disulfide (DADS), 3,30-diindolylmethane (DIM), isothiocyanates, quercetin and alkaloids [29]. These dietary bioactive compounds contribute to the regulation of the expression of genes involved in age-related diseases, inflammation and tumorigenesis [29]. However, dietary intake of these compounds is generally low due to their limited availability in fruits and vegetables. Thus, biotechnological approaches, such as in vitro production of plant materials, are being developed to enhance the production of these beneficial plant-derived molecules.

Nevertheless, food does not only contain bioactive compounds with anti-inflammatory properties. Some dietary components, such as fructose or saturated fatty acids, can promote inflammation when consumed in excess [34], [35]. Consequently, the overall impact of diet on molecular mechanisms represents a complex and intricate network that remains to be fully elucidated.

Bibliography

[1] E. C. Bender, H. S. Tareq, and L. J. Suggs, “Inflammation: a matter of immune cell life and death,” *npj Biomedical Innovations*, vol. 2, no. 1, p. 7, 2025, doi: 10.1038/s44385-025-00010-4.

[2] L. Chen *et al.*, “Inflammatory responses and inflammation-associated diseases in organs.,” *Oncotarget*, vol. 9, no. 6, pp. 7204–7218, Jan. 2018, doi: 10.18632/oncotarget.23208.

[3] J. Zheng *et al.*, “Editorial: Molecular mechanisms and therapeutic strategies in inflammation.,” *Front Immunol*, vol. 16, p. 1626548, 2025, doi: 10.3389/fimmu.2025.1626548.

[4] D. Furman *et al.*, “Chronic inflammation in the etiology of disease across the life span.,” *Nat Med*, vol. 25, no. 12, pp. 1822–1832, Dec. 2019, doi: 10.1038/s41591-019-0675-0.

[5] F. Di Vincenzo, A. Del Gaudio, V. Petito, L. R. Lopetuso, and F. Scaldaferri, “Gut microbiota, intestinal permeability, and systemic inflammation: a narrative review.,” *Intern Emerg Med*, vol. 19, no. 2, pp. 275–293, Mar. 2024, doi: 10.1007/s11739-023-03374-w.

[6] M. Y. Henein, S. Vancheri, G. Longo, and F. Vancheri, “The Role of Inflammation in Cardiovascular Disease.,” *Int J Mol Sci*, vol. 23, no. 21, Oct. 2022, doi: 10.3390/ijms232112906.

[7] C. L. R. Soares *et al.*, “Biochemical aspects of the inflammatory process: A narrative review.,” *Biomed Pharmacother*, vol. 168, p. 115764, Dec. 2023, doi: 10.1016/j.biopha.2023.115764.

[8] J. Guo *et al.*, “Aging and aging-related diseases: from molecular mechanisms to interventions and treatments.,” *Signal Transduct Target Ther*, vol. 7, no. 1, p. 391, Dec. 2022, doi: 10.1038/s41392-022-01251-0.

[9] C. Franceschi, P. Garagnani, P. Parini, C. Giuliani, and A. Santoro, “Inflammaging: a new immune–metabolic viewpoint for age-related diseases,” *Nat Rev Endocrinol*, vol. 14, no. 10, pp. 576–590, 2018, doi: 10.1038/s41574-018-0059-4.

[10] Y. Li, X. Tian, J. Luo, T. Bao, S. Wang, and X. Wu, “Molecular mechanisms of aging and anti-aging strategies.,” *Cell Commun Signal*, vol. 22, no. 1, p. 285, May 2024, doi: 10.1186/s12964-024-01663-1.

[11] L. Ferrucci and E. Fabbri, “Inflammageing: chronic inflammation in ageing, cardiovascular disease, and frailty.,” *Nat Rev Cardiol*, vol. 15, no. 9, pp. 505–522, Sep. 2018, doi: 10.1038/s41569-018-0064-2.

[12] J. F. Aranda, C. M. Ramírez, and M. Mittelbrunn, “Inflammageing, a targetable pathway for preventing cardiovascular diseases.,” *Cardiovasc Res*, vol. 121, no. 10, pp. 1537–1550, Aug. 2025, doi: 10.1093/cvr/cvae240.

[13] T. Takiishi, C. I. M. Fenero, and N. O. S. Câmara, “Intestinal barrier and gut microbiota: Shaping our immune responses throughout life.,” *Tissue Barriers*, vol. 5, no. 4, p. e1373208, Oct. 2017, doi: 10.1080/21688370.2017.1373208.

[14] L. M. Beaver, P. E. Jamieson, C. P. Wong, M. Hosseinikia, J. F. Stevens, and E. Ho, “Promotion of Healthy Aging Through the Nexus of Gut Microbiota and Dietary Phytochemicals.,” *Adv Nutr*, vol. 16, no. 3, p. 100376, Mar. 2025, doi: 10.1016/j.advnut.2025.100376.

[15] L. Spray *et al.*, “Cardiovascular inflammaging: Mechanisms, consequences, and therapeutic perspectives.,” *Cell Rep Med*, vol. 6, no. 9, p. 102264, Sep. 2025, doi: 10.1016/j.xcrm.2025.102264.

[16] S. Golbabapour, M. A. Abdulla, and M. Hajrezaei, “A concise review on epigenetic regulation: insight into molecular mechanisms.,” *Int J Mol Sci*, vol. 12, no. 12, pp. 8661–94, 2011, doi: 10.3390/ijms12128661.

[17] A. T. Davletgildeeva and N. A. Kuznetsov, “The Role of DNMT Methyltransferases and TET Dioxygenases in the Maintenance of the DNA Methylation Level.,” *Biomolecules*, vol. 14, no. 9, Sep. 2024, doi: 10.3390/biom14091117.

[18] L. Wang, X. Zhou, and T. Lu, “Role of mitochondria in physiological activities, diseases, and therapy.,” *Molecular biomedicine*, vol. 6, no. 1, p. 42, Jun. 2025, doi: 10.1186/s43556-025-00284-5.

[19] A. Picca, R. Calvani, H. J. Coelho-Junior, and E. Marzetti, “Cell Death and Inflammation: The Role of Mitochondria in Health and Disease.,” *Cells*, vol. 10, no. 3, Mar. 2021, doi: 10.3390/cells10030537.

[20] J. H. Santos, “Mitochondria signaling to the epigenome: A novel role for an old organelle.,” *Free Radic Biol Med*, vol. 170, pp. 59–69, Jul. 2021, doi: 10.1016/j.freeradbiomed.2020.11.016.

[21] A. L. Morin, P. W. Win, A. Z. Lin, and C. A. Castellani, “Mitochondrial genomic integrity and the nuclear epigenome in health and disease.,” *Front Endocrinol (Lausanne)*, vol. 13, p. 1059085, 2022, doi: 10.3389/fendo.2022.1059085.

[22] Y. An *et al.*, “Epigenetic Regulation of Aging and its Rejuvenation.,” *MedComm (Beijing)*, vol. 6, no. 9, p. e70369, Sep. 2025, doi: 10.1002/mco2.70369.

[23] M. Jung and G. P. Pfeifer, “Aging and DNA methylation.,” *BMC Biol*, vol. 13, p. 7, Jan. 2015, doi: 10.1186/s12915-015-0118-4.

[24] S.-W. Choi and S. Friso, “Modulation of DNA methylation by one-carbon metabolism: a milestone for healthy aging.,” *Nutr Res Pract*, vol. 17, no. 4, pp. 597–615, Aug. 2023, doi: 10.4162/nrp.2023.17.4.597.

[25] X. Xu, Y. Pang, and X. Fan, “Mitochondria in oxidative stress, inflammation and aging: from mechanisms to therapeutic advances.,” *Signal Transduct Target Ther*, vol. 10, no. 1, p. 190, Jun. 2025, doi: 10.1038/s41392-025-02253-4.

[26] S. Marchi, E. Guilbaud, S. W. G. Tait, T. Yamazaki, and L. Galluzzi, “Mitochondrial control of inflammation.,” *Nat Rev Immunol*, vol. 23, no. 3, pp. 159–173, Mar. 2023, doi: 10.1038/s41577-022-00760-x.

[27] N. M. Kassem, Y. A. Abdelmegid, M. K. El-Sayed, R. S. Sayed, M. H. Abdel-Aalla, and H. A. Kassem, “Nutrigenomics and microbiome shaping the future of personalized medicine: a review article.,” *J Genet Eng Biotechnol*, vol. 21, no. 1, p. 134, Nov. 2023, doi: 10.1186/s43141-023-00599-2.

[28] D. Chaudhary *et al.*, “Nutrigenomics and personalized diets - Tailoring nutrition for optimal health,” *Applied Food Research*, vol. 5, no. 1, p. 100980, 2025, doi: https://doi.org/10.1016/j.afres.2025.100980.

[29] A. Kumari, S. Bhawal, S. Kapila, H. Yadav, and R. Kapila, “Health-promoting role of dietary bioactive compounds through epigenetic modulations: a novel

prophylactic and therapeutic approach.," *Crit Rev Food Sci Nutr*, vol. 62, no. 3, pp. 619–639, 2022, doi: 10.1080/10408398.2020.1825286.

[30] A. M. Minihane *et al.*, "Low-grade inflammation, diet composition and health: current research evidence and its translation.," *Br J Nutr*, vol. 114, no. 7, pp. 999–1012, Oct. 2015, doi: 10.1017/S0007114515002093.

[31] M. Cifuentes *et al.*, "Low-Grade Chronic Inflammation: a Shared Mechanism for Chronic Diseases.," *Physiology (Bethesda)*, vol. 40, no. 1, p. 0, Jan. 2025, doi: 10.1152/physiol.00021.2024.

[32] J. Fu, Y. Zheng, Y. Gao, and W. Xu, "Dietary Fiber Intake and Gut Microbiota in Human Health.," *Microorganisms*, vol. 10, no. 12, Dec. 2022, doi: 10.3390/microorganisms10122507.

[33] J. Liu, Y. Tan, H. Cheng, D. Zhang, W. Feng, and C. Peng, "Functions of Gut Microbiota Metabolites, Current Status and Future Perspectives.," *Aging Dis*, vol. 13, no. 4, pp. 1106–1126, Jul. 2022, doi: 10.14336/AD.2022.0104.

[34] Z. Li *et al.*, "Fructose metabolism and its roles in metabolic diseases, inflammatory diseases, and cancer.," *Molecular biomedicine*, vol. 6, no. 1, p. 43, Jun. 2025, doi: 10.1186/s43556-025-00287-2.

[35] O. Ramos-Lopez, D. Martinez-Urbistondo, J. A. Vargas-Nuñez, and J. A. Martinez, "The Role of Nutrition on Meta-inflammation: Insights and Potential Targets in Communicable and Chronic Disease Management.," *Curr Obes Rep*, vol. 11, no. 4, pp. 305–335, Dec. 2022, doi: 10.1007/s13679-022-00490-0.

2. Research objectives

The overall aim of the doctoral research was to investigate the epigenetic, transcriptional and mitochondrial mechanisms underlying inflammation, focusing on the responses to microbial metabolites, nutritional bioactive molecules, aging and cardiovascular disease.

The main research objective was to investigate the epigenetic and transcriptomic effect of Mela Rosa Marchigiana callus extract (MRME), a plant-derived compound with suggested anti-inflammaging properties, using an in vitro model of cellular senescence.

As a secondary objective, the research activity also contributed to the characterization of the role of gut microbiota-derived metabolite Trimethylamine (TMA) in promoting inflammation, with a particular focus on investigating the effect on gene expression regulation and on mitochondrial homeostasis using an in-vitro model of intestinal epithelium.

Then, since cell-free mitochondrial DNA has been proposed as a mediator of inflammation, and given that inflammaging is one of the main factors underpinning the development of cardiovascular disease, the third research objective was to quantify mitochondrial DNA copy number (mtDNAcn) in circulating cell-free DNA and extracellular vesicles by comparing healthy subjects and patients with cardiovascular disease in order to assess whether it is altered in CVD patients and whether it may serve as a predictive biomarker of cardiovascular events.

This doctoral thesis is presented in the format of a thesis by publication. It consists of a general introduction, a series of peer-reviewed articles published during the doctoral period, and a general discussion that integrates the main findings.

3. Results

3.2 Research Article n° 1

THE NUTRIGENOMIC EFFECT OF MELA ROSA MARCHIGIANA CALLUS EXTRACT ON CELLULAR SENESCENCE: INSIGHT FROM A PRELIMINARY IN VITRO STUDY

Chiara Rucci[1,2], Enrica Sordini[3], Giuseppe Persico[4], Eugenia Ciurlia[3], Noemi Pappagallo[5], Giulia Matacchione[6], Marco Giorgio[4], Daniele Fraternale[5], Maria Cristina Albertini[5], Dale Annear[7], Peter De Rijk[8,9], Tim De Pooter[8,9], Mojca Strazisar[8,9], Wim Vanden Berghe[10], Laura Bordoni[2]*, Stefano Amatori[3]*, Rosita Gabbianelli[2]*

[1] School of Advanced Studies, University of Camerino, Camerino, MC, Italy

[2] Unit of Molecular Biology and Nutrigenomics, School of Pharmacy, University of Camerino, Camerino, MC, Italy

[3] Molecular Pathology Laboratory "PaoLa", Department of Biomolecular Sciences, University

[4] Department of Biomedical Sciences, University of Padova, Padova, Italy

[5] Department of Biomolecular Sciences, DISB, University of Urbino Carlo Bo, Urbino, PU, Italy

[6] Center of Clinical Pathology and Innovative Therapy, IRCCS INRCA, Ancona, Italy

[7] Center of Medical Genetics, University of Antwerp, Antwerp, Belgium
of Urbino Carlo Bo, Fano, PU, Italy

[8] Neuromics Support Facility, VIB Center for Molecular Neurology, VIB, Antwerp, Belgium

[9] Department of Biomedical Sciences, University of Antwerp, Antwerp, Belgium

[10] Cell Death Epigenetic Signaling Lab, Department of Biomedical Sciences, University of Antwerp, Antwerp, Belgium

Published in: Molecular Nutrition and Food research (In press)

Abbreviations

AGE: agarose electrophoresis

cPD: cumulative population doubling

CPM: counts per million

DEGs: differentially expressed genes

DMSO: dimethyl sulfoxide

EMT: E2F Targets, G2M checkpoint, epithelial mesenchymal transition

FC: fold change

FDR: false discovery rate

HUVECs: Human umbilical vein endothelial cells

LPS: Lipopolysaccharide

MDS: Multidimensional scaling

MRM: Mela Rosa Marchigiana

MRME: Mela Rosa Marchigiana callus ethanolic extract

MSigDB: Molecular Signatures Database

MTT: (3-(4,5-dimethylthiazol-2-yl)-2,5-diphenyltetrazolium bromide)

PE: paired-end

PTAs: Pentacyclic triterpenic acids

SA: senescence-associated

SASP: senescence-associated secretory phenotype

sHUVECs : senescent Human umbilical vein endothelial cells

sHUVECs MRME: senescent HUVECs treated with Mela Rosa Marchigiana callus ethanolic extract

Key Words: Anti-aging; Anti-inflammatory; DNA methylation; Mela Rosa Marchigiana; Transcriptomic analysis.

Abstract

Scope: Mela Rosa Marchigiana (MRM) is an apple variety cultured in the center of Italy. Calluses derived from in vitro culture of MRM explants were used to obtain an ethanolic extract rich in pentacyclic triterpenic acids with putative anti-inflammatory and anti-aging effect. In this study we investigated the transcriptomic and epigenetic effect of MRM callus extract (MRME) in an in vitro model of cellular senescence. Methods and results: Senescent HUVECs (sHUVECs) were treated with MRME. Transcriptomic analysis was performed to compare young HUVECs (yHUVECs) with sHUVECs and to evaluate the MRME's effect on sHUVECs. Results show that senescence induces major changes in the transcriptome of HUVECs. MRME downregulates TNF-α signaling genes in sHUVECs restoring the expression to those observed in yHUVECs. Genome-wide DNA methylation analysis performed using Oxford-Nanopore sequencing platform didn't reveal significant changes in DNA methylation levels induced by MRME. Conclusion: Our preliminary results provide additional evidence suggesting that MRME exert anti-inflammatory and anti-aging effects, which may be mediated by the modulation of the expression of inflammaging genes via mechanisms independently of DNA methylation. These findings highlight MRME as a promising candidate for further in vivo studies aimed at exploring its clinical translational potential in counteracting inflammaging.

1. INTRODUCTION

Mela Rosa Marchigiana (MRM) is an ancient apple variety peculiar of the center of Italy [1]. It is characterized by the small size, flat shape, green peel with pink reddish colors and an intense sweet taste [1]. The plant (Malus × domestica Borkh, Rosaceae family) is found at altitudes of 400-900 m above the sea level in the Marche region (Italy) where it thrives under the Appenine climatic conditions characteristic of this area.

MRM has been cultivated in the Sibillini region for long, but its production decreased in the past decades until it ceased due to low market demands [2]. However, the productions have recently restarted thanks to the increasing interest in the properties of this variety of fruit. MRM, in fact, has been demonstrated to be an important source of bioactive compounds and it has been suggested as potentially useful to produce nutraceuticals and food supplements [1–3]. MRM contains polyphenols such as flavan-3-ols/procyanidins, dihydrochalcones, flavonols, and hydroxycinnamic acids, as well as triterpenic acids such as annurcoic acid [1]. Pentacyclic triterpenic acids (PTAs) are a class of secondary metabolites present in several medicinal plants and in a great variety of fruit and vegetables [4]. Recently, PTAs have garnered increasing interest due to their potentiality in prompting human health despite their limited availability in food and plants. The presence of secondary metabolites in fresh plant material, in fact, is usually low and depends on factors such as light, temperature and soil composition, which can vary with each season [5–7]. Intriguingly, it has been demonstrated that the cellular plant material (i.e. calluses) obtained from the in vitro culture of fruit pulp contains higher amounts of secondary metabolites, such as PTAs, than the starting material [6,8]. Fraternale et al. developed a technique to obtain in vitro calluses using explants of the mature pulp of the MRM. Interestingly, the chemical analysis of these calluses revealed that the secondary metabolites content in the calluses obtained from Mela Rosa Marchigiana was higher than in the calluses obtained from a common Golden Delicious apple [9]. Furthermore, for both the apple varieties the content in PTAs in the calluses was higher than the starting plant material [2,9]. Several types of extraction were performed on the calluses and the biological activity of the extracts was tested. The aqueous extract of MRM callus showed antiproliferative and antitumorigenic potential, together with chemopreventive

properties [10]. Potenza et al. showed that the ethanolic extract of MRM callus (MRME) has antioxidant properties against free radicals, it reduces ROS production in a cell model of H2O2 induced oxidative stress and it has an anti-inflammatory activity on RAW 264.7 cells treated with LPS [11]. Gubitosa et al. validated in vitro, ex vivo and in vivo the biological effect of the ethanolic extract: all experimental tests confirmed that MRME protects cells, tissues or whole organisms from oxidative stress-induced damage [2]. Finally, Benayada et al. evaluated the in vitro anti-inflammatory activity of MRME in high glucose and senescence conditions. They demonstrated that the treatment of senescent human umbilical vein endothelial cells (sHUVECs) with 1 μg/mL MRME significantly reduces the expression of IL-1β and IL-8 as compared to untreated sHUVEC and it upregulates two microRNAs related to senescence regulation and endothelial function, miR-17 and miR-126, in the same conditions [6]. Furthermore, they showed that MRME downregulates some inflammatory markers in U937 cells exposed to high glucose and/or lipopolysaccharide (LPS) [6]. These results suggest MRME as a possible inhibitor of senescence-associated inflammation and indicate a role of its high PTAs content in this biological activity [6]. The transcriptomic and epigenomic reprogramming potential of PTAs has been demonstrated in different cellular models. The activity seems to be associated with changes in the DNA methylation profile of cells treated with single PTAs molecules or with extracts enriched by PTAs [12–18]. Inflammaging, the chronic, sterile, low-grade inflammation that occurs during aging, is a well-recognized factor contributing to the pathogenesis of age-related diseases (ARDs), such as dementia and cardiovascular diseases [19]. The prevalence of ARDs is rising exponentially due to the growing of the older population and the worsening of lifestyle habits. Aging is characterized by the accumulation of senescent cells (SCs), which are characterized by a state of permanent proliferative arrest; however, they remain metabolically active and acquire a proinflammatory phenotype known as senescence-associated secretory phenotype (SASP), fueling inflammaging [20]. Physical activity and nutrition play a key role in healthy aging, preventing the onset of ARDs[21,22]. In particular, consumption of bioactive natural compounds contained in fruit, vegetables and plants, such as polyphenols, carotenoids and triterpenic acids, has garnered increasing interest for their potential role in prompting longevity [23]. Thus,

given that (i) MRM has been demonstrated to contain bioactive molecules, (ii) the extract obtained from the callus of MRM has been hypothesized to act as a potential inhibitor of senescence-associated inflammation and (iii) its transcriptomic and epigenetic effect has never been investigated before, the present study aims to evaluate the nutrigenomic effect of MRME using an in vitro model of cellular senescence.

2. MATERIALS AND METHODS

2.1 Mela Rosa Marchigiana callus and extract preparation

The MRM callus used in this study was obtained following the method described by Verardo et al. [9] and MRM callus extract was prepared as described by Gubitosa et al. [2].

2.2 Cell culture, senescence characterization and viability assay

HUVEC cells were cultured under standard conditions until replicative senescence and classified as either young (yHUVECs) or senescent (sHUVECs) based on passage number, SA-β-Galactosidase activity, and p16INK4a expression [24][25] . The effect of MRME on sHUVEC viability was evaluated using the MTT assay. Detailed methods for cell culture, characterization, and viability assays are provided in the Supplementary Materials.

2.3 MRME treatment conditions

sHUVECs were treated with MRME at a concentration of 1 µg/mL for 72 h. Untreated sHUVECs (negative control) and yHUVECs were included in the study. Experiments were conducted in triplicate. The selection of the 1 µg/mL concentration was based on cell viability >80% compared to that of the vehicle-treated cells and in accordance with the findings of Benayada et al [6]. After 72 h incubation, cells were collected and stored at -80°C for subsequent analysis.

2.4 DNA and RNA Extraction

Genomic DNA and total RNA were isolated from yHUVECs, sHUVECs, and sHUVECs treated with MRME (sHUVECs MRME) using the RNA/DNA purification

kit (Norgen, Thorold, ON, Canada; cat 48700), quantified by Qubit dsDNA HS Assay Kit and Qubit HS RNA assay kit (Thermo Fisher Scientific, Waltham, MA, USA) and stored at –80 °C. After purification, RNA integrity was evaluated by separating 1 μg of total RNA by agarose gel electrophoresis (AGE).

2.5 RNA sequencing and analysis

Total RNA extracted from yHUVECs, sHUVECs, and sHUVECs MRME was used for transcriptomic analysis via RNA-seq (StarSEQ GmbH, Mainz, Germany). RNA quality and quantity were further evaluated using Agilent 2100 Bionalyzer (Agilent Technologies, Santa Clara, CA, USA). mRNA was isolated, fragmented and reverse transcribed into cDNA which was end-repaired, adapter-ligated and PCR enriched. Libraries were assessed using the Qubit Fluorometer (Thermo Fisher Scientific, Waltham, MA, USA) and Agilent 2100 Bionalyzer (Agilent Technologies, Santa Clara, USA). Sequencing was performed on Illumina NextSeq 2000 platform using XLeap SBS chemistry, generating 150 bp paired-end (PE) reads. Each sample was sequenced to a depth of approximately 25 million paired end reads (2x12.5 million reads per sample, 2x150 bp). Reads were trimmed and aligned to human genome hg38 using Illumina DRAGEN pipeline. Gene expression was quantified with Salmon and differential expression analyzed by edgeR. Low expressed genes (≤2 CPM) were filtered out. Normalization was done using Trimmed Mean of M-values (TMM). A multidimensional scaling (MDS) plot was generated using the plotMDS function from edgeR with default parameters. Genes were identified as differentially expressed (DEGs) when the following criteria were met: false discovery rate (FDR) ≤ 0.05 and fold change (FC) ≥ 2 or ≤ -2. For the comparison of sHUVECs versus sHUVECs MRME, DEGs were filtered for a FC ≥ 1.5 or ≤ -1.5 in consequence of the lower changes monitored. Where not specified, all plots were generated using ggplot2 R package.

2.6 Pathway analysis

Pathway analysis was conducted using iPathwayGuide software (Advaita Bioinformatics, United States) to identify the biological pathways associated with the differentially expressed genes observed in the three experimental conditions. The

Molecular Signatures Database (MSigDB) gene set was used and pathways with FDR below 0.01 were considered significantly enriched.

2.7 DNA methylation analysis

Bisulfite Pyrosequencing was performed to evaluate DNA methylation levels in the promoter regions of twelve genes which were differentially expressed in the comparison between sHUVEC and sHUVEC MRME. To obtain a broader unbiased, genome-wide assessment of DNA methylation changes, Reduced Representation Methylation Sequencing (RRMS) was also conducted using PromethION 24 (Oxford Nanopore Technology, UK) on DNA from three biological replicates of sHUVEC and sHUVEC MRME. Detailed materials and methods for both Pyrosequencing and Nanopore RRMS analysis are provided in the Supplementary Materials.

3. RESULTS

3.1 Differences in the gene expression profile of sHUVECs and yHUVECs

We first decided to investigate the effects induced by senescence on the gene expression profile of HUVEC cells. HUVECs were defined as follows: (i) young HUVECs (yHUVECs), characterized by a replicative passage number <6, (SA)-β-galactosidase activity <20%, and markedly reduced p16^INK4a expression relative to senescent counterparts; (ii) senescent HUVECs (sHUVECs), defined by a replicative passage number >15, (SA)-β-galactosidase activity >60%, and significantly elevated p16^INK4a expression compared with yHUVECs, as reported previously [6].

RNA-seq was conducted using three biological replicates for yHUVECs and sHUVECs. The overall similarity between samples has been assessed through either a hierarchical clustering (Euclidian distance) (Figure 1A) and a multidimensional scaling (MDS) analysis (Figure 1B), allowing the clustering of the triplicates into distinct groups in function of culture passages, suggesting that senescence had a high impact on gene expression. MDS shows that dimension 1 (dim1), which explains 80% of total variability of our dataset, is driven by senescence, while dim2 (6%) variation seems to be related to intragroup variability. Differential enrichment analysis by edgeR package allowed us to identify genes affected by senescence in HUVECs. According

to results, a total of 1,452 differentially expressed genes (DEGs) were identified in sHUVECs compared to yHUVECs (Table S2 of Supplementary materials), with 759 up-regulated and 693 down-regulated genes in sHUVEC (Figure 1C). The DEGs were analyzed for pathway enrichment using the iPathwayGuide software. According to results, we found six pathways as significantly enriched (Figure 1D): E2F Targets ($p < 0.01$), G2M checkpoint ($p < 0.01$), epithelial mesenchymal transition ($p < 0.01$), TNFα signaling via NFKB ($p < 0.01$), KRAS signaling up ($p < 0.01$) and Mitotic spindle ($p < 0.01$). "E2F Targets" pathway included 100 DEGs which were downregulated and only 2 DEGs which were upregulated in sHUVECs compared to yHUVECs, while "G2M checkpoint" included 84 genes which were significantly down-regulated and 1 gene which was up-regulated, indicating the downregulation of both pathways. "Epithelial mesenchymal transition" pathway involved 57 upregulated genes and 5 downregulated genes, "TNFα signaling via NFKB" pathway included 48 upregulated genes and 3 downregulated genes, while "KRAS signaling up" included 36 upregulated genes and 7 downregulated genes suggesting, in this case, the upregulation of these three pathways. Finally, "Mitotic spindle" included 38 downregulated and only 4 upregulated genes. The first twenty differentially expressed genes (DEGs) enriching the six pathways were shown in Figure 2.

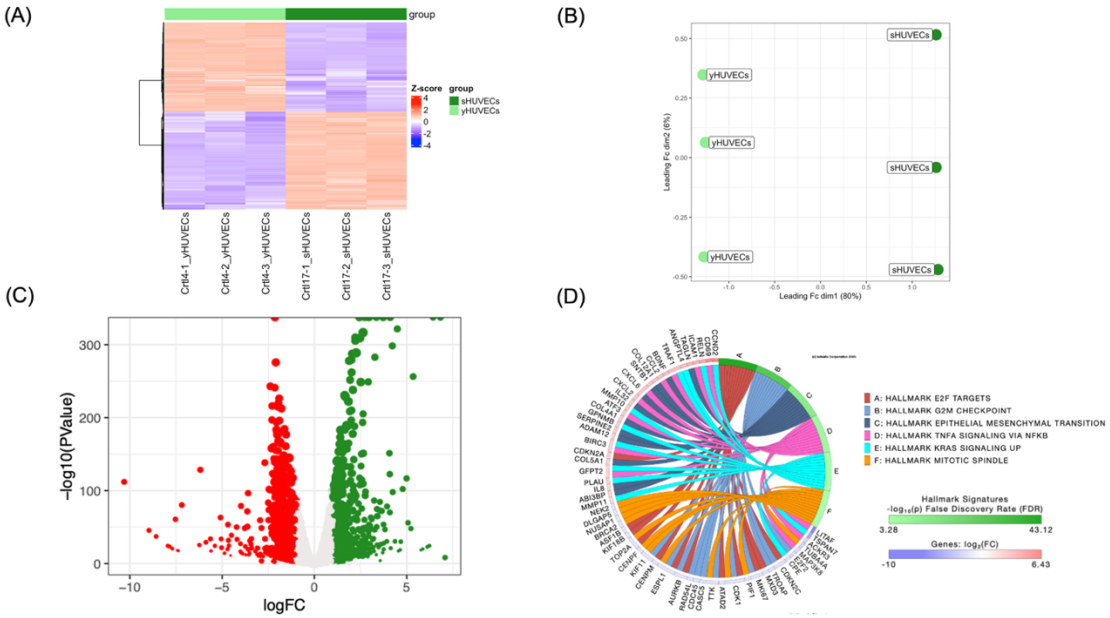

Fig 1. Genome-wide analysis of the gene expression modulations induced by senescence in HUVEC cells.

HUVEC cells were subjected to passage-induced senescence and analyzed by RNA-seq using the R package edgeR with a likelihood ratio test (LRT); the resulting p-values were adjusted using the Benjamini–Hochberg (BH) method. All experiments have been conducted using 3 biological replicates for each condition. (A) Hierarchical clustering heatmap of all DEGs (FDR ≤ 0.05) of yHUVECs and sHUVECs. As reported in the color key, positive Z-scores (red) are associated with higher expression values while negative Z-scores (blue) indicate a lower expression value. (B) Multidimensional scaling (MDS) analysis comparing yHUVECs and sHUVECs. (C) Volcano plot of DEGs obtained comparing yHUVECs and sHUVECs. Significantly downregulated genes in sHUVECs are shown in red, while up-regulated genes are shown in green. (D) Circos plot showing the pathways found modulated using the Molecular Signatures Database (MSigDB) Hallmark signatures and relative DEGs were obtained comparing yHUVECs and sHUVECs. Pathways were considered significantly enriched when p<0.01 and are reported in figure.

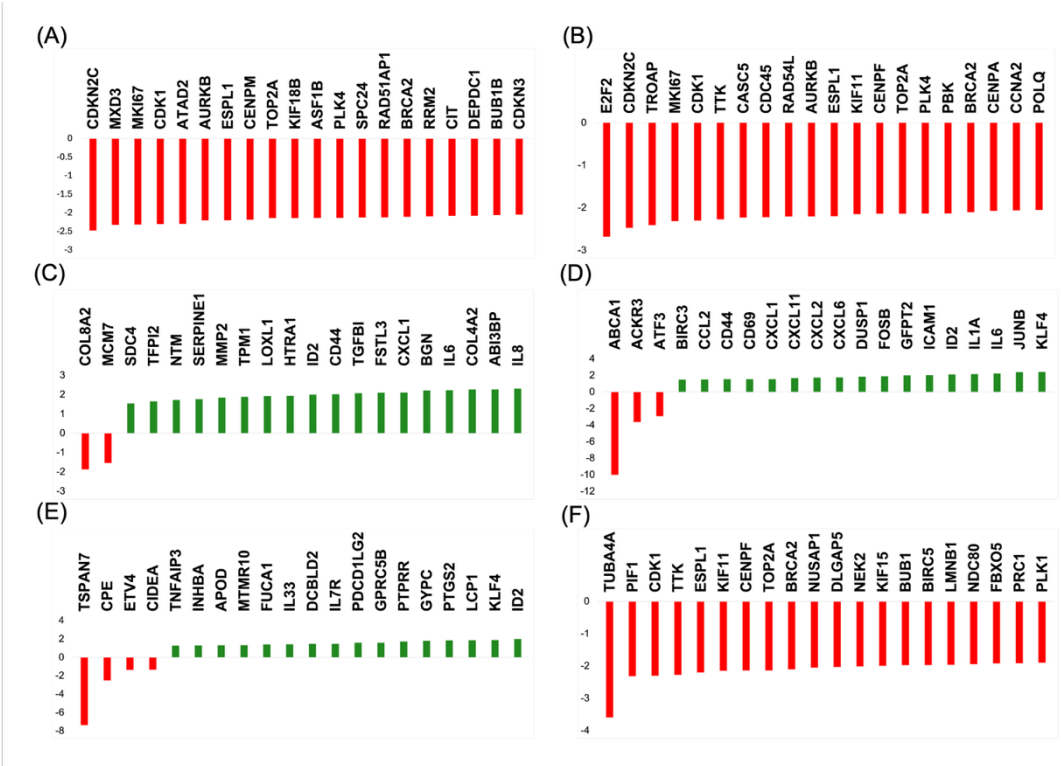

Fig 2. Quantitative transcripts variations of the DEGs belonging to the six pathways modulated by senescence in HUVEC cells. The first twenty differentially expressed genes

(DEGs) enriching the six pathways found modulated by senescence in HUVEC cells are shown as green bars (upregulated DEGs) or red bars (downregulated DEGs). (A) E2F targets pathway; (B) G2M checkpoint pathway; (C) Epithelial mesenchymal transition pathway; (D) TNF-a signaling via NFKB pathway; (E) KRAS signaling up pathway; (F) Mitotic spindle pathway. Data on the y asses are reported as logarithm of the fold change (logFC).

3.2 Modulation of the gene expression profile induced by MRME in sHUVEC

First of all, the effect of MRME on sHUVECs viability has been evaluated treating cells with different concentrations of MRME (ranging from 0.76 to 12.5 μg/ml) for 72 h. MRME treatments didn't show any significant effect on sHUVEC cell viability (Figure S1 of Supplementary Materials). RNA-seq was then conducted on three biological replicates of sHUVECs treated for 72 h with MRME at the concentration of 1 μg/ml and compared to not-treated sHUVECs to evaluate the impact of MRME exposure on the gene expression of sHUVECs. This condition was chosen in consequence of previous works on MRME extracts [6]. Hierarchical clustering (Euclidian distance) was performed showing the clustering of the triplicates into distinct groups (Figure 3A). Regarding MDS analysis, even if only slight differences are present among the two groups, the samples can be anyway clustered matching both dim1 (29%) and dim2 (25%) components (Figure 3B). We found a total of 26 DEGs in sHUVECs MRME compared to untreated sHUVECs with 11 upregulated and 15 downregulated genes (Figure 3C). The list of DEGs is reported in Table S3 of Supplementary materials. Interestingly, iPathwayGuide analysis of DEGs showed that three pathways were significantly enriched by MRME treatments: TNFα signaling via NFKB ($p < 0.01$), UV response up ($p < 0.01$) and TGF-β Signaling ($p < 0.01$) (Figure 3D). "TNFα signaling via NFKB" included 12 DEGs (Figure 4A): ID2, GADD45B, JUNB, HES1, ATF3 NR4A1, KLF4, FOS, FOSB, ZFP36, DUSP1 and SOCS3. All these genes were significantly downregulated by MRME treatments in sHUVECs. The "UV response up" pathway included 5 DEGs which were downregulated in senescent cells treated with the extract (Figure 4B): JUNB, ATF3, NR4A1, FOS and FOSB. Finally, TGF-β Signaling pathway included 3 genes (Figure 4C): ID1, ID2 and JUNB that were, even in this case, downregulated in sHUVEC MRME.

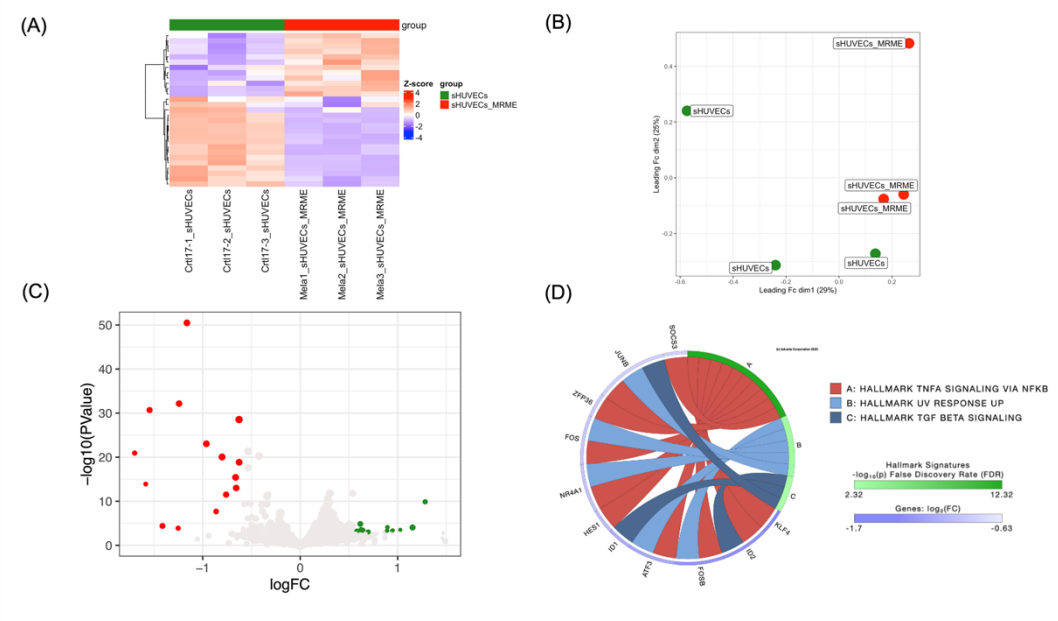

Fig 3. Genome-wide analysis of the gene expression modulations induced by MRME treatments in senescent HUVECs (sHUVECs). HUVECs were treated with at MRME at the concentration of 1 ug/ml for 72 hours and analyzed by RNA-seq using the R package edgeR with a likelihood ratio test (LRT); the resulting p-values were adjusted using the Benjamini–Hochberg (BH) method. All experiments have been conducted using three biological replicates for each condition. (A) Hierarchical clustering heatmap of all DEGs (FDR ≤ 0.05) of untreated and MRME treated sHUVECs. As reported in the color key, positive Z-scores (red) are associated with higher expression values while negative Z-scores (blue) indicate a lower expression value. (B) Multidimensional scaling (MDS) analysis comparing sHUVECs and sHUVECs MRME. (C) Volcano plot of DEGs obtained comparing sHUVECs and sHUVECs MRME. Significantly upregulated genes in sHUVEC MRME are shown in green; downregulated genes are shown in red. (D) Circos plot showing the pathways found modulated using the Molecular Signatures Database (MSigDB) Hallmark signatures and relative DEGs obtained comparing sHUVECs and sHUVECs MRME. Pathways were considered significantly enriched when p<0.01 and are reported in figure.

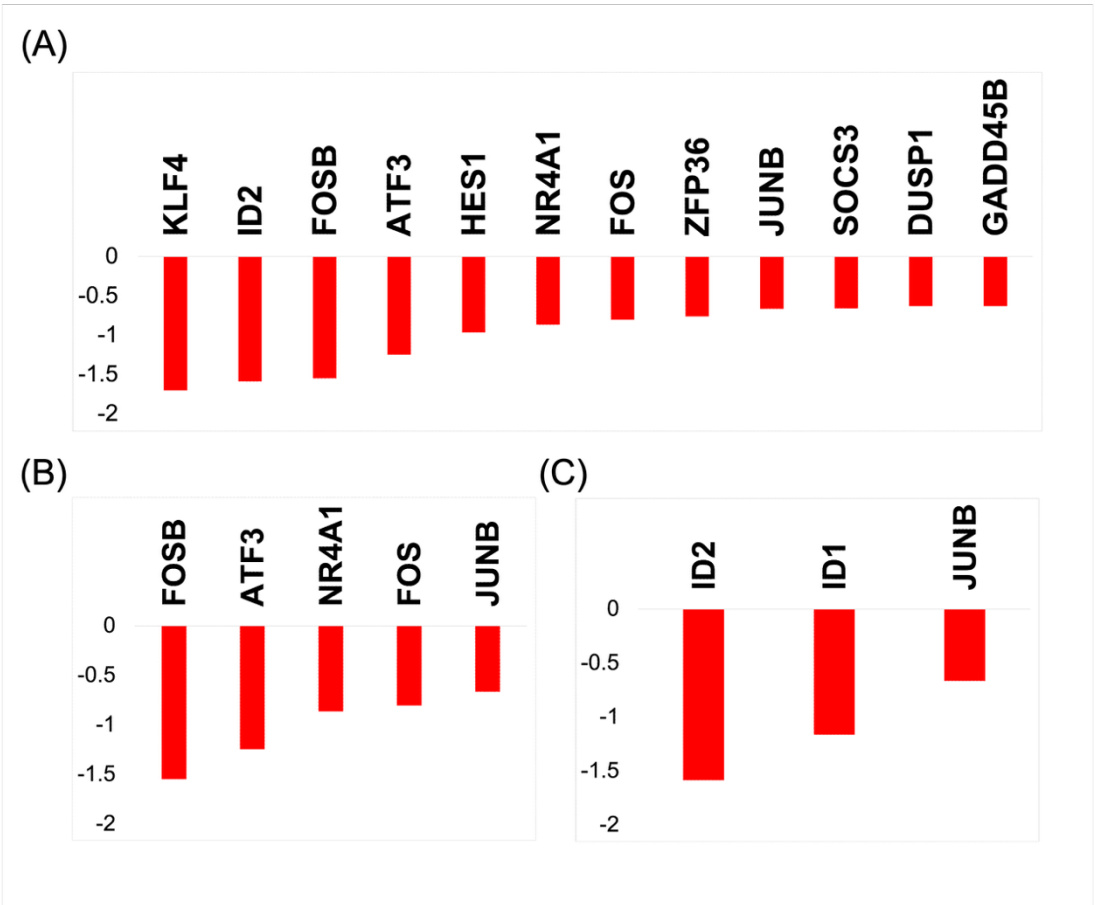

Fig 4. Quantitative transcripts variations of the DEGs belonging to the three pathways modulated by MRME in sHUVECs. DEGs enriching the pathways found modulated by MRME treatments in sHUVEC cells are shown as green bars (upregulated DEGs in sHUVEC MRME) or red bars (downregulated DEGs). (A) TNF-α signaling via NFKB pathway; (B) UV response pathway; (C) TGF-β Signaling pathway). Data on the y asses are reported as logarithm of the fold change (logFC).

3.3 Effect of MRME on DNA methylation in sHUVEC

To explore whether the observed transcriptional changes were associated with DNA methylation, we performed Pyrosequencing analysis in the promoter regions of the 12 DEGs enriched in the TNFα signaling via NFKB pathway. No significant differences in mean promoter methylation levels were observed across conditions (Supplementary Figure S2). However, methylation at a specific CpG site within the SOCS3 promoter was significantly altered by MRME (Figure 5). Along the same line, complementary

genome-wide DNA methylation profiling using PromethION24 (Oxford Nanopore technology, UK) also showed no significant MRME-induced changes in CpG methylation at either single-site (data not shown) or promoter levels (Supplementary Figure S3). Detailed results are provided in the Supplementary Materials.

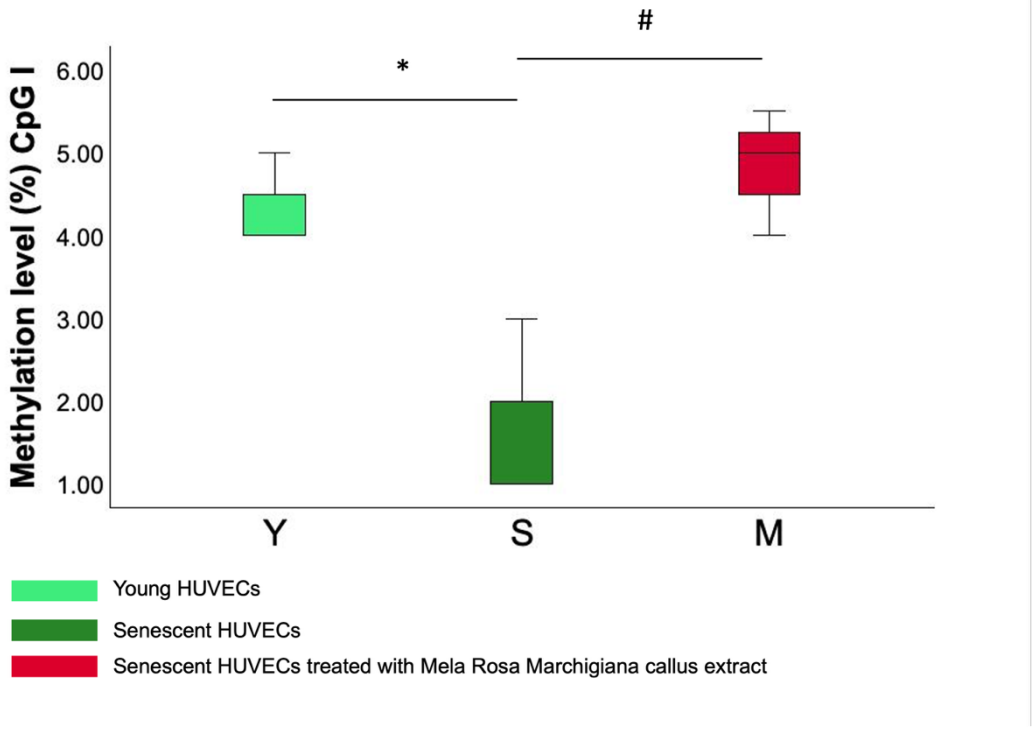

Fig 5: Methylation level of the first CpG site on the selected area of the SOCS3 promoter. Methylation level measured by Pyrosequencing analysis in the I CpG site of the selected area of the SOCS3 promoter in the three groups: Y (young HUVECs), S (senescent HUVECs), M (senescent HUVECs treated with MRME). The experiment was performed using three biological replicates for each condition and two technical replicates for the analysis. There was a statistically significant increase in yHUVECs compared to sHUVECs (, $p < 0.05$) and in sHUVECs MRME compared sHUVECs (#, $p < 0.05$). The boxes represent the interquartile range (25th–75th percentile), the line inside the box indicates the median, and the whiskers extend to the smallest and largest values within 1.5 times the interquartile range. ANOVA test or Kruskall-Wallis test was used to compare differences in methylation levels between groups.*

4. DISCUSSION

Several dietary components have been suggested to affect the genome by regulating the gene expression profile of cells through epigenetic and non-epigenetic mechanisms [26–28]. Among these, bioactive molecules contained in fruit and vegetables have been demonstrated to exert an active role in promoting human health throughout a nutrigenomic effect [28]. In particular, polyphenols, carotenoid and terpenoids have gained increasing attention for their potential role in promoting longevity [23]. Here, we focused the attention on the effects mediated by an ethanolic extract of the callus of Mela Rosa Marchigiana (MRME), an ancient Italian apple containing PTAs [9] secondary metabolites present in small amounts in fruit and vegetables, with known beneficial effects for the human health [29–32]. Its biological effect has been previously investigated using different models, with findings suggesting anti-inflammatory properties and potential anti-aging activity of MRME [2,6]. Although MRM callus is a good source of active compounds, the transcriptomic and epigenetic effect of its extract has never been studied before. This research aimed to investigate the impact of MRME on global gene expression and on DNA methylation using an in vitro model of replicative senescence. First, we focused our attention on the differences between yHUVECs and sHUVECs to identify the transcriptomic variations associated with the senescent phenotype. According to our results, a list of 1,452 DEGs were identified, with 759 genes upregulated and 693 genes downregulated. Gene set enrichment analysis identified 6 significantly enriched biological pathways in senescent cells: E2F Targets, G2M checkpoint, epithelial mesenchymal transition (EMT), TNFα signaling via NFKB, KRAS signaling up and Mitotic spindle. E2F is known to play a major role in cell cycle regulation and its targets includes genes regulating cell cycle, cell proliferation and apoptosis [33]; similarly, G2M checkpoint is a critical stage in cell cycle progression, preventing cells to enter in mitosis when DNA is damaged [34]. Both were downregulated in sHUVECs compared to yHUVECs. This result is not surprising, since the decreased expression levels of cell cycle genes is typical of senescence and is in line with current literature [35]. EMT pathway is responsible for the acquisition of the mesenchymal phenotype by epithelial cells [36]. It is a key regulator of cancer development, favoring metastasis formation, and it has been suggested to be activated by cellular senescence [37]. In fact, the

inflammatory environment characterizing SASP has been demonstrated to drive EMT [37]. Even though this pathway is peculiar of epithelial cells, also endothelial cells have been shown to transit into a mesenchymal phenotype throughout the activation of the endothelial to mesenchymal transition pathway (EndMT) occurring during aging [38,39]. The up-regulation of DEGs involved in EMT pathway in sHUVECs, suggests an activation in replicative senescent cells, possibly due to the inflammatory status characterizing senescent cells. Other enriched pathways were TNFα signaling via NFKB pathway, which regulates inflammation, KRAS signaling pathway, which regulates signal transduction, and mitotic spindle pathway, which is implicated in the mitosis process. TNFα via NFKB is a well-known pathway regulating inflammation [40] and its involvement in aging has been extensively studied. NFKB signaling was suggested to increase with senescence and its activity has been associated with numerous age-related diseases [41,42]. Furthermore, increasing literature suggests that NFKB signaling promotes aging enhancing the manifestation of SASP [41,43]. KRAS signaling stimulate cell growth, cell division, cell survival and regulates cell death [44]. Its upregulation, although paradoxical, could be part of the molecular events associated with the induction of replicative senescence. Activation of a DNA damage response was found to induce senescence in response to overexpression of oncogenic RAS [45]. Finally, mitotic spindle pathway is downregulated in our experimental condition, in line with the reduction of the mitotic process during senescence. Ohori et al. performed RNA-seq on HUVECs at different culture times to study transcriptome changes during senescence, identifying alterations in pathways related to cell cycle, DNA repair, metabolism, and chromosome organization [46]. Notably, G2M checkpoint and mitotic spindle processes were significantly impacted, consistent with our findings [46]. Ramini et al. analyzed HUVECs rendered senescent by high glucose, revealing enrichment of interferon alpha/beta signaling pathway [47]. They also assessed IL-6, IL-1β, and IL-8 expression in yHUVECs (CPD = 15) and sHUVECs (CPD = 35) under standard glucose conditions, reporting changes in IL-6 and IL-8 levels consistent with our results (see Table 2 of Supplementary Materials). Similar results have been described also in another study [48], which also showed Dnmt1 downregulation, consistent with our data (see Table S2 of Supplementary materials). After having analyzed the differences in gene expression between sHUVECs and

yHUVECs, we focused on the effects induced by MRME on sHUVECs. The results suggest an interesting nutrigenomic effect of MRME, highlighting its role in modulating gene expression. Notably, according to transcriptomic analysis results, 26 genes were differentially expressed comparing sHUVECs MRME and sHUVECs. It remains unclear whether the extract's effects are due to the cumulative action of all its individual constituents or to specific polypharmacological compounds even though there is a growing trend toward studying the effects of phytocomplexes rather than their individual isolated compounds (secondary metabolites) since the various chemical components of a plant often act synergistically to produce a more potent and balanced therapeutic effect [49–51] .

Indeed, the impact of individual MRME phytocompounds (e.g., PTAs) on gene remains partly unclear, with some unstudied and others reported to exert modulatory effects [52–55]. In particular, Oleanolic acid was demonstrated to modulate gene expression in HUVECs [53,56]. Pathway analysis was conducted to determine whether the DEGs obtained comparing sHUVECs MRME and sHUVECs were enriched in specifical biological pathways. According to results, MRME significantly modulated three main pathways: TNFα signaling via NFKB pathway, UV response up pathway, and TGF-β Signaling. Interestingly, TNFα signaling via NFKB pathway was the most significantly modulated pathway in sHUVECs MRME respect to sHUVECs. Since the inhibition of NFKB activation has been suggested to delay or revert the aging phenotype [42] the observed downregulation of TNFα /NFKB related genes suggests that MRME may suppress pro-inflammaging processes, driving the senescence phenotype. In line whit this evidence, MRME could be potentially proposed not only as an anti-inflammatory agent but also as a possible modulator of aging. This hypothesis is consistent with previous studies reporting potential anti-aging effects of PTAs in various experimental models [57–62] . However, further comparative in vivo studies, using the phytocomplex are necessary to confirm the anti-aging activity to better elucidate their potential clinical application. Previous literature showed that MRME downregulated the expression of inflammatory markers and upregulated miRNAs involved in inflammation and in the inhibition of cellular senescence [6], in line with our findings[6]. In addition to TNFα via NFKB pathway, MRME also modulated other pathways, including UV response pathway, a process activated in

response to ultraviolet radiation [63] and TGF-β Signaling pathway which regulates various biological mechanisms such as cell proliferation, cell cycle regulation, DNA damage response, telomere regulation and autophagy [64]. Increasing literature suggests that TGF-β signaling is implicated in the aging process and in the occurrence of several age-associated diseases [65] Interestingly, the inhibition of TGF-β signaling has been suggested to retard cellular senescence in human pluripotent stem cells derived endothelial cells [66]. Although only three DEGs in this pathway were downregulated by MRME, these changes indicate its impact on senescence-related mechanisms. After having identified pathways modulated by the MRME and by senescence we concentrated our attention on the expression trends of individual genes, focusing on the twelve genes downregulated by MRME in sHUVEC that are part of the TNFα signaling via NFKB pathway. The aim of this observation was to specifically assess whether the expression levels of these genes changed with senescence and if the treatment of sHUVECs with MRME was able to restore the expression level to those occurring in young cells. Interestingly, we found that the expression levels of most of these twelve genes increased in sHUVECs respect to yHUVECs and were lowered by MRME treatments of sHUVECs, suggesting that the senescence-associated upregulation of these genes can be attenuated by MRME exposure (Figure 6). Among the twelve genes analyzed, transcriptional regulators and factors involved in cytokine response were identified, including FOS, FOSB, and JUNB-components of the AP-1 complex linked to inflammation [67]. Karakaslar et al. showed JUN and FOS activation as markers of immune aging in mice[67] consistent with our findings of increased JUN, JUNB, and FOS expression in senescent HUVECs. A secondary aim of this study was to verify whether the alterations of gene expression levels found in the comparison between sHUVECs MRME and sHUVECs were due to epigenetic alterations in DNA methylation. We focused in the twelve DEGs that were involved in the TNFα via NFKB pathway and we analyzed the DNA methylation levels in selected areas of the promoters of these genes by Pyrosequencing. Results revealed no significant differences in mean methylation levels at promoter regions of the twelve genes involved in the TNFα signaling pathway between yHUVECs, sHUVECs and sHUVECs MRME. Only the first CpG site in the selected area of the SOCS3 promoter showed a significantly different level of

methylation in sHUVECs compared to yHUVECs and in sHUVECs MRME compared to sHUVECs even though the difference observed at this single CpG site is small and close to the lower range of reliable detection by pyrosequencing (as indicated by the low methylation percentages). Therefore, it should be interpreted with caution and may reflect technical or biological variability rather than a consistent epigenetic modification.

Similarly, genome-wide DNA methylation analysis performed using Nanopore sequencing platform also revealed no significant MRME-induced quantitative changes in CpG methylation at either single-site or promoter level in our experimental setting. Thus, although we did not sequence 100% of the genome but only regions highly enriched in CpGs, it is unlikely that the gene expression changes induced by MRME are primarily driven by major DNA methylation variations caused by the extract in this experimental setting. In line with this observation, we found that the expression level of DNA methyltransferase enzymes DNMT1, DNMT3A and DNMT3B, were not influenced by MRME treatments, although DNMT1 and DNMT3B were downregulated in sHUVECs as compared to yHUVEC. This result is in agreement with present literature and with the global hypomethylation occurring during senescence [68]. This study has limitations that need to be addressed. Firstly, it was conducted using three biological replicates per group. Although the number of replicates is relatively small and may not fully capture the underlying variability, it represents a reasonable compromise for an exploratory investigation aimed at generating a preliminary dataset. This design enabled us to capture initial molecular insights that can be further tested and expanded in future studies.

Secondly, since we did not apply ATAC (chromatin accessibility) or HiC (topological association domain) sequencing, our results may not capture the full complexity of 3D chromatin (re)organization upon senescence, which needs further exploration [69–71]. Third, in line with the exploratory aim of this study, our analysis focused exclusively on the expression level of genes without measuring protein levels, enzymatic activities or actual pathway activation, only allowing us to identify preliminary molecular trends in mode of action.

Furthermore, to estimate clinical relevance of our findings, our results need further validation in more complex biological systems to strengthen their translatability.

Nevertheless, this study sheds light, for the first time, on the nutrigenomic effect of MRME, corroborating its interesting anti-inflammatory potential already documented in previous works. Further studies will be necessary to elucidate the mechanisms responsible for the modulation of gene expression induced by MRME and to fully understand if this extract could serve as a potential agent for promoting overall health, as well as its potential applications in specific clinical contexts.

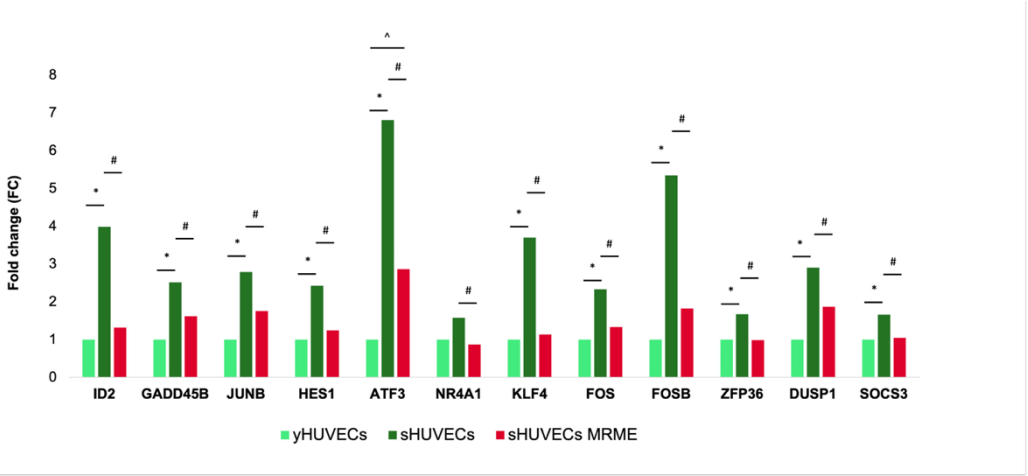

*Fig 6: Expression levels of TNF-α pathway genes modulated by MRME. The relative expression levels of the 12 TNF-α pathway genes in the three conditions: yHUVECs, sHUVECs and sHUVECs MRME. * p<0.05 yHUVECs vs sHUVECs; # p<0.05 sHUVECs vs sHUVECs MRME; ^ p<0.05 yHUVECs vs sHUVECs MRME.*

SUPPLEMENTARY MATERIALS

Supplementary materials and methods: Cell culture, characterization and cell viability assay

Cryopreserved Human umbilical vein endothelial cells (HUVECs) (Clonetics, Lonza, Switzerland) were cultured in endothelial growth medium (EGM-2) (Lonza, Switzerland), composed of endothelial basal medium (EBM-2) (Lonza, Switzerland) and the SingleQuot Bullet Kit (Lonza, Switzerland). The cells were seeded at a density of 5,000/cm^2 in T75 flasks (Corning Costar, Sigma Aldrich, St. Louis, MO, USA), sub-cultured when they reached 70–80% confluence, and maintained in a humidified atmosphere of 5% CO_2 at 37 °C.

Cells were expanded through multiple passages under these conditions until they reached replicative senescence. The cumulative population doubling (cPD) was determined as the sum of PD changes using the formula: log10(F) – log10(I))/log10(2) [36], where **F** represents the number of cells at the end of the passage and **I** the number of seeded cells. Cells were classified as either young (y) or senescent (s) based on replicative passages, senescence-associated (SA) β-Galactosidase activity, and $p16^{INK4a}$ expression levels. Specifically, young HUVECs (yHUVECs) were defined as those with a replicative passage number below 6, SA-β-Galactosidase activity below 20%, and significantly lower $p16^{INK4a}$ expression compared to sHUVEC. In contrast, sHUVEC were identified by a replicative passage number exceeding 15, SA-β-Galactosidase activity above 60%, and significantly higher $p16^{INK4a}$ expression than yHUVECs. To evaluate the effect of MRME on cell viability, sHUVECs were grown in 24-well plates at a density of 5,000 cells/cm^2 and exposed to different doses of MRME (12.5, 6.125, 3.06, 1.57, 0.76 μg/ml) for 72 h. Vehicle (70% ethanol)-treated cells were used as control. Briefly, MTT (5 mg/ml) solution was added to each well (10 μl per every 100 μl) and incubated at 37 °C for 4 h. After the incubation period, the obtained formazan salt was dissolved in dimethyl sulfoxide (DMSO) and the absorbance was measured by a microplate reader (MPT Reader, Invitrogen, Milano, Italy) at the optical density of 570 nm.

Supplementary Materials and Methods: DNA methylation analysis

Isolated genomic DNA was converted with sodium bisulfite using the EZ DNA Methylation Gold kit (ZYMO research, Orange, USA; cat D5006) following manufacturer's instructions. 200 ng of DNA were mixed in PCR tubes with 130 µl of bisulfite mix solution. Samples were incubated in the thermal cycler device (2720 Thermal cycler, Applied Biosystem, Waltham, USA) for 160 min using the following reaction sequence: 98°C for 10 min followed by 150 min min at 64°C. Converted samples were purified using ZYMO spin IC columns and eluted in 20 µL of elution buffer. PCR amplification was performed using PyroMark PCR kit (Qiagen Inc., Venlo, the Netherlands; cat: 978703) in a thermal cycling device (2720 Thermal cycler, Applied Biosystem, Waltham, USA). Primers used to amplify the regions of interests are shown in Table S1 of Supplementary Materials. Briefly, 15 µl of master mix, 3 µl of coral load, 1.2 µl of each primer, 8.6 µl of water, and 1 µl sample (10 ng) were mixed for each reaction and run under the following thermal cycling conditions: 95°C for 15 min, followed by 45 cycles of 30 sec at 94°C, 30 sec at 56°C, and 30 sec at 72°C, followed by a final extension step for 10 min at 72°C. Amplicons were checked for specificity and efficiency of the reaction by gel electrophoresis and then pyrosequenced using the PyroMark Q24 device (Qiagen Inc., Venlo, the Netherlands). PCR products were immobilized on Streptavidin-Sepharose beads (S-GE17-5113-01Streptavidin Sepharose High Performance, Sigma Aldrich) mixing in each well of a 24-well PCR plate 1 µl of Streptavidin-Sepharose beads, 40 µl of Binding Buffer (Qiagen Inc., Venlo, the Netherlands) 30 µl of ultra-distilled water and 9 µl of amplicons from each sample. The mixture was incubated at room temperature with shaking. PyroMark Workstation was prepared using 50 ml 70% ethanol, 40 mL Denaturation Solution (Qiagen Inc., Venlo, the Netherlands), 50 ml Wash Buffer (Qiagen Inc., Venlo, the Netherlands), and 50 ml and 70 ml ultra-distilled water. 0.75 µl of sequencing primer (specific for each sample) and 24.25 µl of Annealing Buffer (Qiagen Inc., Venlo, the Netherlands) were transferred to each well of a PyroMark Q24 plate (Qiagen Inc., Venlo, the Netherlands). The 24-well PCR plate and the Pyromark Q24 plate were transferred to the Workstation. All PCR Sepharose-product complexes were subjected to vacuum filtration and sequentially washed with ethanol, denaturation solution and wash buffer. The vacuum was turned off to allow the transfer

of the complexes in the PyroMark Q24 plate. The vacuum filters were washed extensively in ultra-distilled water. The PyroMark Q24 plates were placed into the Pyromark PyroMark Q24 Sequencer (Qiagen Inc., Venlo, the Netherlands) and sequencing reactions were carried out using cartridges containing enzyme, substrate and nucleotides. The degree of methylation was defined as the percentage of methylated cytosines over the sum of methylated and unmethylated cytosines.

Statistical analysis was performed using SPSS (IBM, version 29, USA). Shapiro-wilk method was used to test for normality of data. ANOVA test or Kruskall-Wallis test was used to compare differences in methylation levels between groups.

PromethION 24 (Oxford Nanopore Technologies, UK) was also used to assess the DNA methylation in sHUVECs and sHUVECs MRME. Adaptive sampling mode was applied to selectively enrich for approximately 310 Mb of the human genome, targeting regions highly enriched in CpG sites, including all annotated CpG islands, shores, shelves, and over 90% of promoter regions.

Three biological replicates for each condition for a total of six samples were sequenced using PromethION24 Instrument (Oxford Nanopore Technologies, Oxford, UK) and R10.4.1 flow cells (Oxford Nanopore Technologies, Oxford, UK) together with four additional samples to reach the recommended DNA molarity for optimal sequencing. In total we sequenced ten samples in two flow cells. Briefly, for all the samples, isolated genomic DNA was quantified using Qubit 4 Fluorometer (Thermo Fisher Scientific) and Qubit dsDNA HS kit (Thermofisher, Dilbeek, Belgium). DNA purity was assessed using Little Lunatic (Pleasanton, CA , USA) and integrity was evaluated with the Fragment Analyzer (Agilent HQ, Santa Clara, CA, USA) using the Agilent DNF-464 HS Large Fragment Kit. After quality control, 1-2 ug of DNA (depending on the sample) was fragmented using Megaruptor 3 (Hologic Diagenode, Ougree, Belgium) to obtain fragments having a size of 6-8 kb. Fragment size was confirmed using Fragment Analyzer, using DNF-492 Standard Sensitivity kit. Then, a volume of 50 ul of fragmented and size selected DNA, corresponding to a range between 732 ng and 1500 ng (equivalent to 154-335 fmol, depending on the sample) was used for library preparation. Libraries were prepared following the protocol for Reduced Representation Methylation Sequencing released By Oxford Nanopore on January 2025 [Ligation sequencing gDNA V14 - reduced representation methylation multiplex

sequencing (RRMS) (SQK-NBD114.24) V RRMS_9209_v114_revE_07Jan2025]. The Ligation sequencing kit SQK-NBD114.24 (Oxford Nanopore Technologies, Oxford, UK) was used to prepare libraries. Briefly, DNA was repaired and end-prepped using NEBNext FFPE DNA Repair Mix (New England Biolab, Ipswich, MA, USA, cat:#M6630) and NEBNext® Ultra II End Repair / dA-tailing Module (New England Biolab, Ipswich, MA, USA, cat: #E7546). Native Barcoding ligation was performed using the NEB Blunt/TA Ligase Master Mix (New England Biolab, Ipswich, MA, USA, cat: #M0367), assigning a unique barcode to each of the 10 samples included in the experiment. Barcoded samples were pooled, and sequencing adapters were ligated to the pooled DNA using the NEBNext Quick Ligation Module (New England Biolab, Ipswich, MA, USA, cat: #E6056). The final multiplexed library was purified, eluted in Elution Buffer and loaded in two flow cells which were sequenced simultaneously on PromethION24 Instrument (Oxford Nanopore Technologies, Oxford, UK). The sequencing run was carried out for 96 hours, after 24 hours and 48 hours of sequencing both the flow cells were flushed, and a fresh library was loaded.

The two flow cells respectively produced an output of 78.46 M and 79.25 M reads, with an estimated N50 of 2.83 kb for the first flow cell and 1.07 kb for the second, resulting in a total base output of 92.63 Gb and 89.9 Gb . Basecalling and methylation calling of the Nanopore data was performed on the instrument by MinKNOW using dorado 7.6.8 (High-accuracy model v4.3.0, 400 bps). The reads were aligned to the hg38 genome reference using minimap2 (https://academic.oup.com/bioinformatics/article/34/18/3094/4994778?login=true) and bedMethyl files were generated per sample using modkit. The edgeR package was used to perform differentially methylation analysis at CpGs loci and Promoter regions following the workflow for Bisulfite Sequencing differentially methylation analysis (section 4.8 in the EdgeR user's guide)

Table S1. Primers used for bisulfite pyrosequencing analysis.

Gene name	Primer forward	Primer reverse	Primer seq
ID2	5'-GGT TTG GGA GAG TTT GGG ATT G-3'	5'-Biotin-AAACCC CCAAACAAACTCTCT AAC-3'	5'-GGG TTTAGTAGG TAT TGATTA GT-3'
GADD45 B	5-AGG AGG GGAGAATGA T TAT TGA G-3'	5'-Biotin-CCAAAA CCT TCC CAC AAAACT AAA-3'	5'-GGG AGAATG AT TATTGAGG T-3'
JUNB	5'-ATT TGT T AGT GGA T TAG GGA AAT TA-3'	5'-Biotin-CAA CTCCCAACT CCC TAC TA C-3'	5'-GGT TAGTGGTAGTTGTIT ATA AGG-3'
HES1	5-AGAGGGAGAGTAGTAAA G GGT TAAAA-3'	5-Biotin-CAA ACT TC T CCC ACAATA ACT TC AA-3'	5'-AGTAGTAAAGGG TTAAAATTT-3'
ATF3	5'-GGTTTGGGT ATT ATT GGT TATGT-3'	5' Biotin-CCAACC C CT CTC TCTCCA T-3'	5'-GTA TTATTG GTT ATG TTT GGA A-3'
NR4A1	5-GTT TAGTGG GTTTGG GAG TT-3'	5'-Biotin-TCT TCT ATACAC TCC CCC AAA TTT-3'	5-'GAG GAG TIT AT TAT AGA TT-3'
KLF4	5-GGG AGG GGG AGGGGA AG A-3'	5'-Biotin-CCCCCTAC CCC AC AAT CTT C-3'	5'-GGTAGTGAAGTT AGT TAG GTAGTT G-3'
FOS	5-AGTTITGGG GGG AGT TAT T-3'	5'-Biotin-CAA CA CTA CT TA TAA CAA-3'	5'-AGG AGGGGGTAG GGA-3'
FOSB	5'-GGT TTAGAGGGT TAT GTAAGT GAT TAGAT-3'	5-Biotin-ACAAAC C CCAACC TAT ATTAT ATA CCC-3'	5-'AGATITTTTGTTGGATAGT G-3'
ZFP36	5-GGG GAT TA T AGT AGATGGTAG TTAGA-3'	5'-Biotin-CCA ATC CAAAAC CAACCAAAC TAC-3'	5'-GAG AGT AGGTTATTT ATAGGAAAT T-3'
DUSP1	5'-GGGGTG T GTT TGA ATG GTGATT A-3'	5-Biotin-TCCTCC TC CCC CTA ACCTA ARA C-3'	5'-ATTAGTTTAGGAGTTGGG T-3'
SOCS3	5'-GGT AGG TTTTTT TGT AAT GTT TAG TTAT-3'	5'-Biotin-CTC TACCAAAAATCAACC T T CTTAAAA-3'	5'-AGG GTG AGG GAG GGG-3'

Supplementary Results

Table S2. *Transcriptomic analysis results: list of differentially expressed genes (DEGs) obtained comparing young HUVECs (yHUVECs) and senescent HUVECs (sHUVECs). Genes were identified as DEGs when the following criteria were met: FDR ≤ 0.05 and FC ≥ 2 or ≤ -2.*

GeneName	FC	FC (2)	logFC	logCPM	LR	PValue	FDR	Tras_ID
MYZAP	134.834988	134.834988	7.07505109	2.23914502	33.4881839	7.1698E-09	2.618E-08	ENSG00000263155.11
TGFB2	113.333693	113.333693	6.82443301	4.9806797	1681.87137	0	0	ENSG00000092969.7
CCND2	86.2898006	86.2898006	6.43111814	4.66078649	1523.33406	0	0	ENSG00000118971.3
DIO2	74.8677025	74.8677025	6.22627158	0.71357553	106.945835	4.575E-25	4.3134E-24	ENSG00000211448.7
CD69	69.1351673	69.1351673	6.11134786	0.61276094	99.9735712	1.5444E-23	1.3615E-22	ENSG00000110848.4
TGFA	58.6439857	58.6439857	5.87391125	0.40494222	86.648603	1.2962E-20	9.9763E-20	ENSG00000163235.11
TTC29	54.4483886	54.4483886	5.76681745	0.31616476	79.9812611	3.7798E-19	2.7119E-18	ENSG00000137473.13
TMEM200A	40.7496278	40.7496278	5.34871498	4.54636659	1172.95518	4.602E-257	2.221E-254	ENSG00000164484.7
GPC5	37.5415483	37.5415483	5.23041624	2.04684397	214.757622	1.2588E-48	2.3885E-47	ENSG00000179399.9
SELP	33.6184917	33.6184917	5.0711831	2.49456619	251.110101	1.4874E-56	3.4787E-55	ENSG00000174175.12
SELE	31.9036761	31.9036761	4.99565076	3.77692921	530.961392	1.745E-117	1.385E-115	ENSG00000007908.11
RELN	27.5260314	27.5260314	4.78272472	3.30412825	463.797687	7.169E-103	4.483E-101	ENSG00000189056.9
SYT14	25.6130211	25.6130211	4.67880552	1.33755944	132.298937	1.287E-30	1.4806E-29	ENSG00000143469.12
RP11-11N9.4	25.1405906	25.1405906	4.65194664	0.48825316	81.5829866	1.6805E-19	1.2262E-18	ENSG00000247134.2
SCUBE1	23.4610213	23.4610213	4.55219391	0.40466266	74.5421917	5.9356E-18	4.0242E-17	ENSG00000159307.14
CCNA1	22.4805119	22.4805119	4.49060298	5.17180347	1473.74768	0	0	ENSG00000133101.5
PCDHB14	20.5623802	20.5623802	4.36193537	1.42508179	134.342556	4.5977E-31	5.3765E-30	ENSG00000120327.4
KCNMA1	18.9271945	18.9271945	4.24238867	3.40616284	444.652869	1.0515E-98	5.768E-97	ENSG00000156113.16
TNFSF15	18.635445	18.635445	4.21997736	5.32171128	1367.2725	2.718E-299	2.05E-296	ENSG00000181634.7
PCDHB15	17.4892334	17.4892334	4.12839514	0.85897828	91.8179221	9.503E-22	7.7331E-21	ENSG00000113248.3
ICAM1	17.1513947	17.1513947	4.10025399	6.42553584	2257.92777	0	0	ENSG00000090339.4
WNK4	16.9927455	16.9927455	4.08684706	2.91677881	316.353208	9.0212E-71	2.8351E-69	ENSG00000126562.12
TAGLN	16.9148278	16.9148278	4.08021659	3.94090469	557.702607	2.657E-123	2.411E-121	ENSG00000149591.12
DIRAS3	16.6937031	16.6937031	4.06123211	4.12603235	689.431741	5.941E-152	8.638E-150	ENSG00000162595.4
NOG	15.2686201	15.2686201	3.93249778	3.07636228	354.547127	4.3347E-79	1.6554E-77	ENSG00000183691.4
ARHGDIG	15.1702848	15.1702848	3.92317627	1.45013093	134.184995	4.9775E-31	5.8149E-30	ENSG00000242173.4

DUSP8	14.1281574	14.1281574	3.82050141	2.40889097	209.131022	2.1255E-47	3.8982E-46	ENSG00000184545.6
GS1-600G8.5	13.5116086	13.5116086	3.75612754	1.52382459	122.666176	1.65E-28	1.7668E-27	ENSG00000235385.1
NTRK2	13.4839383	13.4839383	3.75317002	0.89600591	85.0339127	2.9329E-20	2.2191E-19	ENSG00000148053.11
ADRA1D	13.3825828	13.3825828	3.74228467	2.69177623	240.359099	3.284E-54	7.2719E-53	ENSG00000171873.6
CYTL1	13.2370561	13.2370561	3.7265104	6.95572263	3028.73433	0	0	ENSG00000170891.6
SLC7A14	12.9779028	12.9779028	3.69798536	0.50410231	63.5521863	1.5617E-15	9.2889E-15	ENSG00000013293.5
PCDHGA4	12.5054028	12.5054028	3.64447962	3.62433127	325.919256	7.4404E-73	2.4668E-71	ENSG00000262576.1
SLC44A5	11.9841455	11.9841455	3.58305514	1.94809345	115.809629	5.2318E-27	5.2968E-26	ENSG00000137968.12
FAM21D	11.8191982	11.8191982	3.56306026	0.3521667	14.8790964	0.00011463	0.00027317	ENSG00000174196.5
ANGPTL4	11.711692	11.711692	3.54987762	3.30455989	382.535655	3.4907E-85	1.5319E-83	ENSG00000167772.7
AC011306.2	11.5438137	11.5438137	3.52904802	3.11632597	329.604837	1.1718E-73	3.9723E-72	ENSG00000226702.1
FOXP2	11.1531527	11.1531527	3.47937968	1.18420502	98.5619401	3.1502E-23	2.7409E-22	ENSG00000128573.18
SEMA3G	10.7821048	10.7821048	3.43056693	3.19432593	293.352892	9.2471E-66	2.6633E-64	ENSG00000010319.2
TRAF1	10.4569511	10.4569511	3.38639037	3.50546863	337.73218	1.9896E-75	7.0412E-74	ENSG00000056558.6
TMEM217	10.4428446	10.4428446	3.38444285	3.04491016	292.627901	1.3304E-65	3.8045E-64	ENSG00000172738.7
RP11-356J5.12	10.4420364	10.4420364	3.38433118	1.56226198	112.752802	2.4443E-26	2.4021E-25	ENSG00000250303.2
BDNF	10.3522178	10.3522178	3.37186797	2.64779035	225.457465	5.8349E-51	1.1855E-49	ENSG00000176697.14
CCL2	10.2140145	10.2140145	3.3524781	6.29958417	1489.06511	0	0	ENSG00000108691.5
AC004837.3	10.1966933	10.1966933	3.35002946	0.40424873	51.1929503	8.3719E-13	4.2097E-12	ENSG00000106540.4
COL12A1	9.67498243	9.67498243	3.27425904	5.72397207	1295.21218	1.241E-283	7.487E-281	ENSG00000111799.16
MN1	9.5627941	9.5627941	3.25743223	2.90987438	207.544763	4.7157E-47	8.5449E-46	ENSG00000169184.5
VLDLR	9.4226651	9.4226651	3.23613462	3.65175622	391.094314	4.7824E-87	2.1297E-85	ENSG00000147852.11
CREB3L1	9.3159775	9.3159775	3.21970716	0.85858134	73.2302941	1.1537E-17	7.7093E-17	ENSG00000157613.6
CLDN1	9.1454991	9.1454991	3.19306077	2.41245186	152.185926	5.7702E-35	7.5772E-34	ENSG00000163347.5
RP11-277P12.20	8.9782881	8.9782881	3.1664404	1.7169017	96.0547737	1.1175E-22	9.4704E-22	ENSG00000245648.1
PCDHGA3	8.9365748	8.9365748	3.159722	2.57253247	147.517803	6.047E-34	7.7222E-33	ENSG00000254245.1
ELFN2	8.630962	8.630962	3.10952137	2.98666687	273.824523	1.6649E-61	4.3869E-60	ENSG00000166897.10
NFE4	8.3480292	8.3480292	3.06143565	3.19579381	284.529256	7.7379E-64	2.1566E-62	ENSG00000230257.1
SYTL2	8.2899817	8.2899817	3.05136892	0.83301632	64.8041345	8.2725E-16	4.9892E-15	ENSG00000137501.12
SNTB1	8.216913	8.216913	3.03859649	1.67388631	117.085806	2.7491E-27	2.8116E-26	ENSG00000172164.9
LZTS3	8.1377197	8.1377197	3.02462462	2.72881548	231.561286	2.7218E-52	5.7829E-51	ENSG00000088899.10
CXCL6	8.0458747	8.0458747	3.00824929	1.16398643	61.1793902	5.2104E-15	3.0028E-14	ENSG00000124875.5
CXCL2	8.0426807	8.0426807	3.00767646	3.03812914	210.401377	1.1228E-47	2.0687E-46	ENSG00000081041.8
FANK1	7.9165089	7.9165089	2.98486437	0.78085479	62.4791033	2.6929E-15	1.5764E-14	ENSG00000203780.6

FSTL5	7.89771294	7.89771294	2.98143493	0.7809985	60.6244399	6.9071E-15	3.9505E-14	ENSG00000168843.9
IL32	7.85260121	7.85260121	2.97317063	6.82495185	1743.35128	0	0	ENSG00000008517.12
RSPO3	7.84372507	7.84372507	2.97153897	1.29037787	85.1875128	2.7137E-20	2.0584E-19	ENSG00000146374.9
ABCA4	7.78844987	7.78844987	2.96133622	2.88404261	240.118324	3.706E-54	8.1912E-53	ENSG00000198691.7
LOXL4	7.73084113	7.73084113	2.95062539	2.51974219	167.629233	2.4377E-38	3.4897E-37	ENSG00000138131.3
EPHB1	7.67632213	7.67632213	2.94041525	1.99463657	121.886077	2.4448E-28	2.5972E-27	ENSG00000154928.12
OLFML3	7.61247686	7.61247686	2.92836594	2.97196454	194.889423	2.7236E-44	4.6359E-43	ENSG00000116774.7
MMP10	7.53139918	7.53139918	2.91291791	5.69991014	1139.43922	8.854E-250	3.957E-247	ENSG00000166670.5
TSSC2	7.43124385	7.43124385	2.89360371	1.76415693	90.0328786	2.3423E-21	1.8733E-20	ENSG00000223756.2
IFIT1	7.39819197	7.39819197	2.88717274	0.8958608	41.1787384	1.3893E-10	5.9054E-10	ENSG00000185745.8
GAS6	7.34568424	7.34568424	2.87689688	6.28795645	1640.81395	0	0	ENSG00000183087.10
MGAT5B	7.23654924	7.23654924	2.85530191	3.16010599	225.250348	6.4745E-51	1.3132E-49	ENSG00000167889.8
TNFRSF19	6.95570258	6.95570258	2.79819625	1.35402737	84.6165781	3.6222E-20	2.7201E-19	ENSG00000127863.11
CLDN14	6.95432357	6.95432357	2.79791019	2.29443957	153.515143	2.9559E-35	3.946E-34	ENSG00000159261.6
CACNA2D4	6.91284843	6.91284843	2.78928029	0.9901247	58.3822323	2.1583E-14	1.197E-13	ENSG00000151062.10
ATF3	6.80787838	6.80787838	2.76720526	4.51920273	446.678829	3.81E-99	2.1187E-97	ENSG00000162772.12
ZNF610	6.77413123	6.77413123	2.76003593	1.12230218	64.6585666	8.9068E-16	5.369E-15	ENSG00000167554.10
GLIS3	6.77099671	6.77099671	2.75936822	1.65901106	98.3548595	3.4974E-23	3.0321E-22	ENSG00000107249.17
CPNE7	6.76598581	6.76598581	2.75830015	2.41527287	142.354663	8.1345E-33	1.011E-31	ENSG00000178773.10
ITGA11	6.73705662	6.73705662	2.75211842	2.00568465	125.786257	3.4245E-29	3.7604E-28	ENSG00000137809.12
ERV3-1	6.71839454	6.71839454	2.74811652	5.34454225	422.455332	7.1288E-94	3.5258E-92	ENSG00000213462.4
CTD-3018O17.3	6.66879926	6.66879926	2.73742702	0.36919857	40.9357332	1.5732E-10	6.6451E-10	ENSG00000269834.1
CEACAM1	6.54825928	6.54825928	2.71111145	3.55384359	269.510661	1.4506E-60	3.7327E-59	ENSG00000079385.17
SUSD5	6.53306032	6.53306032	2.70775896	6.50889429	1594.3775	0	0	ENSG00000173705.4
MAMDC2	6.48825179	6.48825179	2.69782981	2.17671552	115.613966	5.7743E-27	5.8314E-26	ENSG00000165072.9
MOBP	6.47408566	6.47408566	2.69467645	0.65578462	48.7913131	2.847E-12	1.3854E-11	ENSG00000168314.13
PCDHGA2	6.43967974	6.43967974	2.68698894	2.23792039	97.0581319	6.7321E-23	5.766E-22	ENSG00000081853.13
LTB	6.43511996	6.43511996	2.68596704	0.9903497	61.9327547	3.5539E-15	2.0639E-14	ENSG00000227507.2
ZNF117	6.34406038	6.34406038	2.6654065	5.91586673	214.415992	1.4944E-48	2.8267E-47	ENSG00000152926.10
LYPD1	6.29131195	6.29131195	2.6533609	6.08316725	689.286544	6.389E-152	9.179E-150	ENSG00000150551.10
DACT3	6.25729467	6.25729467	2.64553904	0.71274794	48.6587041	3.0461E-12	1.4793E-11	ENSG00000197380.6
HTR1D	6.25428805	6.25428805	2.64484567	2.75579491	173.404602	1.3354E-39	1.9896E-38	ENSG00000179546.3
SEMA3D	6.23382164	6.23382164	2.64011688	4.83427304	497.353588	3.579E-110	2.497E-108	ENSG00000153993.9
COL4A1	6.22267472	6.22267472	2.63753483	10.9178875	1451.31317	0	0	ENSG00000187498.10

TRPV2	6.21560208	6.21560208	2.63589415	5.3589748	937.943873	5.539E-206	1.592E-203	ENSG00000187688.10
A2M	6.17795091	6.17795091	2.62712841	4.87593061	496.713663	4.932E-110	3.401E-108	ENSG00000175899.10
AFF3	6.1601764	6.1601764	2.62297166	0.50331498	35.3956877	2.6908E-09	1.0241E-08	ENSG00000144218.14
GPNMB	6.10890776	6.10890776	2.61091446	1.20361034	57.403415	3.5499E-14	1.9402E-13	ENSG00000136235.11
SERPINE2	6.1037422	6.1037422	2.60969403	5.51081788	883.890768	3.118E-194	8.005E-192	ENSG00000135919.8
ADAM12	5.97715685	5.97715685	2.5794594	0.47114136	39.5506354	3.1966E-10	1.3135E-09	ENSG00000148848.10
SHC2	5.9542481	5.9542481	2.57391934	2.46178114	138.210956	6.5532E-32	7.9243E-31	ENSG00000129946.6
KIT	5.94168113	5.94168113	2.57087118	4.41703046	521.098306	2.441E-115	1.888E-113	ENSG00000157404.11
KCNMB4	5.92845757	5.92845757	2.5676568	1.17312725	59.0213512	1.5597E-14	8.7303E-14	ENSG00000135643.4
CDKN2B	5.92580314	5.92580314	2.5670107	3.84264862	340.345699	5.3652E-76	1.9043E-74	ENSG00000147883.9
HIST1H2AC	5.91189471	5.91189471	2.56362057	1.77758986	80.4950441	2.9143E-19	2.1035E-18	ENSG00000180573.8
GRIK4	5.87313574	5.87313574	2.55413098	0.55111454	42.2134776	8.1834E-11	3.541E-10	ENSG00000149403.7
RP1-140K8.5	5.85338734	5.85338734	2.54927175	5.2158617	684.364388	7.513E-151	1.067E-148	ENSG00000260604.1
RNF182	5.79238486	5.79238486	2.53415746	3.36561777	201.654993	9.0925E-46	1.5903E-44	ENSG00000180537.8
BIRC3	5.77458335	5.77458335	2.52971686	1.86080323	93.8793027	3.3536E-22	2.7835E-21	ENSG00000023445.9
PLA2G4C	5.74299404	5.74299404	2.52180307	4.69002738	608.328052	2.585E-134	2.862E-132	ENSG00000105499.9
CDKN2A	5.70046769	5.70046769	2.51108029	4.57450864	495.594796	8.639E-110	5.924E-108	ENSG00000147889.12
SULF2	5.68999527	5.68999527	2.50842745	8.91736371	1137.96525	1.851E-249	7.979E-247	ENSG00000196562.10
PCDHB13	5.66256517	5.66256517	2.50145575	1.12169423	62.5230942	2.6334E-15	1.5435E-14	ENSG00000187372.9
MMP24	5.60985905	5.60985905	2.48796452	1.78982058	92.4777481	6.8086E-22	5.5782E-21	ENSG00000125966.8
CHRNA1	5.59137205	5.59137205	2.48320235	3.16597199	200.401959	1.7065E-45	2.9718E-44	ENSG00000138435.10
COL5A1	5.52664925	5.52664925	2.46640505	9.05867705	1416.40886	0	4.923E-307	ENSG00000130635.11
GFPT2	5.52212063	5.52212063	2.4652224	4.47565419	488.658285	2.791E-108	1.871E-106	ENSG00000131459.8
RP11-482H16.1	5.51561349	5.51561349	2.46352136	1.08982141	40.8107123	1.6771E-10	7.0594E-10	ENSG00000271894.1
PTPRS	5.44173732	5.44173732	2.44406732	4.64012951	534.197647	3.449E-118	2.813E-116	ENSG00000105426.10
PLAU	5.38857965	5.38857965	2.42990505	7.59310652	1668.92834	0	0	ENSG00000122861.11
FOSB	5.34131769	5.34131769	2.41719569	3.86487955	116.399748	3.8853E-27	3.9535E-26	ENSG00000125740.9
PCDHB10	5.30362666	5.30362666	2.40697922	0.91941197	50.4006972	1.2535E-12	6.2483E-12	ENSG00000120324.4
RP11-524D16__A.3	5.2847578	5.2847578	2.40183735	0.69857051	43.401301	4.4589E-11	1.9639E-10	ENSG00000261295.1
ITGA4	5.25819046	5.25819046	2.3945664	3.47309158	210.427328	1.1082E-47	2.045E-46	ENSG00000115232.9
TAF7L	5.25490304	5.25490304	2.39366414	2.28955535	114.237651	1.1559E-26	1.1519E-25	ENSG00000102387.11
NR4A2	5.22991116	5.22991116	2.38678644	0.6118862	35.9911554	1.9822E-09	7.6412E-09	ENSG00000153234.9
PSTPIP2	5.22200995	5.22200995	2.38460521	4.18954016	371.305105	9.7282E-83	4.0623E-81	ENSG00000152229.14
PAPLN	5.15033125	5.15033125	2.36466522	2.03917176	82.5178553	1.0472E-19	7.7059E-19	ENSG00000100767.11

KIAA1217	5.13263837	5.13263837	2.35970062	3.85754017	311.440614	1.0602E-69	3.2892E-68	ENSG00000120549.11
SPINK5	5.1207895	5.1207895	2.35636626	0.88275109	44.4377087	2.6258E-11	1.1758E-10	ENSG00000133710.11
RGS11	5.07851078	5.07851078	2.3444055	2.51032368	122.088694	2.2075E-28	2.3512E-27	ENSG00000076344.11
C8orf4	5.00428456	5.00428456	2.32316383	3.46810121	161.631197	4.9804E-37	6.9243E-36	ENSG00000176907.3
FGF5	4.9846525	4.9846525	2.31749293	2.14659092	77.9416413	1.0613E-18	7.4638E-18	ENSG00000138675.12
PCDHGA7	4.96730063	4.96730063	2.31246206	1.44860301	69.2330549	8.7489E-17	5.5746E-16	ENSG00000253537.1
IL8	4.95209332	4.95209332	2.3080385	4.6105863	267.502309	3.9745E-60	1.0055E-58	ENSG00000169429.6
FAM189A2	4.90077482	4.90077482	2.29300986	2.46902197	124.862753	5.4539E-29	5.9403E-28	ENSG00000135063.13
ROR1	4.85061797	4.85061797	2.27816856	3.92264254	277.2083	3.0477E-62	8.137E-61	ENSG00000185483.7
ABI3BP	4.80851485	4.80851485	2.26559137	4.77111429	421.614185	1.0867E-93	5.3093E-92	ENSG00000154175.12
COL4A2	4.80407586	4.80407586	2.26425893	10.7771715	1323.23459	1.009E-289	7.033E-287	ENSG00000134871.13
RP11-161I2.1	4.72349074	4.72349074	2.23985343	1.15282753	45.1687891	1.8076E-11	8.2102E-11	ENSG00000187229.3
IL6	4.67388328	4.67388328	2.22462171	3.78226101	282.31226	2.3535E-63	6.4698E-62	ENSG00000136244.7
NTN4	4.67182242	4.67182242	2.22398544	7.8462529	1323.15773	1.049E-289	7.033E-287	ENSG00000074527.7
CBLN3	4.65363683	4.65363683	2.21835863	1.19336525	45.8254206	1.2928E-11	5.9682E-11	ENSG00000139899.6
BGN	4.64202623	4.64202623	2.21475468	8.14109871	1419.19566	0	1.315E-307	ENSG00000182492.11
BTBD11	4.64048845	4.64048845	2.21427667	1.92246234	84.3477014	4.1498E-20	3.1067E-19	ENSG00000151136.10
TNFRSF21	4.63568491	4.63568491	2.21278251	7.41985811	1398.13109	5.352E-306	4.306E-303	ENSG00000146072.6
SELM	4.62865424	4.62865424	2.2105928	4.411505	435.511202	1.0266E-96	5.3631E-95	ENSG00000198832.6
WNT9A	4.6098968	4.6098968	2.20473445	2.9698124	152.564235	4.7699E-35	6.2979E-34	ENSG00000143816.7
DENND6B	4.5883734	4.5883734	2.1979828	1.81627501	76.1804753	2.5889E-18	1.7945E-17	ENSG00000205593.7
ABCA6	4.58475965	4.58475965	2.19684611	2.26071909	70.9519754	3.6603E-17	2.3851E-16	ENSG00000154262.8
DSEL	4.56890944	4.56890944	2.19184985	4.5082867	403.487753	9.5874E-90	4.3993E-88	ENSG00000171451.13
TACSTD2	4.49853656	4.49853656	2.16945575	6.30336058	859.439688	6.447E-189	1.526E-186	ENSG00000184292.5
CXCL11	4.43218748	4.43218748	2.14801891	1.48984767	52.3207236	4.7137E-13	2.4165E-12	ENSG00000169248.8
PIK3IP1	4.42809937	4.42809937	2.1466876	3.66911077	196.572517	1.169E-44	2.0039E-43	ENSG00000100100.8
ADAM19	4.37476514	4.37476514	2.12920557	5.91120274	649.643183	2.671E-143	3.504E-141	ENSG00000135074.11
SLC26A4	4.33661557	4.33661557	2.11656956	1.50596395	55.6724575	8.5609E-14	4.5694E-13	ENSG00000091137.7
SLC2A12	4.31856003	4.31856003	2.11055034	1.87352034	67.8215328	1.7898E-16	1.1227E-15	ENSG00000146411.5
FILIP1L	4.29981012	4.29981012	2.10427295	5.40850813	455.436207	4.732E-101	2.799E-99	ENSG00000168386.14
CXCL1	4.29949637	4.29949637	2.10416768	4.79714222	484.196084	2.61E-107	1.694E-105	ENSG00000163739.4
FSTL3	4.2741795	4.2741795	2.0956475	4.50615696	275.222805	8.2539E-62	2.1844E-60	ENSG00000070404.5
FAM89A	4.27408993	4.27408993	2.09561726	4.25682947	323.844804	2.1059E-72	6.8872E-71	ENSG00000182118.5
GDF6	4.26212546	4.26212546	2.09157306	4.15787548	331.852893	3.7951E-74	1.3011E-72	ENSG00000156466.8

MMP11	4.25630723	4.25630723	2.08960229	4.71641941	394.679694	7.9272E-88	3.5563E-86	ENSG00000099953.5
DKK3	4.23999426	4.23999426	2.08406231	8.22638962	1088.73374	9.28E-239	3.613E-236	ENSG00000050165.13
FLRT2	4.21452922	4.21452922	2.07537149	7.63913882	811.503205	1.702E-178	3.314E-176	ENSG00000185070.6
LINC00520	4.20650035	4.20650035	2.07262047	0.80676608	35.93235	2.0429E-09	7.8589E-09	ENSG00000258791.3
TGFBI	4.19189482	4.19189482	2.06760252	4.96017656	562.753696	2.116E-124	1.98E-122	ENSG00000120708.12
ITGB8	4.18787589	4.18787589	2.06621869	3.54011528	209.023572	2.2434E-47	4.0957E-46	ENSG00000105855.5
FILIP1	4.14425941	4.14425941	2.05111431	2.86613283	111.629317	4.3077E-26	4.1924E-25	ENSG00000118407.10
IGFBP7	4.12559494	4.12559494	2.04460218	8.56124711	1316.81098	2.512E-288	1.595E-285	ENSG00000163453.7
IL17D	4.0949447	4.0949447	2.03384397	2.79061968	130.227495	3.654E-30	4.1367E-29	ENSG00000172458.4
SEMA7A	4.09246044	4.09246044	2.03296847	1.24143128	39.0953288	4.0361E-10	1.6427E-09	ENSG00000138623.5
RASA4B	4.07339432	4.07339432	2.02623148	2.29656793	66.9577375	2.7739E-16	1.7193E-15	ENSG00000170667.10
SLC29A4	4.05800676	4.05800676	2.02077127	2.64083019	112.854722	2.3218E-26	2.2854E-25	ENSG00000164638.6
FBXL13	4.04314988	4.04314988	2.01547968	3.15888526	123.266418	1.2193E-28	1.3161E-27	ENSG00000161040.12
CD44	4.0403183	4.0403183	2.01446896	7.9346991	1199.55019	7.639E-263	3.841E-260	ENSG00000026508.12
MFAP2	4.02524994	4.02524994	2.00907837	6.71811961	959.980559	8.979E-211	2.709E-208	ENSG00000117122.9
GALNT15	4.02413837	4.02413837	2.00867991	1.53745304	54.1346106	1.8721E-13	9.8145E-13	ENSG00000131386.13
AGRN	3.99712538	3.99712538	1.99896283	8.28782307	1279.24757	3.656E-280	2.101E-277	ENSG00000188157.9
ARL4C	3.99453224	3.99453224	1.99802657	6.17150006	897.984592	2.691E-197	7.381E-195	ENSG00000188042.5
FAT1	3.99395552	3.99395552	1.99781827	2.67366783	77.5689372	1.2817E-18	8.9823E-18	ENSG00000083857.9
ID2	3.98549824	3.98549824	1.99476009	2.01012238	60.5742563	7.0855E-15	4.0486E-14	ENSG00000115738.5
UNC5C	3.98354628	3.98354628	1.99405334	0.55073188	23.5461814	1.2195E-06	3.6655E-06	ENSG00000182168.10
GLIPR2	3.9517099	3.9517099	1.98247704	5.26235027	562.799742	2.068E-124	1.95E-122	ENSG00000122694.11
FAXC	3.95155702	3.95155702	1.98242123	2.04367671	62.2701874	2.9942E-15	1.749E-14	ENSG00000146267.11
LIMS3L	3.90097975	3.90097975	1.96383651	3.14535444	142.255057	8.5529E-33	1.0619E-31	ENSG00000256671.5
LIMS3L	3.90097975	3.90097975	1.96383651	3.14535444	142.255057	8.5529E-33	1.0619E-31	ENSG00000257207.4
ANTXR1	3.89601906	3.89601906	1.96200073	5.38717242	518.685446	8.176E-115	6.245E-113	ENSG00000169604.15
NRXN3	3.87557641	3.87557641	1.9544109	1.99752094	67.2315915	2.4141E-16	1.5017E-15	ENSG00000021645.13
THSD4	3.87485246	3.87485246	1.95414138	6.94473648	603.031866	3.667E-133	3.987E-131	ENSG00000187720.10
CD200	3.85889259	3.85889259	1.94818689	3.24364888	162.915316	2.6105E-37	3.6547E-36	ENSG00000091972.14
HTRA1	3.82227853	3.82227853	1.93443291	7.32851938	1152.2028	1.49E-252	6.915E-250	ENSG00000166033.7
CD34	3.81391165	3.81391165	1.93127142	7.10201113	378.806038	2.2642E-84	9.7238E-83	ENSG00000174059.12
TM6SF1	3.80632411	3.80632411	1.92839841	4.67182154	419.399877	3.2966E-93	1.5977E-91	ENSG00000136404.11
LOXL1	3.78475219	3.78475219	1.92019884	3.5692369	170.170093	6.7923E-39	9.9477E-38	ENSG00000129038.11
TMEM132A	3.78427649	3.78427649	1.9200175	6.99447269	953.229722	2.634E-209	7.754E-207	ENSG00000006118.10

KIFC2	3.779606 53	3.779606 53	1.918236 05	2.878127 96	88.95444 09	4.0401E- 21	3.1825E- 20	ENSG0000016770 2.7
MOK	3.769558 11	3.769558 11	1.914395 41	2.541095 65	100.1127 48	1.4396E- 23	1.2719E- 22	ENSG0000008082 3.17
CORO2B	3.731059 99	3.731059 99	1.899585 56	2.935183 44	111.0289 63	5.8313E- 26	5.6297E- 25	ENSG0000010364 7.8
IDUA	3.726995 21	3.726995 21	1.898012 97	3.085305 66	73.36490 55	1.0777E- 17	7.213E- 17	ENSG0000012741 5.8
TTC3P1	3.701702 43	3.701702 43	1.888188 93	1.089246 15	26.88832 49	2.1556E- 07	6.9722E- 07	ENSG0000021510 5.3
KLF4	3.700294 62	3.700294 62	1.887640 14	2.617090 56	95.92887 13	1.1909E- 22	1.0057E- 21	ENSG0000013682 6.10
RND1	3.696085 38	3.696085 38	1.885998 08	1.735148 38	57.09348 55	4.1558E- 14	2.2611E- 13	ENSG0000017260 2.5
MIR503HG	3.694859	3.694859	1.885519 31	1.583675 54	51.74819 34	6.3095E- 13	3.1993E- 12	ENSG0000022374 9.3
IFI6	3.692369 74	3.692369 74	1.884547 03	4.276766 45	250.9376 55	1.6219E- 56	3.7859E- 55	ENSG0000012670 9.10
RP5-1070A16.1	3.689001 47	3.689001 47	1.883230 36	0.725876 05	21.75680 83	3.0949E- 06	8.8758E- 06	ENSG0000022605 3.1
TPM1	3.687599 36	3.687599 36	1.882681 92	8.472477 04	1272.562 59	1.037E- 278	5.689E- 276	ENSG0000014041 6.15
CEACAM21	3.684138 02	3.684138 02	1.881327 11	0.740031 83	24.49943 43	7.4332E- 07	2.2796E- 06	ENSG0000000712 9.13
HSD17B2	3.684075 16	3.684075 16	1.881302 49	2.426614 96	66.29925 91	3.874E- 16	2.3841E- 15	ENSG0000008669 6.6
CNIH3	3.662969 91	3.662969 91	1.873013 85	1.575689 68	43.08565 4	5.2395E- 11	2.2959E- 10	ENSG0000014378 6.3
GNA14	3.653995 73	3.653995 73	1.869474 95	1.288752 52	41.14408 84	1.4141E- 10	5.9984E- 10	ENSG0000015604 9.6
LCP1	3.652489 19	3.652489 19	1.86888	2.164741 93	69.22186 07	8.7987E- 17	5.6033E- 16	ENSG0000013616 7.9
GNG2	3.649789 97	3.649789 97	1.867813 45	1.755235 06	38.22250 36	6.312E- 10	2.5349E- 09	ENSG0000018646 9.4
CTSF	3.639964 64	3.639964 64	1.863924 43	4.769995 97	362.8865 59	6.6229E- 81	2.6821E- 79	ENSG0000017408 0.6
MX1	3.613112 32	3.613112 32	1.853242 1	3.228410 44	101.6725 43	6.5502E- 24	5.8772E- 23	ENSG0000015760 1.9
SIRPB1	3.609665 74	3.609665 74	1.851865 25	1.488678 69	42.98018 27	5.5297E- 11	2.4187E- 10	ENSG0000010130 7.11
HAS3	3.609561 27	3.609561 27	1.851823 49	1.621543 34	41.07087 24	1.4681E- 10	6.2164E- 10	ENSG0000010304 4.6
CARD16	3.605019 26	3.605019 26	1.850006 97	5.479955 05	501.5082 38	4.465E- 111	3.188E- 109	ENSG0000020439 7.3
PTGS2	3.587810 93	3.587810 93	1.843103 87	6.205949 1	752.4333 09	1.187E- 165	2.046E- 163	ENSG0000007375 6.7
MMP2	3.583616	3.583616	1.841416 06	9.531694	1016.216 85	5.362E- 223	1.849E- 220	ENSG0000008724 5.8
CXADR	3.546211 09	3.546211 09	1.826278 42	5.128576 55	327.1171 38	4.0803E- 73	1.3602E- 71	ENSG0000015463 9.14
CPA3	3.541757 79	3.541757 79	1.824465 56	2.617531 14	90.02997 8	2.3458E- 21	1.8748E- 20	ENSG0000016375 1.3
SLC40A1	3.520429 02	3.520429 02	1.815751 25	3.438470 78	163.7923 8	1.6793E- 37	2.3647E- 36	ENSG0000013844 9.6
ARSA	3.519157 36	3.519157 36	1.815230 02	4.642828 17	315.2959 24	1.5331E- 70	4.8056E- 69	ENSG0000010029 9.13
ZNF837	3.496433 61	3.496433 61	1.805884 11	0.739645 19	25.29490 27	4.9201E- 07	1.5335E- 06	ENSG0000015247 5.6
PCED1B	3.495632 68	3.495632 68	1.805553 6	0.989478 08	33.38858 94	7.5465E- 09	2.7497E- 08	ENSG0000017971 5.8
PRKG1	3.491490 84	3.491490 84	1.803843 19	1.279543 56	39.29464 23	3.6444E- 10	1.4883E- 09	ENSG0000018553 2.10
GYPC	3.475049 64	3.475049 64	1.797033 58	4.342182 59	289.2437 34	7.2668E- 65	2.0538E- 63	ENSG0000013673 2.10
PRRG1	3.474653 54	3.474653 54	1.796869 13	6.522967 06	864.7059 15	4.619E- 190	1.137E- 187	ENSG0000013096 2.13
SCN3B	3.457645 5	3.457645 5	1.789789 96	1.110393 29	34.31280 7	4.6928E- 09	1.741E- 08	ENSG0000016625 7.4

CYP4X1	3.43820223	3.43820223	1.78165441	1.95148133	48.7753377	2.8703E-12	1.3961E-11	ENSG00000186377.6
SCUBE3	3.42897334	3.42897334	1.77777669	1.82193824	54.1550361	1.8528E-13	9.7173E-13	ENSG00000146197.7
RP11-428J1.4	3.41469334	3.41469334	1.77175602	0.65505576	24.2503978	8.459E-07	2.5837E-06	ENSG00000271978.1
YPEL5	3.41023302	3.41023302	1.76987032	6.07030415	716.735174	6.864E-158	1.062E-155	ENSG00000119801.8
TEKT4P2	3.40472428	3.40472428	1.76753797	2.51274226	76.0190395	2.8094E-18	1.944E-17	ENSG00000188681.7
CNTNAP1	3.393355	3.393355	1.76271237	6.37088792	348.954668	7.1577E-78	2.6497E-76	ENSG00000108797.7
SERPINE1	3.38736854	3.38736854	1.76016496	12.6271239	862.605601	1.322E-189	3.19E-187	ENSG00000106366.7
RASA4	3.37436529	3.37436529	1.75461616	4.2479105	182.895263	1.1306E-41	1.7905E-40	ENSG00000105808.13
APCDD1L	3.37302066	3.37302066	1.75404116	2.90114017	94.1636393	2.9049E-22	2.4177E-21	ENSG00000198768.6
MIR29B1	3.37287481	3.37287481	1.75397877	0.95448046	29.0199565	7.1636E-08	2.4128E-07	ENSG00000226380.3
CPNE5	3.37281565	3.37281565	1.75395347	3.54302508	128.351349	9.4033E-30	1.0537E-28	ENSG00000124772.7
MAP1LC3A	3.3715577	3.3715577	1.75341529	3.53800087	157.875192	3.2954E-36	4.4988E-35	ENSG00000101460.8
FRMD6	3.37133325	3.37133325	1.75331924	7.48160689	865.522885	3.068E-190	7.714E-188	ENSG00000139926.11
IFI44L	3.36880565	3.36880565	1.7522372	1.85361795	49.2196592	2.2885E-12	1.123E-11	ENSG00000137959.11
B4GALNT4	3.36661731	3.36661731	1.75129974	2.54862113	50.0142077	1.5264E-12	7.5524E-12	ENSG00000182272.7
DDIT4L	3.35923433	3.35923433	1.74813244	3.76912831	100.57907	1.1376E-23	1.0087E-22	ENSG00000145358.2
THSD7A	3.32529685	3.32529685	1.73348313	4.08283634	222.122987	3.114E-50	6.2115E-49	ENSG00000005108.11
PDGFD	3.32279855	3.32279855	1.73239883	4.49374657	296.129299	2.2966E-66	6.7598E-65	ENSG00000170962.8
ADCY4	3.31235168	3.31235168	1.72785586	3.90971068	99.5151544	1.9467E-23	1.7048E-22	ENSG00000129467.9
IL1A	3.30780926	3.30780926	1.72587605	1.80883353	44.9317384	2.0402E-11	9.2216E-11	ENSG00000115008.5
PTPRR	3.29924074	3.29924074	1.72213405	1.33463311	34.1842407	5.0133E-09	1.8541E-08	ENSG00000153233.8
LINC00839	3.29432465	3.29432465	1.71998274	0.97752459	27.3669748	1.6828E-07	5.4872E-07	ENSG00000185904.7
NTM	3.2909186	3.2909186	1.71849034	2.2339656	62.9085772	2.1653E-15	1.2784E-14	ENSG00000182667.10
HTRA3	3.29029037	3.29029037	1.71821491	4.80153863	294.206852	6.0248E-66	1.752E-64	ENSG00000170801.5
MB21D2	3.28863534	3.28863534	1.71748904	4.09698029	136.83289	1.3117E-31	1.5689E-30	ENSG00000180611.6
SYNC	3.27360344	3.27360344	1.71087957	3.71767674	152.306824	5.4296E-35	7.1455E-34	ENSG00000162520.10
GPER1	3.26933331	3.26933331	1.70899647	1.28912304	30.0092804	4.2998E-08	1.4742E-07	ENSG00000164850.10
MOV10L1	3.2620564	3.2620564	1.70578173	2.84141561	84.8100666	3.2845E-20	2.4727E-19	ENSG00000073146.11
COL25A1	3.26042533	3.26042533	1.70506018	1.76865018	51.5960362	6.8179E-13	3.4455E-12	ENSG00000188517.10
ZNF365	3.2480533	3.2480533	1.69957531	1.35193143	27.8489112	1.3117E-07	4.3202E-07	ENSG00000138311.11
CCDC178	3.24148437	3.24148437	1.69665462	0.55021424	19.1387951	1.2155E-05	3.2402E-05	ENSG00000166960.12
AMIGO2	3.23108708	3.23108708	1.69201963	4.01970467	180.885757	3.1047E-41	4.8534E-40	ENSG00000139211.5
SIRPB2	3.22174588	3.22174588	1.6878427	2.96112657	103.579372	2.5017E-24	2.2751E-23	ENSG00000196209.8
MEGF6	3.21541386	3.21541386	1.68500444	6.15606876	607.853814	3.278E-134	3.596E-132	ENSG00000162591.11

PDGFC	3.21243343	3.21243343	1.68366656	3.0556623	109.700793	1.1396E-25	1.0923E-24	ENSG00000145431.6
LRRC6	3.21168429	3.21168429	1.68333008	1.30714563	35.642329	2.3708E-09	9.0713E-09	ENSG00000129295.4
RRAGB	3.20057488	3.20057488	1.67833106	4.11605105	181.952037	1.8165E-41	2.8692E-40	ENSG00000083750.8
ISG15	3.19974553	3.19974553	1.67795718	4.90062436	219.284359	1.2956E-49	2.5301E-48	ENSG00000187608.5
MGARP	3.19688684	3.19688684	1.67666768	4.13497475	147.25012	6.9192E-34	8.8081E-33	ENSG00000137463.4
TMEM163	3.19220705	3.19220705	1.67455423	3.29877163	105.49509	9.5133E-25	8.7975E-24	ENSG00000152128.13
PCDHGB4	3.19086339	3.19086339	1.67394684	3.52945226	93.1652917	4.8104E-22	3.9599E-21	ENSG00000253953.1
RELB	3.18855636	3.18855636	1.67290338	3.86949474	163.359098	2.0882E-37	2.9303E-36	ENSG00000104856.9
CTSB	3.18602111	3.18602111	1.67175582	10.0603873	1046.32613	1.531E-229	5.597E-227	ENSG00000164733.16
ADAMTSL1	3.17265829	3.17265829	1.66569214	6.44689374	489.649126	1.699E-108	1.145E-106	ENSG00000178031.11
ARPC4-TTLL3	3.16785941	3.16785941	1.66350831	1.87690619	13.2210093	0.00027683	0.00062189	ENSG00000250151.5
GPR37	3.14966231	3.14966231	1.65519716	3.14341583	111.357742	4.9401E-26	4.7847E-25	ENSG00000170775.2
NCKAP5	3.13871346	3.13871346	1.65017333	0.9311703	24.8251525	6.2773E-07	1.9389E-06	ENSG00000176771.11
TFPI2	3.13389481	3.13389481	1.64795676	6.75793986	835.999942	8.04E-184	1.764E-181	ENSG00000105825.7
MAN2B2	3.13102561	3.13102561	1.64663531	6.13361728	497.254898	3.761E-110	2.608E-108	ENSG00000013288.4
HSD17B14	3.12188354	3.12188354	1.64241672	4.30268528	233.867837	8.5479E-53	1.8258E-51	ENSG00000087076.4
LNX1	3.12013391	3.12013391	1.64160795	2.49991165	78.5304507	7.8775E-19	5.5594E-18	ENSG00000072201.9
CPQ	3.12008715	3.12008715	1.64158633	4.41104278	251.43917	1.2609E-56	2.9605E-55	ENSG00000104324.11
GRN	3.11513903	3.11513903	1.63929655	9.25643132	1055.51548	1.54E-231	5.808E-229	ENSG00000030582.12
RP11-572C15.6	3.10809578	3.10809578	1.63603096	1.72138509	40.9928546	1.5279E-10	6.4583E-10	ENSG00000272761.1
DCHS1	3.07360106	3.07360106	1.61992992	7.78443216	342.666293	1.6757E-76	6.0187E-75	ENSG00000166341.6
PLXNA3	3.06631593	3.06631593	1.61650635	5.46018879	354.601494	4.2181E-79	1.616E-77	ENSG00000130827.5
LINC01013	3.06543046	3.06543046	1.61608968	4.38218612	228.466324	1.2877E-51	2.6886E-50	ENSG00000228495.1
TP53TG1	3.06462797	3.06462797	1.61571195	3.35234202	115.610803	5.7836E-27	5.8358E-26	ENSG00000182165.13
TMEM133	3.05702976	3.05702976	1.6121306	0.98927602	25.2507849	5.0339E-07	1.5677E-06	ENSG00000170647.2
SNED1	3.05429942	3.05429942	1.610841	4.61665399	255.489131	1.6512E-57	3.9227E-56	ENSG00000162804.9
APOE	3.01957101	3.01957101	1.5943436	1.21242416	26.2994835	2.9237E-07	9.3218E-07	ENSG00000130203.5
RP11-14N7.2	3.01936253	3.01936253	1.59424399	3.24882584	117.653587	2.0648E-27	2.1243E-26	ENSG00000232527.3
EPSTI1	3.01825722	3.01825722	1.59371576	0.97749063	26.8027395	2.2532E-07	7.2801E-07	ENSG00000133106.10
NACAD	3.01756934	3.01756934	1.59338692	1.92710475	46.5833422	8.7803E-12	4.107E-11	ENSG00000136274.8
GPRC5B	3.0068526	3.0068526	1.58825414	5.50661348	361.025562	1.6837E-80	6.706E-79	ENSG00000167191.7
PDCD1LG2	3.0047948	3.0047948	1.58726647	4.17731223	175.401255	4.8931E-40	7.409E-39	ENSG00000197646.6
GPR143	3.00272004	3.00272004	1.58626997	4.98568341	350.777653	2.8694E-78	1.0788E-76	ENSG00000101850.8
PLXNB3	3.00129474	3.00129474	1.58558501	4.74575899	250.432154	2.0904E-56	4.8607E-55	ENSG00000198753.7

IL4I1	2.981588 33	2.981588 33	1.576081 08	3.922440 5	181.0174 98	2.9058E- 41	4.5482E- 40	ENSG0000010495 1.11
MMP17	2.978301 83	2.978301 83	1.574489 97	2.689048 3	66.14320 4	4.1932E- 16	2.57E-15	ENSG0000019859 8.2
MXD4	2.974838 22	2.974838 22	1.572811 21	6.858465 67	645.9675 6	1.683E- 142	2.138E- 140	ENSG0000012393 3.10
TMEM140	2.961392 5	2.961392 5	1.566275 72	4.535712 97	242.2573 95	1.2662E- 54	2.8245E- 53	ENSG0000014685 9.6
TGFB3	2.956522 9	2.956522 9	1.563901 45	1.589954 07	36.01517 55	1.9579E- 09	7.5511E- 09	ENSG0000011969 9.3
MEG3	2.953880 18	2.953880 18	1.562611 31	5.464654 31	89.39309 35	3.2366E- 21	2.563E- 20	ENSG0000021454 8.10
HERC2P2	2.934885 56	2.934885 56	1.553304 25	6.368839 35	233.9804 88	8.0779E- 53	1.7315E- 51	ENSG0000014018 1.10
PTGIS	2.932480 04	2.932480 04	1.552121 29	1.613273 81	37.18178 21	1.0761E- 09	4.2524E- 09	ENSG0000012421 2.5
ACCS	2.928227 78	2.928227 78	1.550027 78	1.938655 12	47.97893 91	4.3082E- 12	2.073E- 11	ENSG0000011045 5.9
TMEM86A	2.917838 17	2.917838 17	1.544899 87	1.496689 19	34.53754 59	4.1811E- 09	1.5597E- 08	ENSG0000015111 7.4
NDRG4	2.917806 88	2.917806 88	1.544884 4	5.809584 85	358.1591 48	7.0864E- 80	2.7676E- 78	ENSG0000010303 4.10
PYROXD2	2.908649 03	2.908649 03	1.540349 23	1.575158 12	37.10400 39	1.1199E- 09	4.4197E- 09	ENSG0000011994 3.6
CADM4	2.905656 15	2.905656 15	1.538863 99	2.831613 91	75.12448 01	4.4195E- 18	3.0218E- 17	ENSG0000010576 7.2
SDC4	2.899712 52	2.899712 52	1.535909 88	6.215676 85	552.8670 4	2.994E- 122	2.638E- 120	ENSG0000012414 5.5
DUSP1	2.899309 59	2.899309 59	1.535709 39	6.357513 58	431.0790 71	9.463E- 96	4.7983E- 94	ENSG0000012012 9.5
PNPLA7	2.898944 8	2.898944 8	1.535527 86	1.067538 58	19.36029 72	1.0823E- 05	2.9007E- 05	ENSG0000013065 3.11
PLK2	2.896748	2.896748	1.534434 18	8.180767 04	750.5102 13	3.108E- 165	5.209E- 163	ENSG0000014563 2.10
ARSD	2.893541 75	2.893541 75	1.532836 46	5.578132 99	451.1205 71	4.114E- 100	2.3641E- 98	ENSG0000000675 6.11
ZNF804A	2.891623 8	2.891623 8	1.531879 87	1.567017 49	32.97773 49	9.322E- 09	3.3682E- 08	ENSG0000017039 6.6
C15orf52	2.886687 15	2.886687 15	1.529414 76	4.689708 3	230.5794 16	4.4564E- 52	9.4185E- 51	ENSG0000018854 9.8
PBXIP1	2.885511 25	2.885511 25	1.528826 96	6.753008 92	720.3638 4	1.116E- 158	1.749E- 156	ENSG0000016334 6.12
LEPREL1	2.868016 92	2.868016 92	1.520053 53	2.487679 74	64.20224 72	1.1228E- 15	6.7413E- 15	ENSG0000009053 0.5
ACSF2	2.863219 45	2.863219 45	1.517638 25	4.131753 51	191.7184 13	1.3404E- 43	2.2467E- 42	ENSG0000016710 7.8
ASTN2	2.861925 29	2.861925 29	1.516986 01	0.965319 49	21.98113 73	2.7534E- 06	7.9399E- 06	ENSG0000014821 9.12
CREG2	2.852298 09	2.852298 09	1.512124 76	1.260283 56	26.74042 97	2.327E- 07	7.5147E- 07	ENSG0000017587 4.5
ITGAV	2.844904 82	2.844904 82	1.508380 39	8.296526 75	695.0709 29	3.528E- 153	5.193E- 151	ENSG0000013844 8.7
MYL5	2.844594 51	2.844594 51	1.508223 01	1.933017 11	41.59419 48	1.1233E- 10	4.812E- 10	ENSG0000021537 5.2
LHX6	2.835673 44	2.835673 44	1.503691 4	4.953813	322.9613 9	3.2799E- 72	1.0612E- 70	ENSG0000010685 2.11
FBXL2	2.834656 26	2.834656 26	1.503173 8	4.156016 67	176.6242 16	2.6456E- 40	4.0569E- 39	ENSG0000015355 8.9
ABCA1	2.828716 91	2.828716 91	1.500147 8	4.509902 26	128.5338 28	8.5773E- 30	9.6199E- 29	ENSG0000016502 9.11
WDR52	2.828701 6	2.828701 6	1.50014	1.316390 33	29.40887 86	5.8609E- 08	1.9879E- 07	ENSG0000020653 0.4
CTD-3232M19.2	2.828109 16	2.828109 16	1.499837 81	3.357074 33	13.87063 68	0.000195 83	0.000450 24	ENSG0000020477 1.5
LINC00607	2.823729 08	2.823729 08	1.497601 68	5.257749 05	211.6124 56	6.1105E- 48	1.138E- 46	ENSG0000023577 0.1
GTF2IRD2B	2.822568 05	2.822568 05	1.497008 36	2.524852 59	24.56026 06	7.2022E- 07	2.2127E- 06	ENSG0000017442 8.12

KANK3	2.81747384	2.81747384	1.49440221	4.1649613	168.884419	1.2967E-38	1.874E-37	ENSG00000186994.7
SYT1	2.81217056	2.81217056	1.4916841	4.52372911	236.256695	2.576E-53	5.5811E-52	ENSG00000067715.9
GOLGA8B	2.79902933	2.79902933	1.4849266	3.60729319	35.2096176	2.9606E-09	1.1176E-08	ENSG00000215252.7
ASS1	2.7915299	2.7915299	1.48105601	0.906261	19.9879917	7.793E-06	2.1249E-05	ENSG00000130707.13
HHAT	2.78992595	2.78992595	1.48022683	1.39633689	28.9744063	7.3341E-08	2.4663E-07	ENSG00000054392.8
AC007362.1	2.7842598	2.7842598	1.47729383	5.40704042	295.216747	3.63E-66	1.0659E-64	ENSG00000180672.4
JUNB	2.78413355	2.78413355	1.47722842	5.17128352	187.52895	1.1008E-42	1.8124E-41	ENSG00000171223.4
OAS1	2.77486988	2.77486988	1.47242012	3.09302852	68.637103	1.1836E-16	7.4664E-16	ENSG00000089127.8
ENC1	2.77443666	2.77443666	1.47219487	6.95972182	535.559459	1.744E-118	1.441E-116	ENSG00000171617.9
MYL9	2.77199966	2.77199966	1.47092708	5.76614349	369.492099	2.4142E-82	1.0012E-80	ENSG00000101335.5
TNFRSF10C	2.7672902	2.7672902	1.46847395	5.7213458	237.752433	1.2156E-53	2.6432E-52	ENSG00000173535.9
TUBB3	2.76710297	2.76710297	1.46837633	7.84714298	641.439157	1.625E-141	2.001E-139	ENSG00000198211.8
TUBB3	2.76710297	2.76710297	1.46837633	7.84714298	641.439157	1.625E-141	2.001E-139	ENSG00000258947.2
IL7R	2.76667951	2.76667951	1.46815553	1.90210886	40.2952607	2.1834E-10	9.1047E-10	ENSG00000168685.10
DCBLD2	2.76457607	2.76457607	1.46705827	7.92517128	594.997655	2.05E-131	2.133E-129	ENSG00000057019.11
DCLK1	2.75351782	2.75351782	1.46127594	1.85911633	35.7507544	2.2425E-09	8.5965E-09	ENSG00000133083.10
LMF1	2.74856412	2.74856412	1.45867813	2.48722104	56.0454123	7.0816E-14	3.8067E-13	ENSG00000103227.14
MST1	2.74645839	2.74645839	1.45757243	1.31580447	26.5431787	2.5771E-07	8.2825E-07	ENSG00000173531.11
APLP1	2.74636382	2.74636382	1.45752276	2.26256218	50.1919758	1.3942E-12	6.9124E-12	ENSG00000105290.7
SMPD1	2.7389076	2.7389076	1.4536006	6.62183979	636.498099	1.93E-140	2.329E-138	ENSG00000166311.5
MYLK2	2.73759262	2.73759262	1.45290777	1.78824182	34.3388965	4.6303E-09	1.7194E-08	ENSG00000101306.6
C1orf110	2.73539938	2.73539938	1.45175149	1.25046717	21.7363564	3.1281E-06	8.9602E-06	ENSG00000185860.9
FAM214B	2.73507171	2.73507171	1.45157866	5.79579497	362.85524	6.7278E-81	2.7154E-79	ENSG00000005238.15
LTBP1	2.72762183	2.72762183	1.44764364	7.59137021	571.769468	2.314E-126	2.271E-124	ENSG00000049323.11
MARCH4	2.71932555	2.71932555	1.44324888	6.16570696	458.908678	8.306E-102	5.037E-100	ENSG00000144583.4
RP13-631K18.2	2.70929765	2.70929765	1.4379189	2.32744862	49.0390867	2.5091E-12	1.2269E-11	ENSG00000254486.1
TUFT1	2.70056795	2.70056795	1.43326285	2.83417741	69.0080456	9.8063E-17	6.2252E-16	ENSG00000143367.11
CHN2	2.69324122	2.69324122	1.42934345	2.29134121	47.0920787	6.7729E-12	3.2015E-11	ENSG00000106069.16
TP53I11	2.69093129	2.69093129	1.42810555	7.00514861	542.719728	4.828E-120	4.132E-118	ENSG00000175274.14
PSAP	2.68537151	2.68537151	1.42512169	10.8665491	835.07086	1.28E-183	2.759E-181	ENSG00000197746.9
AC046143.3	2.6842423	2.6842423	1.42451491	0.73937858	18.208122	1.9803E-05	5.1628E-05	ENSG00000229334.1
CAPS	2.67988329	2.67988329	1.42217017	0.95481146	13.1389028	0.00028923	0.00064769	ENSG00000105519.8
RNF207	2.67841583	2.67841583	1.42137996	0.98894444	19.8829954	8.2329E-06	2.2403E-05	ENSG00000158286.8
IL33	2.6744833	2.6744833	1.4192602	1.02310976	22.1028379	2.5843E-06	7.4753E-06	ENSG00000137033.7

ALX1	2.66820817	2.66820817	1.41587123	2.67356436	56.3174851	6.1665E-14	3.3237E-13	ENSG00000180318.3
EVA1A	2.66617527	2.66617527	1.41477163	5.32420784	350.42633	3.4222E-78	1.282E-76	ENSG00000115363.9
FOXF1	2.65974083	2.65974083	1.41128567	1.88334465	32.2900859	1.3279E-08	4.7439E-08	ENSG00000103241.5
FUCA1	2.65891881	2.65891881	1.41083973	3.28246993	75.6870442	3.3238E-18	2.2895E-17	ENSG00000179163.11
YAE1D1	2.65805552	2.65805552	1.41037124	3.78626956	127.270197	1.6213E-29	1.7967E-28	ENSG00000241127.3
GLIPR1	2.65582662	2.65582662	1.40916096	6.33751899	470.652345	2.311E-104	1.46E-102	ENSG00000139278.5
BMP1	2.65559672	2.65559672	1.40903608	6.42404269	305.691487	1.8959E-68	5.7201E-67	ENSG00000168487.13
GPR116	2.65082876	2.65082876	1.40644348	7.5950347	330.682866	6.8243E-74	2.3199E-72	ENSG00000069122.14
CSF1	2.64447579	2.64447579	1.40298177	6.07337091	174.279646	8.6003E-40	1.2925E-38	ENSG00000184371.9
SPATA18	2.6410883	2.6410883	1.40113253	3.73612508	125.158846	4.6979E-29	5.1354E-28	ENSG00000163071.6
PLSCR4	2.640648	2.640648	1.400892	4.93348219	284.521807	7.7668E-64	2.1597E-62	ENSG00000114698.10
RP11-359E10.1	2.63997989	2.63997989	1.40052694	2.1589731	45.8731748	1.2616E-11	5.8289E-11	ENSG00000270607.1
MDK	2.63759093	2.63759093	1.39922083	7.79439023	790.768241	5.486E-174	1.003E-171	ENSG00000110492.11
ZMAT3	2.63213236	2.63213236	1.39623204	7.14655719	331.720192	4.0563E-74	1.3867E-72	ENSG00000172667.6
CLIP3	2.63138931	2.63138931	1.39582471	4.74898308	132.513219	1.1553E-30	1.3304E-29	ENSG00000105270.10
BACH2	2.6268591	2.6268591	1.39333882	1.97402198	33.9199542	5.7427E-09	2.1084E-08	ENSG00000112182.10
ANKRD1	2.62152742	2.62152742	1.39040763	9.48458889	596.868416	8.034E-132	8.505E-130	ENSG00000148677.6
TRNP1	2.61271866	2.61271866	1.38555178	4.51228013	212.029292	4.9561E-48	9.2586E-47	ENSG00000253368.3
PLXNB1	2.61179661	2.61179661	1.38504255	5.76784987	277.832615	2.228E-62	5.9883E-61	ENSG00000164050.8
SAMD14	2.61012257	2.61012257	1.38411756	3.14964997	74.271271	6.8087E-18	4.5981E-17	ENSG00000167100.10
SEC31B	2.60809883	2.60809883	1.38299854	1.47185537	26.38263	2.8005E-07	8.9556E-07	ENSG00000075826.12
DNAH8	2.60731816	2.60731816	1.38256664	2.31850581	45.0965245	1.8756E-11	8.5092E-11	ENSG00000124721.13
SAMD4A	2.60659146	2.60659146	1.38216448	6.60661137	425.607216	1.4689E-94	7.325E-93	ENSG00000020577.9
XXYLT1-AS2	2.59693667	2.59693667	1.37681083	2.36440874	43.2368098	4.85E-11	2.1314E-10	ENSG00000230266.1
CD163L1	2.59475551	2.59475551	1.37559861	2.87782874	52.0089399	5.5249E-13	2.818E-12	ENSG00000177675.4
BST1	2.5921004	2.5921004	1.3741216	3.20248062	69.2140516	8.8336E-17	5.6226E-16	ENSG00000109743.6
EDN1	2.59062457	2.59062457	1.37329996	8.97124353	746.980591	1.819E-164	3.008E-162	ENSG00000078401.6
FAM131B	2.58842574	2.58842574	1.37207493	1.3254698	22.9063048	1.7009E-06	5.0311E-06	ENSG00000159784.13
NUAK1	2.58401208	2.58401208	1.36961281	6.15721436	364.932613	2.3743E-81	9.7793E-80	ENSG00000074590.9
PMAIP1	2.57878667	2.57878667	1.36669243	4.85510377	229.862645	6.387E-52	1.3405E-50	ENSG00000141682.11
SELL	2.57766947	2.57766947	1.36606728	0.83128975	17.6240232	2.6917E-05	6.9039E-05	ENSG00000188404.4
SIAE	2.57523871	2.57523871	1.36470617	5.44666974	346.424019	2.5461E-77	9.3109E-76	ENSG00000110013.8
ZFHX2	2.57472328	2.57472328	1.36441739	0.98907881	20.0794322	7.4291E-06	2.0316E-05	ENSG00000136367.12
SDC3	2.57315499	2.57315499	1.36353836	5.66957989	313.805188	3.2382E-70	1.0124E-68	ENSG00000162512.11

COL4A5	2.569057 07	2.569057 07	1.361238 94	6.273204 62	335.2322 93	6.9697E- 75	2.438E- 73	ENSG0000018815 3.8
APOL4	2.563462 72	2.563462 72	1.358093 91	1.559193 87	27.01367 99	2.0202E- 07	6.552E- 07	ENSG0000010033 6.13
ST3GAL5	2.558507 24	2.558507 24	1.355302 32	4.398010 94	169.5210 75	9.4139E- 39	1.3721E- 37	ENSG0000011552 5.12
TANK	2.553233 23	2.553233 23	1.352325 33	6.158873 49	485.0590 56	1.694E- 107	1.105E- 105	ENSG0000013656 0.9
NOVA1	2.548198 34	2.548198 34	1.349477 58	1.882933 4	27.73931 62	1.3881E- 07	4.5559E- 07	ENSG0000013991 0.15
UGCG	2.547997 51	2.547997 51	1.349363 87	6.003036 63	448.9340 09	1.231E- 99	6.9072E- 98	ENSG0000014815 4.5
SEZ6L2	2.546777 65	2.546777 65	1.348673 01	1.120230 35	20.63325 37	5.5622E- 06	1.5431E- 05	ENSG0000017493 8.10
GOLGA6L5	2.538618 35	2.538618 35	1.344043 52	2.515458 03	44.01407 98	3.2602E- 11	1.4508E- 10	ENSG0000023037 3.4
CDH13	2.534295 21	2.534295 21	1.341584 59	7.163790 19	351.5191 38	1.9785E- 78	7.4613E- 77	ENSG0000014094 5.11
TNFSF9	2.530592 75	2.530592 75	1.339475 35	1.495866 97	25.64991 92	4.0931E- 07	1.2857E- 06	ENSG0000012565 7.3
TPP1	2.527301 74	2.527301 74	1.337597 92	8.025724 07	360.8727 61	1.8178E- 80	7.1925E- 79	ENSG0000016634 0.10
MBP	2.523597 4	2.523597 4	1.335481 77	3.437682 54	84.85057 37	3.2179E- 20	2.4241E- 19	ENSG0000019797 1.10
IL3RA.1	2.516799 44	2.516799 44	1.331590 25	3.262580 78	13.14827 98	0.000287 78	0.000645 17	
MTMR10	2.515093 37	2.515093 37	1.330611 96	6.985886 64	455.8394 35	3.866E- 101	2.31E-99	ENSG0000016691 2.12
RP11-66N24.3	2.514195 89	2.514195 89	1.330097 06	1.521089 55	21.04817 43	4.4788E- 06	1.2561E- 05	ENSG0000025872 7.1
HLA-B	2.513968 51	2.513968 51	1.329966 58	6.872449 42	353.4003 86	7.7031E- 79	2.9233E- 77	ENSG0000023474 5.5
LGR4	2.511671 87	2.511671 87	1.328648	3.529642 41	98.27582 42	3.6398E- 23	3.1533E- 22	ENSG0000020521 3.9
GADD45B	2.510983 38	2.510983 38	1.328252 48	5.184425 21	278.7167 47	1.4297E- 62	3.8606E- 61	ENSG0000009986 0.4
PCED1A	2.500365 09	2.500365 09	1.322138 77	3.520149 51	93.11457 03	4.9353E- 22	4.0572E- 21	ENSG0000013263 5.12
PRSS23	2.499428 19	2.499428 19	1.321598 08	9.461808 12	699.4246 21	3.989E- 154	5.943E- 152	ENSG0000015068 7.7
SRPX2	2.498617 36	2.498617 36	1.321129 98	5.836678 47	217.8004 18	2.7301E- 49	5.28E-48	ENSG0000010235 9.5
APOD	2.494826 4	2.494826 4	1.318939 43	1.034149 31	17.97887 08	2.2337E- 05	5.7896E- 05	ENSG0000018905 8.4
FCGRT	2.494711 11	2.494711 11	1.318872 76	6.255179 13	318.9211 44	2.4883E- 71	7.8815E- 70	ENSG0000010487 0.8
BOK	2.493821 94	2.493821 94	1.318358 46	6.530708 96	451.0551 84	4.251E- 100	2.4313E- 98	ENSG0000017672 0.3
SLFN5	2.491894 07	2.491894 07	1.317242 74	5.663991 68	232.3893 66	1.7959E- 52	3.8223E- 51	ENSG0000016675 0.5
TICAM2	2.491828 53	2.491828 53	1.317204 79	1.420907 9	6.769375 74	0.009273 53	0.016219 26	ENSG0000024341 4.4
PLTP	2.490592 05	2.490592 05	1.316488 73	6.400439 13	321.9062 43	5.5678E- 72	1.787E- 70	ENSG0000010097 9.10
GPR155	2.489379 51	2.489379 51	1.315786 19	1.883729 22	33.92806 55	5.7188E- 09	2.1003E- 08	ENSG0000016332 8.9
TRPM4	2.486869 37	2.486869 37	1.314330 73	4.262805 74	145.5454 57	1.632E- 33	2.0666E- 32	ENSG0000013052 9.11
EFNA4	2.486318 87	2.486318 87	1.314011 33	3.706341 45	93.65348 41	3.7589E- 22	3.1113E- 21	ENSG0000024336 4.3
PLEKHO1	2.484749 17	2.484749 17	1.313100 22	7.022306 57	564.3071 88	9.72E- 125	9.31E- 123	ENSG0000002390 2.9
SIK1	2.482692 8	2.482692 8	1.311905 76	3.832502 14	109.6744 08	1.1548E- 25	1.1058E- 24	ENSG0000014217 8.7
FHL2	2.481081 47	2.481081 47	1.310969 11	7.589595 19	460.3567 94	4.02E- 102	2.463E- 100	ENSG0000011564 1.14
CCDC176	2.481056 22	2.481056 22	1.310954 43	1.161195 78	20.02913 81	7.6271E- 06	2.0824E- 05	ENSG0000011963 6.11

DAPK3	2.47854356	2.47854356	1.30949261	6.58907911	498.008226	2.578E-110	1.82E-108	ENSG00000167657.7
FAXDC2	2.47308123	2.47308123	1.30630963	2.19494877	24.4132855	7.7731E-07	2.3809E-06	ENSG00000170271.6
HOXB9	2.47109793	2.47109793	1.30515219	3.10802053	72.8734107	1.3824E-17	9.2067E-17	ENSG00000170689.8
INHBA	2.47095967	2.47095967	1.30507146	5.73661548	321.818526	5.8182E-72	1.8624E-70	ENSG00000122641.9
PLA2G15	2.4588415	2.4588415	1.29797874	5.45010433	254.414772	2.8315E-57	6.7132E-56	ENSG00000103066.8
MFGE8	2.4561059	2.4561059	1.29637277	6.67610358	422.351825	7.5084E-94	3.6984E-92	ENSG00000140545.10
C1orf54	2.45207382	2.45207382	1.29400241	3.17530658	59.3791658	1.3004E-14	7.3059E-14	ENSG00000118292.4
HES4	2.45175516	2.45175516	1.29381492	1.70654388	27.8419361	1.3164E-07	4.3335E-07	ENSG00000188290.6
MMP7	2.45174111	2.45174111	1.29380665	1.54421967	24.0269276	9.4998E-07	2.8914E-06	ENSG00000137673.4
OGFRL1	2.44523886	2.44523886	1.2899754	6.90504674	569.074031	8.928E-126	8.689E-124	ENSG00000119900.7
RP11-212P7.2	2.44240237	2.44240237	1.28830089	2.34532648	36.4469432	1.5688E-09	6.1066E-09	ENSG00000273270.1
TUBB2B	2.43965201	2.43965201	1.28667538	1.46324417	21.5297369	3.4838E-06	9.9275E-06	ENSG00000137285.9
FKBP9	2.43870845	2.43870845	1.28611729	7.60998241	595.054945	1.992E-131	2.091E-129	ENSG00000122642.6
LTBP3	2.43659455	2.43659455	1.28486621	6.91680963	492.937202	3.271E-109	2.23E-107	ENSG00000168056.10
RP11-420G6.4	2.43583039	2.43583039	1.28441368	2.44949335	40.7104993	1.7654E-10	7.4128E-10	ENSG00000230438.5
TNFAIP3	2.43461258	2.43461258	1.28369221	3.06756301	68.921141	1.0248E-16	6.4886E-16	ENSG00000118503.10
AC027612.6	2.4321818	2.4321818	1.28225107	3.73120576	83.4978112	6.3787E-20	4.7313E-19	ENSG00000143429.5
MURC	2.43149606	2.43149606	1.28184426	1.35175133	21.9395318	2.8138E-06	8.109E-06	ENSG00000170681.6
WARS	2.4307327	2.4307327	1.28139126	8.4696954	535.593345	1.714E-118	1.427E-116	ENSG00000140105.13
ACTA2	2.42963668	2.42963668	1.2807406	4.51605193	183.117108	1.0113E-41	1.6037E-40	ENSG00000107796.8
HES1	2.42855596	2.42855596	1.28009873	5.24671635	69.2768563	8.5568E-17	5.455E-16	ENSG00000114315.3
TCF7L1	2.42197386	2.42197386	1.2761833	4.43251941	115.450578	6.2702E-27	6.3216E-26	ENSG00000152284.4
USP54	2.42197242	2.42197242	1.27618243	4.27944357	103.605891	2.4684E-24	2.2499E-23	ENSG00000166348.13
TUBA1A	2.42144608	2.42144608	1.27586888	9.98881627	575.692725	3.243E-127	3.208E-125	ENSG00000167552.9
SLC30A3	2.4196818	2.4196818	1.27481734	3.30397722	78.5970733	7.6162E-19	5.3813E-18	ENSG00000115194.6
TRIL	2.41929644	2.41929644	1.27458756	0.81889347	14.3657741	0.00015051	0.00035174	ENSG00000176734.3
PCDHGB3	2.41577331	2.41577331	1.27248508	0.92971029	14.2998372	0.00015588	0.00036372	ENSG00000262209.1
FN1	2.41144801	2.41144801	1.26989971	11.3817757	245.946553	1.9868E-55	4.5154E-54	ENSG00000115414.14
KITLG	2.40893215	2.40893215	1.26839376	7.15859125	546.89166	5.973E-121	5.149E-119	ENSG00000049130.9
FKBP9L	2.40685534	2.40685534	1.26714943	1.52783678	19.5610813	9.7434E-06	2.6246E-05	ENSG00000176826.11
MICAL1	2.40554032	2.40554032	1.26636098	5.04503453	196.194381	1.4137E-44	2.4198E-43	ENSG00000135596.13
G0S2	2.40382203	2.40382203	1.26533009	1.90047873	15.3243273	9.0543E-05	0.00021849	ENSG00000123689.5
NIPAL2	2.40305651	2.40305651	1.26487058	3.69359389	76.3015449	2.4349E-18	1.6888E-17	ENSG00000104361.5
LPXN	2.39582283	2.39582283	1.26052123	3.66041378	82.6628029	9.7315E-20	7.1697E-19	ENSG00000110031.8

TMEM63B	2.39577317	2.39577317	1.26049132	5.99122429	337.294741	2.4776E-75	8.7427E-74	ENSG00000137216.14
B3GALT4	2.39511199	2.39511199	1.26009312	1.76761561	28.7050592	8.4283E-08	2.8175E-07	ENSG00000235863.2
BCL2L11	2.39193637	2.39193637	1.25817901	4.47537292	127.697251	1.3074E-29	1.4515E-28	ENSG00000153094.17
HES2	2.39073836	2.39073836	1.25745625	4.34276199	120.501601	4.9127E-28	5.1554E-27	ENSG00000069812.7
CEACAM19	2.38644233	2.38644233	1.25486147	0.76604079	12.6613538	0.00037329	0.00082212	ENSG00000186567.8
SPARC	2.38473313	2.38473313	1.25382782	10.8975648	583.702657	5.871E-129	5.953E-127	ENSG00000113140.6
ZNF71	2.38295162	2.38295162	1.25274966	4.1820189	122.445293	1.8443E-28	1.9679E-27	ENSG00000197951.4
FZD8	2.38232272	2.38232272	1.25236886	3.59075611	82.4432201	1.0875E-19	7.9926E-19	ENSG00000177283.4
CRYL1	2.38161872	2.38161872	1.25194246	4.73413184	171.43782	3.5904E-39	5.2904E-38	ENSG00000165475.9
NFKBIZ	2.38065804	2.38065804	1.2513604	3.93759418	62.7125433	2.3919E-15	1.4067E-14	ENSG00000144802.7
RHOD	2.37892955	2.37892955	1.25031255	3.58007507	94.6735365	2.2452E-22	1.8751E-21	ENSG00000173156.2
PVR	2.37482734	2.37482734	1.24782263	8.20121538	485.764995	1.189E-107	7.843E-106	ENSG00000073008.10
OPTN	2.37466283	2.37466283	1.24772269	7.02619012	377.543718	4.2632E-84	1.8116E-82	ENSG00000123240.12
EFEMP2	2.3733374	2.3733374	1.24691721	5.71126111	349.455292	5.5688E-78	2.0678E-76	ENSG00000172638.8
SOCS2	2.36703395	2.36703395	1.2430804	3.2369926	65.3304521	6.3335E-16	3.8447E-15	ENSG00000120833.9
ZNF425	2.36409645	2.36409645	1.2412889	1.08899649	15.8810126	6.7452E-05	0.00016538	ENSG00000204947.4
TSPAN9	2.36311324	2.36311324	1.24068876	6.58328949	403.259393	1.075E-89	4.9141E-88	ENSG00000011105.7
SPRY2	2.36301812	2.36301812	1.24063069	5.46879727	191.692063	1.3583E-43	2.2735E-42	ENSG00000136158.6
TMEM150A	2.36244315	2.36244315	1.24027962	4.11386234	102.884461	3.5528E-24	3.2188E-23	ENSG00000168890.9
LINC00152	2.35945493	2.35945493	1.23845361	5.80201402	356.908768	1.3265E-79	5.1143E-78	ENSG00000222041.6
BCAS3	2.35804053	2.35804053	1.23758851	3.42144049	79.4252136	5.0083E-19	3.5763E-18	ENSG00000141376.16
PDP1	2.35769696	2.35769696	1.2373783	6.66509415	454.868265	6.29E-101	3.703E-99	ENSG00000164951.11
MALAT1	2.35735537	2.35735537	1.23716926	8.82794431	62.8760953	2.2013E-15	1.2984E-14	ENSG00000251562.3
COLEC12	2.3567026	2.3567026	1.23676971	5.03039247	184.164968	5.9717E-42	9.5705E-41	ENSG00000158270.10
GATS	2.35603207	2.35603207	1.23635918	2.40686158	39.1480521	3.9286E-10	1.6011E-09	ENSG00000160844.6
GATS	2.35603207	2.35603207	1.23635918	2.40686158	39.1480521	3.9286E-10	1.6011E-09	ENSG00000239521.3
RP1-74M1.3	2.3489275	2.3489275	1.23200219	2.47814991	42.0873044	8.7288E-11	3.7594E-10	ENSG00000272796.1
C14orf37	2.34766446	2.34766446	1.23122623	0.9771357	16.6813538	4.4213E-05	0.00011074	ENSG00000139971.11
SARM1	2.34695261	2.34695261	1.23078871	4.23763172	117.311783	2.4531E-27	2.5173E-26	ENSG00000004139.9
AMT	2.34522202	2.34522202	1.22972451	0.9421864	14.4239669	0.00014593	0.0003421	ENSG00000145020.10
RGCC	2.34505455	2.34505455	1.22962148	5.63253265	145.141977	1.9995E-33	2.5293E-32	ENSG00000102760.12
CDKN1A	2.34466184	2.34466184	1.22937987	8.67587282	644.670883	3.222E-142	4.05E-140	ENSG00000124762.9
SERINC2	2.34408864	2.34408864	1.22902712	4.89474083	215.72866	7.7288E-49	1.4805E-47	ENSG00000168528.7
ZNF345	2.34098264	2.34098264	1.22711424	1.07762284	17.3276581	3.1457E-05	8.0175E-05	ENSG00000251247.5

LIMCH1	2.340099 2	2.340099 2	1.226569 69	4.148244 19	120.9089 14	4.0009E-28	4.2168E-27	ENSG0000006404 2.13
PMEPA1	2.339862 38	2.339862 38	1.226423 68	4.842265 61	161.4486 51	5.4594E-37	7.5729E-36	ENSG0000012422 5.11
F2RL1	2.337752 81	2.337752 81	1.225122 39	5.782619 45	275.2142 84	8.2893E-62	2.189E-60	ENSG0000016425 1.4
MMP14	2.333843 46	2.333843 46	1.222707 8	10.32814 96	637.8983 76	9.572E-141	1.167E-138	ENSG0000015722 7.8
FOS	2.332417 6	2.332417 6	1.221826 11	5.595114 42	99.65367 68	1.8152E-23	1.5931E-22	ENSG0000017034 5.5
JUP	2.332088 97	2.332088 97	1.221622 83	8.152541 76	350.4005 34	3.4667E-78	1.2912E-76	ENSG0000017380 1.12
TTLL3	2.331259 32	2.331259 32	1.221109 5	3.185863 48	22.91999 01	1.6889E-06	5.0003E-06	ENSG0000021402 1.11
COL18A1	2.328001 81	2.328001 81	1.219092 18	9.466635 62	552.9345 13	2.895E-122	2.588E-120	ENSG0000018287 1.10
CCDC80	2.325362 34	2.325362 34	1.217455 54	6.191528 29	398.7615 19	1.0246E-88	4.6136E-87	ENSG0000009198 6.11
SYNGR1	2.320984 53	2.320984 53	1.214736 9	2.001786 52	31.32814 17	2.179E-08	7.6553E-08	ENSG0000010032 1.10
POFUT2	2.320263 62	2.320263 62	1.214288 73	5.956038 52	309.3763 98	2.9859E-69	9.1224E-68	ENSG0000018686 6.12
DAB2	2.317487 82	2.317487 82	1.212561 76	8.378000 22	377.9945 4	3.4008E-84	1.4554E-82	ENSG0000015307 1.10
F2RL3	2.316637 4	2.316637 4	1.212032 25	1.535832 48	21.35429 37	3.8176E-06	1.082E-05	ENSG0000012753 3.3
LTBP2	2.314600 02	2.314600 02	1.210762 91	9.958916 79	343.1834 57	1.2929E-76	4.6857E-75	ENSG0000011968 1.7
PCDHGB2	2.313713 13	2.313713 13	1.21021	1.067046 78	14.39674 9	0.000148 06	0.000346 61	ENSG0000025391 0.1
ZSWIM4	2.313630 17	2.313630 17	1.210158 27	4.848831 64	144.9903 64	2.1581E-33	2.7214E-32	ENSG0000013200 3.5
LAMC2	2.313125 12	2.313125 12	1.209843 31	2.716114 21	45.93637 88	1.2216E-11	5.6504E-11	ENSG0000005808 5.10
FBLN7	2.307339 01	2.307339 01	1.206229 99	1.692171 91	25.52459 95	4.3678E-07	1.3673E-06	ENSG0000014415 2.8
SPTBN5	2.301388 6	2.301388 6	1.202504 61	4.621972 5	106.0414 98	7.2207E-25	6.7289E-24	ENSG0000013787 7.8
WFS1	2.298375 11	2.298375 11	1.200614 28	6.968418 88	354.3677 04	4.7427E-79	1.8055E-77	ENSG0000010950 1.9
RP11-693N9.2	2.297555 77	2.297555 77	1.200099 88	3.144713 71	56.02265 7	7.1641E-14	3.8459E-13	ENSG0000023550 5.3
TRANK1	2.295314 91	2.295314 91	1.198692 1	4.287351 3	84.50922 37	3.8243E-20	2.8683E-19	ENSG0000016801 6.9
GNPTG	2.294804 6	2.294804 6	1.198371 31	5.426511 07	209.0257 85	2.2409E-47	4.0957E-46	ENSG0000009058 1.5
GSTM3	2.294410 44	2.294410 44	1.198123 5	2.644801 62	46.55838 22	8.8929E-12	4.1565E-11	ENSG0000013420 2.6
HOXD1	2.292993 57	2.292993 57	1.197232 31	3.481010 8	71.56625 17	2.681E-17	1.7613E-16	ENSG0000012864 5.11
EME2	2.291317 12	2.291317 12	1.196177 14	3.107015 37	34.51115 25	4.2382E-09	1.5796E-08	ENSG0000019777 4.8
KIAA1324L	2.290891 74	2.290891 74	1.195909 28	5.671899 2	222.6859 82	2.347E-50	4.7128E-49	ENSG0000016465 9.10
ATHL1	2.290278 84	2.290278 84	1.195523 26	4.532459 65	105.3526 36	1.0222E-24	9.4315E-24	ENSG0000014210 2.11
LRP1	2.287942 72	2.287942 72	1.194050 94	3.418515 7	41.46676 02	1.1989E-10	5.1253E-10	ENSG0000012338 4.9
LYRM9	2.287862 91	2.287862 91	1.194000 61	1.181191 29	16.68276 26	4.4181E-05	0.000110 71	ENSG0000023285 9.5
RP11-680F8.1	2.283822 93	2.283822 93	1.191450 8	0.953931 44	13.74993 71	0.000208 83	0.000478 11	ENSG0000025680 2.2
BEND6	2.283098 2	2.283098 2	1.190992 91	1.150958 43	14.88667 81	0.000114 17	0.000272 23	ENSG0000015191 7.13
PRNP	2.282884 6	2.282884 6	1.190857 93	7.601590 77	448.1747 72	1.8E-99	1.0058E-97	ENSG0000017186 7.12
TRAPPC6A	2.279506 06	2.279506 06	1.188721 24	2.585314 42	37.41088 86	9.5686E-10	3.791E-09	ENSG0000000725 5.6

DDX58	2.279489 14	2.279489 14	1.188710 54	5.432379 84	265.1793 83	1.2752E-59	3.1994E-58	ENSG0000010720 1.5
NISCH	2.278291 96	2.278291 96	1.187952 64	7.098928 11	221.7904 13	3.6801E-50	7.3165E-49	ENSG0000001032 2.11
RGAG4	2.275241 84	2.275241 84	1.186019 9	2.289766 68	35.58546 52	2.441E-09	9.3281E-09	ENSG0000024273 2.3
CCNJL	2.274440 36	2.274440 36	1.185511 6	4.481248 66	126.2962 42	2.6484E-29	2.9189E-28	ENSG0000013508 3.10
SEL1L3	2.270427 27	2.270427 27	1.182963 82	7.664142 88	407.7975 14	1.1055E-90	5.1115E-89	ENSG0000009149 0.6
CCDC159	2.270138 9	2.270138 9	1.182780 57	2.691305 41	35.68116 76	2.324E-09	8.895E-09	ENSG0000018340 1.7
SLC6A8	2.268864 68	2.268864 68	1.181970 56	5.697161 32	250.1032 92	2.4656E-56	5.7111E-55	ENSG0000013082 1.11
PTGIR	2.266137 2	2.266137 2	1.180235 21	1.369170 86	19.07555 65	1.2564E-05	3.3442E-05	ENSG0000016001 3.4
ASMTL.1	2.264870 86	2.264870 86	1.179428 79	4.076326 96	23.90383 82	1.0127E-06	3.0707E-06	
ANXA3	2.264112 67	2.264112 67	1.178945 76	6.156048 03	293.4310 81	8.8914E-66	2.567E-64	ENSG0000013877 2.8
TSPAN11	2.263585 58	2.263585 58	1.178609 85	3.852921 36	90.70030 44	1.6717E-21	1.3458E-20	ENSG0000011090 0.10
GAL3ST4	2.263029 86	2.263029 86	1.178255 62	2.826514 64	49.97781 18	1.5549E-12	7.6906E-12	ENSG0000019709 3.6
CYB5D2	2.261695 16	2.261695 16	1.177404 49	4.113523 19	95.55224 78	1.4404E-22	1.2113E-21	ENSG0000016774 0.5
CASC15	2.261462 21	2.261462 21	1.177255 89	1.870265 86	23.13702 44	1.5086E-06	4.4908E-06	ENSG0000027216 8.1
RRAS	2.260722 16	2.260722 16	1.176783 7	6.085329 77	324.1173 01	1.8369E-72	6.0238E-71	ENSG0000012645 8.3
CTSS	2.259695 8	2.259695 8	1.176128 57	4.042984 14	97.38418 9	5.71E-23	4.9115E-22	ENSG0000016313 1.6
GPRC5A	2.257184 71	2.257184 71	1.174524 48	5.805861 83	198.2661 74	4.9911E-45	8.617E-44	ENSG0000001358 8.5
SLC9A7P1	2.257115 1	2.257115 1	1.174479 99	0.830976 69	13.05553 85	0.000302 39	0.000675 41	ENSG0000022782 5.3
FADS3	2.255271 68	2.255271 68	1.173301 23	7.044972 41	428.9039 36	2.8148E-95	1.4213E-93	ENSG0000022196 8.4
TXNDC5	2.254946 44	2.254946 44	1.173093 16	10.92702 27	515.7126 45	3.625E-114	2.734E-112	ENSG0000023926 4.4
PTPRM	2.252761 79	2.252761 79	1.171694 77	6.172357 5	227.9248 52	1.6901E-51	3.5105E-50	ENSG0000017348 2.12
C17orf103	2.252630 45	2.252630 45	1.171610 66	3.965236 54	61.45703 65	4.5251E-15	2.6154E-14	ENSG0000015403 5.6
KCTD13	2.252292 61	2.252292 61	1.171394 27	3.281597 3	55.73923 07	8.275E-14	4.4226E-13	ENSG0000017494 3.5
DOK3	2.252072 6	2.252072 6	1.171253 34	2.183862 14	26.44663 42	2.7092E-07	8.6815E-07	ENSG0000014609 4.9
THBS3	2.251560 2	2.251560 2	1.170925 05	3.656192 97	78.86512 62	6.6498E-19	4.7068E-18	ENSG0000016923 1.9
GLCE	2.251077 74	2.251077 74	1.170615 88	7.937396 28	449.8385 46	7.821E-100	4.4311E-98	ENSG0000013860 4.5
TP53I3	2.249721 74	2.249721 74	1.169746 57	6.726320 12	417.9299 77	6.8867E-93	3.3111E-91	ENSG0000011512 9.9
SEMA3A	2.249135 88	2.249135 88	1.169370 82	3.197652 3	33.16423 17	8.4694E-09	3.0721E-08	ENSG0000007521 3.6
PNMA6C	2.248538 95	2.248538 95	1.168987 87	0.941803 3	12.06649 72	0.000513 36	0.001110 46	ENSG0000023596 1.3
MANBA	2.248207 76	2.248207 76	1.168775 37	4.106013 99	86.31165 64	1.537E-20	1.1784E-19	ENSG0000010932 3.4
P2RX4	2.247813 6	2.247813 6	1.168522 41	5.958236 87	261.0721 03	1.0019E-58	2.4377E-57	ENSG0000013512 4.10
GAA	2.245980 4	2.245980 4	1.167345 34	6.391931 31	376.5492 63	7.0186E-84	2.9719E-82	ENSG0000017129 8.8
LY96	2.245023 19	2.245023 19	1.166730 35	3.274395 18	57.09686 07	4.1487E-14	2.2583E-13	ENSG0000015458 9.2
BBS2	2.242472 49	2.242472 49	1.165090 29	5.553833 39	277.4947 65	2.6396E-62	7.0788E-61	ENSG0000012512 4.7

MAPK11	2.24182589	2.24182589	1.16467423	4.85262364	189.299302	4.5215E-43	7.5262E-42	ENSG00000185386.10
ZFP14	2.24108405	2.24108405	1.16419676	1.25040415	14.4619811	0.00014302	0.00033598	ENSG00000142065.9
DNAH11	2.23849502	2.23849502	1.16252911	2.30442241	32.7119979	1.0688E-08	3.842E-08	ENSG00000105877.13
SLC7A11-AS1	2.23790232	2.23790232	1.16214707	2.01882649	30.1303344	4.0396E-08	1.3893E-07	ENSG00000250033.1
LAMP1	2.23542177	2.23542177	1.16054706	9.13275876	540.664825	1.351E-119	1.141E-117	ENSG00000185896.9
MIR4435-1HG	2.23438468	2.23438468	1.15987758	5.6309165	185.912171	2.4812E-42	4.0031E-41	ENSG00000172965.10
HBEGF	2.23399693	2.23399693	1.1596272	6.0880426	348.727204	8.0225E-78	2.9607E-76	ENSG00000113070.6
CROT	2.23300129	2.23300129	1.15898408	3.27481269	40.1313834	2.3744E-10	9.8673E-10	ENSG00000005469.7
PLD3	2.22780716	2.22780716	1.15562436	7.53402961	530.695979	1.993E-117	1.572E-115	ENSG00000105223.14
GPR137B	2.22762033	2.22762033	1.15550336	3.82949043	90.5984496	1.76E-21	1.416E-20	ENSG00000077585.9
KLHDC8B	2.22612646	2.22612646	1.15453555	5.02340913	166.679515	3.9304E-38	5.5868E-37	ENSG00000185909.10
PDLIM7	2.22538787	2.22538787	1.15405681	7.24387622	500.950135	5.905E-111	4.192E-109	ENSG00000196923.9
FNDC3B	2.22529145	2.22529145	1.1539943	8.21789874	416.70035	1.2754E-92	6.108E-91	ENSG00000075420.8
HIST2H2AA4	2.22470309	2.22470309	1.15361281	1.43030411	17.810472	2.4404E-05	6.2982E-05	ENSG00000203812.2
RHBDF1	2.22337267	2.22337267	1.15274979	5.65945929	264.69152	1.629E-59	4.0533E-58	ENSG00000007384.11
RP11-311C24.1	2.22297006	2.22297006	1.15248852	2.23381808	22.7345798	1.8599E-06	5.4785E-06	ENSG00000260772.1
KIAA1161	2.22252339	2.22252339	1.1521986	4.79564471	101.088634	8.7958E-24	7.8512E-23	ENSG00000164976.8
SLC43A2	2.22201197	2.22201197	1.15186659	6.49003978	409.044393	5.9175E-91	2.7572E-89	ENSG00000167703.10
STK32B	2.21971015	2.21971015	1.1503713	4.8295018	166.302748	4.7504E-38	6.7445E-37	ENSG00000152953.8
SDSL	2.2189625	2.2189625	1.14988528	2.88314112	45.6802946	1.3922E-11	6.4027E-11	ENSG00000139410.10
SOGA2	2.21741221	2.21741221	1.14887699	5.1475258	174.269378	8.6449E-40	1.2976E-38	ENSG00000168502.13
PGAP3	2.21468987	2.21468987	1.14710468	2.88970923	43.6836867	3.8598E-11	1.71E-10	ENSG00000161395.8
ZDHHC1	2.2143629	2.2143629	1.14689168	3.00160908	43.4000485	4.4618E-11	1.9644E-10	ENSG00000159714.6
RHOF	2.21417097	2.21417097	1.14676663	4.0172023	73.9067965	8.1894E-18	5.5028E-17	ENSG00000139725.3
GALNT7	2.21146148	2.21146148	1.14500011	7.33610111	426.031226	1.1877E-94	5.9473E-93	ENSG00000109586.7
ARHGEF10L	2.2113064	2.2113064	1.14489894	3.56212517	62.0893558	3.2822E-15	1.9098E-14	ENSG00000074964.12
KCNG1	2.20999586	2.20999586	1.14404367	1.69164037	20.7849676	5.1385E-06	1.4321E-05	ENSG00000026559.9
RAB32	2.20972143	2.20972143	1.1438645	6.14274235	291.792375	2.0231E-65	5.7582E-64	ENSG00000118508.4
RND3	2.20808916	2.20808916	1.14279843	6.84311493	342.985358	1.428E-76	5.1441E-75	ENSG00000115963.9
SDC1	2.20750604	2.20750604	1.14241738	3.78138493	92.1470512	8.0469E-22	6.5615E-21	ENSG00000115884.6
CDC42EP5	2.20734093	2.20734093	1.14230948	4.52880069	124.036421	8.2711E-29	8.9763E-28	ENSG00000167617.2
TMEM175	2.20641787	2.20641787	1.14170604	3.03040139	43.2524214	4.8114E-11	2.116E-10	ENSG00000127419.12
LINC00963	2.20641642	2.20641642	1.1417051	4.94696936	156.383833	6.979E-36	9.4738E-35	ENSG00000204054.7
GABARAPL1	2.20603275	2.20603275	1.14145421	5.79045097	186.647797	1.7143E-42	2.8032E-41	ENSG00000139112.6

SLC7A7	2.20569467	2.20569467	1.14123309	4.64060183	144.848398	2.318E-33	2.9199E-32	ENSG00000155465.14
LIMS1	2.20555458	2.20555458	1.14114146	7.88696332	435.448927	1.0591E-96	5.5093E-95	ENSG00000169756.12
CLDN11	2.20507426	2.20507426	1.14082724	9.55366832	411.220831	1.9879E-91	9.2982E-90	ENSG00000013297.6
EDIL3	2.20188135	2.20188135	1.13873673	4.69975072	160.899984	7.1948E-37	9.9344E-36	ENSG00000164176.8
CDH5	2.19850178	2.19850178	1.1365207	10.589215	440.47812	8.519E-98	4.6102E-96	ENSG00000179776.13
HEXA	2.19820854	2.19820854	1.13632826	6.65239993	398.961806	9.267E-89	4.1885E-87	ENSG00000213614.5
GDF15	2.19707191	2.19707191	1.13558209	7.69582067	462.912927	1.117E-102	6.947E-101	ENSG00000130513.6
LPHN1	2.19215716	2.19215716	1.13235123	1.74730998	21.701485	3.1855E-06	9.1096E-06	ENSG00000072071.12
HYI	2.19070113	2.19070113	1.13139267	6.73392105	381.699375	5.3086E-85	2.3212E-83	ENSG00000178922.12
CERS4	2.19004203	2.19004203	1.13095856	1.23042097	14.7773639	0.00012098	0.00028694	ENSG00000090661.7
ECM1	2.18916359	2.18916359	1.13037977	3.74285187	67.4317432	2.1811E-16	1.3589E-15	ENSG00000143369.10
BMF	2.18901292	2.18901292	1.13028047	3.51946603	53.5685265	2.4973E-13	1.2961E-12	ENSG00000104081.9
MRC2	2.18830251	2.18830251	1.12981219	5.30688891	211.344269	6.9918E-48	1.2981E-46	ENSG00000011028.9
RGS3	2.18828648	2.18828648	1.12980162	7.84388105	470.975063	1.966E-104	1.249E-102	ENSG00000138835.18
MEX3A	2.17944156	2.17944156	1.12395852	5.78781526	258.975784	2.8693E-58	6.8977E-57	ENSG00000254726.2
VWCE	2.17771908	2.17771908	1.12281786	3.48601262	57.7212806	3.0202E-14	1.656E-13	ENSG00000167992.8
KLF5	2.17290533	2.17290533	1.11962532	1.85186828	24.3016764	8.2367E-07	2.5203E-06	ENSG00000102554.9
FAM109A	2.17211726	2.17211726	1.11910199	4.48820429	120.786577	4.2553E-28	4.4772E-27	ENSG00000198324.10
MAP1LC3B	2.16850242	2.16850242	1.11669905	7.63308643	458.481429	1.029E-101	6.208E-100	ENSG00000140941.8
ALDH1A3	2.16831321	2.16831321	1.11657316	3.78834782	59.6143028	1.1539E-14	6.5043E-14	ENSG00000184254.12
OAS2	2.16424432	2.16424432	1.11386337	3.18961033	53.7628915	2.2621E-13	1.1797E-12	ENSG00000111335.8
TIMP2	2.1642189	2.1642189	1.11384643	9.26193202	435.00908	1.3203E-96	6.8384E-95	ENSG00000035862.8
C10orf54	2.16344293	2.16344293	1.11332906	2.65581962	35.8670804	2.1125E-09	8.1112E-09	ENSG00000107738.15
RP3-522D1.1	2.15951612	2.15951612	1.11070808	1.03342353	12.2095144	0.00047546	0.00103367	ENSG00000224167.1
EVI5L	2.15848559	2.15848559	1.11001946	4.72992685	146.148581	1.2046E-33	1.5287E-32	ENSG00000142459.4
DRAXIN	2.1574822	2.1574822	1.10934866	2.66264336	35.4042652	2.679E-09	1.0199E-08	ENSG00000162490.6
SPOCK1	2.15618251	2.15618251	1.1084793	8.45958996	399.783407	6.1388E-89	2.7851E-87	ENSG00000152377.8
TNKS1BP1	2.15282996	2.15282996	1.10623437	7.19054983	304.222861	3.9607E-68	1.189E-66	ENSG00000149115.9
PLAT	2.15220474	2.15220474	1.10581533	8.21194517	322.394568	4.3583E-72	1.4026E-70	ENSG00000104368.13
ZNF136	2.15017623	2.15017623	1.10445491	1.80702827	22.3508891	2.2711E-06	6.6201E-06	ENSG00000196646.7
SHC3	2.14664809	2.14664809	1.1020857	2.17810796	22.7957128	1.8017E-06	5.3108E-06	ENSG00000148082.5
NEDD9	2.14609673	2.14609673	1.1017151	6.63629265	279.309657	1.0618E-62	2.8925E-61	ENSG00000111859.12
PAM	2.14376761	2.14376761	1.10014852	7.65042079	364.292025	3.2736E-81	1.3392E-79	ENSG00000145730.16
TNFAIP1	2.14305628	2.14305628	1.09966974	7.0899347	402.164484	1.861E-89	8.4751E-88	ENSG00000109079.5

PLOD1	2.14278827	2.14278827	1.0994893	8.69585462	455.479143	4.631E-101	2.753E-99	ENSG00000083444.12
EGFR	2.1401539	2.1401539	1.09771455	3.47422146	52.4951662	4.3131E-13	2.214E-12	ENSG00000146648.11
DNASE2	2.13914753	2.13914753	1.09703598	5.66937721	239.420383	5.2612E-54	1.1565E-52	ENSG00000105612.4
PSMG3-AS1	2.13732914	2.13732914	1.09580909	2.35404183	31.0754978	2.4818E-08	8.6865E-08	ENSG00000230487.3
CERCAM	2.13379526	2.13379526	1.09342176	5.97637336	310.081724	2.0961E-69	6.4204E-68	ENSG00000167123.14
PIK3CD	2.13340032	2.13340032	1.0931547	4.09990362	86.895286	1.1442E-20	8.8346E-20	ENSG00000171608.11
CAP2	2.13325931	2.13325931	1.09305934	4.2154169	89.9500757	2.4425E-21	1.9482E-20	ENSG00000112186.7
CD99P1	2.13224107	2.13224107	1.09237055	1.90229239	7.25116779	0.00708549	0.01266031	ENSGR0000223773.2
CD99P1	2.13224107	2.13224107	1.09237055	1.90229239	7.25116779	0.00708549	0.01266031	ENSG00000223773.2
LIMS3L.1	2.13025536	2.13025536	1.09102638	2.63745576	20.6360951	5.5539E-06	1.5411E-05	
CTSD	2.12758228	2.12758228	1.08921492	8.54916681	437.578208	3.6436E-97	1.937E-95	ENSG00000117984.8
ARHGAP42	2.12676544	2.12676544	1.08866093	2.83190187	42.9439336	5.6331E-11	2.4622E-10	ENSG00000165895.13
CABLES1	2.1239487	2.1239487	1.08674892	6.20293507	337.21481	2.5789E-75	9.0737E-74	ENSG00000134508.8
GRINA	2.12156794	2.12156794	1.08513088	7.38599295	434.607712	1.6145E-96	8.3263E-95	ENSG00000178719.12
SNAI1	2.12135121	2.12135121	1.08498349	3.47094511	65.9198248	4.6964E-16	2.8741E-15	ENSG00000124216.3
ATOH8	2.12081176	2.12081176	1.08461657	2.9194632	45.4395418	1.5742E-11	7.2044E-11	ENSG00000168874.8
TTLL1	2.11920451	2.11920451	1.08352282	3.41888803	53.8540703	2.1595E-13	1.1277E-12	ENSG00000100271.12
KDR	2.11751336	2.11751336	1.08237107	8.90966644	281.179988	4.1539E-63	1.1393E-61	ENSG00000128052.8
BSDC1	2.11666338	2.11666338	1.08179185	6.31684886	261.468377	8.212E-59	2.0021E-57	ENSG00000160058.14
OTUB2	2.11476884	2.11476884	1.08049997	2.56459818	24.8797623	6.102E-07	1.8872E-06	ENSG00000089723.5
VWF	2.11215287	2.11215287	1.07871425	12.1867697	185.64739	2.8344E-42	4.5608E-41	ENSG00000110799.9
CTSZ	2.11141083	2.11141083	1.07820732	7.91370293	444.4414	1.1691E-98	6.3838E-97	ENSG00000101160.9
FAM167B	2.1073626	2.1073626	1.07543857	1.99613321	22.2789499	2.3578E-06	6.8563E-06	ENSG00000183615.5
AC006547.14	2.10728768	2.10728768	1.07538728	0.88117777	10.9862904	0.00091788	0.00190556	ENSG00000234409.4
CTSO	2.10625493	2.10625493	1.07468006	3.73730528	66.2203811	4.0322E-16	2.4776E-15	ENSG00000256043.2
GOLGA8A	2.10602338	2.10602338	1.07452145	4.18397367	47.8147033	4.6847E-12	2.2479E-11	ENSG00000175265.13
JAK3	2.10529546	2.10529546	1.07402272	1.69208856	19.7859617	8.6617E-06	2.3474E-05	ENSG00000105639.14
SLC2A6	2.10190629	2.10190629	1.07169835	5.934309	285.18764	5.561E-64	1.5571E-62	ENSG00000160326.9
C2CD4B	2.10181634	2.10181634	1.07163661	3.2121097	34.3667763	4.5645E-09	1.6965E-08	ENSG00000205502.3
KCNJ2-AS1	2.09991734	2.09991734	1.07033254	1.61222368	14.4527696	0.00014372	0.00033743	ENSG00000267365.1
MEX3B	2.09950783	2.09950783	1.07005117	5.00558986	181.270693	2.5585E-41	4.0098E-40	ENSG00000183496.5
PLA2R1	2.09841049	2.09841049	1.06929693	4.45795322	87.2191126	9.7141E-21	7.534E-20	ENSG00000153246.7
PRKCE	2.09507674	2.09507674	1.06700309	5.83916822	172.510865	2.0931E-39	3.0993E-38	ENSG00000171132.9
CD274	2.09504936	2.09504936	1.06698423	5.02838653	92.0530314	8.4385E-22	6.8761E-21	ENSG00000120217.9

FBXO44	2.093976 51	2.093976 51	1.066245 26	3.411897 08	58.01523 33	2.601E-14	1.4326E-13	ENSG0000013287 9.9
GPR153	2.091916 95	2.091916 95	1.064825 58	2.308717 31	25.77819 81	3.8299E-07	1.2052E-06	ENSG0000015829 2.6
FABP4	2.090467 08	2.090467 08	1.063825 32	4.868057 17	97.62018 75	5.0685E-23	4.3721E-22	ENSG0000017032 3.4
DYRK1B	2.087194 82	2.087194 82	1.061565 27	4.688744 18	111.9884 57	3.594E-26	3.5091E-25	ENSG0000010520 4.9
CRELD1	2.087132 28	2.087132 28	1.061522 04	4.475254 51	96.65205 22	8.2647E-23	7.0536E-22	ENSG0000016370 3.13
HMCN1	2.082272 98	2.082272 98	1.058159 22	3.298122	29.47718 78	5.6579E-08	1.9228E-07	ENSG0000014334 1.7
RP11-479G22.8	2.082234 02	2.082234 02	1.058132 22	3.245542 45	50.9324	9.5602E-13	4.7907E-12	ENSG0000027303 8.1
MIR24-2	2.081726 4	2.081726 4	1.057780 47	1.719773 88	16.36986 26	5.2107E-05	0.000129 68	ENSG0000026751 9.2
ITGB5	2.080177 52	2.080177 52	1.056706 65	8.039403 41	488.3335 47	3.284E-108	2.178E-106	ENSG0000008278 1.7
CHPF2	2.079756 24	2.079756 24	1.056414 45	7.367995 92	334.0870 27	1.2378E-74	4.3172E-73	ENSG0000003310 0.10
PHLDA3	2.079554 32	2.079554 32	1.056274 37	5.362147 9	168.6476 37	1.4606E-38	2.1085E-37	ENSG0000017430 7.5
RNF122	2.079078 36	2.079078 36	1.055944 13	4.472848 76	122.6731 99	1.6442E-28	1.7622E-27	ENSG0000013387 4.1
P4HA2	2.076259 77	2.076259 77	1.053986 96	5.617660 37	229.7623 46	6.7169E-52	1.4073E-50	ENSG0000007268 2.14
LOXL2	2.075932 45	2.075932 45	1.053759 5	9.707926 82	418.8400 82	4.3643E-93	2.1067E-91	ENSG0000013401 3.11
TEF	2.074980 54	2.074980 54	1.053097 8	2.326208 64	28.94825 94	7.4338E-08	2.4975E-07	ENSG0000016707 4.10
F11R.1	2.074961 8	2.074961 8	1.053084 78	5.121071 3	97.67047 54	4.9414E-23	4.2655E-22	
TMEM159	2.073421 18	2.073421 18	1.052013 21	4.709457 78	132.6570 38	1.0746E-30	1.2386E-29	ENSG0000001163 8.6
HEY1	2.072531 56	2.072531 56	1.051394 07	2.368223 62	13.98112 21	0.000184 66	0.000426 57	ENSG0000016468 3.12
CHST2	2.071475 42	2.071475 42	1.050658 7	4.057699 83	87.49693 95	8.441E-21	6.5551E-20	ENSG0000017504 0.4
LYVE1	2.070458 98	2.070458 98	1.049950 62	6.369789 05	286.0597 96	3.5901E-64	1.0076E-62	ENSG0000013380 0.4
ZNF516	2.069764 61	2.069764 61	1.049466 71	4.021269 82	68.36018 21	1.362E-16	8.5697E-16	ENSG0000010149 3.6
TMEM256-PLSCR3	2.066261 49	2.066261 49	1.047022 84	5.967628 11	192.9918 8	7.068E-44	1.1946E-42	ENSG0000018783 8.12
CELF2	2.066258 34	2.066258 34	1.047020 64	5.596528 07	182.8237 7	1.1719E-41	1.8536E-40	ENSG0000004874 0.13
RP11-597D13.9	2.065470 85	2.065470 85	1.046470 7	1.259329 07	14.21225 1	0.000163 3	0.000380 31	ENSG0000024842 9.1
PALLD	2.064205 72	2.064205 72	1.045586 76	5.872148 74	268.2684 03	2.7059E-60	6.9183E-59	ENSG0000012911 6.13
HOMER3	2.064184 44	2.064184 44	1.045571 89	6.626709 65	235.0053 07	4.8286E-53	1.0443E-51	ENSG0000005112 8.14
ACYP2	2.063385 47	2.063385 47	1.045013 37	1.876593 67	22.55026 37	2.0472E-06	5.9993E-06	ENSG0000017063 4.8
SGIP1	2.062505 7	2.062505 7	1.044398 11	3.404103 78	48.22906 02	3.7923E-12	1.8313E-11	ENSG0000011847 3.17
CTNNBIP1	2.061959 12	2.061959 12	1.044015 73	5.710062 55	150.8606 21	1.1242E-34	1.4667E-33	ENSG0000017858 5.10
B3GNT9	2.060662 48	2.060662 48	1.043108 22	1.670388 23	16.92120 53	3.8964E-05	9.8125E-05	ENSG0000023717 2.3
SQSTM1	2.060648 13	2.060648 13	1.043098 17	9.211387 65	414.4068	4.0262E-92	1.9129E-90	ENSG0000016101 1.15
KIAA1211	2.060421 91	2.060421 91	1.042939 79	3.884447 14	78.39018 32	8.4571E-19	5.9615E-18	ENSG0000010926 5.8
CLU	2.059719 38	2.059719 38	1.042447 8	7.854059 07	264.9587 74	1.4245E-59	3.5592E-58	ENSG0000012088 5.15
SLC12A4	2.057805 55	2.057805 55	1.041106 66	6.581158 77	214.9946 73	1.1175E-48	2.127E-47	ENSG0000012406 7.12

C6orf141	2.057076 72	2.057076 72	1.040595 6	2.729348 21	35.24946 14	2.9006E-09	1.0963E-08	ENSG0000019726 1.7
SUMF1	2.055800 39	2.055800 39	1.039700 19	5.797783 43	240.5868 2	2.9292E-54	6.5101E-53	ENSG0000014445 5.9
MAN2B1	2.055536 55	2.055536 55	1.039515 02	6.536540 62	319.8602 97	1.5536E-71	4.9599E-70	ENSG0000010477 4.8
IFI27L2	2.054571 93	2.054571 93	1.038837 84	2.832326 23	30.08171 47	4.1422E-08	1.4238E-07	ENSG0000011963 2.3
CTD-2228K2.7	2.051599 1	2.051599 1	1.036748 85	1.454981 72	14.80394 77	0.000119 29	0.000283 21	ENSG0000022513 8.3
HIST1H2BK	2.051089 89	2.051089 89	1.036390 72	3.142084 44	36.17019 03	1.8082E-09	6.9938E-09	ENSG0000019790 3.6
ERC2	2.049515 85	2.049515 85	1.035283 15	2.401912 33	30.62715 56	3.1269E-08	1.0856E-07	ENSG0000018767 2.8
SPSB1	2.049206 54	2.049206 54	1.035065 4	5.227973 38	152.0440 26	6.1973E-35	8.1293E-34	ENSG0000017162 1.9
GLB1	2.047707 66	2.047707 66	1.034009 77	6.831166 15	292.1197 01	1.7167E-65	4.8977E-64	ENSG0000017026 6.11
TXNRD3	2.045923 85	2.045923 85	1.032752 45	2.969474 26	44.12555 1	3.0797E-11	1.373E-10	ENSG0000019776 3.8
BMP4	2.045866 51	2.045866 51	1.032712 02	7.156762 93	286.1535 04	3.4252E-64	9.6354E-63	ENSG0000012537 8.11
MARCH2	2.045745 51	2.045745 51	1.032626 68	5.240554 87	159.9442 62	1.1637E-36	1.6013E-35	ENSG0000009978 5.6
SAMD9L	2.043396 39	2.043396 39	1.030969 09	5.088632 69	132.1104 09	1.4153E-30	1.625E-29	ENSG0000017740 9.7
AC093673.5	2.042927 75	2.042927 75	1.030638 18	2.269840 1	23.47484 03	1.2656E-06	3.7917E-06	ENSG0000023253 3.1
OPRL1	2.042268 95	2.042268 95	1.030172 87	1.306048 57	11.88713 5	0.000565 23	0.001216 55	ENSG0000012551 0.11
RCN1P2	2.042027 81	2.042027 81	1.030002 51	3.267787 25	35.28968 82	2.8413E-09	1.0759E-08	ENSG0000021445 5.3
PODXL2	2.041571 94	2.041571 94	1.029680 41	2.779721 68	28.56989 49	9.0376E-08	3.0162E-07	ENSG0000011463 1.10
COL8A1	2.040746 79	2.040746 79	1.029097 19	7.096968 14	238.7469 54	7.3778E-54	1.6159E-52	ENSG0000014481 0.11
NUAK2	2.040728 89	2.040728 89	1.029084 54	2.178248 61	24.56051 52	7.2012E-07	2.2127E-06	ENSG0000016354 5.7
METRNL	2.038613 75	2.038613 75	1.027588 46	4.390303 28	98.12545 14	3.927E-23	3.3972E-22	ENSG0000017684 5.8
DKFZP761J1410	2.038276 34	2.038276 34	1.027349 66	4.918804 85	158.8567 78	2.0111E-36	2.7517E-35	ENSG0000010552 0.6
LGALS3	2.036773 6	2.036773 6	1.026285 62	4.785646 62	149.7892 32	1.9277E-34	2.496E-33	ENSG0000013198 1.11
REC8	2.036318 71	2.036318 71	1.025963 38	5.562428 66	191.0394 26	1.8856E-43	3.1517E-42	ENSG0000010091 8.8
IRF9	2.036071 53	2.036071 53	1.025788 25	3.791328 07	56.33860 94	6.1006E-14	3.2896E-13	ENSG0000021392 8.4
LURAP1L	2.035968 79	2.035968 79	1.025715 45	1.351751 99	14.47427 16	0.000142 09	0.000334 12	ENSG0000015371 4.5
C18orf32	2.035783 87	2.035783 87	1.025584 4	4.516237 2	112.6181 63	2.616E-26	2.5667E-25	ENSG0000017757 6.6
GALNT10	2.032643 6	2.032643 6	1.023357 27	7.203915 67	262.7086 51	4.4066E-59	1.0809E-57	ENSG0000016457 4.11
RAB3B	2.032004 62	2.032004 62	1.022903 68	5.880980 51	222.2970 88	2.8533E-50	5.7103E-49	ENSG0000016921 3.6
ZNF583	2.031773 34	2.031773 34	1.022739 46	1.774155 83	16.64903 01	4.4973E-05	0.000112 6	ENSG0000019844 0.5
CTSA	2.027204 05	2.027204 05	1.019491 31	7.691802 44	361.5648 28	1.2848E-80	5.1513E-79	ENSG0000006460 1.12
RP11-690G19.3	2.026526 61	2.026526 61	1.019009 12	1.487137 08	16.14972 25	5.8527E-05	0.000144 88	ENSG0000026675 3.2
RASSF9	2.025512 57	2.025512 57	1.018287 04	1.160295 43	8.424712 08	0.003701 55	0.006966 68	ENSG0000019877 4.3
TMC7	2.024249 42	2.024249 42	1.017387 07	3.352746 35	31.41398 89	2.0847E-08	7.3349E-08	ENSG0000017053 7.8
APLP2	2.023897 21	2.023897 21	1.017136 02	10.75155 73	422.1920 51	8.1344E-94	3.9905E-92	ENSG0000008423 4.12

PAOX	2.02125768	2.02125768	1.01525326	1.29735153	12.7904889	0.00034839	0.0007703	ENSG00000148832.10
ROGDI	2.02077759	2.02077759	1.01491055	3.60000628	55.2588823	1.0566E-13	5.6244E-13	ENSG00000067836.8
SGSH	2.0170522	2.0170522	1.01224842	6.27299765	267.727119	3.5504E-60	9.0014E-59	ENSG00000181523.8
GPR126	2.016735	2.016735	1.01202152	7.46584042	215.595624	8.2629E-49	1.5803E-47	ENSG00000112414.10
CALCOCO1	2.01557962	2.01557962	1.01119478	5.28487823	114.43831	1.0447E-26	1.0436E-25	ENSG00000012822.11
IL27RA	2.01554959	2.01554959	1.01117328	2.8083367	27.8645738	1.3011E-07	4.2866E-07	ENSG00000104998.2
RAG1	2.01189147	2.01189147	1.00855248	1.72569158	17.295659	3.1992E-05	8.1451E-05	ENSG00000166349.5
F2R	2.01166765	2.01166765	1.00839198	9.4212199	450.494775	5.629E-100	3.2043E-98	ENSG00000181104.6
MLLT11	2.01137023	2.01137023	1.00817866	6.90324764	319.249666	2.1103E-71	6.7018E-70	ENSG00000213190.2
ARHGEF37	2.01064601	2.01064601	1.00765911	3.06658996	35.0267508	3.2521E-09	1.2215E-08	ENSG00000183111.7
RP11-658F2.8	2.01060092	2.01060092	1.00762676	2.19290536	23.0479312	1.5801E-06	4.6899E-06	ENSG00000258297.1
C1RL	2.01021323	2.01021323	1.00734854	4.05416278	61.8809449	3.6486E-15	2.1179E-14	ENSG00000139178.6
ARVCF	2.00674923	2.00674923	1.00486034	6.12791478	205.133005	1.584E-46	2.8278E-45	ENSG00000099889.9
S100A11	2.00666771	2.00666771	1.00480174	7.44780324	300.859112	2.1409E-67	6.3637E-66	ENSG00000163191.5
GBA	2.00537224	2.00537224	1.00387005	6.78509047	289.998481	4.9761E-65	1.4097E-63	ENSG00000177628.11
LAMB2	2.00384492	2.00384492	1.00277086	8.07056809	200.559321	1.5768E-45	2.7498E-44	ENSG00000172037.9
PPP1R3B	2.00327748	2.00327748	1.00236227	6.41055863	229.982097	6.0152E-52	1.2669E-50	ENSG00000173281.4
MAGED2	2.00122279	2.00122279	1.00088179	7.52839737	328.046	2.5608E-73	8.5844E-72	ENSG00000102316.12
SORT1	2.00094886	2.00094886	1.00068429	5.07365857	150.83785	1.1372E-34	1.482E-33	ENSG00000134243.7
GIMAP8	0.49995695	-2.0001722	-1.0001242	5.94704536	212.245232	4.4466E-48	8.3197E-47	ENSG00000171115.3
ALG10B	0.49925624	-2.0029795	-1.0021476	1.24645221	11.3696274	0.00074655	0.00157094	ENSG00000175548.4
AR	0.4992272	-2.003096	-1.0022315	4.37220776	85.8550644	1.9362E-20	1.4798E-19	ENSG00000169083.11
PDLIM3	0.49900459	-2.0039896	-1.002875	2.28172933	23.6135934	1.1775E-06	3.5446E-06	ENSG00000154553.9
PAN2	0.49877939	-2.0048944	-1.0035263	3.1688559	39.0446507	4.1422E-10	1.6842E-09	ENSG00000135473.10
NUP155	0.49853989	-2.0058576	-1.0042192	5.92019048	218.300881	2.1233E-49	4.1262E-48	ENSG00000113569.11
TFAP4	0.4984581	-2.0061867	-1.0044559	3.51427994	49.0799966	2.4573E-12	1.2026E-11	ENSG00000090447.7
SLC25A40	0.49836524	-2.0065605	-1.0047246	3.95864489	51.6743909	6.5512E-13	3.3176E-12	ENSG00000075303.8
LIN54	0.49809048	-2.0076674	-1.0055203	4.35296254	95.4508431	1.5161E-22	1.2741E-21	ENSG00000189308.6
C4orf46	0.49701499	-2.0120117	-1.0086387	5.16706676	93.3361385	4.4126E-22	3.6399E-21	ENSG00000205208.4

KLHL3	0.49695786	-2.0122431	-1.0088046	3.11243242	35.686281	2.3179E-09	8.8745E-09	ENSG00000146021.10
SNHG3	0.49640571	-2.0144812	-1.0104084	5.73894795	142.401802	7.9438E-33	9.8932E-32	ENSG00000242125.2
MIR3654	0.49637209	-2.0146177	-1.0105061	3.03646289	31.054318	2.5091E-08	8.7792E-08	ENSG00000255508.3
CALHM2	0.49609659	-2.0157365	-1.0113071	3.74545207	59.389819	1.2934E-14	7.2708E-14	ENSG00000138172.6
TFEB	0.49608875	-2.0157684	-1.0113299	1.72851225	15.087342	0.00010265	0.00024608	ENSG00000112561.13
NUP107	0.49555113	-2.0179552	-1.0128942	5.83652528	213.84209	1.9937E-48	3.7594E-47	ENSG00000111581.5
LMNB2	0.49491894	-2.0205329	-1.0147358	8.25028426	389.374718	1.1324E-86	5.0242E-85	ENSG00000176619.6
KLHL15	0.49319231	-2.0276066	-1.0197778	3.05028233	42.759049	6.1915E-11	2.6984E-10	ENSG00000174010.9
CEP72	0.49310784	-2.027954	-1.0200249	2.02312958	20.308343	6.5913E-06	1.8123E-05	ENSG00000112877.6
GPR3	0.49280868	-2.0291851	-1.0209004	1.71444309	13.109773	0.00029376	0.00065723	ENSG00000181773.6
CCP110	0.49138993	-2.0350437	-1.0250598	4.99324455	152.248731	5.5907E-35	7.3495E-34	ENSG00000103540.12
PRKAR2B	0.4908433	-2.0373101	-1.0266656	6.84154235	284.86595	6.5351E-64	1.8256E-62	ENSG00000005249.8
CYP2S1	0.49038479	-2.0392149	-1.0280139	1.85189649	18.923531	1.3606E-05	3.6041E-05	ENSG00000167600.9
FRY	0.48998134	-2.040894	-1.0292013	5.45531388	183.319507	9.1342E-42	1.4542E-40	ENSG00000073910.15
DARS2	0.48961856	-2.0424062	-1.0302698	5.65642589	162.043383	4.0477E-37	5.6406E-36	ENSG00000117593.8
NR2C2AP	0.48957848	-2.0425735	-1.030388	3.35895769	51.662891	6.5899E-13	3.3359E-12	ENSG00000184162.10
MTHFD1	0.48931292	-2.043682	-1.0311707	7.09712321	311.419715	1.0714E-69	3.3153E-68	ENSG00000100714.11
DNAJC6	0.48875758	-2.0460041	-1.032809	2.975101	40.199676	2.2929E-10	9.5415E-10	ENSG00000116675.11
HMGB1	0.48803493	-2.0490337	-1.0349437	9.14296698	304.316152	3.7796E-68	1.1375E-66	ENSG00000189403.10
SYNE3	0.48744751	-2.0515029	-1.0366812	3.58689214	52.233525	4.9278E-13	2.5209E-12	ENSG00000176438.8
LRR1	0.48742398	-2.051602	-1.0367509	4.34095459	100.892631	9.7107E-24	8.6486E-23	ENSG00000165501.12
ATP6V0E2-AS1	0.48732351	-2.052025	-1.0370483	1.03005173	11.588419	0.00066364	0.00140975	ENSG00000204934.6
C19orf33	0.48730157	-2.0521173	-1.0371132	1.30202155	13.866335	0.00019628	0.00045102	ENSG00000167644.7

TTC32	0.48701482	-2.0533256	-1.0379624	1.3019269	13.7903315	0.00020439	0.00046856	ENSG00000183891.5
PSIP1	0.48695385	-2.0535827	-1.038143	6.36787594	283.644617	1.2061E-63	3.3308E-62	ENSG00000164985.10
DCLRE1A	0.48547644	-2.0598322	-1.0425268	3.6764387	59.7559231	1.0738E-14	6.0725E-14	ENSG00000198924.3
OSGEPL1	0.48456005	-2.0637277	-1.0452526	2.49691537	29.9475465	4.4389E-08	1.521E-07	ENSG00000128694.7
RP11-673C5.1	0.48389186	-2.0665774	-1.0472434	5.58420733	225.701754	5.1613E-51	1.0539E-49	ENSG00000259781.1
ITGA1	0.48349879	-2.0682575	-1.0484158	2.35770886	26.239439	3.016E-07	9.5933E-07	ENSG00000213949.4
TTF2	0.48334465	-2.0689171	-1.0488758	5.2536211	139.567618	3.3095E-32	4.0548E-31	ENSG00000116830.7
CABYR	0.48253963	-2.0723686	-1.0512806	1.96661177	21.3093598	3.9082E-06	1.1064E-05	ENSG00000154040.16
HYLS1	0.48248752	-2.0725925	-1.0514365	3.21734935	50.3479914	1.2876E-12	6.4085E-12	ENSG00000198331.6
PARP1	0.48236074	-2.0731372	-1.0518156	8.05207587	363.802158	4.1849E-81	1.7062E-79	ENSG00000143799.8
PLEKHH2	0.48081431	-2.079805	-1.0564483	0.87881012	9.01268595	0.00268112	0.00515383	ENSG00000152527.9
MFSD2A	0.4807341	-2.080152	-1.056689	2.59615883	27.4645994	1.6E-07	5.2298E-07	ENSG00000168389.13
IGFBP3	0.48036354	-2.0817567	-1.0578014	2.3627059	25.3739631	4.7225E-07	1.4742E-06	ENSG00000146674.10
CENPQ	0.47854372	-2.0896732	-1.0632774	2.98430631	26.4774061	2.6664E-07	8.558E-07	ENSG00000031691.6
POLD3	0.47827398	-2.0908518	-1.0640908	4.62276562	119.822758	6.9173E-28	7.2088E-27	ENSG00000077514.4
HSPA1B	0.47714604	-2.0957944	-1.0674972	6.72728862	294.538943	5.1002E-66	1.4867E-64	ENSG00000204388.5
FAM13A	0.47651293	-2.098579	-1.0694127	2.85900117	40.3154287	2.161E-10	9.0174E-10	ENSG00000138640.10
MB21D1	0.47647929	-2.0987271	-1.0695146	2.81673492	35.2630134	2.8805E-09	1.089E-08	ENSG00000164430.11
RP11-660L16.2	0.47629548	-2.099537	-1.0700712	1.94239006	17.4744526	2.9119E-05	7.442E-05	ENSG00000254682.1
NASP	0.47608191	-2.1004789	-1.0707183	6.88181804	332.292945	3.0436E-74	1.0494E-72	ENSG00000132780.12
SPDL1	0.47594019	-2.1011043	-1.0711478	5.62682911	201.907031	8.011E-46	1.4031E-44	ENSG00000040275.12
NKX3-1	0.47569633	-2.1021814	-1.0718872	0.76339748	9.59985252	0.00194593	0.0038342	ENSG00000167034.9
PEG10	0.4755875	-2.1026625	-1.0722173	5.73740922	261.785221	7.0046E-59	1.7112E-57	ENSG00000242265.1

IRF6	0.4751841	-2.1044475	-1.0734415	3.48771422	60.2624784	8.3015E-15	4.73E-14	ENSG00000117595.6
FKBP5	0.4748412 8	-2.1059669	-1.0744827	7.0188791 8	370.742366	1.2899E-82	5.3678E-81	ENSG00000096060.10
POLA2	0.4745256 9	-2.1073675	-1.0754419	4.9766552 9	137.573642	9.033E-32	1.0868E-30	ENSG00000014138.4
MSMP	0.4739684 3	-2.1098452	-1.0771371	3.4544325 2	53.687355 8	2.3507E-13	1.2238E-12	ENSG00000215183.4
CLEC1A	0.4739656 8	-2.1098574	-1.0771455	3.3308340 2	56.201461 6	6.5413E-14	3.5194E-13	ENSG00000150048.6
PLS1	0.4733623 8	-2.1125464	-1.0789831	1.4243546 8	13.116201 2	0.0002927 5	0.0006552 2	ENSG00000120756.8
RN7SL3	0.4727112 6	-2.1154563	-1.0809689	0.9845463 1	10.282973 2	0.0013426 3	0.0027186 1	ENSG00000266037.1
ZNF296	0.4722167 6	-2.1176715	-1.0824788	0.9025605 5	11.438886 2	0.0007192 3	0.0015182 2	ENSG00000170684.4
CSRP2	0.4714091 8	-2.1212994	-1.0849482	2.2246937 3	28.945756 3	7.4434E-08	2.5E-07	ENSG00000175183.5
RPA3	0.4691466 1	-2.1315298	-1.0918892	3.2691838 3	47.813142 9	4.6884E-12	2.2488E-11	ENSG00000106399.7
MAP2K6	0.4688110 1	-2.1330557	-1.0929216	2.7602039 4	28.905592 9	7.5993E-08	2.5489E-07	ENSG00000108984.9
SLC15A3	0.4687420 9	-2.1333693	-1.0931338	1.1052185 6	10.535559 2	0.0011709 9	0.0023915 3	ENSG00000110446.5
MPHOSPH9	0.4685837 3	-2.1340903	-1.0936212	4.6652440 3	131.15673 7	2.2881E-30	2.605E-29	ENSG00000051825.10
TOPBP1	0.4685553 8	-2.1342194	-1.0937085	5.9439291 5	269.80163 2	1.2536E-60	3.2325E-59	ENSG00000163781.8
RTKN	0.4683228 3	-2.1352792	-1.0944247	2.248795	24.424768 6	7.7269E-07	2.3673E-06	ENSG00000114993.11
SMCHD1	0.4678007 1	-2.1376624	-1.096034	5.9876609 5	253.21444 7	5.1722E-57	1.2215E-55	ENSG00000101596.10
MTX3	0.4670463	-2.1411153	-1.0983625	2.0394664 4	23.974532 2	9.7618E-07	2.9667E-06	ENSG00000177034.10
HMGN2P5	0.4669514 9	-2.1415501	-1.0986554	0.8281318 2	10.766591 7	0.0010334 9	0.0021294 4	ENSG00000234664.1
GTF2H2B	0.4668748 9	-2.1419015	-1.0988921	2.7022580 8	21.638994 2	3.2909E-06	9.4089E-06	ENSG00000226259.6
G2E3	0.4663298	-2.1444051	-1.1005775	5.0189376 6	167.84182 1	2.1905E-38	3.1433E-37	ENSG00000092140.10
ZNF714	0.4658325 3	-2.1466942	-1.1021167	3.2944369 1	51.599194 3	6.807E-13	3.4414E-12	ENSG00000160352.11
RFWD3	0.4648221 9	-2.1513603	-1.1052491	5.8899808	270.47625 6	8.9354E-61	2.319E-59	ENSG00000168411.9
SFRP1	0.4644402 3	-2.1531296	-1.1064351	2.3801245 2	21.934875 3	2.8206E-06	8.1258E-06	ENSG00000104332.7

YOD1	0.46405144	-2.1549335	-1.1076434	3.54364863	53.476267	2.6174E-13	1.3562E-12	ENSG00000180667.6
HSD17B7	0.46398999	-2.1552189	-1.1078344	4.33271497	115.828813	5.1815E-27	5.2502E-26	ENSG00000132196.9
HAUS6	0.46371658	-2.1564897	-1.1086848	5.67090326	255.660703	1.515E-57	3.6061E-56	ENSG00000147874.6
CYP1A1	0.46306772	-2.1595114	-1.1107049	2.09942623	23.1035775	1.535E-06	4.5639E-06	ENSG00000140465.9
HOXD3	0.46228408	-2.163172	-1.1131484	1.27546647	9.98057505	0.001582	0.00316139	ENSG00000128652.7
NRN1	0.4609098	-2.1696219	-1.1174436	3.64715622	56.817337	4.7823E-14	2.595E-13	ENSG00000124785.4
TMEM170B	0.46048416	-2.1716274	-1.1187766	3.86479707	72.537023	1.6393E-17	1.087E-16	ENSG00000205269.4
PRDM1	0.46028211	-2.1725806	-1.1194097	1.65866272	13.311661	0.00026376	0.00059452	ENSG00000057657.10
RTKN2	0.45927639	-2.1773381	-1.1225655	2.58977624	33.243208	8.1323E-09	2.9543E-08	ENSG00000182010.6
SPINT2	0.45914426	-2.1779647	-1.1229806	3.55989286	58.932466	1.6318E-14	9.121E-14	ENSG00000167642.8
ARHGAP19	0.45842239	-2.1813943	-1.1252506	5.30654251	214.399782	1.5066E-48	2.8454E-47	ENSG00000213390.6
HPDL	0.45830116	-2.1819714	-1.1256322	2.85488974	37.701825	8.2427E-10	3.2819E-09	ENSG00000186603.4
H1F0	0.4581364	-2.1827561	-1.1261509	6.69605051	408.911304	6.3257E-91	2.9361E-89	ENSG00000189060.4
NRM	0.4581108	-2.182878	-1.1262315	4.27769564	65.126951	7.0226E-16	4.2545E-15	ENSG00000137404.10
DCLRE1B	0.45810889	-2.1828871	-1.1262375	4.20764527	98.510964	3.2323E-23	2.8083E-22	ENSG00000118655.4
RAB30-AS1	0.45787075	-2.1840225	-1.1269877	1.91861003	21.447258	3.637E-06	1.0344E-05	ENSG00000246067.3
TMEM106C	0.457854	-2.1841024	-1.1270405	5.74996011	256.602003	9.4453E-58	2.2616E-56	ENSG00000134291.7
PAGR1.1	0.45724474	-2.1870126	-1.1289615	3.66066344	63.256439	1.8147E-15	1.0746E-14	
MTL5	0.45639604	-2.1910795	-1.1316418	0.8024303	11.771911	0.00060131	0.00128801	ENSG00000132749.6
HMGN2	0.45537669	-2.1959842	-1.1348677	8.67486613	311.122654	1.2436E-69	3.8381E-68	ENSG00000198830.6
H2AFZ	0.45473999	-2.1990589	-1.1368862	8.49528788	327.883241	2.7786E-73	9.2887E-72	ENSG00000164032.7
ANKRD36C	0.45459611	-2.1997549	-1.1373428	2.81805001	35.151903	3.0496E-09	1.1501E-08	ENSG00000174501.10
C12orf66	0.4543348	-2.20102	-1.1381723	1.88281705	24.590688	7.0893E-07	2.1802E-06	ENSG00000174206.8

ZWILCH	0.45314622	-2.2067932	-1.1419514	5.67614453	210.478028	1.0804E-47	1.9966E-46	ENSG00000174442.7
CYBA	0.45273228	-2.2088109	-1.1432699	2.33109842	27.333282	1.7124E-07	5.5791E-07	ENSG00000051523.6
CSGALNACT1	0.45259301	-2.2094906	-1.1437138	3.53535755	66.741291	3.0958E-16	1.9149E-15	ENSG00000147408.10
RP1-193H18.2	0.45199843	-2.2123971	-1.1456103	1.13656622	13.654608	0.0002197	0.0005012	ENSG00000267194.1
MIS18A	0.45167857	-2.2139638	-1.1466316	4.28804758	106.028536	7.2681E-25	6.7679E-24	ENSG00000159055.3
DUT	0.45136367	-2.2155084	-1.1476378	6.18292517	260.265571	1.5019E-58	3.6394E-57	ENSG00000128951.9
POLE	0.45081622	-2.2181988	-1.1493887	5.88899267	270.076663	1.0919E-60	2.8218E-59	ENSG00000177084.12
C9orf64	0.45034639	-2.2205129	-1.150893	3.20362206	54.158226	1.8498E-13	9.7057E-13	ENSG00000165118.10
ACAT2	0.45014333	-2.2215147	-1.1515437	7.02700294	291.688083	2.1318E-65	6.0532E-64	ENSG00000120437.7
LRFN1	0.44853304	-2.2294902	-1.1567138	0.81588971	10.863049	0.00098102	0.00202687	ENSG00000128011.4
PHGDH	0.44733377	-2.2354673	-1.1605764	5.64147577	183.730485	7.4293E-42	1.1859E-40	ENSG00000092621.7
PCNA	0.44562104	-2.2440592	-1.1661107	7.14174415	259.104746	2.6894E-58	6.4783E-57	ENSG00000132646.6
GNB3	0.44517743	-2.2462954	-1.1675476	1.34788012	12.154431	0.00048971	0.00106197	ENSG00000111664.6
RAD21	0.44503486	-2.247015	-1.1680098	7.68060831	533.910782	3.982E-118	3.204E-116	ENSG00000164754.8
ALG10	0.44484355	-2.2479813	-1.1686301	2.12442662	27.358957	1.6898E-07	5.5085E-07	ENSG00000139133.2
C9orf40	0.44470454	-2.248684	-1.169081	3.15170253	51.778203	6.2138E-13	3.1521E-12	ENSG00000135045.6
SCLT1	0.44468468	-2.2487844	-1.1691454	3.88303707	99.089668	2.4132E-23	2.1073E-22	ENSG00000151466.7
CDKN2D	0.44448947	-2.2497721	-1.1697788	1.83850677	23.871066	1.0301E-06	3.1195E-06	ENSG00000129355.6
DLL4	0.44443536	-2.250046	-1.1699545	5.26971175	124.415367	6.8332E-29	7.4225E-28	ENSG00000128917.5
RP11-296I10.6	0.44433558	-2.2505513	-1.1702784	0.99693628	8.9339304	0.00279921	0.00536972	ENSG00000261556.4
SLC37A4	0.44297775	-2.2574497	-1.1746939	4.59323145	122.00532	2.3023E-28	2.4501E-27	ENSG00000137700.12
TNFRSF1B	0.44280645	-2.258323	-1.1752519	5.33413601	211.20707	7.4907E-48	1.3886E-46	ENSG00000028137.12
LLGL2	0.44191335	-2.2628871	-1.1781646	1.72116507	19.683747	9.1376E-06	2.4675E-05	ENSG00000073350.9

ROBO3	0.44086897	-2.2682476	-1.1815782	1.80010292	20.5804287	5.7178E-06	1.583E-05	ENSG00000154134.10
PKDCC	0.44007097	-2.2723607	-1.1841919	1.39894544	18.1616306	2.0293E-05	5.279E-05	ENSG00000162878.8
ECHDC3	0.44004311	-2.2725046	-1.1842832	1.754179	23.8955857	1.017E-06	3.0831E-06	ENSG00000134463.10
FAM161A	0.43985803	-2.2734608	-1.1848901	2.75844048	46.1961417	1.0699E-11	4.9601E-11	ENSG00000170264.8
SLC1A4	0.43979865	-2.2737678	-1.1850849	3.63776225	60.4382046	7.5925E-15	4.3302E-14	ENSG00000115902.6
KNSTRN	0.43936531	-2.2760104	-1.1865071	5.14939788	159.21771	1.6771E-36	2.3026E-35	ENSG00000128944.9
CENPL	0.43913102	-2.2772247	-1.1872767	3.69787845	79.215966	5.5678E-19	3.9642E-18	ENSG00000120334.11
XRCC3	0.43870283	-2.2794473	-1.1886841	4.03182012	105.731283	8.4444E-25	7.8329E-24	ENSG00000126215.9
DAW1	0.438261	-2.2817454	-1.1901378	1.57656338	21.3463699	3.8335E-06	1.086E-05	ENSG00000123977.5
LINC00341	0.43737883	-2.2863475	-1.1930447	2.84261333	37.0875419	1.1294E-09	4.4557E-09	ENSG00000229645.4
ACACB	0.43689702	-2.2888689	-1.1946348	1.01833692	13.7548761	0.00020828	0.00047695	ENSG00000076555.11
RUNDC3B	0.43662778	-2.2902803	-1.1955242	1.31035312	16.5191383	4.8161E-05	0.00012026	ENSG00000105784.11
MCM3	0.43657924	-2.2905349	-1.1956846	6.9081686	379.238662	1.8227E-84	7.8559E-83	ENSG00000112118.13
MALT1	0.43473327	-2.300261	-1.2017976	3.45552684	66.9386149	2.8009E-16	1.7352E-15	ENSG00000172175.8
LIPE	0.43266968	-2.311232	-1.2086621	3.69320735	85.0209578	2.9522E-20	2.2309E-19	ENSG00000079435.5
SYNE2	0.43244699	-2.3124222	-1.2094048	5.40342963	29.4458819	5.75E-08	1.9519E-07	ENSG00000054654.11
BRI3BP	0.43236991	-2.3128344	-1.209662	4.76145323	121.966005	2.3483E-28	2.4968E-27	ENSG00000184992.10
RNASEH2A	0.43227618	-2.3133359	-1.2099748	4.38928458	115.914765	4.9617E-27	5.0364E-26	ENSG00000104889.4
PXN-AS1	0.43207393	-2.3144187	-1.2106499	0.76267419	10.6927935	0.00107554	0.00220779	ENSG00000255857.1
RTTN	0.43139295	-2.3180722	-1.2129255	3.85275507	93.8145813	3.4651E-22	2.874E-21	ENSG00000176225.8
MYCL	0.43050631	-2.3228463	-1.2158937	0.98545945	13.7686127	0.00020676	0.00047374	ENSG00000116990.9
TSPYL5	0.43021543	-2.3244169	-1.2168688	2.84156197	44.443432	2.6181E-11	1.1728E-10	ENSG00000180543.3
PIM1	0.43015406	-2.3247485	-1.2170747	2.93790303	39.0144564	4.2068E-10	1.7082E-09	ENSG00000137193.9

CCDC77	0.42978576	-2.3267406	-1.2183104	3.474171	78.0585594	1.0003E-18	7.043E-18	ENSG00000120647.5
THAP10	0.42970245	-2.3271917	-1.2185901	2.27794362	25.2059119	5.1524E-07	1.6034E-06	ENSG00000129028.4
C5	0.4292913	-2.3294206	-1.2199712	1.0737679	15.4203083	8.6058E-05	0.00020813	ENSG00000106804.6
H1FX	0.42909698	-2.3304755	-1.2206243	6.26504152	201.190358	1.1483E-45	2.0055E-44	ENSG00000184897.4
ENTPD1	0.42876486	-2.3322807	-1.2217414	3.81110958	73.4619242	1.026E-17	6.8747E-17	ENSG00000138185.12
RMI1	0.42787937	-2.3371073	-1.224724	4.00170061	90.7633096	1.6193E-21	1.3054E-20	ENSG00000178966.11
CCSAP	0.42717909	-2.3409386	-1.2270871	3.61525887	77.3178384	1.4555E-18	1.0182E-17	ENSG00000154429.6
SLC2A10	0.42668263	-2.3436623	-1.2287647	3.09209092	62.7754864	2.3166E-15	1.3651E-14	ENSG00000197496.4
SUV39H2	0.42655484	-2.3443645	-1.2291969	4.56511067	150.624663	1.266E-34	1.6481E-33	ENSG00000152455.11
MYBL1	0.42628976	-2.3458222	-1.2300937	2.74121993	33.4093724	7.4663E-09	2.7213E-08	ENSG00000185697.12
CCDC15	0.4262784	-2.3458848	-1.2301322	2.32625029	35.265696	2.8765E-09	1.0884E-08	ENSG00000149548.10
ARL4D	0.42596173	-2.3476287	-1.2312043	1.78143888	19.6795149	9.1578E-06	2.4724E-05	ENSG00000175906.4
ANP32E	0.42573716	-2.3488671	-1.2319651	6.98454492	434.35627	1.8313E-96	9.4043E-95	ENSG00000143401.10
GLDC	0.42547941	-2.35029	-1.2328388	2.49941066	36.4089326	1.5997E-09	6.2214E-09	ENSG00000178445.8
VRK1	0.42535031	-2.3510033	-1.2332766	4.68129824	146.607883	9.5598E-34	1.2144E-32	ENSG00000100749.3
SH2D4A	0.42518853	-2.3518978	-1.2338254	1.04081936	15.4625839	8.4155E-05	0.00020391	ENSG00000104611.7
CBR3	0.42410013	-2.3579337	-1.2375232	3.49460662	76.650413	2.0406E-18	1.421E-17	ENSG00000159231.5
P2RX7	0.42308064	-2.3636156	-1.2409954	2.39735565	36.8887543	1.2507E-09	4.9162E-09	ENSG00000089041.12
C16orf59	0.42301714	-2.3639704	-1.241212	3.15703986	66.3468601	3.7816E-16	2.3284E-15	ENSG00000162062.10
CELSR2	0.42301084	-2.3640056	-1.2412335	1.52328759	15.9692998	6.4378E-05	0.00015817	ENSG00000143126.7
CSNK2B-LY6G5B-1181	0.42295206	-2.3643341	-1.2414339	1.23613991	17.2275776	3.3159E-05	8.4298E-05	ENSG00000263020.1
TIMELESS	0.42277695	-2.3653134	-1.2420314	5.8463917	323.022113	3.1815E-72	1.0321E-70	ENSG00000111602.7
ART4	0.42143118	-2.3728667	-1.246631	2.3845516	37.7170332	8.1787E-10	3.2585E-09	ENSG00000111339.6

ADAMTS9	0.42121622	-2.3740776	-1.2473671	5.93793688	266.047487	8.2483E-60	2.0738E-58	ENSG00000163638.9
SELENBP1	0.42086279	-2.3760713	-1.2485781	2.58148814	46.9200116	7.3944E-12	3.4817E-11	ENSG00000143416.16
HSPB6	0.42036179	-2.3789032	-1.2502966	2.08675654	26.4540931	2.6988E-07	8.6527E-07	ENSG00000004776.7
BRICD5	0.4200739	-2.3805335	-1.2512849	1.05225699	16.0952149	6.0236E-05	0.00014881	ENSG00000182685.3
AGMAT	0.41988995	-2.3815764	-1.2519168	0.7356687	13.4244022	0.00024837	0.00056225	ENSG00000116771.5
LBR	0.41914183	-2.3858273	-1.2544896	7.11680049	439.879055	1.1502E-97	6.1966E-96	ENSG00000143815.10
TRIM59	0.41903062	-2.3864604	-1.2548724	5.21664787	224.426821	9.7909E-51	1.9792E-49	ENSG00000213186.3
E2F7	0.41849088	-2.3895383	-1.2567319	5.27057345	239.06467	6.29E-54	1.3801E-52	ENSG00000165891.11
KCNJ12	0.41745467	-2.3954697	-1.2603085	1.01849707	16.3642167	5.2263E-05	0.00013004	ENSG00000184185.5
TBC1D30	0.41738818	-2.3958513	-1.2605384	2.54723819	42.1944092	8.2636E-11	3.5731E-10	ENSG00000111490.8
ELOVL6	0.41718409	-2.3970234	-1.261244	5.926862	316.420466	8.722E-71	2.7554E-69	ENSG00000170522.5
TRAIP	0.41703026	-2.3979075	-1.261776	2.65903442	46.5114878	9.1083E-12	4.2505E-11	ENSG00000183763.4
GEN1	0.4170162	-2.3979884	-1.2618247	4.07986639	88.7488178	4.4827E-21	3.5196E-20	ENSG00000178295.10
KCNK6	0.41673665	-2.399597	-1.2627921	3.28878769	70.0072878	5.9086E-17	3.809E-16	ENSG00000099337.3
ICA1L	0.41667057	-2.3999775	-1.2630209	1.59251307	18.6936358	1.5349E-05	4.0489E-05	ENSG00000163596.12
POLA1	0.4163985	-2.4015456	-1.2639632	5.04150873	213.827693	2.0082E-48	3.7808E-47	ENSG00000101868.6
IGFLR1	0.41618672	-2.4027677	-1.2646972	0.69420228	12.0604253	0.00051504	0.00111348	ENSG00000126246.5
ZNF467	0.41604124	-2.4036079	-1.2652015	1.48306669	17.7252085	2.5522E-05	6.5742E-05	ENSG00000181444.8
DNMT1	0.41582174	-2.4048767	-1.2659629	7.48489744	503.972034	1.299E-111	9.39E-110	ENSG00000130816.10
EZH2	0.41524384	-2.4082236	-1.2679693	5.15985468	249.145626	3.9875E-56	9.1835E-55	ENSG00000106462.6
DBNDD2	0.41521269	-2.4084042	-1.2680776	3.17653723	67.0887118	2.5956E-16	1.6113E-15	ENSG00000244274.3
CENPO	0.41391793	-2.4159379	-1.2725834	5.50498591	264.833908	1.5166E-59	3.7815E-58	ENSG00000138092.6
PASK	0.4135315	-2.4181955	-1.2739309	3.91999549	75.0826359	4.5142E-18	3.0839E-17	ENSG00000115687.9

CCDC138	0.41314387	-2.4204643	-1.2752838	2.71010019	44.5556489	2.4723E-11	1.1095E-10	ENSG00000163006.7
WHSC1	0.41250081	-2.4242377	-1.2775311	7.70463364	575.912453	2.905E-127	2.898E-125	ENSG00000109685.13
DNMT3B	0.40976708	-2.4404108	-1.287124	3.28335945	60.6631659	6.7726E-15	3.8772E-14	ENSG00000088305.14
SNHG1	0.4074505	-2.4542858	-1.2953033	4.99089098	157.306029	4.3881E-36	5.977E-35	ENSG00000255717.2
FCHO1	0.406056	-2.4627145	-1.3002494	1.59267983	19.0680405	1.2614E-05	3.3567E-05	ENSG00000130475.10
SMIM10	0.40603986	-2.4628124	-1.3003067	2.4357501	36.4912807	1.5335E-09	5.9775E-09	ENSG00000184785.4
CENPW	0.40569905	-2.4648813	-1.3015182	3.87766404	58.5227664	2.0095E-14	1.1181E-13	ENSG00000203760.4
SMAD9	0.40568773	-2.4649501	-1.3015584	2.72768126	51.9561013	5.6755E-13	2.8875E-12	ENSG00000120693.9
DONSON	0.40515982	-2.4681618	-1.303437	4.56877612	163.675665	1.7808E-37	2.5018E-36	ENSG00000159147.13
RP11-468E2.4	0.40503908	-2.4688976	-1.303867	0.76378157	9.40893547	0.00215931	0.00421522	ENSG00000259529.1
RHPN2	0.40452998	-2.4720047	-1.3056815	1.38245181	20.8240544	5.0347E-06	1.4048E-05	ENSG00000131941.3
MYSM1	0.40392131	-2.4757298	-1.3078538	3.85609074	85.0668511	2.8845E-20	2.1838E-19	ENSG00000162601.5
CDC25A	0.40369037	-2.477146	-1.3086789	4.96333676	220.510061	7.0005E-50	1.3759E-48	ENSG00000164045.7
NDC1	0.4036862	-2.4771716	-1.3086938	6.15487897	308.990435	3.6237E-69	1.1015E-67	ENSG00000058804.10
LINC00342	0.40245005	-2.4847804	-1.3131184	1.80838361	15.8181314	6.9731E-05	0.00017066	ENSG00000232931.1
CDC25B	0.40229618	-2.4857308	-1.31367	6.37484782	443.24233	2.132E-98	1.159E-96	ENSG00000101224.13
EXOSC8	0.40169105	-2.4894754	-1.3158418	4.9936234	133.106126	8.5706E-31	9.8976E-30	ENSG00000120699.8
MMS22L	0.40137577	-2.4914309	-1.3169746	4.3665795	105.916529	7.6907E-25	7.1449E-24	ENSG00000146263.7
MIR4453	0.400645	-2.4959752	-1.3196036	1.25466792	20.5223872	5.8938E-06	1.6287E-05	ENSG00000268471.3
WDHD1	0.40064304	-2.4959875	-1.3196107	5.03313397	247.368838	9.729E-56	2.2237E-54	ENSG00000198554.7
DSN1	0.40004671	-2.4997081	-1.3217596	4.71214275	171.42771	3.6087E-39	5.3109E-38	ENSG00000149636.11
RAD18	0.39986752	-2.5008283	-1.322406	4.49946141	176.325048	3.0751E-40	4.7094E-39	ENSG00000070950.5
FOXC1	0.39942381	-2.5036064	-1.3240078	3.93681945	81.4805025	1.77E-19	1.2907E-18	ENSG00000054598.5

FIGNL1	0.39773629	-2.5142287	-1.3301159	5.4623235	247.075194	1.1274E-55	2.572E-54	ENSG00000132436.7
VDR	0.39738006	-2.5164792	-1.3314067	0.7891363	15.639099	7.6653E-05	0.0001868	ENSG00000111424.6
CCDC171	0.39728269	-2.5170993	-1.3317621	1.0631197	14.644758	0.0001298	0.0003068	ENSG00000164989.11
SLC1A1	0.39669222	-2.520846	-1.333908	4.1357495	140.528212	2.0404E-32	2.5049E-31	ENSG00000106688.7
PCDH7	0.39602905	-2.5250673	-1.3363218	4.6340285	192.784353	7.8449E-44	1.3241E-42	ENSG00000169851.11
PLCXD1.1	0.39573715	-2.5269298	-1.3373856	1.6208212	23.120989	1.5212E-06	4.5261E-06	
CKAP2	0.39503942	-2.5313929	-1.3399315	6.5842902	426.423156	9.7588E-95	4.907E-93	ENSG00000136108.10
CLDN7	0.39479621	-2.5329524	-1.3408199	3.0489841	58.046952	2.5594E-14	1.4116E-13	ENSG00000181885.14
DHRS13	0.39464095	-2.5339489	-1.3413874	1.7872536	31.196518	2.3323E-08	8.182E-08	ENSG00000167536.9
PELI2	0.39432626	-2.5359711	-1.3425383	2.4052120	32.288601	1.3289E-08	4.7462E-08	ENSG00000139946.5
SLC27A5	0.39347832	-2.5414361	-1.345644	1.1158035	19.366818	1.0787E-05	2.8921E-05	ENSG00000083807.5
GINS4	0.39320818	-2.5431821	-1.3466348	4.6271862	186.03708	2.3302E-42	3.7696E-41	ENSG00000147536.7
CYB5R2	0.39229623	-2.5490941	-1.3499846	2.0925127	35.300083	2.8262E-09	1.0708E-08	ENSG00000166394.10
RP11-424C20.2	0.39111182	-2.5568135	-1.3543469	4.0931115	100.982965	9.2778E-24	8.2692E-23	ENSG00000256663.1
CIDEA	0.39106901	-2.5570934	-1.3545049	2.2900381	40.389885	2.0802E-10	8.6953E-10	ENSG00000176194.13
AC005562.1	0.39068983	-2.5595752	-1.3559044	2.0330789	34.720579	3.8059E-09	1.4242E-08	ENSG00000214719.7
DIAPH3	0.39023256	-2.5625745	-1.3575939	5.681422	383.333702	2.3398E-85	1.0305E-83	ENSG00000139734.13
C10orf128	0.38910345	-2.5700106	-1.3617743	2.9514938	58.071130	2.5281E-14	1.395E-13	ENSG00000204161.9
DANCR	0.38891057	-2.5712852	-1.3624896	4.9826257	264.420476	1.8663E-59	4.6153E-58	ENSG00000226950.2
DCP2	0.3888391	-2.5717579	-1.3627548	5.0503491	190.897515	2.025E-43	3.38E-42	ENSG00000172795.11
CEP152	0.38776315	-2.5788939	-1.3667524	3.7949396	93.646318	3.7726E-22	3.1204E-21	ENSG00000103995.9
ETV4	0.38729849	-2.5819879	-1.3684822	4.9198238	225.83947	4.8164E-51	9.8515E-50	ENSG00000175832.8
ECT2	0.38637334	-2.5881703	-1.3719325	5.9411694	336.108956	4.4904E-75	1.5753E-73	ENSG00000114346.9

EFEMP1	0.38528824	-2.5954594	-1.3759899	10.5092425	659.988164	1.503E-145	2.061E-143	ENSG00000115380.14
LIN9	0.38511087	-2.5966548	-1.3766543	3.61682517	88.8268786	4.3092E-21	3.3901E-20	ENSG00000183814.11
SHMT1	0.38270836	-2.6129557	-1.3856827	4.70740268	217.888163	2.6124E-49	5.0604E-48	ENSG00000176974.13
ZBTB16	0.38253767	-2.6141216	-1.3863263	1.56886559	22.6215895	1.9726E-06	5.7919E-06	ENSG00000109906.9
GINS3	0.38242587	-2.6148859	-1.386748	4.41510201	171.904048	2.84E-39	4.195E-38	ENSG00000181938.9
UBE2S	0.3824045	-2.615032	-1.3868286	6.91080789	323.636598	2.3377E-72	7.6246E-71	ENSG00000108106.9
EVI2B	0.38238312	-2.6151782	-1.3869093	2.66559175	52.1377235	5.1741E-13	2.6402E-12	ENSG00000185862.5
RFC3	0.38166641	-2.6200891	-1.3896159	4.66870116	186.053378	2.3112E-42	3.7439E-41	ENSG00000133119.8
DBF4B	0.38123299	-2.6230678	-1.3912551	3.62595522	88.2509511	5.7656E-21	4.5093E-20	ENSG00000161692.13
HIF3A	0.37999868	-2.6315881	-1.3959337	1.22688553	20.0151158	7.6832E-06	2.0968E-05	ENSG00000124440.11
C14orf80	0.37949823	-2.6350584	-1.3978349	3.50994713	90.5737774	1.7821E-21	1.4318E-20	ENSG00000185347.13
TPD52	0.37923405	-2.636894	-1.3988396	4.38861454	148.726357	3.2912E-34	4.2254E-33	ENSG00000076554.11
TMEM194A	0.37903154	-2.6383029	-1.3996102	4.92368925	231.241137	3.1965E-52	6.7795E-51	ENSG00000166881.5
TCF7	0.37897639	-2.6386868	-1.3998201	1.07286486	18.8375027	1.4234E-05	3.7637E-05	ENSG00000081059.15
DEK	0.37764703	-2.6479753	-1.4048897	7.63473145	598.618537	3.344E-132	3.603E-130	ENSG00000124795.10
PHF19	0.37690886	-2.6531613	-1.4077124	6.47039229	372.937355	4.2919E-83	1.811E-81	ENSG00000119403.9
TONSL	0.37595181	-2.6599154	-1.4113804	4.49074549	178.631309	9.6442E-41	1.4921E-39	ENSG00000160949.12
CEP128	0.37583316	-2.6607551	-1.4118357	3.5760373	111.645646	4.2724E-26	4.1613E-25	ENSG00000100629.12
SUV39H1	0.37529197	-2.664592	-1.4139147	4.66219216	208.898149	2.3892E-47	4.3555E-46	ENSG00000101945.12
C1orf21	0.37520677	-2.6651971	-1.4142422	3.06876186	64.1521324	1.1517E-15	6.9081E-15	ENSG00000116667.8
DHH	0.37432027	-2.6715091	-1.4176549	1.591093	29.1770038	6.6059E-08	2.2312E-07	ENSG00000139549.2
CHTF18	0.37427265	-2.671849	-1.4178385	4.53739046	181.635568	2.1297E-41	3.3509E-40	ENSG00000127586.12
CDKN1C	0.37412792	-2.6728826	-1.4183965	0.62285506	14.6879247	0.00012686	0.00030024	ENSG00000129757.8

RAD54B	0.37394669	-2.674178	-1.4190955	3.28550826	90.0563774	2.3147E-21	1.8524E-20	ENSG00000197275.8
U82695.10	0.37334802	-2.678466	-1.421407	0.4346741	12.9122534	0.00032644	0.0007247	ENSG00000259886.1
ADRBK2	0.37269451	-2.6831627	-1.4239345	0.9962402	20.3365264	6.4949E-06	1.7875E-05	ENSG00000100077.10
CHAF1B	0.37066158	-2.6978787	-1.4318255	4.4271251	167.329954	2.8337E-38	4.0426E-37	ENSG00000159259.7
GMFG	0.36976872	-2.7043931	-1.4353049	3.4639775	87.051208	1.0575E-20	8.1805E-20	ENSG00000130755.8
CENPJ	0.36966469	-2.7051542	-1.4357109	4.2154483	152.674309	4.5129E-35	5.9651E-34	ENSG00000151849.10
ZNF695	0.36884044	-2.7111995	-1.4389313	0.9610638	17.9460971	2.2725E-05	5.8851E-05	ENSG00000197472.10
TMEM121	0.36760401	-2.7203185	-1.4437756	0.9620003	19.3222633	1.1041E-05	2.9564E-05	ENSG00000184986.6
CENPP	0.3667144	-2.7269177	-1.4472712	2.8194435	70.2780462	5.1508E-17	3.3365E-16	ENSG00000188312.9
AC004381.6	0.36655983	-2.7280676	-1.4478794	1.7548195	31.0016059	2.5782E-08	9.0105E-08	ENSG00000005189.15
FANCG	0.36636395	-2.7295262	-1.4486505	4.6330862	205.57834	1.2665E-46	2.271E-45	ENSG00000221829.5
FANCE	0.36527597	-2.7376561	-1.4529412	3.4786714	109.593092	1.2032E-25	1.1487E-24	ENSG00000112039.3
IGFBP2	0.36494623	-2.7401297	-1.4542442	5.8787238	453.706222	1.126E-100	6.565E-99	ENSG00000115457.5
CCNF	0.36488708	-2.7405739	-1.454478	6.1273283	310.127155	2.0489E-69	6.2917E-68	ENSG00000162063.8
TMEM97	0.36487858	-2.7406377	-1.4545116	5.8896550	362.439185	8.2883E-81	3.3341E-79	ENSG00000109084.9
DNA2	0.36401493	-2.7471401	-1.4579305	3.8416778	137.39372	9.8897E-32	1.1887E-30	ENSG00000138346.10
PM20D2	0.36393562	-2.7477387	-1.4582448	4.6637552	202.109626	7.2356E-46	1.271E-44	ENSG00000146281.5
TBC1D31	0.36384161	-2.7484487	-1.4586176	3.1777174	78.1901158	9.3586E-19	6.5931E-18	ENSG00000156787.12
SFXN2	0.36330501	-2.7525082	-1.4607468	3.156762	75.2371923	4.1743E-18	2.8622E-17	ENSG00000156398.8
BORA	0.36259773	-2.7578771	-1.4635582	3.7872364	120.765028	4.3018E-28	4.5222E-27	ENSG00000136122.11
ANKRD32	0.36258888	-2.7579444	-1.4635934	3.3093739	79.0796456	5.9656E-19	4.2423E-18	ENSG00000133302.8
C18orf54	0.36031066	-2.7753828	-1.4726867	4.7682489	249.312346	3.6674E-56	8.4623E-55	ENSG00000166845.9
UHRF1	0.35996223	-2.7780693	-1.4740826	6.4602850	461.444606	2.331E-102	1.435E-100	ENSG00000034063.9

STEAP1	0.35977928	-2.7794819	-1.474816	5.07945957	305.771087	1.8217E-68	5.5099E-67	ENSG00000164647.4
RRM1	0.35956159	-2.7811647	-1.4756892	6.94547846	657.34563	5.644E-145	7.653E-143	ENSG00000167325.10
LRRCC1	0.35910415	-2.7847075	-1.4775258	2.18427475	45.3266315	1.6677E-11	7.6088E-11	ENSG00000133739.11
HMHA1	0.3590954	-2.7847753	-1.4775609	3.38435125	69.2883906	8.5069E-17	5.4261E-16	ENSG00000180448.6
GIPC2	0.35891717	-2.7861582	-1.4782772	3.63145244	112.909176	2.2589E-26	2.2253E-25	ENSG00000137960.5
DBF4	0.3583822	-2.7903171	-1.4804291	4.93524037	264.458681	1.8309E-59	4.537E-58	ENSG00000006634.3
CCDC18	0.3576984	-2.7956513	-1.4831844	3.50897679	96.0006113	1.1485E-22	9.7194E-22	ENSG00000122483.13
USP1	0.35647906	-2.8052139	-1.4881108	6.08910008	539.963327	1.92E-119	1.609E-117	ENSG00000162607.8
SALL2	0.35454529	-2.8205141	-1.4959582	1.08502182	17.1950534	3.3731E-05	8.5609E-05	ENSG00000165821.7
PBX1	0.35428459	-2.8225896	-1.4970194	3.31373495	74.6965147	5.4893E-18	3.7258E-17	ENSG00000185630.14
STC1	0.35409664	-2.8240878	-1.497785	3.92838569	150.596794	1.2839E-34	1.6696E-33	ENSG00000159167.7
PLA2G3	0.35388061	-2.8258118	-1.4986654	0.90219538	20.5247883	5.8864E-06	1.6271E-05	ENSG00000100078.3
SCML1	0.35387282	-2.825874	-1.4986971	3.83917211	138.574977	5.4556E-32	6.6303E-31	ENSG00000047634.10
GK	0.35345496	-2.8292148	-1.5004017	2.89641645	68.8468204	1.0642E-16	6.7308E-16	ENSG00000198814.8
TDRP	0.35306674	-2.8323257	-1.5019872	1.85093604	39.9204226	2.6452E-10	1.0944E-09	ENSG00000180190.7
MTBP	0.3530645	-2.8323437	-1.5019963	3.11510627	61.6954466	4.0091E-15	2.3193E-14	ENSG00000172167.3
RFC5	0.35288442	-2.833789	-1.5027323	4.42707554	226.752694	3.0447E-51	6.2703E-50	ENSG00000111445.9
SLC16A9	0.35278607	-2.834579	-1.5031345	2.02232699	30.2111785	3.8747E-08	1.3341E-07	ENSG00000165449.7
ADAMTS3	0.35271864	-2.8351209	-1.5034103	0.62225634	17.2974574	3.1961E-05	8.1391E-05	ENSG00000156140.4
RBPMS2	0.35233241	-2.8382289	-1.5049909	1.49028242	32.032966	1.5158E-08	5.3944E-08	ENSG00000166831.4
TAF5	0.35165071	-2.8437309	-1.507785	3.45974854	112.364655	2.9728E-26	2.9096E-25	ENSG00000148835.9
RPGR	0.35097834	-2.8491787	-1.5105461	3.85999876	119.923048	6.5763E-28	6.8653E-27	ENSG00000156313.8
MASTL	0.35081632	-2.8504945	-1.5112122	4.39326431	225.955353	4.5441E-51	9.3103E-50	ENSG00000120539.10

CHAF1A	0.35079211	-2.8506913	-1.5113118	5.78980968	372.03744	6.7388E-83	2.8238E-81	ENSG00000167670.11
ANKRD33	0.35006109	-2.8566442	-1.5143214	0.96203339	20.2279713	6.874E-06	1.8849E-05	ENSG00000167612.8
IMPA2	0.34998269	-2.8572842	-1.5146445	2.01542676	34.203397	4.9642E-09	1.8371E-08	ENSG00000141401.7
RP11-798M19.6	0.34961631	-2.8602785	-1.5161556	0.74937593	16.8774024	3.9873E-05	0.00010027	ENSG00000272870.1
FAM72A	0.34957392	-2.8606253	-1.5163305	2.59530123	62.7337825	2.3662E-15	1.3923E-14	ENSG00000196550.6
KIF18A	0.34848507	-2.8695634	-1.5208312	4.22241664	169.392856	1.0041E-38	1.4617E-37	ENSG00000121621.6
SULT1C4	0.34787893	-2.8745633	-1.5233428	2.56639861	47.218542	6.3497E-12	3.0062E-11	ENSG00000198075.5
CDC7	0.34690236	-2.8826555	-1.5273984	3.78613369	130.216014	3.6752E-30	4.1568E-29	ENSG00000097046.8
CGN	0.34683621	-2.8832053	-1.5276736	1.47337195	29.5480988	5.4546E-08	1.8548E-07	ENSG00000143375.10
C1orf112	0.34646818	-2.8862679	-1.5292052	3.72279334	132.876353	9.6222E-31	1.1101E-29	ENSG00000000460.12
HSPA2	0.34564504	-2.8931415	-1.5326369	1.97606944	39.6007907	3.1156E-10	1.281E-09	ENSG00000126803.8
ZNF366	0.34485432	-2.8997752	-1.5359411	1.43304669	18.8500307	1.4141E-05	3.7399E-05	ENSG00000178175.7
MIS18BP1	0.344783	-2.900375	-1.5362395	5.43294673	275.774504	6.2579E-62	1.6598E-60	ENSG00000129534.9
MCM7	0.34384039	-2.9083262	-1.5401891	7.66523755	807.800122	1.087E-177	2.082E-175	ENSG00000166508.13
CTSH	0.34320051	-2.9137486	-1.5428764	1.48169593	28.2851286	1.047E-07	3.473E-07	ENSG00000103811.11
LURAP1	0.34183159	-2.9254171	-1.5486424	0.93802663	21.4224695	3.6843E-06	1.0469E-05	ENSG00000171357.5
FEN1	0.34171229	-2.9264385	-1.549146	6.28783092	436.213377	7.2205E-97	3.8051E-95	ENSG00000168496.3
RPL39L	0.34100866	-2.9324768	-1.5521197	3.22423121	86.3901786	1.4772E-20	1.1333E-19	ENSG00000163923.5
SLAIN1	0.34096772	-2.9328289	-1.5522929	1.98813451	42.501538	7.0627E-11	3.0681E-10	ENSG00000139737.17
PIK3CG	0.33929898	-2.9472532	-1.559371	3.65731765	101.302087	7.8973E-24	7.0648E-23	ENSG00000105851.6
SHROOM3	0.33921057	-2.9480213	-1.559747	3.96777428	153.33111	3.2427E-35	4.3193E-34	ENSG00000138771.10
NAGS	0.33893536	-2.9504151	-1.5609179	3.15741543	95.9427494	1.1825E-22	9.9936E-22	ENSG00000161653.6
TYMS	0.33861324	-2.9532218	-1.5622897	7.27573919	733.81314	1.328E-161	2.165E-159	ENSG00000176890.11

RBL1	0.33776903	-2.960603	-1.5658911	4.74302759	297.339789	1.2513E-66	3.7011E-65	ENSG00000269846.1
RBL1	0.33776903	-2.960603	-1.5658911	4.74302759	297.339789	1.2513E-66	3.7011E-65	ENSG00000080839.7
C17orf96	0.33691439	-2.9681131	-1.5695461	2.42947696	35.909748	2.0667E-09	7.9431E-09	ENSG00000179294.5
SNHG10	0.33577716	-2.9781656	-1.574424	2.56003772	50.372598	1.2716E-12	6.3332E-12	ENSG00000247092.2
CENPK	0.33536502	-2.9818256	-1.5761959	4.32375038	206.731945	7.094E-47	1.2778E-45	ENSG00000123219.8
AC137932.6	0.33535629	-2.9819032	-1.5762334	0.90217949	22.551896	2.0454E-06	5.9957E-06	ENSG00000261253.1
TMPO-AS1	0.33517685	-2.9834996	-1.5770056	1.85112754	39.488889	3.2994E-10	1.3534E-09	ENSG00000257167.2
CLSPN	0.33455854	-2.9890135	-1.5796694	5.56402537	433.623233	2.6442E-96	1.3464E-94	ENSG00000092853.9
INCENP	0.33434603	-2.9909133	-1.5805861	5.92594799	533.9881	3.831E-118	3.103E-116	ENSG00000149503.8
TMPO	0.33402153	-2.993819	-1.581987	7.40360685	617.582517	2.509E-136	2.857E-134	ENSG00000120802.9
C21orf58	0.33380176	-2.9957901	-1.5829365	2.7064523	67.382249	2.2365E-16	1.3927E-15	ENSG00000160298.13
MCM2	0.33358468	-2.9977396	-1.5838751	6.63751721	526.746552	1.441E-116	1.122E-114	ENSG00000073111.9
GMNN	0.33297502	-3.0032283	-1.5865142	5.04687093	300.620832	2.4128E-67	7.1541E-66	ENSG00000112312.5
C4orf21	0.3303471	-3.027119	-1.5979454	3.02069999	92.322562	7.364E-22	6.0168E-21	ENSG00000138658.11
TRIP13	0.33005726	-3.0297773	-1.5992118	5.734854	361.27364	1.4868E-80	5.9413E-79	ENSG00000071539.9
C21orf91	0.33005288	-3.0298175	-1.5992309	2.18921961	50.327263	1.3013E-12	6.4732E-12	ENSG00000154642.6
NCAPD3	0.33005136	-3.0298315	-1.5992376	5.95956173	466.514553	1.838E-103	1.155E-101	ENSG00000151503.8
MCM4	0.32821488	-3.0467845	-1.6072874	7.04782229	596.905288	7.887E-132	8.423E-130	ENSG00000104738.12
FANCA	0.32815176	-3.0473705	-1.6075649	4.56670779	257.027553	7.6287E-58	1.8303E-56	ENSG00000187741.10
ANKRD55	0.32800624	-3.0487225	-1.6082048	1.30111528	31.312074	2.1971E-08	7.7145E-08	ENSG00000164512.13
BAIAP2L1	0.32723917	-3.0558689	-1.6115827	0.41741065	15.137148	9.9977E-05	0.0002401	ENSG00000006453.9
LBH	0.32562872	-3.0709822	-1.6187001	0.76230493	20.691678	5.395E-06	1.4984E-05	ENSG00000213626.7
DSCC1	0.3251729	-3.075287	-1.6207211	2.37319116	54.442517	1.6006E-13	8.4424E-13	ENSG00000136982.5

PRR11	0.32507217	-3.07624	-1.6211681	6.15822768	612.433204	3.308E-135	3.696E-133	ENSG00000068489.8
ORC6	0.32491451	-3.0777327	-1.6218679	4.30784729	218.427162	1.9928E-49	3.8789E-48	ENSG00000091651.4
IRAK3	0.32490191	-3.077852	-1.6219239	3.43854543	111.86469	3.8255E-26	3.7321E-25	ENSG00000090376.4
NCAPD2	0.32426381	-3.0839087	-1.6247601	7.27852219	842.610376	2.938E-185	6.819E-183	ENSG00000010292.8
HAUS8	0.32393652	-3.0870246	-1.626217	3.63290036	133.597266	6.6922E-31	7.773E-30	ENSG00000131351.10
MCM6	0.32385686	-3.0877839	-1.6265718	6.49897789	533.85253	4.1E-118	3.277E-116	ENSG00000076003.4
UBE2T	0.32350881	-3.0911059	-1.6281231	4.63536107	296.351684	2.0542E-66	6.061E-65	ENSG00000077152.5
CKS1B	0.32331968	-3.0929141	-1.6289668	5.45675182	372.148542	6.3737E-83	2.6801E-81	ENSG00000173207.8
CKS1B	0.32331968	-3.0929141	-1.6289668	5.45675182	372.148542	6.3737E-83	2.6801E-81	ENSG00000268942.1
CENPE	0.3233168	-3.0929416	-1.6289796	6.26773697	381.020527	7.4607E-85	3.2504E-83	ENSG00000138778.7
SLCO4A1	0.32266024	-3.0992352	-1.6319123	2.64652369	64.4750702	9.7761E-16	5.8842E-15	ENSG00000101187.11
MCM8	0.32079168	-3.1172878	-1.6402914	4.28659053	201.985348	7.7018E-46	1.351E-44	ENSG00000125885.9
DHFR	0.32063488	-3.1188122	-1.6409967	6.0976965	355.093539	3.2959E-79	1.2667E-77	ENSG00000228716.2
TPX2	0.320041	-3.1245997	-1.6436714	7.47787808	823.817915	3.579E-181	7.198E-179	ENSG00000088325.11
MCM5	0.31950397	-3.1298516	-1.6460942	6.93585184	485.531569	1.337E-107	8.768E-106	ENSG00000100297.11
TBXAS1	0.31934577	-3.131402	-1.6468087	0.84047103	23.227385	1.4393E-06	4.2963E-06	ENSG00000059377.11
RFC4	0.31919483	-3.1328828	-1.6474908	4.2545583	226.193266	4.0323E-51	8.2759E-50	ENSG00000163918.6
AURKA	0.31891658	-3.1356162	-1.648749	5.87699948	497.671687	3.052E-110	2.141E-108	ENSG00000087586.13
DHFRP1	0.31877711	-3.1369881	-1.64938	3.73900365	148.188651	4.3141E-34	5.5151E-33	ENSG00000188985.5
IQCC	0.31861559	-3.1385784	-1.6501112	1.20607475	23.5082166	1.2438E-06	3.7321E-06	ENSG00000160051.7
PARPBP	0.31834121	-3.1412835	-1.6513542	4.09850579	199.869711	2.2298E-45	3.8718E-44	ENSG00000185480.7
H2AFX	0.31747995	-3.1498052	-1.6552626	6.70368341	677.406053	2.449E-149	3.437E-147	ENSG00000188486.3
C17orf53	0.31729569	-3.1516344	-1.6561002	2.8506712	74.7051031	5.4655E-18	3.7117E-17	ENSG00000125319.10

OIP5	0.31572137	-3.1673498	-1.6632762	3.15492379	109.059282	1.575E-25	1.4978E-24	ENSG00000104147.4
MBOAT1	0.31551055	-3.1694661	-1.6642398	1.88730997	45.5697776	1.473E-11	6.7589E-11	ENSG00000172197.9
ANKLE1	0.31512358	-3.1733582	-1.6660104	2.44272505	64.2655903	1.0873E-15	6.5313E-15	ENSG00000160117.10
SOX18	0.31478773	-3.1767439	-1.6675488	6.01632143	138.796928	4.8787E-32	5.9411E-31	ENSG00000203883.5
PAQR4	0.31421019	-3.182583	-1.6701981	4.69059382	267.291762	4.4174E-60	1.1153E-58	ENSG00000162073.9
DNM3	0.31404054	-3.1843022	-1.6709773	0.80129875	22.5786277	2.0172E-06	5.92E-06	ENSG00000197959.9
KIF23	0.31272457	-3.1977021	-1.6770355	5.98990075	558.653292	1.65E-123	1.52E-121	ENSG00000137807.9
TACC3	0.31267555	-3.1982034	-1.6772617	6.98644244	641.83953	1.33E-141	1.655E-139	ENSG00000013810.14
MELK	0.31234164	-3.2016224	-1.6788032	5.58196981	507.355369	2.386E-112	1.745E-110	ENSG00000165304.3
FANCI	0.31215813	-3.2035046	-1.679651	6.05002365	393.168463	1.6909E-87	7.5575E-86	ENSG00000140525.13
SMC4	0.31214728	-3.203616	-1.6797012	7.63648489	829.618612	1.961E-182	4.081E-180	ENSG00000113810.11
GPSM2	0.31127402	-3.2126034	-1.6837429	4.46949453	215.361664	9.2933E-49	1.7746E-47	ENSG00000121957.8
LMO7	0.31026709	-3.2230295	-1.6884174	3.73675756	127.89667	1.1824E-29	1.3164E-28	ENSG00000136153.15
PSMC3IP	0.31000263	-3.2257791	-1.6896477	3.65613352	156.233245	7.5283E-36	1.0197E-34	ENSG00000131470.10
SMC2	0.30893902	-3.2368848	-1.694606	6.16118031	490.974259	8.746E-109	5.93E-107	ENSG00000136824.14
SLC7A2	0.30792354	-3.2475595	-1.6993559	4.32799297	199.255327	3.0363E-45	5.2646E-44	ENSG00000003989.12
CCNB1	0.30783558	-3.2484874	-1.6997681	6.89113255	501.635421	4.189E-111	3.009E-109	ENSG00000134057.10
RECQL4	0.30774517	-3.2494418	-1.7001919	4.59711666	252.093747	9.078E-57	2.1355E-55	ENSG00000160957.8
EBF3	0.30651871	-3.2624436	-1.705953	1.19661233	30.7369658	2.9548E-08	1.0276E-07	ENSG00000108001.9
RACGAP1	0.30633468	-3.2644035	-1.7068194	5.54574842	386.992973	3.7369E-86	1.6519E-84	ENSG00000161800.8
POC1A	0.30568188	-3.2713748	-1.7098971	4.12558231	199.104545	3.2752E-45	5.6708E-44	ENSG00000164087.3
ARHGEF39	0.30437519	-3.2854189	-1.7160773	2.40361152	70.3550236	4.9537E-17	3.214E-16	ENSG00000137135.13
HMGB1P5	0.3042132	-3.2871684	-1.7168454	3.63432121	131.653599	1.7814E-30	2.0397E-29	ENSG00000132967.9

CDC20	0.30388767	-3.2906896	-1.71839	6.96005502	664.760906	1.377E-146	1.91E-144	ENSG00000117399.9
PDE3B	0.30350574	-3.2948306	-1.7202043	1.61271318	34.3976355	4.4927E-09	1.6724E-08	ENSG00000152270.4
ZWINT	0.30316773	-3.2985041	-1.7218119	6.0149732	420.774203	1.6555E-93	8.0559E-92	ENSG00000122952.12
RFTN2	0.30229907	-3.3079824	-1.7259516	1.25498875	29.3608629	6.0079E-08	2.0355E-07	ENSG00000162944.6
FAM83D	0.30180942	-3.3133492	-1.7282903	5.63497216	576.575852	2.084E-127	2.096E-125	ENSG00000101447.9
YAP1	0.30066427	-3.3259689	-1.7337747	5.09938241	413.151886	7.5518E-92	3.5599E-90	ENSG00000137693.9
AGAP5	0.30058299	-3.3268682	-1.7341647	0.57768615	20.7810043	5.1491E-06	1.4344E-05	ENSG00000172650.8
ZNF141	0.30055941	-3.3271292	-1.7342779	1.21598276	32.182038	1.4038E-08	5.0063E-08	ENSG00000131127.9
PTTG1	0.30050899	-3.3276874	-1.7345199	5.48640074	263.258332	3.3442E-59	8.2532E-58	ENSG00000164611.8
CDCA7	0.29998782	-3.3334687	-1.7370242	5.15306773	358.662547	5.5057E-80	2.1572E-78	ENSG00000144354.9
AUNIP	0.29961451	-3.337622	-1.7388206	1.85635324	48.5975787	3.1426E-12	1.5249E-11	ENSG00000127423.6
HELLS	0.29897518	-3.3447593	-1.7419024	4.77816336	343.061751	1.3743E-76	4.9656E-75	ENSG00000119969.10
BARD1	0.29888419	-3.3457775	-1.7423415	3.51155062	128.290465	9.6962E-30	1.0835E-28	ENSG00000138376.6
KIAA1524	0.29868673	-3.3479893	-1.7432949	5.07177254	424.58858	2.4474E-94	1.2154E-92	ENSG00000163507.9
STIL	0.29867992	-3.3480657	-1.7433278	5.25168617	379.601353	1.5197E-84	6.5733E-83	ENSG00000123473.11
DEPDC1B	0.29726141	-3.3640425	-1.7501959	4.15069399	187.651195	1.0352E-42	1.7091E-41	ENSG00000035499.8
MSH5	0.29501356	-3.3896747	-1.7611468	2.8580908	88.3274158	5.5469E-21	4.344E-20	ENSG00000204410.10
SGOL2	0.29497237	-3.390148	-1.7613483	5.12654845	444.730747	1.0113E-98	5.5726E-97	ENSG00000163535.13
MAD2L1	0.29448603	-3.3957468	-1.7637289	5.68828783	438.424145	2.3846E-97	1.2733E-95	ENSG00000164109.9
RAD51	0.29361365	-3.4058363	-1.7680091	4.12119592	234.589791	5.9488E-53	1.2797E-51	ENSG00000051180.12
SKA1	0.29360645	-3.4059198	-1.7680444	4.56132187	217.65165	2.9419E-49	5.6805E-48	ENSG00000154839.5
DLEU2	0.29307621	-3.4120818	-1.7706522	2.42522286	74.1465798	7.2527E-18	4.8924E-17	ENSG00000231607.4
GINS2	0.29304667	-3.4124258	-1.7707977	4.5828922	160.204744	1.0207E-36	1.4062E-35	ENSG00000131153.4

MPP2	0.29083717	-3.4383501	-1.7817164	0.68036484	22.6731409	1.9203E-06	5.6427E-06	ENSG00000108852.10
CDCA8	0.29022502	-3.4456024	-1.7847562	5.67846951	563.226617	1.67E-124	1.587E-122	ENSG00000134690.6
ANLN	0.28995974	-3.4487546	-1.7860755	7.45288332	971.796762	2.425E-213	7.504E-211	ENSG00000011426.6
ARHGAP11A	0.28956727	-3.453429	-1.7880296	6.36016487	648.63099	4.434E-143	5.754E-141	ENSG00000198826.6
CDCA3	0.28938169	-3.4556436	-1.7889544	4.36290834	220.199492	8.1822E-50	1.6056E-48	ENSG00000111665.7
RP11-22B23.1	0.28937731	-3.4556959	-1.7889763	1.5138453	34.3869135	4.5175E-09	1.68E-08	ENSG00000111788.9
CPT1C	0.28677683	-3.4870321	-1.8019996	2.14926815	50.6783499	1.0881E-12	5.4375E-12	ENSG00000169169.10
PRKAA2	0.28660515	-3.4891208	-1.8028635	2.79592355	87.5127295	8.3739E-21	6.5072E-20	ENSG00000162409.6
XRCC2	0.2864945	-3.4904684	-1.8034206	3.88654784	178.97624	8.1087E-41	1.2578E-39	ENSG00000196584.2
FANCD2	0.28647184	-3.4907445	-1.8035347	4.59755476	316.405804	8.7864E-71	2.7685E-69	ENSG00000144554.6
KCNK1	0.28559198	-3.5014989	-1.8079726	1.07230824	29.8288829	4.7191E-08	1.6124E-07	ENSG00000135750.10
PARD6A	0.28423586	-3.5182049	-1.8148395	0.96111671	28.7976201	8.035E-08	2.6905E-07	ENSG00000102981.5
KIF24	0.28385332	-3.5229463	-1.8167825	3.29515308	134.892967	3.4846E-31	4.1066E-30	ENSG00000186638.11
SSTR1	0.28349371	-3.5274151	-1.8186114	0.63659294	22.8146411	1.784E-06	5.2652E-06	ENSG00000139874.5
PROX1	0.28278355	-3.5362736	-1.8222299	2.03242471	48.932091	2.6498E-12	1.2926E-11	ENSG00000117707.11
ACSL5	0.28277154	-3.5364237	-1.8222912	2.24194326	71.1865266	3.25E-17	2.1223E-16	ENSG00000197142.6
C11orf82	0.28237599	-3.5413775	-1.8243107	3.75152564	174.223179	8.848E-40	1.3264E-38	ENSG00000165490.8
RUNX1T1	0.28206696	-3.5452575	-1.8258904	3.16957179	120.450849	5.04E-28	5.2844E-27	ENSG00000079102.12
HMGB2	0.28111733	-3.5572335	-1.8307557	7.44879802	751.243855	2.152E-165	3.659E-163	ENSG00000164104.7
CDCA5	0.28110593	-3.5573779	-1.8308142	5.39596345	566.161811	3.839E-125	3.706E-123	ENSG00000146670.5
CDT1	0.27992026	-3.5724459	-1.8369122	4.84019419	350.421044	3.4312E-78	1.282E-76	ENSG00000167513.4
SASS6	0.27949539	-3.5778765	-1.8391036	3.2789127	125.501929	3.9521E-29	4.3279E-28	ENSG00000156876.8
NCAPG2	0.27790266	-3.5983822	-1.8473484	6.19874257	616.226885	4.948E-136	5.58E-134	ENSG00000146918.15

KIF22	0.27781905	-3.5994652	-1.8477826	5.99104284	552.912416	2.927E-122	2.597E-120	ENSG00000079616.8
KIF20B	0.2773818	-3.6051392	-1.850055	5.73168727	636.373458	2.054E-140	2.455E-138	ENSG00000138182.10
NCAPG	0.27724776	-3.6068821	-1.8507523	6.2343572	762.718836	6.885E-168	1.222E-165	ENSG00000109805.5
KIF4A	0.27696324	-3.6105875	-1.8522336	5.84974786	435.609116	9.7742E-97	5.1285E-95	ENSG00000090889.10
KNTC1	0.27616661	-3.6210026	-1.8563892	5.02997494	459.504976	6.161E-102	3.755E-100	ENSG00000184445.7
NCOA2	0.27575768	-3.6263722	-1.858527	3.57047856	153.444355	3.0631E-35	4.0846E-34	ENSG00000140396.8
COX7A1	0.27574331	-3.6265612	-1.8586022	1.10497082	33.2078246	8.2817E-09	3.0058E-08	ENSG00000161281.6
CCNE2	0.27549506	-3.6298292	-1.8599017	4.06215419	187.857934	9.3306E-43	1.5467E-41	ENSG00000175305.12
FAM72D	0.27530124	-3.6323846	-1.860917	2.41133059	74.7332507	5.3881E-18	3.6654E-17	ENSG00000215784.4
GINS1	0.27460797	-3.6415549	-1.8645546	4.68125089	278.716334	1.43E-62	3.8606E-61	ENSG00000101003.8
WDR76	0.273742	-3.6530748	-1.8691113	4.44405845	161.915773	4.3161E-37	6.0077E-36	ENSG00000092470.7
COL8A2	0.27342349	-3.6573303	-1.8707909	0.87759386	26.7146714	2.3582E-07	7.6054E-07	ENSG00000171812.6
CDC6	0.2722124	-3.6736019	-1.8771953	5.61681	433.81033	2.4076E-96	1.2311E-94	ENSG00000094804.5
SH3BP1	0.27215613	-3.6743614	-1.8774935	1.27308153	36.2210889	1.7615E-09	6.8267E-09	ENSG00000100092.16
BRCA1	0.2716915	-3.6806452	-1.8799587	5.22595224	449.398421	9.751E-100	5.4987E-98	ENSG00000012048.15
IQGAP3	0.27161458	-3.6816875	-1.8803672	5.42133059	535.465125	1.828E-118	1.501E-116	ENSG00000183856.6
KIF2C	0.27132947	-3.6855562	-1.8818824	5.65172362	514.841498	5.609E-114	4.204E-112	ENSG00000142945.8
MTFR2	0.27097199	-3.6904184	-1.8837844	3.14660891	92.4433871	6.9279E-22	5.6682E-21	ENSG00000146410.7
CCNB2	0.26914082	-3.7155271	-1.8935669	5.50445105	540.693843	1.332E-119	1.132E-117	ENSG00000157456.3
FST	0.26850034	-3.72439	-1.8970042	2.20213954	64.0963613	1.1848E-15	7.0994E-15	ENSG00000134363.7
CENPH	0.26840236	-3.7257497	-1.8975308	3.30259005	127.507573	1.4385E-29	1.5956E-28	ENSG00000153044.5
PPP1R9A	0.26826791	-3.7276169	-1.8982536	1.18673197	36.3885035	1.6165E-09	6.2829E-09	ENSG00000158528.7
PLK1	0.26796904	-3.7317744	-1.8998618	6.7190434	895.83675	7.886E-197	2.115E-194	ENSG00000166851.10

UBE2C	0.2674962	-3.7383708	-1.9024097	5.35189854	454.250334	8.573E-101	5.022E-99	ENSG00000175063.12
POLE2	0.2674176	-3.7394697	-1.9028337	3.11238347	133.880912	5.8013E-31	6.7642E-30	ENSG00000100479.8
VASH2	0.2670126	-3.7451408	-1.9050199	0.62211097	25.5302407	4.355E-07	1.3637E-06	ENSG00000143494.11
PRC1	0.2658261	-3.7618568	-1.9114449	6.96396058	1035.58218	3.312E-227	1.176E-224	ENSG00000198901.9
NLRP2	0.2651164	-3.771927	-1.9153018	3.55664606	165.297675	7.8756E-38	1.1129E-36	ENSG00000022556.11
FBXO5	0.2643354	-3.7830705	-1.9195577	4.55731001	247.43491	9.4116E-56	2.1552E-54	ENSG00000112029.5
RP11-389C8.2	0.2621193	-3.8150475	-1.931701	1.20676887	30.578407	3.2064E-08	1.1116E-07	ENSG00000261269.1
FANCB	0.2616555	-3.821818	-1.9342591	2.00412465	68.524479	1.2531E-16	7.8928E-16	ENSG00000181544.9
KIF14	0.2611534	-3.829168	-1.937031	5.03001489	476.1458	1.474E-105	9.46E-104	ENSG00000118193.7
SPC25	0.2608983	-3.8329101	-1.9384401	3.96447778	141.364434	1.3392E-32	1.6525E-31	ENSG00000152253.4
DTL	0.2608807	-3.8331685	-1.9385374	5.00795818	380.882389	7.9956E-85	3.4709E-83	ENSG00000143476.13
NDC80	0.2606897	-3.8360036	-1.9396041	5.15595732	360.860162	1.8293E-80	7.2144E-79	ENSG00000080986.8
CEP55	0.2604053	-3.840179	-1.9411736	6.40274636	820.082997	2.321E-180	4.592E-178	ENSG00000138180.11
DDX12P	0.2602786	-3.8420627	-1.9418811	2.45011126	75.1730397	4.3122E-18	2.9517E-17	ENSG00000214826.4
CKAP2L	0.2599174	-3.8473752	-1.9438745	5.08879117	451.723179	3.042E-100	1.7563E-98	ENSG00000169607.8
E2F1	0.2597404	-3.8499971	-1.9448573	4.46366793	309.089848	3.4474E-69	1.0506E-67	ENSG00000101412.9
HMMR	0.2586007	-3.866965	-1.9512017	5.54664461	488.496932	3.026E-108	2.018E-106	ENSG00000072571.15
CENPI	0.2583685	-3.8704356	-1.9524959	4.52384507	294.981899	4.0839E-66	1.1962E-64	ENSG00000102384.9
NEIL3	0.2581348	-3.8738897	-1.9537829	3.20283523	89.6177742	2.8892E-21	2.2954E-20	ENSG00000109674.3
LMNB1	0.2575379	-3.8829232	-1.9571432	7.18290558	1003.50432	3.109E-220	1.042E-217	ENSG00000113368.7
KIF20A	0.2565295	-3.8981862	-1.962803	6.46556441	759.664452	3.177E-167	5.557E-165	ENSG00000112984.7
RAB38	0.2561714	-3.9036358	-1.9648184	1.56731349	51.5992063	6.8069E-13	3.4414E-12	ENSG00000123892.7
ZNF503	0.2559202	-3.9074708	-1.9662351	1.76033643	53.2190631	2.9835E-13	1.5426E-12	ENSG00000165655.14

SAPCD2	0.25549319	-3.9139987	-1.9686433	5.43077139	646.734395	1.146E-142	1.472E-140	ENSG00000186193.7
BIRC5	0.25548795	-3.9140789	-1.9686728	6.54026058	557.802481	2.527E-123	2.311E-121	ENSG00000089685.10
ATAD5	0.25528716	-3.9171575	-1.9698071	3.66892041	204.583293	2.0879E-46	3.7218E-45	ENSG00000176208.4
CGREF1	0.25526567	-3.9174872	-1.9699286	1.44007964	47.1262191	6.6559E-12	3.1475E-11	ENSG00000138028.10
KIFC1	0.25525649	-3.9176281	-1.9699804	5.90426014	704.074087	3.888E-155	5.866E-153	ENSG00000237649.3
SHCBP1	0.25521146	-3.9183194	-1.970235	6.00079951	628.200684	1.231E-138	1.428E-136	ENSG00000171241.4
SKA3	0.25507339	-3.9204403	-1.9710157	4.75247808	341.456062	3.0745E-76	1.101E-74	ENSG00000165480.11
RP11-122A3.2	0.25498663	-3.9217742	-1.9715065	1.01751231	32.869564	9.8554E-09	3.5535E-08	ENSG00000253250.2
BUB1	0.25481803	-3.9243691	-1.9724608	6.03963823	766.366969	1.108E-168	1.996E-166	ENSG00000169679.10
EXO1	0.25407718	-3.935812	-1.9766613	3.93150826	212.437434	4.0374E-48	7.5657E-47	ENSG00000174371.12
MYBL2	0.2536753	-3.9420472	-1.9789451	6.72671754	982.678547	1.046E-215	3.321E-213	ENSG00000101057.11
WDR62	0.25319491	-3.9495264	-1.9816797	4.3323078	326.622536	5.229E-73	1.7384E-71	ENSG00000075702.12
BLM	0.25202322	-3.9678884	-1.9883714	4.44361895	269.093427	1.7885E-60	4.5923E-59	ENSG00000197299.6
FAM72B	0.25131322	-3.9790982	-1.9924415	2.63786861	97.3775307	5.7292E-23	4.9245E-22	ENSG00000188610.8
KIF15	0.25124695	-3.9801479	-1.992822	4.65252862	413.257398	7.1628E-92	3.3898E-90	ENSG00000163808.12
KIAA0101	0.25109431	-3.9825673	-1.9936988	5.43051755	528.422862	6.224E-117	4.877E-115	ENSG00000166803.6
FOXM1	0.25102574	-3.9836553	-1.9940928	6.8991421	803.272289	1.049E-176	1.947E-174	ENSG00000111206.8
RMI2	0.25065568	-3.9895366	-1.9962212	2.91349926	114.822856	8.6051E-27	8.6251E-26	ENSG00000175643.7
LONRF3	0.25042038	-3.9932852	-1.9975761	2.11250644	54.4918604	1.5609E-13	8.2403E-13	ENSG00000175556.12
E2F8	0.2498617	-4.0022141	-2.0007983	4.56166824	204.263308	2.4521E-46	4.3645E-45	ENSG00000129173.8
NEK2	0.24794441	-4.0331621	-2.0119114	4.33176101	344.748627	5.8983E-77	2.144E-75	ENSG00000117650.8
HYAL1	0.24753246	-4.0398742	-2.0143104	0.77565981	30.3421148	3.6218E-08	1.2499E-07	ENSG00000114378.12
CDCA2	0.24742574	-4.0416166	-2.0149325	5.14819258	478.976833	3.568E-106	2.302E-104	ENSG00000184661.9

TK1	0.2451413	-4.07928	-2.0283145	6.43596732	806.408651	2.181E-177	4.113E-175	ENSG00000167900.7
TCF19	0.2450252	-4.0812076	-2.0289961	5.49351198	589.458649	3.286E-130	3.389E-128	ENSG00000137310.7
HJURP	0.2448775	-4.0836741	-2.0298677	5.42839724	620.675043	5.333E-137	6.129E-135	ENSG00000123485.7
DLGAP5	0.2446953	-4.0867448	-2.0309522	6.71706392	823.996144	3.273E-181	6.695E-179	ENSG00000126787.8
GTSE1	0.2441258	-4.096248	-2.0343031	5.61133912	653.060689	4.825E-144	6.398E-142	ENSG00000075218.14
NUF2	0.2439738	-4.0987999	-2.0352016	4.69576851	452.959858	1.637E-100	9.496E-99	ENSG00000143228.8
SPAG5	0.2433858	-4.1087031	-2.0386831	6.03836433	836.165196	7.401E-184	1.654E-181	ENSG00000076382.12
ZNF395	0.2431001	-4.1135312	-2.0403774	3.09207548	135.620927	2.415E-31	2.8629E-30	ENSG00000186918.9
ERCC6L	0.2429901	-4.1153937	-2.0410305	3.80082725	208.872075	2.4208E-47	4.4063E-46	ENSG00000186871.5
EME1	0.2427576	-4.1193329	-2.0424107	2.38643263	84.3958607	4.0499E-20	3.0338E-19	ENSG00000154920.10
CDKN3	0.2423260	-4.126671	-2.0449784	4.13705585	276.559788	4.2198E-62	1.1217E-60	ENSG00000100526.15
PKMYT1	0.2417389	-4.1366934	-2.048478	4.49694266	325.191352	1.0719E-72	3.5246E-71	ENSG00000127564.12
NUSAP1	0.2416973	-4.1374677	-2.048748	5.9902596	883.973867	2.991E-194	7.846E-192	ENSG00000137804.8
POLQ	0.2414740	-4.1412323	-2.0500601	4.08996216	247.59348	8.6915E-56	1.9941E-54	ENSG00000051341.9
CYP26B1	0.2409047	-4.1510175	-2.053465	1.13633982	37.5395963	8.9576E-10	3.5559E-09	ENSG00000003137.4
BUB1B	0.2404914	-4.1581524	-2.0559426	5.90314114	833.649175	2.608E-183	5.522E-181	ENSG00000156970.8
SGOL1	0.2403479	-4.1606348	-2.0568036	3.71042674	192.453919	9.2621E-44	1.5589E-42	ENSG00000129810.10
MEOX2	0.2403293	-4.1609575	-2.0569155	4.00151044	233.919322	8.3298E-53	1.7823E-51	ENSG00000106511.5
NPR1	0.2400457	-4.1658733	-2.058619	3.19322093	154.846118	1.5129E-35	2.0309E-34	ENSG00000169418.9
EPS8	0.2400194	-4.1663287	-2.0587767	3.40687071	155.388366	1.1517E-35	1.5529E-34	ENSG00000151491.8
KAZN	0.2398508	-4.1692575	-2.0597905	2.00903449	70.3014283	5.0901E-17	3.299E-16	ENSG00000189337.11
CCNA2	0.2395685	-4.1741654	-2.0614878	6.65497752	839.410261	1.458E-184	3.32E-182	ENSG00000145386.5
SLFN13	0.2394959	-4.1754367	-2.0619271	2.10583777	64.8119146	8.2399E-16	4.972E-15	ENSG00000154760.9

CENPA	0.23790517	-4.2033554	-2.0715415	4.1438674	302.745236	8.3116E-68	2.4828E-66	ENSG00000115163.10
ZNF736	0.23765277	-4.2078196	-2.0730729	1.21488535	40.4231985	2.045E-10	8.5512E-10	ENSG00000234444.5
DEPDC1	0.23764598	-4.20794	-2.0731141	5.58881364	510.504006	4.927E-113	3.648E-111	ENSG00000024526.12
CIT	0.2365775	-4.2269447	-2.0796152	5.60958655	706.775738	1.005E-155	1.536E-153	ENSG00000122966.9
MNS1	0.23558486	-4.2447549	-2.0856812	2.12206661	78.9386756	6.4068E-19	4.5427E-18	ENSG00000138587.5
LYPD6	0.23538712	-4.2483208	-2.0868927	1.92883442	66.1843563	4.1066E-16	2.5195E-15	ENSG00000187123.10
TMEM88	0.23538387	-4.2483794	-2.0869126	3.50847917	173.695324	1.1538E-39	1.7275E-38	ENSG00000167874.6
SLC47A1	0.23493685	-4.2564629	-2.0896551	1.61956026	51.9923325	5.5718E-13	2.8402E-12	ENSG00000142494.9
ZNF724P	0.2347063	-4.2606441	-2.0910715	0.59202835	27.8001343	1.3452E-07	4.4245E-07	ENSG00000196081.5
RRM2	0.23464712	-4.2617186	-2.0914353	7.85569233	1262.08286	1.964E-276	1.031E-273	ENSG00000171848.9
MLF1IP	0.234234	-4.2692351	-2.0939776	5.02090848	552.228677	4.123E-122	3.605E-120	ENSG00000151725.7
FAM64A	0.23320231	-4.2881222	-2.100346	4.5451371	328.935229	1.6394E-73	5.5265E-72	ENSG00000129195.11
MCM10	0.2328063	-4.2954164	-2.102798	4.85788915	512.473535	1.837E-113	1.368E-111	ENSG00000065328.12
BRCA2	0.23277957	-4.2959097	-2.1029637	4.40982055	243.334286	7.374E-55	1.651E-53	ENSG00000139618.10
GSG2	0.23252812	-4.3005552	-2.1045229	3.4541279	174.420962	8.0104E-40	1.2084E-38	ENSG00000177602.4
RAD51AP1	0.23045768	-4.3391915	-2.1174263	4.09069865	294.859586	4.3424E-66	1.2689E-64	ENSG00000111247.10
SPC24	0.22963525	-4.354732	-2.1225839	4.21470511	319.683659	1.6975E-71	5.4051E-70	ENSG00000161888.7
RNFT2	0.229037	-4.3661068	-2.1263474	1.25368149	45.4638567	1.5548E-11	7.1182E-11	ENSG00000135119.10
PSRC1	0.2286412	-4.3736649	-2.1288427	4.13872369	292.74655	1.2535E-65	3.5931E-64	ENSG00000134222.12
HIST1H2BH	0.22844226	-4.3774739	-2.1300986	1.19586521	44.0440796	3.2106E-11	1.4292E-10	ENSG00000197459.2
C5orf34	0.22840809	-4.3781287	-2.1303144	2.43549431	91.3629562	1.1959E-21	9.681E-21	ENSG00000172244.4
PBK	0.22801883	-4.3856028	-2.1327751	5.34757863	473.726961	4.952E-105	3.162E-103	ENSG00000168078.5
MFSD7	0.22789731	-4.3879412	-2.1335442	0.86522999	35.2180557	2.9478E-09	1.1134E-08	ENSG00000169026.8

PLK4	0.22780902	-4.3896418	-2.1341032	4.89710105	520.191379	3.845E-115	2.956E-113	ENSG00000142731.6
CCDC150	0.22778367	-4.3901304	-2.1342638	1.19630431	40.2736029	2.2077E-10	9.203E-10	ENSG00000144395.13
ASF1B	0.22711021	-4.4031486	-2.1385355	5.20963987	439.763763	1.2186E-97	6.536E-96	ENSG00000105011.4
LPIN3	0.22709659	-4.4034126	-2.138622	1.26313757	45.2641939	1.7217E-11	7.8316E-11	ENSG00000132793.7
KIF18B	0.22691497	-4.406937	-2.1397763	5.05875361	411.486515	1.74E-91	8.1706E-90	ENSG00000186185.9
TOP2A	0.22689296	-4.4073647	-2.1399163	7.79204955	1485.16465	0	0	ENSG00000131747.10
CENPF	0.22689011	-4.4074201	-2.1399344	7.38901358	634.44449	5.397E-140	6.386E-138	ENSG00000117724.8
KIF11	0.225631	-4.432015	-2.1479628	6.31224502	1103.04068	7.211E-242	2.901E-239	ENSG00000138160.4
TICRR	0.22520344	-4.4404295	-2.1506992	4.43105541	364.313722	3.2382E-81	1.3292E-79	ENSG00000140534.9
ZNF486	0.22481373	-4.4481269	-2.1531979	2.2646344	93.4078401	4.2556E-22	3.5128E-21	ENSG00000256229.3
NCAPH	0.2245922	-4.4525144	-2.1546203	4.98789078	551.255329	6.713E-122	5.828E-120	ENSG00000121152.5
ZNF788	0.22291983	-4.4859177	-2.1654032	0.92328353	8.52151412	0.00350972	0.00662942	ENSG00000188474.6
ZNF788	0.22291983	-4.4859177	-2.1654032	0.92328353	8.52151412	0.00350972	0.00662942	ENSG00000214189.4
FAM111B	0.22234658	-4.4974831	-2.1691179	4.75956649	515.953929	3.212E-114	2.438E-112	ENSG00000189057.6
PTER	0.2220043	-4.5044173	-2.1713405	2.09586655	86.5117425	1.3891E-20	1.0671E-19	ENSG00000165983.10
DERL3	0.22167825	-4.5110424	-2.1734609	0.56173911	28.4493786	9.6181E-08	3.2002E-07	ENSG00000099958.10
AQP1	0.2208219	-4.5285364	-2.1790449	2.73709281	72.9959286	1.2992E-17	8.6666E-17	ENSG00000240583.6
AQP1	0.2208219	-4.5285364	-2.1790449	2.73709281	72.9959286	1.2992E-17	8.6666E-17	ENSG00000250424.3
PRIM1	0.22059968	-4.533098	-2.1804974	3.14239655	152.514507	4.8908E-35	6.4505E-34	ENSG00000198056.9
CENPM	0.22011063	-4.54317	-2.1836993	3.63234139	195.550188	1.954E-44	3.3354E-43	ENSG00000100162.10
ZNF626	0.21898976	-4.5664236	-2.1910647	1.69836647	64.5281158	9.5165E-16	5.7308E-15	ENSG00000188171.10
MND1	0.21874798	-4.5714707	-2.1926584	1.94072668	67.6525185	1.95E-16	1.2193E-15	ENSG00000121211.3
ARHGAP11B	0.21838606	-4.5790469	-2.1950473	3.55143889	222.226581	2.9561E-50	5.9063E-49	ENSG00000187951.6

ORC1	0.21798891	-4.5873894	-2.1976734	4.05181569	293.916888	6.9682E-66	2.0215E-64	ENSG00000085840.8
ESPL1	0.21788071	-4.5896675	-2.1983896	5.14586407	654.824466	1.995E-144	2.675E-142	ENSG00000135476.7
AURKB	0.21744737	-4.5988141	-2.2012619	5.35669566	507.058584	2.768E-112	2.012E-110	ENSG00000178999.8
RAD54L	0.21693424	-4.609692	-2.2046703	3.95184588	277.316963	2.8859E-62	7.7223E-61	ENSG00000085999.7
EXOC3L1	0.21693339	-4.6097099	-2.204676	2.60863122	88.8057958	4.3554E-21	3.4242E-20	ENSG00000179044.11
CDC45	0.21488179	-4.6537215	-2.2183849	4.88265399	554.278677	1.476E-122	1.33E-120	ENSG00000093009.5
MBNL3	0.21414391	-4.6697568	-2.2233474	2.55633338	84.8840712	3.1638E-20	2.3848E-19	ENSG00000076770.10
CASC5	0.21320791	-4.6902574	-2.2296671	5.73771728	731.78503	3.665E-161	5.897E-159	ENSG00000137812.15
RP11-977G19.10	0.21167424	-4.7242404	-2.2400824	0.80041746	11.5694277	0.00067045	0.00142247	ENSG00000144785.4
NEFH	0.21058839	-4.7486	-2.2475022	3.34835864	177.470989	1.7283E-40	2.6672E-39	ENSG00000100285.9
ZNF367	0.2069342	-4.8324541	-2.272756	3.80463097	228.44879	1.2991E-51	2.7077E-50	ENSG00000165244.6
TTK	0.20690124	-4.8332239	-2.2729858	5.02014576	561.697553	3.592E-124	3.335E-122	ENSG00000112742.5
BRIP1	0.20653868	-4.8417081	-2.2755161	3.98307209	308.940165	3.7162E-69	1.1268E-67	ENSG00000136492.4
ESCO2	0.20549904	-4.8662027	-2.2827964	4.31036734	359.575334	3.4838E-80	1.3695E-78	ENSG00000171320.10
ALDH1L2	0.20478046	-4.8832784	-2.28785	2.08999709	83.3237934	6.9656E-20	5.1603E-19	ENSG00000136010.9
APOBEC3B	0.20446023	-4.8909266	-2.2901078	4.10162579	268.296992	2.6673E-60	6.8343E-59	ENSG00000179750.11
ATAD2	0.2039866	-4.9022828	-2.2934537	5.96885406	988.041864	7.138E-217	2.328E-214	ENSG00000156802.8
GIMAP5	0.20360107	-4.9115656	-2.296183	2.09182465	63.7783149	1.3924E-15	8.302E-15	ENSG00000196329.6
ARHGAP20	0.20350781	-4.9138164	-2.296844	2.35432723	94.6037096	2.3258E-22	1.9387E-21	ENSG00000137727.8
CDK1	0.20302147	-4.9255874	-2.3002958	5.91348235	899.715534	1.132E-197	3.176E-195	ENSG00000170312.11
PIF1	0.20132526	-4.9670867	-2.3123999	3.32575009	176.139897	3.3751E-40	5.1493E-39	ENSG00000140451.8
MKI67	0.20130889	-4.9674905	-2.3125172	8.32626529	721.05676	7.886E-159	1.252E-156	ENSG00000148773.8
STEAP2	0.20096195	-4.9760663	-2.3150057	1.61877474	53.5679091	2.4981E-13	1.2961E-12	ENSG00000157214.9

MXD3	0.20017235	-4.9956951	-2.3206854	3.21065785	188.321617	7.3908E-43	1.2269E-41	ENSG00000213347.6
ITPRIPL1	0.19981234	-5.0046958	-2.3232824	1.89216298	75.8875044	3.0029E-18	2.0756E-17	ENSG00000198885.5
CDC25C	0.19541533	-5.1173058	-2.3553844	3.3638587	219.807094	9.9646E-50	1.9522E-48	ENSG00000158402.14
KHK	0.19515886	-5.1240307	-2.3572791	2.48507285	93.1598499	4.8237E-22	3.9681E-21	ENSG00000138030.8
FOXD2-AS1	0.19487946	-5.1313771	-2.3593461	1.03977504	43.7829689	3.6688E-11	1.6272E-10	ENSG00000237424.1
AIF1L	0.19240275	-5.197431	-2.3777987	4.21541101	345.58071	3.8862E-77	1.4169E-75	ENSG00000126878.8
SCML2	0.19132997	-5.2265726	-2.3858652	1.20542842	53.0168526	3.307E-13	1.7026E-12	ENSG00000102098.13
ASPM	0.19086384	-5.2393371	-2.3893843	6.72751344	1111.9198	8.476E-244	3.527E-241	ENSG00000066279.12
TROAP	0.18839556	-5.3079808	-2.4081632	4.4203471	457.712991	1.512E-101	9.079E-100	ENSG00000135451.8
PLEKHA7	0.18239243	-5.4826838	-2.4548823	2.11226548	89.9725377	2.4149E-21	1.9274E-20	ENSG00000166689.10
SCN5A	0.18127971	-5.5163371	-2.4637106	4.69741278	462.587914	1.314E-102	8.134E-101	ENSG00000183873.11
CDKN2C	0.18004422	-5.5541912	-2.4735768	4.0632732	332.517954	2.7188E-74	9.4013E-73	ENSG00000123080.6
HLA-DPB1	0.17965127	-5.5663397	-2.476729	2.36919863	89.2821578	3.4233E-21	2.7055E-20	ENSG00000223865.6
METTL7A	0.17842464	-5.6046071	-2.4866132	3.61486253	267.901916	3.2523E-60	8.2628E-59	ENSG00000185432.10
HLA-DPA1	0.1770898	-5.6468525	-2.497447	2.03114746	93.7389339	3.6001E-22	2.9819E-21	ENSG00000231389.3
RCAN3	0.17684818	-5.6545675	-2.4994167	1.48877304	69.7794331	6.6321E-17	4.264E-16	ENSG00000117602.7
EMP2	0.1764405	-5.667633	-2.5027463	4.13414137	377.604771	4.1347E-84	1.7632E-82	ENSG00000213853.5
CPE	0.17512361	-5.7102523	-2.5135545	1.08296859	53.7305242	2.2996E-13	1.1983E-12	ENSG00000109472.9
ITGB4	0.16509606	-6.0570797	-2.5986224	1.73892057	80.1182198	3.5267E-19	2.5363E-18	ENSG00000132470.9
SLC29A2	0.16435371	-6.0844381	-2.605124	2.20164783	96.040743	1.1254E-22	9.531E-22	ENSG00000174669.7
FRAS1	0.16215236	-6.1670396	-2.6245781	2.00382421	78.9614897	6.3333E-19	4.4932E-18	ENSG00000138759.13
ZNF826P	0.15824775	-6.3192051	-2.6597431	1.28108299	63.8571113	1.3378E-15	7.9883E-15	ENSG00000231205.7
LRP4	0.15659444	-6.3859229	-2.6748951	1.69059336	88.3422876	5.5054E-21	4.3142E-20	ENSG00000134569.5

E2F2	0.15608108	-6.4069263	-2.6796324	2.72462332	150.309554	1.4835E-34	1.9272E-33	ENSG00000007968.6
NUDT11	0.15520849	-6.4429464	-2.6877206	1.75905717	91.0264267	1.4177E-21	1.1451E-20	ENSG00000196368.4
SLC38A5	0.15496039	-6.4532619	-2.6900286	4.66774691	629.766132	5.619E-139	6.584E-137	ENSG00000017483.10
C14orf132	0.14654818	-6.8236944	-2.770553	0.56163239	41.1715054	1.3944E-10	5.9211E-10	ENSG00000227051.4
ENPP4	0.13720155	-7.2885476	-2.8656314	3.07074922	217.925067	2.5644E-49	4.9755E-48	ENSG00000001561.6
MAGED4	0.13719755	-7.2887599	-2.8656734	2.13297151	13.1773489	0.00028335	0.0006356	ENSG00000154545.12
FBXO43	0.13471055	-7.4233237	-2.8920653	0.78767476	53.039971	3.2683E-13	1.6848E-12	ENSG00000156509.9
AMPH	0.13125185	-7.61894	-2.9295903	0.38223722	40.043965	2.4831E-10	1.0298E-09	ENSG00000078053.12
MAP3K8	0.13111931	-7.6266419	-2.931048	0.93708798	56.9325468	4.5102E-14	2.4507E-13	ENSG00000107968.5
KIF26A	0.13013389	-7.6843932	-2.9419313	3.32467403	266.99037	5.1388E-60	1.2947E-58	ENSG00000066735.10
RNF180	0.12201114	-8.1959731	-3.0349152	0.46615758	43.7982454	3.6403E-11	1.6157E-10	ENSG00000164197.7
ZNF506	0.12113512	-8.255244	-3.0453109	0.63584275	50.1360103	1.4345E-12	7.1036E-12	ENSG00000081665.9
SHISA3	0.11957076	-8.3632489	-3.0640635	1.53526011	91.6475448	1.0357E-21	8.4114E-21	ENSG00000178343.4
PTPRN2	0.11656138	-8.5791711	-3.1008383	1.48023166	93.4245341	4.2199E-22	3.488E-21	ENSG00000155093.13
ZNF844	0.11643966	-8.5881391	-3.1023456	0.67916308	53.4378181	2.6691E-13	1.3824E-12	ENSG00000223547.5
ZNF93	0.1090353	-9.1713418	-3.1971328	1.15564431	72.6713069	1.5314E-17	1.0166E-16	ENSG00000184635.9
AC016683.6	0.09477515	-10.551289	-3.3993474	1.54409761	91.7673111	9.7492E-22	7.9228E-21	ENSG00000189223.9
TPBG	0.09375084	-10.666571	-3.4150246	2.13627036	151.338468	8.8392E-35	1.1544E-33	ENSG00000146242.5
CRISPLD1	0.09232798	-10.830953	-3.4370883	1.85478357	116.665973	3.3973E-27	3.4656E-26	ENSG00000121005.4
MYO7A	0.08825801	-11.330417	-3.502129	1.91491318	137.581482	8.9975E-32	1.0836E-30	ENSG00000137474.15
TMEM200B	0.08746994	-11.432498	-3.5150688	0.66478101	60.8693835	6.099E-15	3.5016E-14	ENSG00000253304.1
PCDH18	0.08532274	-11.720205	-3.5509259	0.48215545	50.5242294	1.177E-12	5.8744E-12	ENSG00000189184.7
F8A3	0.08342464	-11.986866	-3.5833826	1.48029281	84.0648862	4.788E-20	3.5734E-19	ENSG00000185990.6

TUBA4A	0.08288885	-12.064349	-3.5926782	3.71867036	437.49101	3.8063E-97	2.0147E-95	ENSG00000127824.9
ACKR3	0.08080434	-12.375573	-3.6294234	3.05432344	227.10864	2.5463E-51	5.2619E-50	ENSG00000144476.5
EHD3	0.08059003	-12.408482	-3.6332547	3.7273017	323.25113	2.8363E-72	9.2258E-71	ENSG00000013016.10
ANO5	0.07643776	-13.082539	-3.7095707	0.34713237	50.315071	1.3094E-12	6.511E-12	ENSG00000171714.10
PCDHAC2	0.07444467	-13.432796	-3.7476877	1.37106433	102.57734	4.1485E-24	3.7529E-23	ENSG00000243232.3
PTPRD	0.07304229	-13.690698	-3.7751241	2.81758391	217.01857	4.0432E-49	7.7945E-48	ENSG00000153707.11
RASAL3	0.06804001	-14.697234	-3.8774728	0.48274008	57.085843	4.172E-14	2.2689E-13	ENSG00000105122.8
CCDC36	0.06377063	-15.681199	-3.970964	0.56131162	62.217163	3.076E-15	1.795E-14	ENSG00000173421.12
KRT7	0.06346075	-15.757772	-3.9779916	3.15553451	357.22910	1.1297E-79	4.3976E-78	ENSG00000135480.10
VGLL3	0.06219607	-16.078185	-4.0070327	1.44694972	119.43015	8.4312E-28	8.7714E-27	ENSG00000206538.3
TUB	0.06215651	-16.088418	-4.0079506	0.86326564	71.333302	3.017E-17	1.9745E-16	ENSG00000166402.4
RGS7BP	0.05473214	-18.2708	-4.1914679	1.76436933	146.80041	8.6768E-34	1.1034E-32	ENSG00000186479.4
EMILIN1	0.05378924	-18.591079	-4.2165386	2.46698885	223.90028	1.2755E-50	2.5739E-49	ENSG00000138080.9
MGMT	0.04430721	-22.569692	-4.4963148	1.88499563	172.51369	2.0901E-39	3.0987E-38	ENSG00000170430.9
CCDC144A	0.04293925	-23.288717	-4.5415593	0.25564406	46.211219	1.0617E-11	4.924E-11	ENSG00000170160.12
ZNF253	0.04025067	-24.844308	-4.6348435	1.1339417	107.47024	3.5114E-25	3.3219E-24	ENSG00000256771.2
FAM46A	0.03959115	-25.258173	-4.6586784	1.86515948	140.83197	1.751E-32	2.154E-31	ENSG00000112773.11
TBX1	0.03893041	-25.686859	-4.6829586	2.70204162	239.46915	5.134E-54	1.1306E-52	ENSG00000184058.8
TRO	0.03807374	-26.264821	-4.7150599	0.86323658	85.240966	2.6413E-20	2.0047E-19	ENSG00000067445.16
USP32P1	0.03421577	-29.22629	-4.8691948	0.53077931	60.18042	8.6549E-15	4.9268E-14	ENSG00000188933.10
GBP4	0.03055336	-32.729623	-5.0325251	1.47315671	94.941187	1.9613E-22	1.6414E-21	ENSG00000162654.8
XYLT1	0.0300831	-33.241253	-5.0549029	1.51107511	149.32941	2.4296E-34	3.1292E-33	ENSG00000103489.7
NUP210	0.02944189	-33.965215	-5.0859861	2.58958193	284.18526	9.1956E-64	2.5511E-62	ENSG00000132182.7

DCAF12L1	0.02379782	-42.020664	-5.3930271	0.99416084	106.36111	6.1452E-25	5.7489E-24	ENSG00000198889.3
NLGN4Y	0.02058013	-48.590557	-5.6026041	0.46595351	74.3216579	6.6371E-18	4.4872E-17	ENSG00000165246.8
CCDC152	0.02013962	-49.653358	-5.6338194	1.69485354	149.817511	1.9004E-34	2.4634E-33	ENSG00000198865.5
IGFBP1	0.0169902	-58.85745	-5.8791531	1.43039733	128.697144	7.8998E-30	8.8683E-29	ENSG00000146678.5
RPS4Y1	0.01378254	-72.555551	-6.1810141	3.47252019	585.022127	3.032E-129	3.1E-127	ENSG00000129824.11
ZNF711	0.01326515	-75.385525	-6.2362156	1.02674764	111.482309	4.6393E-26	4.5042E-25	ENSG00000147180.12
NDN	0.00687616	-145.42999	-7.184181	2.66209335	363.145701	5.816E-81	2.3632E-79	ENSG00000182636.4
TSPAN7	0.00604058	-165.54703	-7.3710973	0.29229532	75.3638072	3.915E-18	2.689E-17	ENSG00000156298.8
EIF1AY	0.00586683	-170.44983	-7.4132033	0.32865279	77.9350228	1.0649E-18	7.4844E-18	ENSG00000198692.5
DDX3Y	0.00540499	-185.01413	-7.5314917	2.22770426	273.385875	2.0749E-61	5.4552E-60	ENSG00000067048.12
USP9Y	0.00480379	-208.16912	-7.7016123	0.57628201	89.0697512	3.8113E-21	3.0043E-20	ENSG00000114374.8
KDM5D	0.00434848	-229.96557	-7.845274	0.70602028	101.861743	5.9535E-24	5.3498E-23	ENSG00000012817.11
GPAT2	0.00404744	-247.07001	-7.9487761	0.79953185	106.673616	5.2487E-25	4.9293E-24	ENSG00000186281.8
PTPLAD2	0.00261675	-382.15371	-8.5780092	1.36986984	165.3441	7.6938E-38	1.0885E-36	ENSG00000188921.12
RP11-512M8.5	0.00199981	-500.04861	-8.9659245	1.73030324	203.342699	3.8941E-46	6.9008E-45	ENSG00000256861.1
LITAF	0.00078881	-1267.7266	-10.308028	3.01543358	508.92954	1.084E-112	7.978E-111	ENSG00000189067.8

Fig S1. Effects of MRME treatments on HUVECs viability. *HUVECs were treated at different MRME concentrations for 72 hours and viability was evaluated by MTT assay. Untreated sHUVECs were used as reference in the study. The data represent the mean values of three independent experiments. Error bands represent standard deviation.*

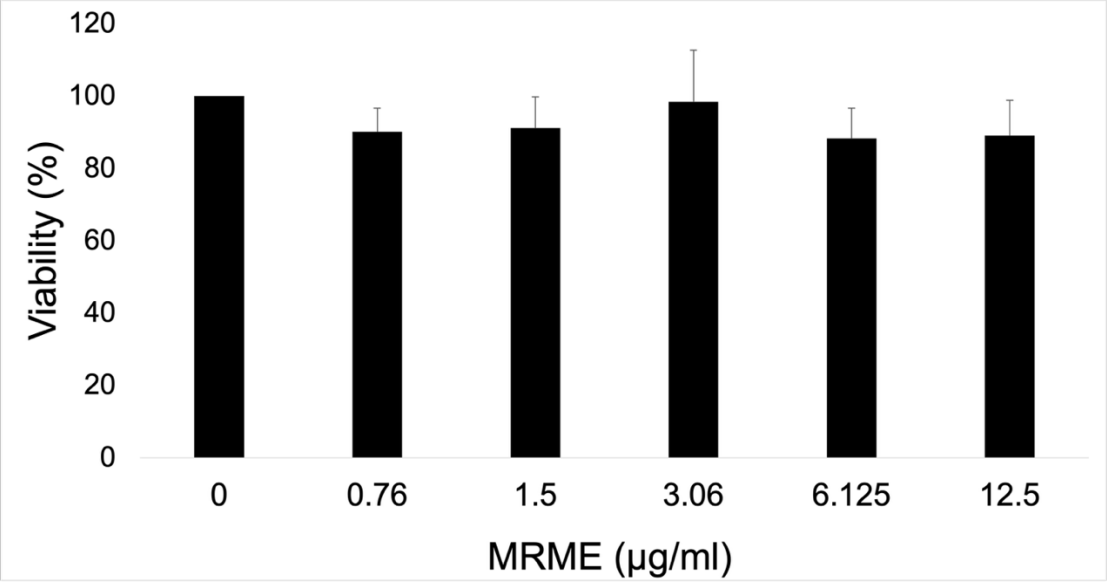

Table S3: Transcriptomic analysis results*. List of differentially expressed genes (DEGs) obtained comparing senescent HUVECs (sHUVECs) untreated and treated with Mela Rosa Marchigiana callus extract (MRME). 11 genes were up regulated and 15 genes were downregulated in sHUVEC MRME. Genes were identified as DEGs when the following criteria were met: FDR ≤ 0.05 and FC ≥ 1.5 or ≤ -1.5.*

GeneName	**FC**	**logFC**	**FDR**	**Tras_ID**
RASD1	2.43232674	1.28233705	7.4999E-08	ENSG00000108551.4
GTPBP6	2.22379949	1.15302672	0.00938402	ENSGR0000178605.8
HYPK	2.03790606	1.02708755	0.02101529	ENSG00000242028.1
ZNF230	1.93036227	0.94887162	0.02513974	ENSG00000159882.8
PRDM1	1.9223511	0.94287185	0.03189461	ENSG00000057657.10
RP11-33B1.1	1.85957503	0.89497296	0.0085504	ENSG00000245958.2
C19orf68	1.85554675	0.89184435	0.02840498	ENSG00000185453.8
WDR5B	1.62247632	0.69819743	0.04410006	ENSG00000196981.2
ZC3HAV1L	1.56251998	0.64387464	0.02488436	ENSG00000146858.7
SEMA6D	1.54324401	0.62596619	0.02046903	ENSG00000137872.11
LYST	1.53293775	0.61629911	0.00226989	ENSG00000143669.9
GADD45B	0.64753955	-0.6269598	1.6667E-16	ENSG00000099860.4

DUSP1	0.64726647	-0.6275683	8.4214E-26	ENSG00000120129.5
SOCS3	0.63422732	-0.6569281	8.119E-11	ENSG00000184557.3
JUNB	0.63154877	-0.6630339	3.6939E-13	ENSG00000171223.4
ZFP36	0.59042179	-0.7601821	2.1287E-09	ENSG00000128016.4
FOS	0.57349019	-0.8021593	1.1722E-17	ENSG00000170345.5
NR4A1	0.54984418	-0.8629053	7.3596E-06	ENSG00000123358.15
HES1	0.51299762	-0.962976	2.1149E-20	ENSG00000114315.3
ID1	0.44667004	-1.1627186	3.8519E-47	ENSG00000125968.7
ATF3	0.42248007	-1.2430448	4.0286E-29	ENSG00000162772.12
RABGEF1	0.4196816	-1.2526329	0.01186952	ENSG00000154710.11
BOLA2B	0.37540602	-1.4134763	0.00534688	ENSG00000169627.7
FOSB	0.34248538	-1.5458857	7.9483E-28	ENSG00000125740.9
ID2	0.3332742	-1.5852185	1.1603E-11	ENSG00000115738.5
KLF4	0.3080516	-1.6987561	1.9549E-18	ENSG00000136826.10

Supplementary results: Effect of MRME on DNA methylation in sHUVEC

To explore potential epigenetic mechanisms underlying MRME-induced gene expression changes we investigated DNA methylation in the promoter region of the 12 genes (ID2, GADD45B, JUNB, HES1, ATF3 NR4A1, KLF4, FOS, FOSB, ZFP36, DUSP1 and SOCS3) identified as differentially expressed in sHUVECs treated with MRME compared to untreated senescent cells and implicated in the TNF-α via NFKB signalling. Pyrosequencing analysis was conducted on yHUVECs, sHUVECs and sHUVECs MRME to assess the DNA methylation levels across the three conditions. The analysis revealed no significant differences in the mean methylation levels of the promoter regions of the selected genes between yHUVECs, sHUVECs and sHUVECs MRME (Figure S2). However, when the analysis was extended to single CpG sites, we found that the methylation level of the first CpG site in the selected area of SOCS3 promoter region significantly changes between the three conditions (Overall p-value = 0.009 ANOVA). In particular, the methylation level of this CpG decreases with senescence ($p < 0.05$), while is increased by MRME treatments of sHUVECs ($p < 0.05$) (Figure 5). To further investigate whether MRME influences DNA methylation

levels, we extended our analysis by performing Reduced Representation Methylation Sequencing (RRMS) using PromethION24 (Oxford Nanopore Technology, UK) on DNA extracted from three biological replicates of sHUVECs and sHUVECs MRME. While pyrosequencing provides quantification of DNA methylation at specific CpG sites, it is limited by its targeted design, allowing analysis only within short, pre-amplified regions, typically 100 base pairs, of selected promoters. As a result, it cannot detect methylation changes outside the predefined loci, nor capture broader epigenetic alterations across the genome. Therefore, we employed Nanopore adaptive sampling RRMS protocol to obtain a broader, genome-wide perspective, specifically enriching for CpG-dense regions, and to detect potential epigenetic changes beyond the predefined promoter targets.

The average coverage across all the samples was approximately 20x per sample. Differential methylation analysis was firstly performed at CpGs locus level. No significant differences in DNA methylation levels were observed after adjustment for multiple comparisons comparing sHUVECs and sHUVECs MRME in any CpG site (data not shown) . Similarly, no significant differences were detected when the analysis was extended to promoter regions (Figure S3).

Fig. S2 Analysis of the methylation status in the promoter regions of the 12 selected genes. *Average methylation level measured by Pyrosequencing analysis in the selected area of the ID2 promoter (A), GADD45B promoter (B), JUNB promoter (C), HES1 promoter (D), ATF3 promoter (E), NR4A1 promoter (F), KLF4 promoter (G), FOS promoter (H), FOSB promoter (I), ZFP36 promoter (L), DUSP1 promoter (M), SOCS3 promoter (N) in the three groups: Y (young HUVECs), S (senescent HUVECs), M (Senescent HUVECs treated with the Mela Rosa Marchigiana callus extract). There was no significant difference in the mean methylation levels of the promoter regions of the selected genes comparing yHUVECs, sHUVECs and sHUVECs MRME. The boxes represent the interquartile range (25th–75th percentile), the line inside the box indicates the median, and the whiskers extend to the smallest and largest values within 1.5 times the interquartile range.*

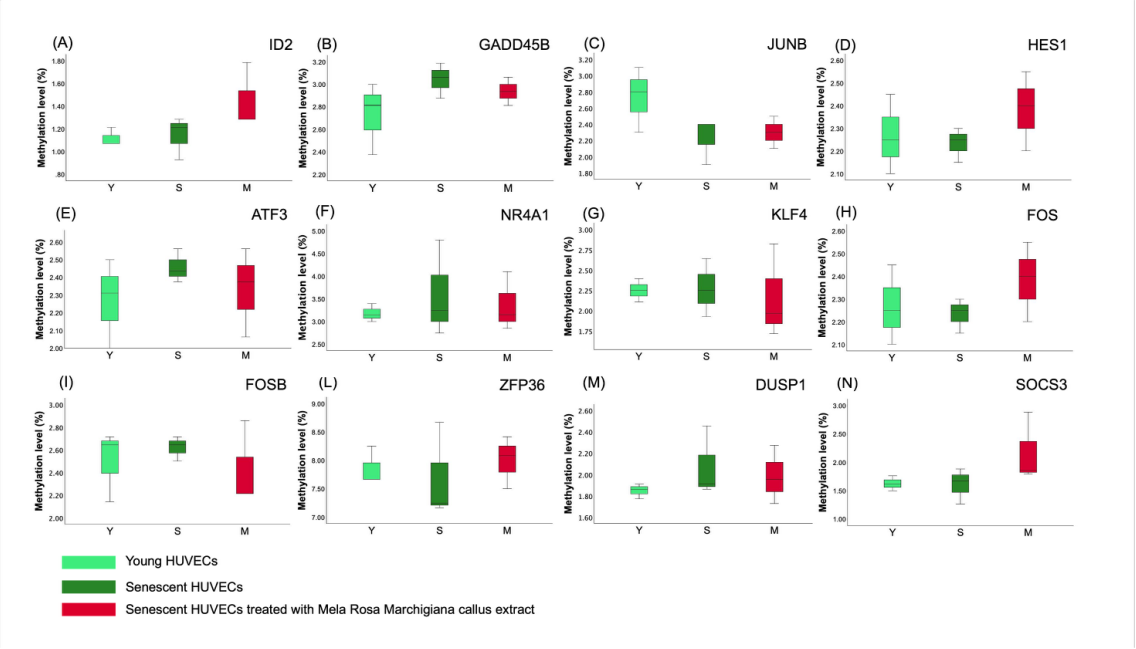

Fig. S3: Analysis of genome-wide methylation by Oxford Nanopore sequencing (RRMS). *MD plot showing the log-fold-change of the methylation level in gene promoters, representing the difference between senescent HUVECs treated with MRME and untreated senescent HUVECs, plotted against the average CpG abundance within each gene promoter. No significant differences in DNA methylation levels were observed between groups after correction for multiple testing (Bonferroni correction). Promoters not significantly differentially methylated (FDR > 0.05) are shown in black.*

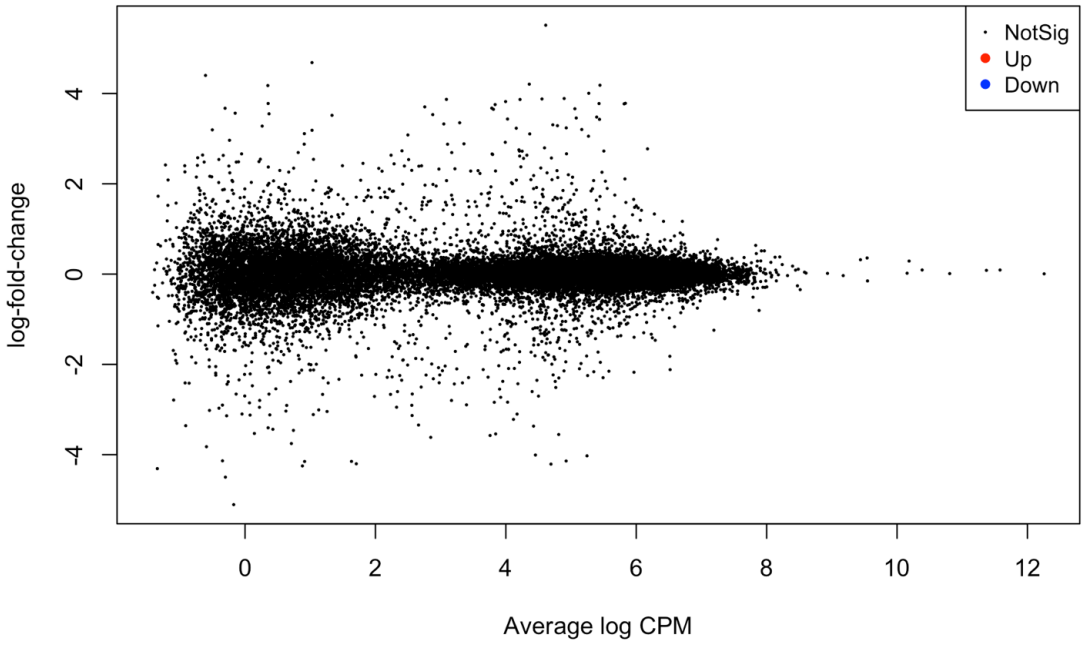
NotSig
Up
Down
log-fold-change
4
2
0
-2
-4
0
2
4
6
8
10
12
Average log CPM

References

[1] J. G. Nkuimi Wandjou, S. Sut, C. Giuliani, G. Fico, F. Papa, S. Ferraro, G. Caprioli, F. Maggi, S. Dall'Acqua, Int J Food Sci Nutr 2019, 70, 796–812.

[2] F. Gubitosa, L. Benayada, D. Fraternale, R. De Bellis, S. Carloni, L. Potenza, L. Chiarantini, A. Gorassini, G. Verardo, C. Roselli, L. Valentini, P. Gobbi, W. Balduini, N. Ventura, F. Giannaccini, G. E. N. Kass, M. Colomba, M. C. Albertini, J Funct Foods 2024, 114, 106073.

[3] H. Yousefi-Manesh, S. Hemmati, S. Shirooie, S. M. Nabavi, A. Talebzadeh Bonakdar, R. Fayaznia, M. H. Asgardoon, A. Zare Dehnavi, M. Ghafouri, J. G. Nkuimi Wandjou, G. Caprioli, S. Sut, F. Maggi, S. Dall'Acqua, Food Funct 2019, 10, 7544–7552.

[4] N. A. J. C. Furtado, L. Pirson, H. Edelberg, L. M. Miranda, C. Loira-Pastoriza, V. Preat, Y. Larondelle, C. M. André, Molecules 2017, 22, DOI 10.3390/molecules22030400.

[5] Y. Li, D. Kong, Y. Fu, M. R. Sussman, H. Wu, Plant Physiology and Biochemistry 2020, 148, 80–89.

[6] L. Benayada, F. Gubitosa, D. Fraternale, S. Carloni, L. Cerioni, G. Matacchione, F. Olivieri, L. Potenza, R. De Bellis, L. Chiarantini, C. Roselli, L. Valentini, P. Gobbi, W. Balduini, N. Pappagallo, N. Ventura, G. E. N. Kass, M. Colomba, M. C. Albertini, J Funct Foods 2024, 121, 106420.

[7] T. Lavecchia, G. Rea, A. Antonacci, M. T. Giardi, Crit Rev Food Sci Nutr 2013, 53, 198–213.

[8] G. Verardo, A. Gorassini, D. Fraternale, Food Research International 2019, 119, 596–604.

[9] G. Verardo, A. Gorassini, D. Ricci, D. Fraternale, Phytochemical Analysis 2017, 28, 5–15.

[10] G. Baldelli, M. De Santi, D. Fraternale, G. Brandi, M. Fanelli, G. F. Schiavano, J Med Food 2019, 22, 614–622.

[11] L. Potenza, M. Minutelli, V. Stocchi, D. Fraternale, J Funct Foods 2020, 75, 104269.

[12] H. Kim, C. N. Ramirez, Z.-Y. Su, A.-N. T. Kong, J Nutr Biochem 2016, 33, 54–62.

[13] S. Li, R. Wu, L. Wang, H.-C. Dina Kuo, D. Sargsyan, X. Zheng, Y. Wang, X. Su, A.-N. Kong, Mol Carcinog 2022, 61, 111–121.

[14] R. R. Hudlikar, D. Sargsyan, R. Wu, S. Su, M. Zheng, A.-N. Kong, Chem Biol Interact 2020, 321, 109025.

[15] Y. Yang, R. Yin, R. Wu, C. N. Ramirez, D. Sargsyan, S. Li, L. Wang, D. Cheng, C. Wang, R. Hudlikar, H. C. Kuo, Y. Lu, A. N. Kong, Mol Carcinog 2019, 58, 1738–1753.

[16] J. Yang, R. Wu, W. Li, L. Gao, Y. Yang, P. Li, A.-N. Kong, Mol Carcinog 2018, 57, 512–521.

[17] M. S. Sarwar, C. N. Ramirez, H.-C. D. Kuo, P. Chou, R. Wu, D. Sargsyan, Y. Yang, A. Shannar, R. M. Peter, R. Yin, Y. Wang, X. Su, A.-N. Kong, Carcinogenesis 2024, 45, 288–299.

[18] H. C. D. Kuo, R. Wu, M. S. Sarwar, M. Zheng, C. Wang, D. Sargsyan, N. Suh, A. N. T. Kong, AAPS Journal 2022, 24, DOI 10.1208/s12248-022-00763-5.

[19] C. Franceschi, P. Garagnani, P. Parini, C. Giuliani, A. Santoro, Nat Rev Endocrinol 2018, 14, 576–590.

[20] R. Kumari, P. Jat, Front Cell Dev Biol 2021, 9.

[21] M. Fekete, Z. Szarvas, V. Fazekas-Pongor, A. Feher, T. Csipo, J. Forrai, N. Dosa, A. Peterfi, A. Lehoczki, S. Tarantini, J. T. Varga, Nutrients 2023, 15, DOI 10.3390/nu15010047.

[22] A. Szychowska, W. Drygas, Aging Clin Exp Res 2022, 34, 1209–1214.

[23] L. Song, S. Zhang, Biomolecules 2023, 13, DOI 10.3390/biom13111600.

[24] F. Prattichizzo, V. De Nigris, E. Mancuso, R. Spiga, A. Giuliani, G. Matacchione, R. Lazzarini, F. Marcheselli, R. Recchioni, R. Testa, L. La Sala, M. R. Rippo, A. D. Procopio, F. Olivieri, A. Ceriello, Redox Biol 2018, 15, 170–181.

[25] G. Matacchione, D. Valli, A. Silvestrini, A. Giuliani, J. Sabbatinelli, C. Giordani, S. Coppari, M. R. Rippo, M. C. Albertini, F. Olivieri, Antioxidants 2022, 11, DOI 10.3390/antiox11061037.

[26] L. Bordoni, R. Gabbianelli, Biochimie 2019, 160, 156–171.

[27] S. W. Choi, S. Friso, Advances in Nutrition 2010, 1, 8–16.

[28] J. Mierziak, K. Kostyn, A. Boba, M. Czemplik, A. Kulma, W. Wojtasik, Nutrients 2021, 13, DOI 10.3390/nu13113673.

[29] M. Nistor, D. Rugina, Z. Diaconeasa, C. Socaciu, M. A. Socaciu, Int J Mol Sci 2023, 24, DOI 10.3390/ijms241612923.

[30] M. Hibi, Y. Matsui, S. Niwa, S. Oishi, A. Yanagimoto, T. Ono, T. Yamaguchi, J Funct Foods 2022, 97, 105256.

[31] D. Kashyap, A. Sharma, H. S. Tuli, S. Punia, A. K. Sharma, Recent Pat Inflamm Allergy Drug Discov 2016, 10, 21–33.

[32] J. Deng, H. Wang, X. Mu, X. He, F. Zhao, Q. Meng, Mini Rev Med Chem 2021, 21, 79–89.

[33] H.-Z. Chen, S.-Y. Tsai, G. Leone, Nat Rev Cancer 2009, 9, 785–797.

[34] G. R. Stark, W. R. Taylor, in Checkpoint Controls and Cancer: Volume 1: Reviews and Model Systems (Ed.: A.H. Schönthal), Humana Press, Totowa, NJ 2004, pp. 51–82.

[35] L. Roger, F. Tomas, V. Gire, Int J Mol Sci 2021, 22, 13173.

[36] S. Lamouille, J. Xu, R. Derynck, Nat Rev Mol Cell Biol 2014, 15, 178–196.

[37] R. Thapa, S. Gupta, G. Gupta, A. A. Bhat, Smriti, M. Singla, H. Ali, S. K. Singh, K. Dua, M. K. Kashyap, Ageing Res Rev 2024, 102, 102576.

[38] B. S. Fleenor, K. D. Marshall, C. Rippe, D. R. Seals, J Vasc Res 2012, 49, 59–64.

[39] S. Piera-Velazquez, S. A. Jimenez, Physiol Rev 2019, 99, 1281–1324.

[40] T. Liu, L. Zhang, D. Joo, S.-C. Sun, Signal Transduct Target Ther 2017, 2, 17023.

[41] A. Salminen, A. Kauppinen, K. Kaarniranta, Cell Signal 2012, 24, 835–845.

[42] V. A. García-García, J. P. Alameda, A. Page, M. L. Casanova, Cells 2021, 10, 1906.

[43] M. Haga, M. Okada, Biochemical Journal 2022, 479, 161–183.

[44] P. K. Tripathi, K. R. Mittal, N. Jain, N. Sharma, C. K. Jain, Recent Pat Anticancer Drug Discov 2024, 19, 268–279.

[45] G. M. DeNicola, D. A. Tuveson, Eur J Cancer 2009, 45 Suppl 1, 211–6.

[46] M. Ohori, Y. Nakayama, M. Ogasawara-Shimizu, H. Toyoshiba, A. Nakanishi, S. Aparicio, S. Araki, BMC Genomics 2021, 22, 869.

[47] D. Ramini, A. Giuliani, K. M. Kwiatkowska, M. Guescini, G. Storci, E. Mensà, R. Recchioni, L. Xumerle, E. Zago, J. Sabbatinelli, S. Santi, P. Garagnani, M. Bonafè, F. Olivieri, Cell Death Discov 2024, 10, 184.

[48] E. Mensà, M. Guescini, A. Giuliani, M. G. Bacalini, D. Ramini, G. Corleone, M. Ferracin, G. Fulgenzi, L. Graciotti, F. Prattichizzo, L. Sorci, M. Battistelli, V. Monsurrò, A. R. Bonfigli, M. Cardelli, R. Recchioni, F. Marcheselli, S. Latini, S. Maggio, M. Fanelli, S. Amatori, G. Storci, A. Ceriello, V. Stocchi, M. De Luca, L. Magnani, M. R. Rippo, A. D. Procopio, C. Sala, I. Budimir, C. Bassi, M. Negrini, P. Garagnani, C. Franceschi, J. Sabbatinelli, M. Bonafè, F. Olivieri, J Extracell Vesicles 2020, 9, 1725285.

[49] G. Rigillo, G. Baini, R. Bruni, G. Puja, E. Miraldi, L. Pani, F. Tascedda, M. Biagi, Phytotherapy Research 2025, 39, 264–281.

[50] M. Fumagalli, G. Martinelli, G. Paladino, N. Rossini, U. Ciriello, V. Nicolaci, N. Maranta, C. Pozzoli, S. M. El Haddad, E. Sonzogni, M. Dell'Agli, S. Piazza, E. Sangiovanni, Pharmaceuticals 2025, 18, 647.

[51] L. Vesci, G. Martinelli, Y. Liu, L. Tagliavento, M. Dell'Agli, Y. Wu, S. Soldi, V. Sagheddu, S. Piazza, E. Sangiovanni, F. Meneguzzo, Biomedicines 2025, 13, 686.

[52] M. O. Radwan, S. F. Kadasah, S. M. Aljubiri, A. F. Alrefaei, M. H. El-Maghrabey, M. A. El Hamd, H. Tateishi, M. Otsuka, M. Fujita, Biomolecules 2023, 13, 1465.

[53] S. Bai, B. Zhao, Q. Zhao, Y. Ge, M. Li, C. Zhao, X. Wu, X. Wang, Sci Rep 2024, 14, 21852.

[54] S. Li, R. Wu, L. Wang, H. Dina Kuo, D. Sargsyan, X. Zheng, Y. Wang, X. Su, A. Kong, Mol Carcinog 2022, 61, 111–121.

[55] S. Li, H.-C. D. Kuo, R. Yin, R. Wu, X. Liu, L. Wang, R. Hudlikar, R. M. Peter, A.-N. Kong, Biochem Pharmacol 2020, 175, 113890.

[56] J. Stelling-Férez, I. Cappellacci, A. Pandolfi, J. A. Gabaldón, C. Pipino, F. J. Nicolás, Front Endocrinol (Lausanne) 2023, 14, DOI 10.3389/fendo.2023.1308606.

[57] R. Samivel, R. P. Nagarajan, U. Subramanian, A. A. Khan, A. Masmali, T. Almubrad, S. Akhtar, Oxid Med Cell Longev 2020, 2020, 1246510.

[58] Y. Xu, J. Wei, W. Wang, Z. Mao, D. Wang, T. Zhang, P. Zhang, Molecules 2025, 30, DOI 10.3390/molecules30030740.

[59] Y. Gong, Y. Luo, S. Liu, J. Ma, F. Liu, Y. Fang, F. Cao, L. Wang, Z. Pei, J. Ren, Biochim Biophys Acta Mol Basis Dis 2022, 1868, 166402.

[60] S. A. Bahrami, N. Bakhtiari, Biomed Pharmacother 2016, 82, 8–14.

[61] A. Viggiano, A. Viggiano, M. Monda, I. Turco, L. Incarnato, V. Vinno, E. Viggiano, M. E. Baccari, B. De Luca, Exp Neurol 2006, 199, 354–61.

[62] S. Tsai, M. Yin, Eur J Pharmacol 2012, 689, 81–8.

[63] P. Herrlich, M. Karin, C. Weiss, Mol Cell 2008, 29, 279–290.

[64] K. Tominaga, H. I. Suzuki, Int J Mol Sci 2019, 20, 5002.

[65] K. K. Yamamoto, C. Savage-Dunn, Front Genet 2023, 14, DOI 10.3389/fgene.2023.1220068.

[66] H. Bai, Y. Gao, D. L. Hoyle, T. Cheng, Z. Z. Wang, Stem Cells Transl Med 2017, 6, 589–600.

[67] E. O. Karakaslar, N. Katiyar, M. Hasham, A. Youn, S. Sharma, C. han Chung, R. Marches, R. Korstanje, J. Banchereau, D. Ucar, Aging Cell 2023, 22, DOI 10.1111/acel.13792.

[68] H. A. Cruickshanks, T. McBryan, D. M. Nelson, N. D. VanderKraats, P. P. Shah, J. van Tuyn, T. Singh Rai, C. Brock, G. Donahue, D. S. Dunican, M. E. Drotar, R. R. Meehan, J. R. Edwards, S. L. Berger, P. D. Adams, Nat Cell Biol 2013, 15, 1495–1506.

[69] M. G. Basilicata, E. Sommella, L. Scisciola, G. Tortorella, M. Malavolta, C. Giordani, M. Barbieri, P. Campiglia, G. Paolisso, Ageing Res Rev 2025, 111, 102824.

[70] Q. Song, Y. Hou, Y. Zhang, J. Liu, Y. Wang, J. Fu, C. Zhang, M. Cao, Y. Cui, X. Zhang, X. Wang, J. Zhang, C. Liu, Y. Zhang, P. Wang, Nucleic Acids Res 2022, 50, 10947–10963.

[71] H. A. Shaban, S. M. Gasser, Cell Death Differ 2025, 32, 9–15.

3.1 Research Article n. 2

Gut Microbiota-Derived Trimethylamine Promotes Inflammation with a Potential Impact on Epigenetic and Mitochondrial Homeostasis in Caco-2 Cells

Laura Bordoni[1], Irene Petracci[1], Giulia Feliziani[2], Gaia de Simone[2], Chiara Rucci[2], Rosita Gabbinelli[1]

[1] Unit of Molecular Biology and Nutrigenomics, School of Pharmacy and Health Products, University of Camerino, 62032 Camerino, Italy;

[2] School of Advanced Studies, University of Camerino, 62032 Camerino, Italy;

Published in: Antioxidants (Basel). 2024 Aug 30;13(9):1061. doi: 10.3390/antiox13091061. PMID: 39334721; PMCID: PMC11428692.

Abstract: Trimethylamine (TMA), a byproduct of gut microbiota metabolism from dietary precursors, is not only the precursor of trimethylamine-N-oxide (TMAO) but may also affect gut health. An in vitro model of intestinal epithelium of Caco-2 cells was used to evaluate the impact of TMA on inflammation, paracellular permeability, epigenetics and mitochondrial functions. The expression levels of pro-inflammatory cytokines (IL-6, IL-1β) increased significantly after 24 h exposure to TMA 1 mM. TMA exposure was associated with an upregulation of SIRT1 (TMA 1 mM, 400 μM, 10 μM) and DNMT1 (TMA 1 mM, 400 μM) genes, while DNMT3A expression decreased (TMA 1 mM). In a cell-free model, TMA (from 0.1 μM to 1 mM) induced a dose-dependent reduction in Sirtuin enzyme activity. In Caco-2 cells, TMA reduced total ATP levels and significantly downregulated ND6 expression (TMA 1 mM). TMA excess (1 mM) reduced intracellular mitochondrial DNA copy numbers and increased the methylation of the light-strand promoter in the D-loop area of mtDNA. Also, TMA (1 mM, 400 μM, 10 μM) increased the permeability of Caco-2 epithelium, as evidenced by the reduced transepithelial electrical resistance values. Based on our preliminary results, TMA excess might promote inflammation in intestinal cells and disturb epigenetic and mitochondrial homeostasis.

1. Introduction

Trimethylamine (TMA) is an amine generated in the colon by the gut microbiota through the processing of nutritional substrates like choline, betaine, L-carnitine, and dimethylglycine and their precursors (phosphatidylcholine, crono-betaine, and g-butyrobeaine) [1,2]. These substrates are commonly found in red meat, fish, eggs, and related sources. TMA generated in the gut is absorbed through passive diffusion and then transported via the portal circulation to the liver, where it is oxidized into trimethylamine-N-Oxide (TMAO) by hepatic flavin monooxygenases (FMOs) [3]. TMAO is a low-molecular-weight compound which has been associated with the development of several chronic non-communicable diseases and proposed as a possible biomarker of cardiovascular diseases (CVDs) [4]. Despite a body of literature about the potential harmful effects of TMA and TMAO, evidence on this topic is still fragmentary. Although being a well-known uremic toxin, TMA has been understudied concerning its effects on human health, largely due to the predominant focus on its derivative, TMAO. While it has been suggested that TMA may pose significant health risks [5], only a limited number of studies have delved into the mechanistic effects of TMA on health. Jalandra and collaborators showed that TMA has toxic effects in vitro, with acute exposure leading to decreased cell viability and ATP production in HCT116 and HT29 cells [5]. In this model, TMA induces oxidative stress by increasing cellular superoxide production [5], potentially impacting mitochondrial dynamics, although the precise mechanism remains unknown. Additionally, intrarectal and intraperitoneal injections of TMA in FVB/J mice led to a significant increase in inflammatory cell infiltration in the colon and rectum, also supporting the idea of the local pro-inflammatory action of TMA in vivo [5].

However, due to the limited literature on this topic, the exact mechanism by which TMA promotes inflammation is still unclear. Nonetheless, recent evidence suggests that TMA induced inflammation may result from the perturbation of mitochondrial homeostasis [5].

Indeed, the connection between inflammation and mitochondrial functions is well documented [6]: by releasing reactive oxygen species during aerobic respiration,

mitochondria can contribute to oxidative stress, thereby sustaining inflammation and causing cellular damage. Simultaneously, inflammation disrupts mitochondrial dynamics and function, promoting the production of reactive oxygen species [6].

Moreover, the mitochondrial damage induced by inflammation may also manifest with an aberrant mitochondrial DNA copy number (mtDNAcn), which is defined as the number of copies of mitochondrial DNA present in a cell. The maintenance of an appropriate mtDNAcn in the cell is essential for the regular expression of mitochondrial proteins, which overall control and determine the mitochondrial function [7]. For this reason, mtDNAcn has been considered a proxy indicator for mitochondrial activity and a biomarker of mitochondrial health [7,8]. New conjectures propose the potential influence of mtDNA methylation on mitochondrial functions, especially in the context of cardiovascular and metabolic diseases [9,10]. Notably, studies have measured DNA methylation in the displacement loop (D-loop) of mtDNA, a region that being crucial for mtDNA replication and transcription, might also affect mtDNAcn [11]. Furthermore, mtDNA methylation has been hypothesized to be linked to multifactorial diseases (such as obesity and metabolic diseases) and to environmental exposures such as diet [10,12–14]. However, this remains a contentious topic, as certain evidence contradicts the presence of the methylation on mtDNA, despite the identification of enzymes accountable for DNA methylation within mitochondria [15].

Epigenetic regulations can also affect inflammation: epigenetic mechanisms are responsible for the regulation of inflammatory genes' expression, but in turn, inflammation can affect chromatin remodeling and epigenetic enzymes activity [16,17]. Among the numerous enzymes involved in these complex regulations, DNA methyltransferases (DNMTs) (major determinants of DNA methylation) and Sirtuins (SIRTs) (histone deacetylases connected with both nuclear and mitochondrial functions) are central mediators linking epigenetic regulations to inflammation, mitochondrial dysfunctions and oxidative stress [18–25].

Lastly, mitochondrial dysfunction may compromise the ATP production system and alter the mitochondrial membrane potential ($\Delta\psi m$) of the cell [26–28]. Changes in the mitochondrial membrane potential trigger apoptotic signaling pathways that culminate

in the release of mitochondrial components, including mtDNA, into the extracellular environment, potentially fostering inflammation [8,29–31].

This study aims at testing the hypothesis that disturbances in ATP production and mitochondrial membrane potential, as well as alterations of mtDNAcn and cell-free mito- chondrial DNA (cf-mtDNA) released can be induced by TMA exposure in an intestinal model of Caco-2 cells. Additionally, given the well-established association between inflammation and epigenetic homeostasis, we aimed at testing the capacity of TMA to affect the expression levels and activity of DNMTs and SIRTs—pivotal enzymes in the epigenetic landscape.

2. Materials and Methods

2.1. Cell Culture

To investigate the impact of TMA on intestinal cells, Caco-2 cells, which are a human colonic epithelial cell line (ATCC, Rockville, MD, USA), were selected. Cells were provided by Professor Ivan Nabissi, University of Camerino. Caco-2 cells were cultured in Dulbecco's modified Eagle's medium (DMEM) supplemented with 10% heat-inactivated fetal bovine serum (FBS), 1% L-glutamine, 1% non-essential amino acids (NEAAs), and 1% penicillin/streptomycin. The cells were maintained at 37 ◦C in a humidified atmosphere with 5% CO2. The medium was refreshed every 2 days, and cells were passaged when reaching 80% confluence.

In addition, to test the effect of TMA on intestinal permeability, these cells were cultured in a transwell-based system, as described by Kyeong Jin Kim et al. [32]. Briefly, Caco-2 cells were seeded on non-coated transwell inserts (0.4 μm pore size, ThinCert®, Greiner Bio-one, Frickenhausen, Germany) at the density of 1×10^5 cells/insert in a 6- well plate and maintained in complete medium. The culture medium was added in both apical (AP) and basal (BL) compartments and replaced every 2 days. The 6-well plates were incubated in atmosphere of 5% CO2 at 37 °C. Cells were cultured in transwells until differentiation and complete epithelium formation. In order to assess the evolution of the intestinal epithelium formation, the transepithelial electrical resistance (TEER), which indicates the integrity of Caco-2 epithelium, was

measured using Millicell® ERS (Millipore, Merk, Darmstadt, Germany) after 4, 7, 10, 14, and 17 days post seeding.

2.2. Cell Viability Assay

The cytotoxic impact of TMA was assessed through the 3-(4,5-Di-2-yl)-2,5-ditetrazolium bromide (MTT) assay (Thiazolyl blue tetrazolium bromide 98%, code 158990050, Acros Organic, Fair Lawn, NJ, USA). In brief, Caco-2 cells were plated in 96-well plates at a density of 1×10^4 cells/well in complete medium and exposed to various concentrations of TMA (1 nM, 10 nM, 0.1 µM, 1 µM, 10 µM, 100 µM, 1 mM, 10 mM, 100 mM) for 24 h. Following the incubation period, the cells were treated with a 5 mg/mL MTT solution. After four hours, the absorbance was measured at 540 nm using a spectrometer reader (FLUOstar Omega, BMG LABTECH's, Ortenberg, Germany). The experiment was performed in biological quadruplicates.

2.3. Treatments

Caco-2 cells were exposed to TMA at concentrations of 10 µM, 400 µM, and 1 mM (directly solved in complete medium as a vehicle) for a duration of 24 h. The selection of the lowest TMA concentration was based on average physiological fecal TMA concentrations [33]. The other two concentrations tested (400 µM and 1 mM) were determined by the MTT assay results: TMA 1 mM represented the highest non-cytotoxic concentration, while TMA 400 µM was chosen as an intermediate value between 10 µM and 1 mM. A negative control (vehicle only) and two positive controls, lipopolysaccharide (LPS), at 100 ng/mL and 10 µg/mL, were included in the experimental settings. Experiments were conducted in triplicate. After 24-h incubation, both cells and medium were collected. The cell pellets were promptly frozen in liquid nitrogen and stored at −80 °C for subsequent analysis. The cell medium was centrifuged at 13,248× g for 5 min, and the clear supernatant was aliquoted into new nuclease-free conical tubes, then stored at −80 ◦C for future use.

To evaluate the inflammatory activity of TMA on the intestinal epithelium model, cells previously differentiated and grown in transwells were treated as follows: TMA at different concentrations (1 mM, 400 µM, and 10 µM) was added to the AP compartment and cells were incubated for 24 h. Two positive controls for

inflammatory conditions, LPS 100 ng/mL and 10 μg/mL, were also included. The treatments were performed in biological triplicates.

2.4. Assessment of DNMT and SIRT Activities after Exposure to TMA

The nuclear protein fraction was isolated from Caco-2 cells using the Nuclear Extraction kit (Abcam, Waltham, MA, USA) according to the manufacturer's instructions. Briefly, untreated Caco-2 cells were first lysed and then the nuclear protein fraction was isolated from the cytoplasmic fraction. The protein concentration of the nuclear extract was quantified by Bradford Assay, using bovine serum albumin (BSA) as a calibrator. The nuclear extract was used to evaluate the activity of DNMTs and SIRTs. The effect of TMA on DNMTs activity was evaluated using the EpiQuikTM DNA Methyltransferase Activity/Inhibition Assay Kit (EpigenTek, Farmingdale, NY, USA) according to manufacturer's instructions. Briefly, 5 μg of nuclear proteins were transferred to a 96-well plate and incubated with various concentrations of TMA (1 mM, 400 μM, 100 μM, 50 μM, 10 μM, 1 μM, 100 nM, 10 nM, 1 nM, 0.01 nM, 0.001 nM, 0.000001 nM) for 120 min at 37 °C. The absorbance was measured at 450 nm using a microplate reader (FLUOstar Omega, BMG LABTECH's, Ortenberg, Germany), and DNMT activity (OD/h/mg) was calculated.
The effect of TMA on SIRT activity was evaluated using the Universal SIRT Activity Assay Kit (Abcam, Waltham, MA, USA) following the manufacturer's guidelines. In brief, 4 μg of nuclear proteins were transferred to a 96-well plate and incubated with various concentrations of TMA (1 mM, 400 μM, 100 μM, 50 μM, 10 μM, 1 μM, 100 nM, 1 nM, 0.01 nM, 0.001 nM, 0.000001 nM) for 90 min. The absorbance was recorded at 450 nm and SIRT activity (OD/min/mg) was calculated. The experiment was performed in technical duplicates.

2.5. MtDNAcn Quantification

Genomic DNA was extracted from Caco-2 cell pellets using DNAzol Reagent (Invitrogen, Carlsbad, CA, USA). Briefly, the cell pellets were lysed with DNAzol, 100% ethanol was added to the lysate to precipitate genomic DNA and two washes in 75% ethanol were performed to remove any contaminants from the isolated DNA.

Cf-DNA was extracted from the culture medium of treated Caco-2 cells using the Plasma/Serum Cell-Free Circulating DNA Purification Kit (Norgen, Biotek, Thorold, ON, Canada) according to manufacturer's instructions. The concentration and purity of genomic DNA was measured using NanoDrop spectrophotometer (Thermo Fisher Scientific, Waltham, MA, USA) while the concentration of cf-DNA was assessed using Qubit Fluorometer (Thermo Fisher Scientific, Monza, Italy).

Genomic DNA was used to quantify relative mtDNAcn by quantitative Real Time Polymerase Chain Reaction (qPCR) (CFX connect, Biorad, Hercules, CA, USA) while cf- DNA was used to perform both relative and absolute quantification of cf-mtDNA and cell- free nuclear DNA (cf-nDNA) by digital PCR (QIAcuity, Qiagen, Venlo, The Netherlands).

For relative quantification of mtDNAcn, mtDNA-tRNALeu (RefSeq accession number NC_012920.1) (Fw: 5′-CACCCAAGAACAGGGTTTGT-3′; Rv: 5′-TGGCCATGGGTATGTTGTTA- 3′) and Beta 2 microglobulin (B2M) (RefSeq accession number NC_000015.10) primers (Fw: 5′-TGCTGTCTCCATGTTTGATGTATCT-3′; Rv: 5′-TCTCTGCTCCCCACCTCTAAGT-3′) were chosen to amplify mtDNA and nuclear DNA (nDNA), respectively. Each analysis was run in technical duplicate. The mitochondrial primers were previously validated for their specificity (unique amplification of mtDNA) and the absence of coamplified nuclear insertions of mitochondrial origin (NUMTs) [34].

2.6. MtDNA Methylation

Bisulfite pyrosequencing was used to evaluate the methylation level of the mtDNA in two areas of the D-loop region [the promoter of the heavy strand (HSP) and the promoter of the light strand (LSP)] and in the ND6 gene. To avoid potential confounding factor due to NUMTs, mtDNA was isolated from nDNA by means of magnetic beads (Agencourt AMPure XP, Beckman Coulter, Brea, CA, USA) that selectively bind to mtDNA, and nDNA specific enzymatic digestion (Plasmid-SafeTM ATP-Dependent DNase, Lucigen Biosearch Technologies, Middlesex, UK). To improve the efficiency of bisulfite conversion, the solution enriched with mtDNA was linearized using BamHI enzyme and then, converted with sodium bisulfite using the

EZ-96 DNA Methylation-Gold kit (Zymo Research, Orange, CA, USA). PCR amplification was performed using the PyroMark PCR kit (Qiagen, Venlo, The Netherlands) in a thermal cycling device (2720 Thermal cycler, Applied Biosystem, Waltham, MA, USA). The selected areas of the mtDNA were investigated for methylation as previously described (primer sequences available in the original manuscript by Sun et al.) [35]. Gel electrophoresis was used to check the amplification accuracy. Amplicons were pyrosequenced using the PyroMark Q24 device (Qiagen, Venlo, The Netherlands) [35]. Biological triplicates for each treatment were analyzed.

2.7. Gene Expression Analysis

Total RNA was extracted from Caco-2 cells with the Total RNA Purification Plus Kit (Norgen Biotek, Thorold, ON, Canada), according to the manufacturer's instructions and quantified (NanoDrop, Thermo Fisher Scientific, Italy). 1 μg of RNA was retrotranscribed to cDNA using the PrimeScript RT-PCR Kit (Takara Bio, Göteborg, Sweden) and quantitative real-time PCR (Biorad CFX96) was used to perform the gene expression analysis using TB Green® Premix Ex TaqTM (Takara Bio, Göteborg, Sweden). The amplification conditions were: 30 s at 95 ◦C (denaturation), 5 s at 95 ◦C (annealing) and 30 s at 60 ◦C (extension) repeated for 40 cycles. The expression levels of the target genes were normalized rela- tive to β-actin, using the $2^{-\Delta\Delta Ct}$ method. Each analysis was run in technical duplicate. An inter-run calibrator sample was applied to adjust the results obtained from different amplification plates. The target genes analyzed from Caco-2 cells were the epigenetic genes DNA methyltransferase 1 (DNMT1), DNA methyltransferase-3A (DNMT3A), DNA methyltransferase-3B (DNMT3B), Sirtuin-1 (SIRT1), Sirtuin-6 (SIRT6), and Sirtuin-7 (SIRT7), the pro-inflammatory genes interleukin-6 (IL-6) and interleukin 1β (IL-1β), the mitochondrial genes NADH dehydrogenase 6 (ND6), Cytochrome B (CYTB), Cytochrome c oxidase 1 (CO1), ATP synthase membrane 6 (ATP6) and the thigh junctions genes Zonulin 1 (ZO-1), Occludin (OCLN) and Claudin (CLDN1). The sequences of the primers used in the study are listed in Table S1 of Supplementary Materials. Biological triplicates for each treatment were analyzed.

2.8. ATP Quantification

The ATP content from treated Caco-2 cells was quantified using the ATP Colorimetric Assay Kit (Sigma-Aldrich, Darmstadt, Germany) according to the manufacturer's instructions. Briefly, pellets from treated Caco-2 cells were lysed, and the ATP content was determined by phosphorylating glycerol. To correct for background in samples, especially background caused by glycerol phosphate, we included a Sample Blank by omitting the ATP Converter, as detailed in the manufacturer's instructions. The Sample Blank readings were then be subtracted from the sample readings. The absorbance was read at 570 nm with a spectrometer (FLUOstar Omega, BMG LABTECH's, Ortenberg, Germany). An ATP calibration curve using specific standards was generated and used for accurate ATP quantification. All analyses were run in triplicate. The effects of TMA on ATP levels were compared to the negative control (cells not exposed to TMA).

2.9. Mitochondrial Membrane Potential

The mitochondrial membrane potential ($\Delta\Psi m$) was assessed by the Mitochondrial Membrane Potential Kit (Sigma-Aldrich, Germany). This assay utilizes the cationic, lipophilic dye JC-10, which can distinguish between living and apoptotic cells based on variations in their $\Delta\Psi m$. In brief, 8×10^4 cells were seeded into a 96-well plate, and various concentrations of TMA (0.01 µM, 0.1 µM, 1 µM, 10 µM, 100 µM, 200 µM, 400 µM, and 1 mM) were added to the cells. Additionally, two positive controls (LPS at 100 ng/mL and 10 µg/mL) and a negative control (vehicle only) were included. The treated cells were then incubated for 24 h at 37 °C. Subsequently, the cells were exposed to the JC-10 dye at 37 °C for 60 min, and the fluorescence was measured at two wavelengths (red at $\lambda ex = 490/\lambda em = 525$ nm and at $\lambda ex = 540/\lambda em = 590$ nm) using a fluorometer (FLUOstar Omega, BMG LABTECH's, Ortenberg, Germany). Each experimental condition was set up in technical duplicate.

2.10. Permeability Assay

The TEER measurement was performed in cells cultured in transwells at 0, 6, and 24 h post treatment with TMA at different concentrations (10 µM, 400 µM, and 1 mM) or LPS (100 nM, 10 µM). Three values were measured for each well, which were then averaged and expressed as percentages. Also, the Lucifer Yellow (LY) (Sigma-Aldrich

Life Science, Burlington, MA, USA) assay was used to measure the permeability of the Caco-2 multilayer. Briefly, the medium from both the AP and BL compartments was collected 24 h after treatments and stored at −80 ◦C for further analysis. Caco-2 cells on the AP side were gently washed twice with Phosphate-Buffered Saline (PBS) with Ca2+ and Mg2+ (Corning, Glendale, AZ, USA). LY at a concentration of 100 µM (in PBS with Ca2+ and Mg2+) was introduced into the AP compartment, while PBS (with Ca2+ and Mg2+) was added to the BL compartment. Subsequently, 150 µL of the solution from both compartments were promptly transferred to a 96-well plate, and fluorescence readings were taken using a fluorometer (FLUOstar Omega, BMG LABTECH's, Ortenberg, Germany) at λEx/λEm = 485/520 nm. These measurements were repeated at 30, 60, and 120 min after the addition of the LY solution in the AP. The cells were maintained at 37 ◦C in a humidified atmosphere containing 5% CO2 between each reading. All analyses were conducted in biological duplicate.

2.11. Statistics Analyses

Statistical analyses were performed by using SPSS (IBM SPSS Statistics for Windows, Version 24.0, Armonk, NY, USA) and R version 3.5.3 (R Core Team, Vienna, Austria). An ANOVA test with Bonferroni's correction for multiple testing was used to compare the difference between group means. A p-value < 0.05 was considered significant throughout the study. Results are shown as means ± SD.

3. Results

3.1. Cell Viability

The results from the MTT assay revealed that 24 h exposure to TMA at 100 mM ($p < 0.05$) and 10 mM ($p < 0.05$) concentrations exhibit significant cytotoxicity (Figure 1). Specifically, the residual viability of cells that were treated with 100 mM TMA is 10.01 ± 4.6%, while cells that were treated with 10 mM TMA show a viability of 72.66 ± 16.3%. No significant decrease in cell viability was measured for the other concentrations tested (Figure 1).

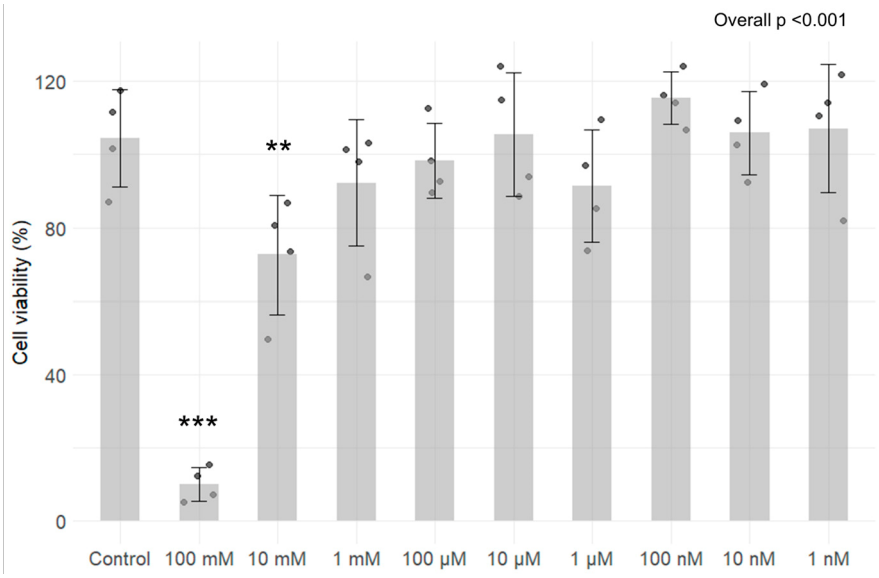

*Figure 1. Assessment of cytotoxicity of TMA on Caco-2 cells after 24 h exposure to different concentrations (ranging from 100 mM to 1 nM). Cell viability is expressed in percentages with standard deviation for each condition. Results revealed that exposure for 24 h to TMA at 100 mM and 10 mM exhibit significant cytotoxicity. ** p < 0.01; *** p < 0.001 vs. Control.*

3.2. Expression Levels of Pro-Inflammatory Genes

Expression levels of the pro-inflammatory cytokines IL-1β and IL-6 were measured in Caco-2 cells exposed to various concentrations of TMA (10 µM, 400 µM, and 1 mM) and to LPS at 100 ng/mL. A statistically significant increase in the expression levels of both analyzed genes was measured in cells treated with TMA at 1 mM (IL-1β, $p < 0.001$; IL-6, $p < 0.001$), while no significant changes were observed at lower TMA concentrations (Figure 2A,B).

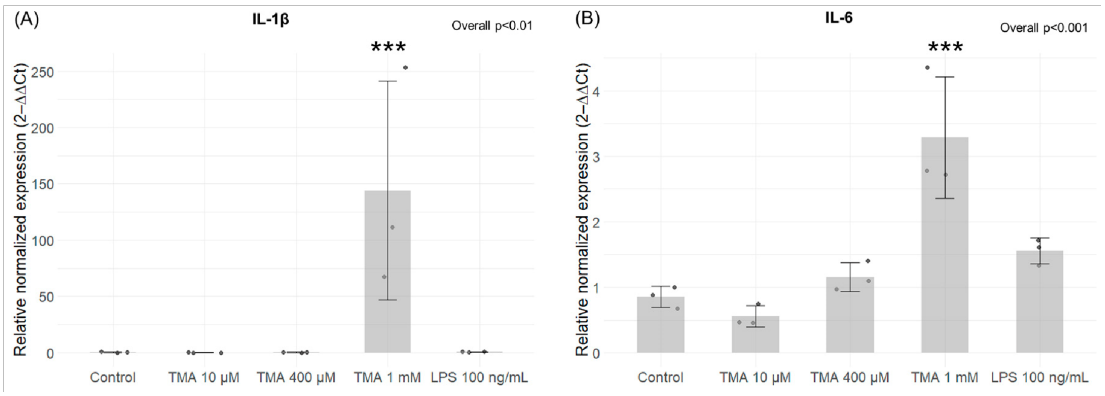

*Figure 2. Expression levels of inflammatory genes. Expression levels of IL-1β (A) and IL-6 (B) in Caco-2 cells measured by qPCR after TMA treatments at different concentrations (10 μM, 400 μM, and 1 mM) for 24 h. A statistically significant increase in the expression levels of both genes was measured in cells treated with TMA at 1 mM. *** $p < 0.001$ vs. Control.*

3.3. Expression Levels of DNMTs and SIRTs

A significant increase in DNMT1 expression was induced by TMA at 10 μM ($p < 0.05$) and 400 μM ($p < 0.05$) (Figure 3A). Conversely, a statistically significant decrease in DNMT3A expression was observed after exposure for 24 h to TMA at 1 mM ($p < 0.05$) and LPS at 100 ng/mL ($p < 0.05$) (Figure 3B). On the other hand, DNMT3B expression remained unaffected by both TMA and LPS treatments ($p > 0.05$) (Figure 3C). Significantly elevated levels of SIRT1 were measured in Caco-2 cells exposed to TMA at all tested concentrations (10 μM, $p < 0.05$; 400 μM, $p < 0.01$; 1 mM, $p < 0.01$) (Figure 4A). In contrast, the expression of SIRT6 and SIRT7 was affected only by LPS 10 μg/mL (Figure 4B,C).

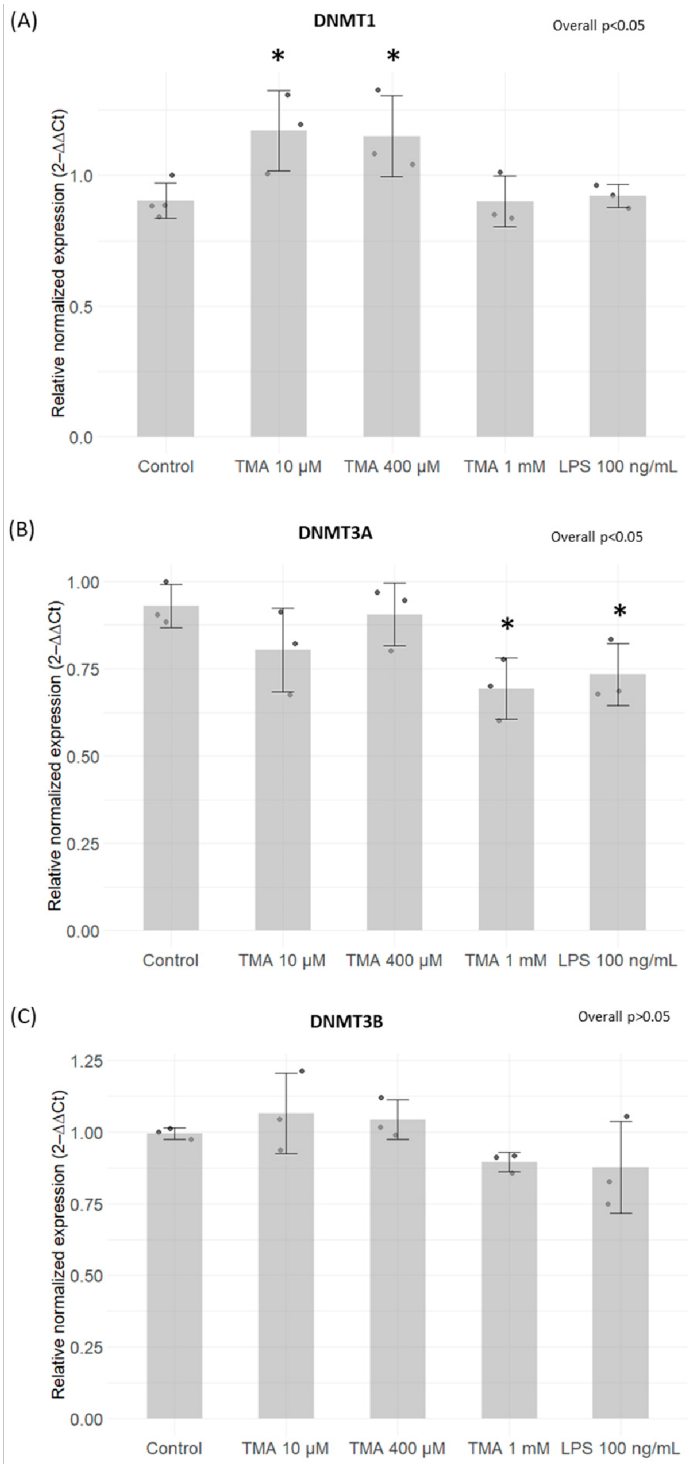

Figure 3. Expression levels of DNMTs measured by qPCR. DNMT1 (A), DNMT3A (B) and DNMT3B (C) expression levels on Caco-2 cells after TMA treatments measured with the qPCR. A significant increase in DNMT1 expression was induced by TMA at 10 µM and 400 µM (A). A statistically significant decrease in DNMT3A expression was observed after

*exposure for 24 h to TMA at 1 mM and LPS at 100 ng/mL (B). DNMT3B expression remained unaffected by both TMA and LPS treatments (C). * p < 0.05 vs. Control.*

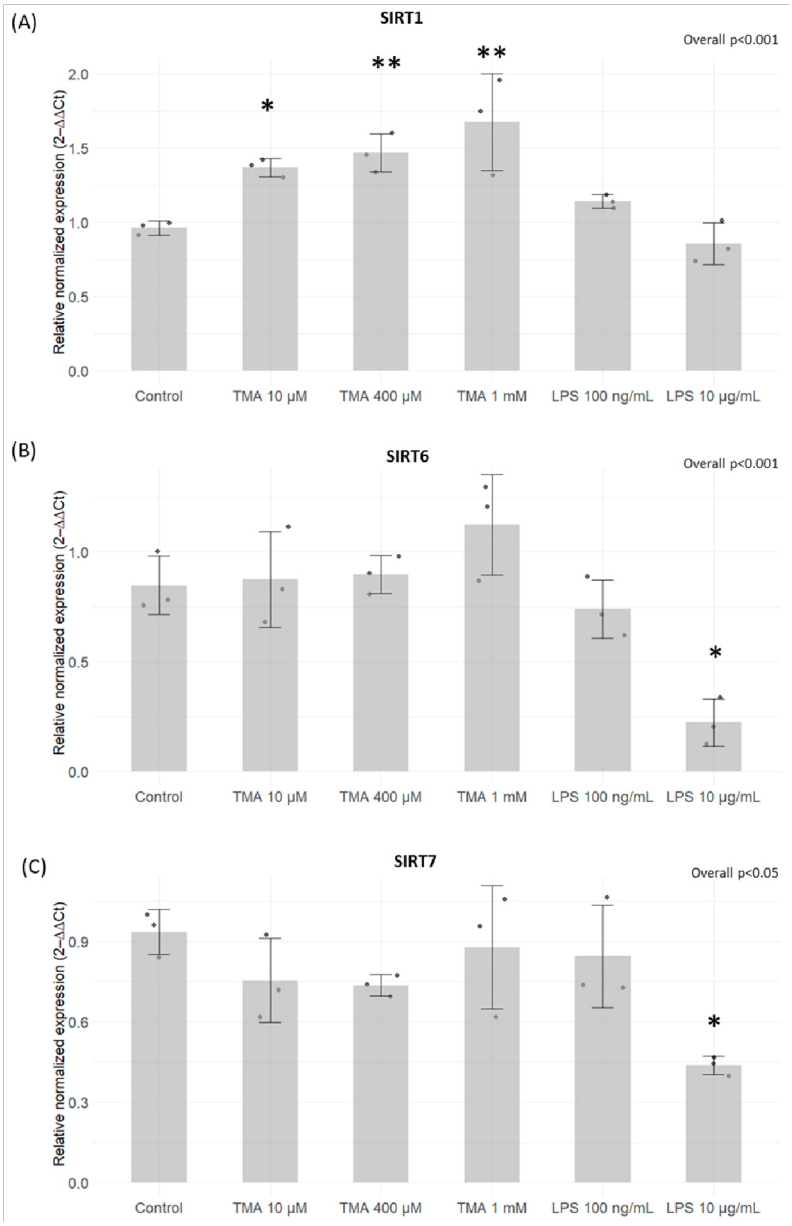

Figure 4. Expression levels of SIRTs. SIRT1 (A), SIRT6 (B), and SIRT7 (C) expression levels on Caco-2 cells after TMA treatments measured with the qPCR. Significantly elevated levels of SIRT1 were measured in Caco-2 cells exposed to TMA at all tested concentrations (A). The

*expression of SIRT6 and SIRT7 was affected only by LPS 10 µg/mL (B,C). * $p < 0.05$; ** $p < 0.01$ vs. Control.*

3.4. DNMT and SIRT Enzymatic Activity

The ability of different TMA concentrations to modulate the activity of SIRTs and DNMTs isolated from Caco-2 cells was tested in a cell-free experimental setting. TMA did not elicit any notable changes in DNMT activity at any of the concentrations tested (overall $p > 0.05$) (Figure 5A). Conversely, the results indicate that TMA can hamper SIRTs' activity in a concentration-dependent manner. The inhibition of their activity was significant within the concentration range of 0.1 µM to 1 mM (overall $p < 0.001$) (Figure 5B).

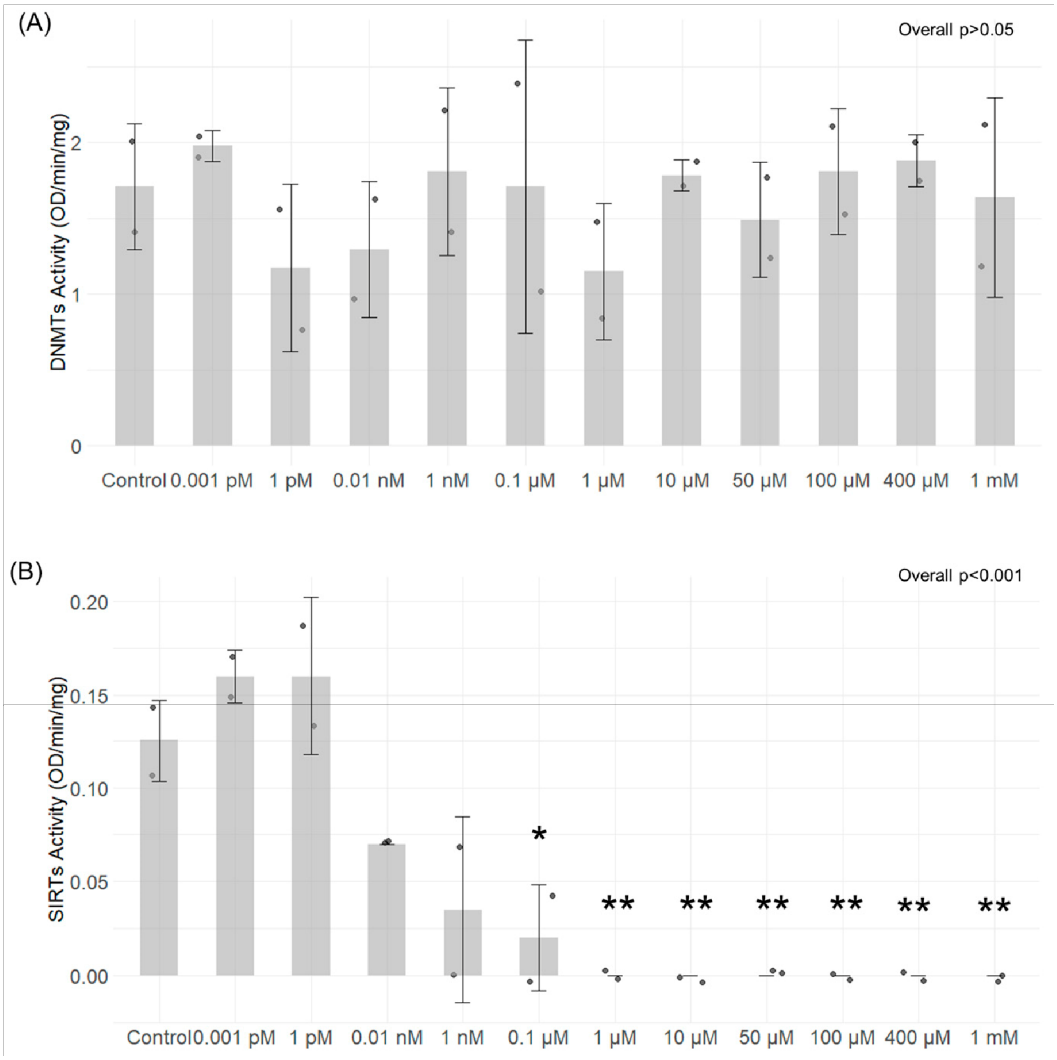

*Figure 5. DNMTs and SIRTs enzymatic activity after exposure to different concentrations of TMA. DNMTs activity (A) and SIRTs' activity (B) were tested in a cell-free experimental setting after exposure of nuclear extract to different concentrations of TMA using the EpiQuik™ DNA Methyltransferase Activity/Inhibition Assay Kit (EpigenTek, Farmingdale, NY, USA) and the Universal SIRT Activity Assay Kit (Abcam, Waltham, MA, USA), respectively. TMA did not provoke any notable changes in DNMT activity at any of the concentrations tested (A). In contrast, the results indicate that TMA can hamper SIRTs' activity in a concentration-dependent manner; the inhibition of their activity was significant within the concentration range of 0.1 μM to 1 mM (B). * $p < 0.05$; ** $p < 0.01$ vs. Control.*

3.5. mtDNA Quantification and Methylation

The treatment with TMA 1 mM induced a significant decrease in intracellular mtDNAcn ($p < 0.05$) (relative to nDNA copies). Neither the lower TMA concentrations nor LPS 100 ng/mL were able to affect mtDNAcn (Figure 6A). As for the release of mtDNA from the cell following an induction of the inflammatory condition, the relative quantification analysis revealed a significant increase in cf-mtDNA (over cf-nDNAcn) released into the medium by Caco-2 cells after exposure to 1 mM TMA ($p < 0.05$) and LPS 100 ng/mL ($p < 0.01$) (Figure 6B). Of note, the absolute quantification analysis of cell-free mtDNAcn (cf-mtDNAcn) performed by Qiacuity digital PCR confirmed a significant increase in the absolute copies/mL of cf-mtDNA released in the medium only upon TMA 1 mM treatment ($p < 0.05$) (Figure 6C). The methylation levels were investigated in three areas of mtDNA: the regulatory regions HSP and LSP as well as in the ND6 mitochondrial gene. Methylation levels detected by bisulfite pyrosequencing were very low in all the three areas (around 2–3%). A significant increase in the methylation of the LSP area was measured after TMA 1 mM treatment with respect to controls ($p < 0.01$), with a signal which was almost doubled compared to the control (Supplementary Materials Figure S1A). This increase was driven by the effect of the second CpG (CpG2) analyzed in the LSP area ($p < 0.001$) (Supplementary Materials Figure S1B).

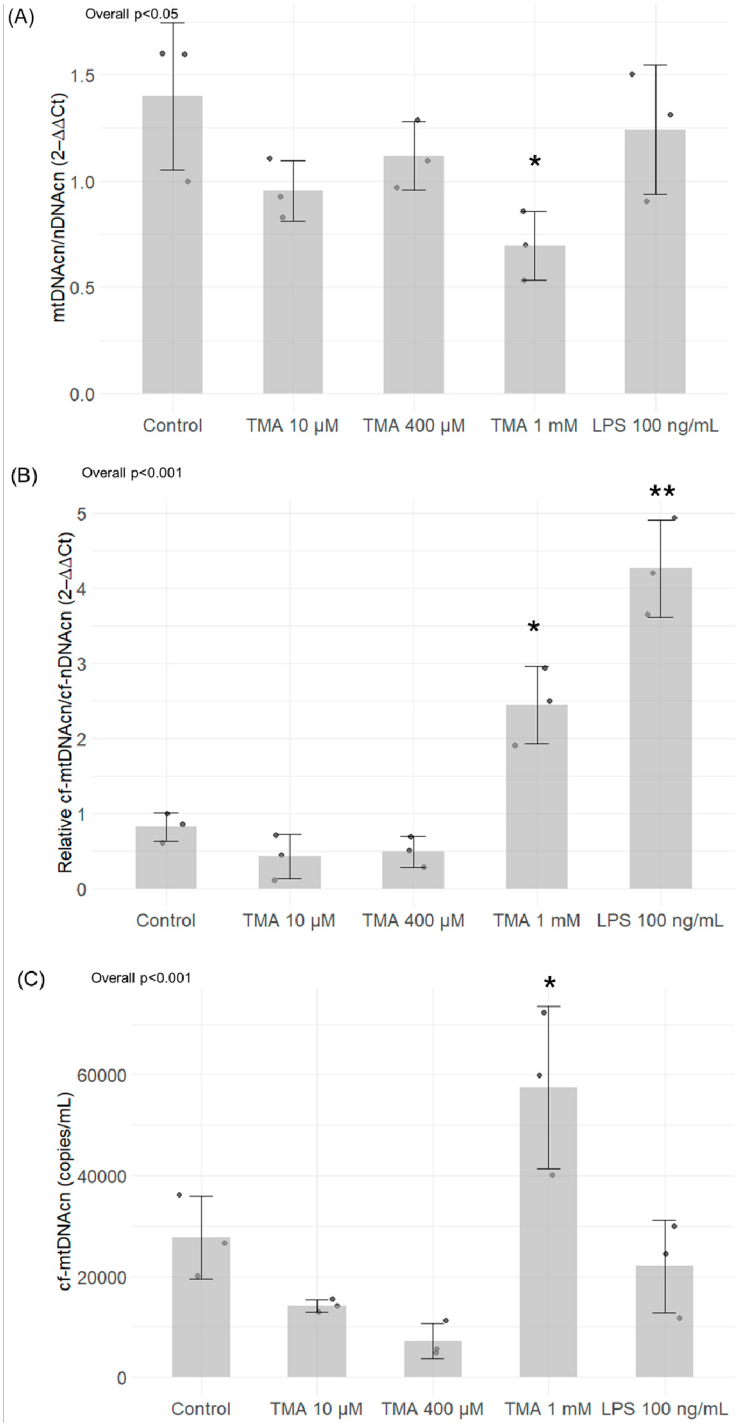

Figure 6. MtDNA quantification in Caco-2 cells exposed to different concentrations of TMA and in the cell culture medium. Intracellular mtDNAcn (A) and cf-mtDNA released in the culture medium (B,C) were assessed by Caco-2 cells after TMA treatments. Panel (B) shows values of cf-mtDNAcn normalized for cf-nDNAcn, while panel (C) shows the absolute

*quantification of mtDNAcn/mL of medium. Significant variations in mtDNAcn were observed in the treatment with TMA 1 mM, while neither the lower TMA concentrations nor LPS 100 ng/mL were able to affect intracellular mtDNAcn (A). As for the release of mtDNA from the cell following an induction of the inflammatory condition, the relative quantification analysis revealed a significant increase in cf-mtDNA after exposure to 1 mM TMA and LPS 100 ng/mL (B). The absolute quantification analysis of cf-mtDNAcn by digital PCR confirmed a significant increase in cf-mtDNA only upon TMA 1 mM treatment (C). * $p < 0.05$; ** $p < 0.01$ vs. Control.*

3.6. Expression of Mitochondrial Genes

The expression levels of ND6 significantly decreased with the highest TMA concentration (TMA 1 mM, $p < 0.05$), as well as both LPS treatments ($p < 0.05$) (Figure 7B). Conversely, CO1 showed significant downregulation after treatments with the lowest TMA concentration (TMA 10 µM, $p < 0.05$) and LPS 10 µg/mL ($p < 0.05$) (Figure 7C). The expression levels of ATP6 and CYTB were not affected by TMA treatments but only by LPS 10 µg/mL ($p < 0.05$ for both genes) (Figure 7A,D).

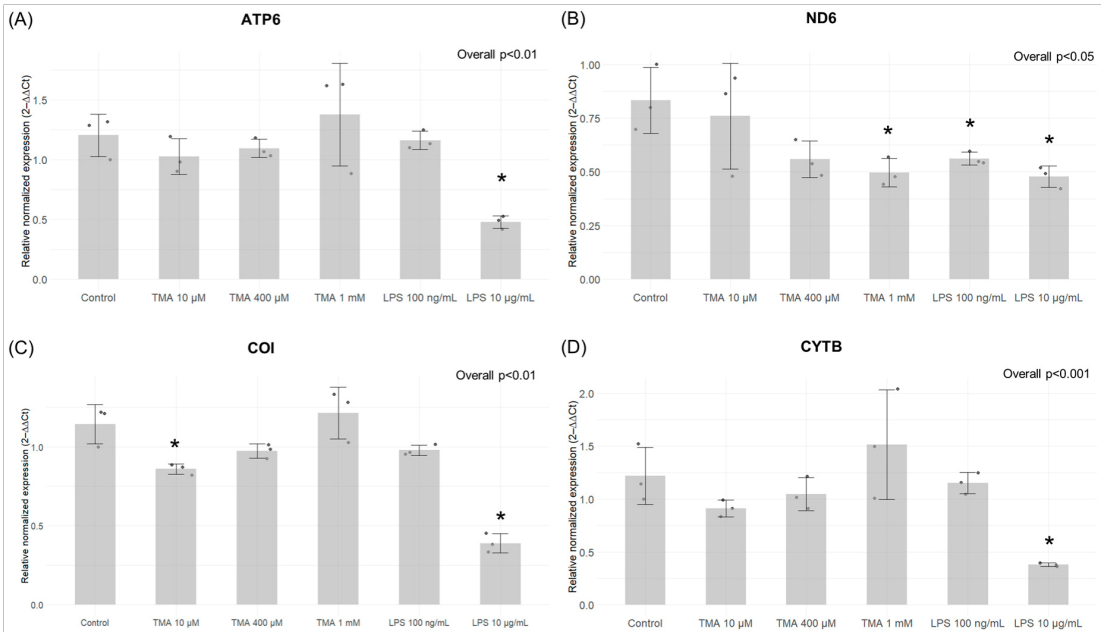

Figure 7. Expression of mitochondrial genes by qPCR. The gene expression of ATP6 (A), ND6 (B), CO1 (C), CYTB (D) in the different experimental conditions. The expression levels of ND6 significantly decreased with the highest TMA concentration (TMA 1 mM), as well as both LPS

*treatments (B). Conversely, CO1 showed significant downregulation after treatments with the lowest TMA concentration (TMA 10 µM) and LPS 10 µg/mL (C). The expression levels of ATP6 and CYTB were not affected by TMA treatments but only by LPS 10 µg/mL (A,D). * p < 0.05 vs. Control.*

3.7. ATP Quantification

To assess the impact of TMA on intracellular ATP levels, Caco-2 cells were cultured in the presence of different concentrations of TMA (10 µM, 400 µM, and 1 mM). After 24 h, intracellular ATP was quantified on lysed cells. ATP contents is expressed as nmoles ATP per 1 million cells. A decrease in ATP content was observed for all TMA concentrations tested (10 µM TMA, $p < 0.001$; 400 µM TMA, $p < 0.01$ and 1 mM TMA, $p < 0.001$), as well as exposing cells to 100 ng/mL LPS ($p < 0.01$) (Figure 8). As ATP content reflects the metabolic activity of cells, here, we confirm that TMA slows down the cellular metabolism in Caco-2 cells.

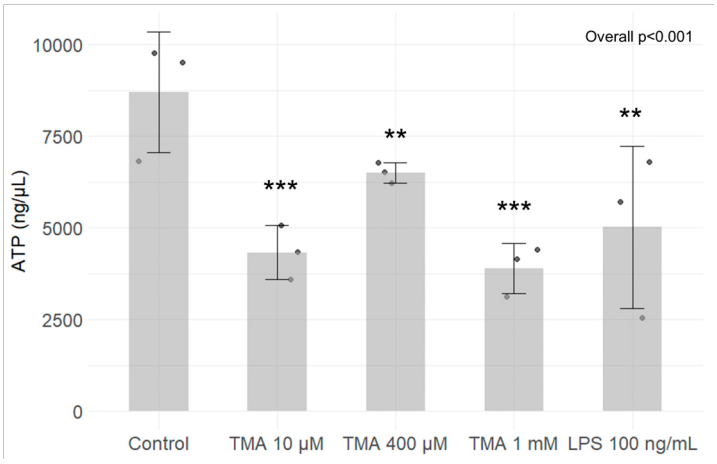

*Figure 8. ATP quantification. ATP levels in Caco-2 cells exposed to different TMA concentrations and LPS (as positive control) was measured using the ATP Colorimetric Assay Kit (Sigma-Aldrich, Germany). A decrease in ATP content was observed for all TMA concentrations tested, as well as exposing cells to 100 ng/mL LPS. ** p < 0.01; *** p < 0.001 vs. Control.*

3.8. Mitochondrial Membrane Potential

The mitochondrial membrane potential (ΔΨm) serves as a crucial gauge not only for mitochondrial activity, indicating ATP production, but also as a marker for overall

cellular well-being. In this study, the impact of different doses of TMA on the mitochondrial membrane potential was explored. Following a 24 h exposure to various TMA concentrations, (from 0.01 µM to 1 mM), and to two LPS concentrations (100 ng/mL and 10 µg/mL), no notable changes in the mitochondrial membrane potential were discerned across the tested concentrations (overall $p > 0.05$) (Supplementary Materials Figure S2).

3.9. Assessment of the Intestinal Permeability

The integrity of the intestinal monolayer after 24 h exposure to different concentrations of TMA was investigated using the TEER assay. The epithelium integrity was significantly affected by TMA exposure at time 0, and after 6 h and 24 h, decreasing significantly when compared with the control group at the same time points (Figure 9). Similarly, a significant reduction in the epithelium integrity was measured after exposure to LPS (100 ng/mL, 10 µg/mL), used as positive control for a pro-inflammatory condition (Figure 9). In contrast, no significant differences in permeability were measured between the different treatments with the Lucifer Yellow assay (Supplementary Materials Figure S3). To evaluate the effect of TMA on intestinal permeability, the expression levels of the thigh junctions ZO-1, CLDN1 and OCLN were also measured in Caco-2 cells after the exposure to various concentrations of TMA (10 µM, 400 µM, and 1 mM) and to LPS (100 ng/mL and 10 µg/mL). No significant difference was measured in the expression levels of either ZO-1, CLDN1 or OCLN genes when compared to the control (Supplementary Materials Figure S4).

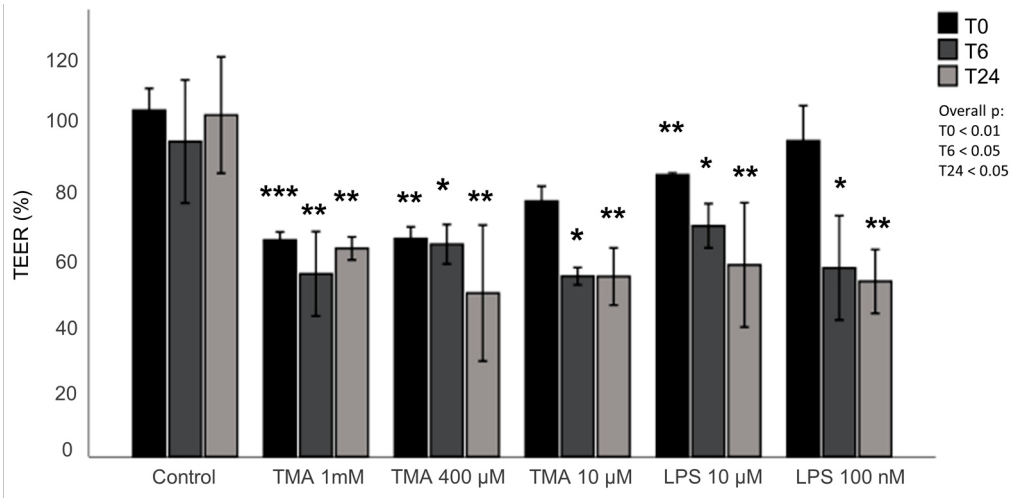

*Figure 9. Assessment of the intestinal permeability. The effect of TMA on intestinal barrier was assessed performing TEER measurement in cells cultured in transwells during the treatment with TMA (1 mM, 400 µM, 10 µM) and LPS (10 µg/mL, 100 ng/mL) at time 0, 6 and 24 h post treatment. The values shown in the figure are expressed as a percent of control. * p < 0.05; ** p < 0.01; *** p < 0.001 vs. Control measured at the same time (T0 or T6 or T24, respectively).*

4. Discussion

Numerous studies have proven the existence of a causal link between diet, gut microbiota and human diseases [36]. Addressing the gut microbiota and their metabolites emerges as a promising approach in managing complex multifactorial pathologies, including cardiovascular [37] and metabolic diseases [38,39]. Among diet-derived metabolites suggested as potentially dangerous for the human health, TMAO and TMA have attracted increasing attention [4,40]. As TMAO in the bloodstream is predominantly derived from a nearly complete hepatic oxidation of TMA, most scientific inquiries have focused on TMAO [37,41], with only a limited number of studies exploring the impact of TMA on health. Jaworska et al. indicated that cardiovascular patients exhibit more than double the plasma TMA levels than their healthy counterparts, accompanied by a comparatively smaller disparity in TMAO levels [42]. Altered levels of circulating TMA was also associated to CVD [43]. Despite its systemic role, considering that TMA is produced in the gut, exploring its local impact on the intestinal environment becomes particularly intriguing. The results from our study support the hypothesis that an excess of dietary derived TMA can affect gut health by modulating intestinal permeability, inflammation and epigenetic homeostasis.

In particular, elevated TMA levels stimulated pro-inflammatory signaling in Caco-2 cells, as evidenced by the heightened expression of pro-inflammatory cytokines IL-6 and IL1β (Figure 2). The pro-inflammatory effect associated to TMA aligns with prior research [5]. Pro-inflammatory effects were observed at the highest concentration tested (where the increase was higher than in cells exposed to LPS 100 ng/mL) but not at the lowest. This suggests that low and physiological levels of this molecule likely have no adverse effects on the gut, whereas conditions that lead to an excess of TMA may pose a risk due to its pro-inflammatory effects.

Of note, previous findings showed that inflammation has the potential to cause epigenetic alterations [17]. Foran et al. observed that IL-6 increases DNMT1 expression, causing the excessive methylation of tumor suppressor genes [44]. Yang et al. confirmed this observation by showing that IL-6 silences the expression of suppressor of cytokine signaling 3 (SOCS 3) by inducing high expression levels of DNMT1 [45]. Despite the fact that changes in gene expression have been linked to

inflammation, the resulting impact on the methylome varies across different contexts, making the overall picture complex. Changes in methylation patterns, as well as disturbances in the function and abundance of SIRTs, have been previously linked to various biological conditions and human disorders, including inflammatory responses [46,47]. In our study, TMA was not able to modulate DNMT activity in cell-free in vitro tests. We found a mild modulation of the expression of genes encoding for DNMTs after their exposure to different TMA concentrations in the cellular model. Despite the fact that our findings suggest the potential ability of TMA to perturb DNMT expression, we could not detect a clear association between inflammation induced by TMA (which was especially observed at a high concentration, i.e., 1 mM) and DNMT expression. In contrast, TMA was able to significantly modulate SIRT activity, with a dose-dependent effect.

Notably, SIRT1 expression was upregulated in Caco-2 cells exposed to the highest dose of TMA (1 mM), suggesting a potential compensatory response to offset the decline in enzymatic activity. Also, the inhibition of SIRT activity might be associated with the TMA's pro-inflammatory action, given that the suppression of SIRTs is a recognized facet of the acute inflammatory response measured both in laboratory settings and within living organisms [48]. Indeed, NAD+-dependent SIRTs play essential, distinct roles in both chronic and acute inflammation, with chronic inflammatory diseases often associated with a deficient "low-sirtuin" state. Maintaining an adaptive phenotype relies on continuous NAD+ generation, along with heightened SIRT1 expression and activation [49]. The substantial depletion of NAD+ within cells during inflammatory responses [50] could explain the reduction in SIRT activity, as these enzymes depend on intracellular NAD+ as a cofactor. Of note, previous evidence showed that TMAO represses SIRT expression [51]. Luo T. et al. [52] documented an upregulation of DNMTs in response to TMAO in a study where mice received TMAO-supplemented water. Additionally, TMAO treatment in RAW264.7 cells was associated with an elevated expression of both DNMT1 and DNMT3B. Altogether, these findings suggest that both TMA and TMAO might affect epigenetic regulations by affecting these pathways. As observed for proinflammatory cytokines, TMA can upregulate the gene expression of DNMT1 (Figure 3) and SIRT1 (Figure 4) more than what is observed with LPS. This suggests that alterations of these

parameters are driven by TMA specifically, rather than by inflammation per se. However, while we can speculate that TMA may directly affect Sirtuin homeostasis, as indicated by its ability to suppress Sirtuins' activity (Figure 5), we cannot draw the same conclusion for DNMT1. Further studies are needed to determine whether TMA directly impacts DNMT1 expression independently of inflammation, especially considering the central role of this enzyme in maintaining overall DNA methylation patterns within the cell. Considering the widely recognized involvement of mitochondria in inflammation, we tested if intestinal cells exposed to different TMA concentrations undergo changes in mitochondrial functions. The capacity of TMAO to alter the mitochondrial energy metabolism has been previously demonstrated in cardiac tissues [53]. Previous evidence also showed that administration of TMAO into WT mice lead to a reduction in ATP levels in cardiac tissue throughout the suppression of mitochondrial complex IV activity [54]. However, little is known about the action of TMA on the subunits of the respiratory chain. In our study, TMA induced a decrease in intracellular ATP concentration. This evidence is in line with the results revealed by Jalandra et al. [5]. Despite the effect of TMA on ATP levels, no significant alteration of the mitochondrial membrane potential after TMA treatments was measured. Nevertheless, the gene expression of CO1 and ND6, two components of the electron transport chain, is downregulated by TMA. CO1 and ND6 have a crucial role in the process of energy homeostasis and the decrease in their expression caused by TMA treatment corroborates the hypothesis of a direct TMA-induced mitochondrial dynamics damage. The mechanism of regulation of the mitochondrial gene expression has not been totally elucidated yet: whether it is regulated by the methylation on the mtDNA is still a matter of debate. In our experimental settings, we measured by bisulfite pyrosequencing low levels of mtDNA methylation in the light strand promoter region (LPS), which doubled in cells exposed to the highest dose of TMA (1 mM). Alterations of DNA methylation in this area, in association with a decreased expression of the ND6 gene, suggest a potential correlation between these phenomena (in particular, considering that ND6 is the only gene under the control of LSP promoter). Of note, previous evidence demonstrated that higher ND6 methylation levels were associated with lower ND6 expression in a liver sample of patients with Metabolic Steatohepatitis (MeSH) and in leukocytes of diabetic patients [10,55,56].

Although intriguing, further studies are necessary to confirm this preliminary evidence and clarify the role of mtDNA methylation in this context.

Remarkably, we found that TMA has a significant impact on mtDNAcn, both in the intracellular and extracellular context. In our study, Caco-2 cells exposed to TMA 1 mM showed lower levels of intracellular mtDNAcn over nDNA copies. The mtDNAcn has been considered a biomarker of mitochondrial health: a high mtDNAcn level has been hypothesized to reflect a proper mitochondrial DNA translation leading to mitochondrial genome stability, while a decrease in mtDNAcn has been associated with the downregulation of mitochondrial transcription and a decline in OXPHOS proteins levels [7]. This evidence corroborates the hypothesis of a detrimental effect of TMA on mitochondrial functions. The potential alteration of mtDNA functions is reflected also in the increased cf-mtDNA measured in the medium of cells exposed to 1 mM TMA. Cf-mtDNA has been suggested to be released by cells throughout cellular death/breakdown processes or throughout an active regulated process probably linked to inflammation [57]. Indeed, cf-mtDNA has been found increased in plasma of inflammatory pathologies patients, even though the mechanistic explanation for this association has not been elucidated yet [29,58,59]. In vitro studies showed that the treatment of cells with purified mtDNA and proinflammatory compounds trigger pro-inflammatory responses [57]. In particular, the co-stimulation of monocytes with purified cf-mtDNA and LPS potentiated the pro-inflammatory action of LPS [57,60]. Furthermore, the combination of mtDNA and N-Formylmethionyl-leucylphenylalanine (fMLS) in polymorphonuclear leukocytes induced IL-8 more than fMLF alone [57,61]. Thus, we can speculate that the released cf-mtDNA might foster the local pro-inflammatory action of TMA in the gut. Of note, while both TMA 1 mM and LPS were associated to increased mtDNAcn/nDNAcn ratio, the absolute quantity of cf-mtDNA released into the medium measured by digital PCR was higher in cells exposed to TMA compared to LPS. This finding suggests that TMA has a specific effect on mitochondrial dynamics, which aligns with our additional results.

Our findings also suggest that exposure to TMA can damage the intestinal epithelium integrity, potentially promoting a leaky gut, which is often associated with a proinflammatory condition. Although preliminary, this result supports further studies investigating how factors that increase gut TMA levels (including dietary precursors

and microbiome composition) affect intestinal barrier functions and possibly contribute to leaky gut.

This study has several limitations. Firstly, we were able to perform the experiment only in vitro and in a singular cell line. Further investigations aimed at confirming these preliminary findings in other cell lines and in vivo are necessary before addressing the TMA of potentially harmful effects and driving therapeutic or dietetic intervention. Also, despite the fact that Caco-2 cells are a widely used to generate a surrogate of intestinal epithelium and testing diet-derived molecules, we have to keep in mind that they are a tumoral cell line, with potential responses that might not be replicated in more physiological conditions. Similar studies on different cellular models (non-transformed cells or organoids) that might be able to simulate better physiological condition of healthy humans are warranted. Also, given the potential effect of TMA on mitochondrial homeostasis, further investigations showing the impact of TMA on mitochondrial morphology and functionality (e.g., respiration measured with Seahorse Analyzer or Oroboros O2k) would add valuable insights to this complex picture. Finally, further studies are needed to assess the physiological levels of TMA in the gut to determine the concentrations to which the gut can be exposed in real-life contexts. This is crucial due to the significant variability in TMA levels, which are directly influenced by diet and microbiome composition.

Despite these limitations, our study provides preliminary evidence that TMA excess in the gut might not only endorse an increase in circulating TMAO levels but also promote in situ inflammation, disrupting both epigenetic and mitochondrial homeostasis. Despite the fact that alterations induced by TMA in the conditions we tested did not induce a complete disruption of cellular functions, a prolonged activation of the pro-inflammatory state induced by TMA may lead to increased intestinal permeability and compromised mitochondrial functions. Further studies corroborating these preliminary findings in different experimental context could prompt a reassessment of dietary recommendations concerning TMA precursors and microbiome modulation strategies designed to reduce TMA accumulation and its potential adverse effects.

Supplementary Materials

Supplementary Table S1. *Primer sequences used for gene expression analysis.*

	Fw (5'-3')	Rv (5'-3')	RefSeq accession number
SIRT1	ACGCTGGAACAGGTTGCGGG	AGCGGTTCATCAGCTGGGCAC	NM_001314049.2
SIRT6	AGTTCGACACCACCTTTGAG	CGTACTGCGTCTTACACTTG	XM_054321190.1
SIRT7	CGTCCGGAACGCCAAATAC	GACGCTGCCGTGCTGATT	XM_054316405.1
IL-6	TGCAATAACCACCCCTGACC	GTGCCCATGCTACATTTGCC	XM_054358146.1
IL-1β	AGATGATAAGCCCACTCTACAG	ACATTCAGCACAGGACTCTC	XM_047444175.1
ND6	CAAACAATGTTCAACCAGTAACCACTAC	ATATACTACAGCGATGGCTATTGAGGA	NM_005006
CYTB	ATCACTCGAGACGTAAATTATGGCT	TGAACTAGGTCTGTCCCAATGTATG	NM_001031702
CO1	GACGTAGACACACGAGCATATTTCA	AGGACATAGTGGAAGTGAGCTACAAC	NM_001114.4
ATP6	TAGCCATACACAACACTAAAGGACGA	GGGCATTTTTAATCTTAGAGCGAAA	NM_001686.4
ZONULIN	TTCACGCAGTTACGAGCAAG	TTGGTGTTTGAAGGCAGAGC	XM_054378717.1
OCCLUDIN	GGGCATTGCTCATCCTGAAG	GCCTGTAAGGAGGTGGACTT	XM_054351382.1
CLAUDIN	TGGTCAGGCTCTCTTCACTG	TTGGATAGGGCCTTGGTGTT	NM_021101.5
DNMT1	Biorad PrimePCR™ SYBR® Green Assay: DNMT1, Human Unique Assay ID:qHsaCED0044343		NM_001130549.2
DNMT3A	Biorad PrimePCR™ SYBR® Green Assay: DNMT3a, Human Unique Assay ID: qMmuCED0037493		NM_006892.5
DNMT3B	Biorad PrimePCR™ SYBR® Green Assay: DNMT3b, Human Unique Assay ID: qHsaCED0042577		NM_006892.4

Supplementary Figure S1*. Evaluation of mtDNA methylation by bisulfite pyrosequencing. Percentage of average methyla on of the LSP area (A) and focus on the second CpG (CpG2) of the LSP area (B) for the different treatments. A significant increase in the methyla on of the LSP D-Loop area has been measured a er TMA 1mM*

*treatment (A); this increase was driven by the effect of the CpG2 analysed in the LSP D-Loop area (B). **p <0.01; ***p <0.001***p <0.001 vs Naif.*

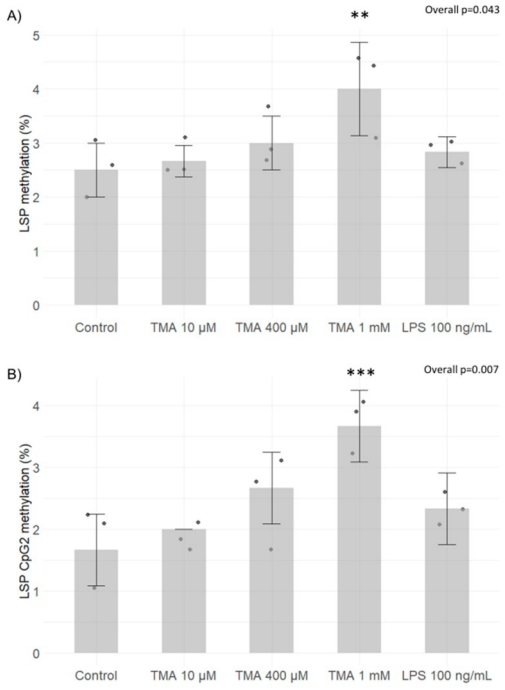

Supplementary Figure S2. *Evaluation of Mitochondrial membrane poten al. Mitochondrial membrane poten al (ΔΨm) in Caco-2 cells a er 24h TMA treatments. The analysis was conducted in technical duplicates.*

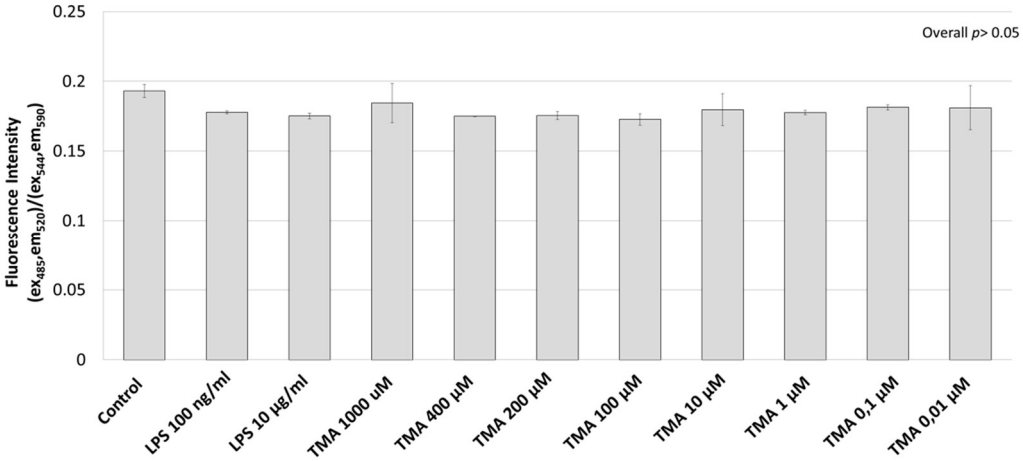

Supplementary Figure S3. *Assessment of the intes nal permeability. Intes nal permeability of Caco2 cells epithelium model measured by the Lucifer Yellow (LY) assay. The plot shows the permeability of the epithelium at me 0, 30, 60 and 120 minutes a er the addi on of the LY on the AP compartment. The analysis was conducted in duplicates.*

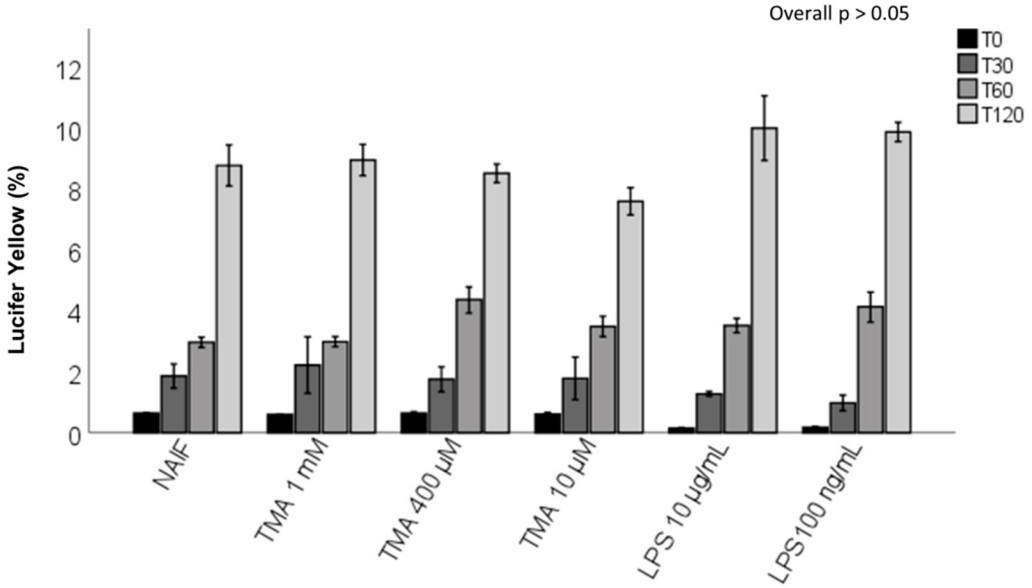

Supplementary Figure S4. *Expression levels of ght junc ons. Expression levels of ZO-1 (A), OCLN (B) and CLDN1 (C) in Caco-2 cells treated with TMA (10µM, 400µM, and 1mM), and LPS (100 ng/ml and 10 µg/ml) was measured by qPCR. No significant difference was observed in the expression levels of either ZO-1, OCLN or CLDN1 genes when compared to the control.*

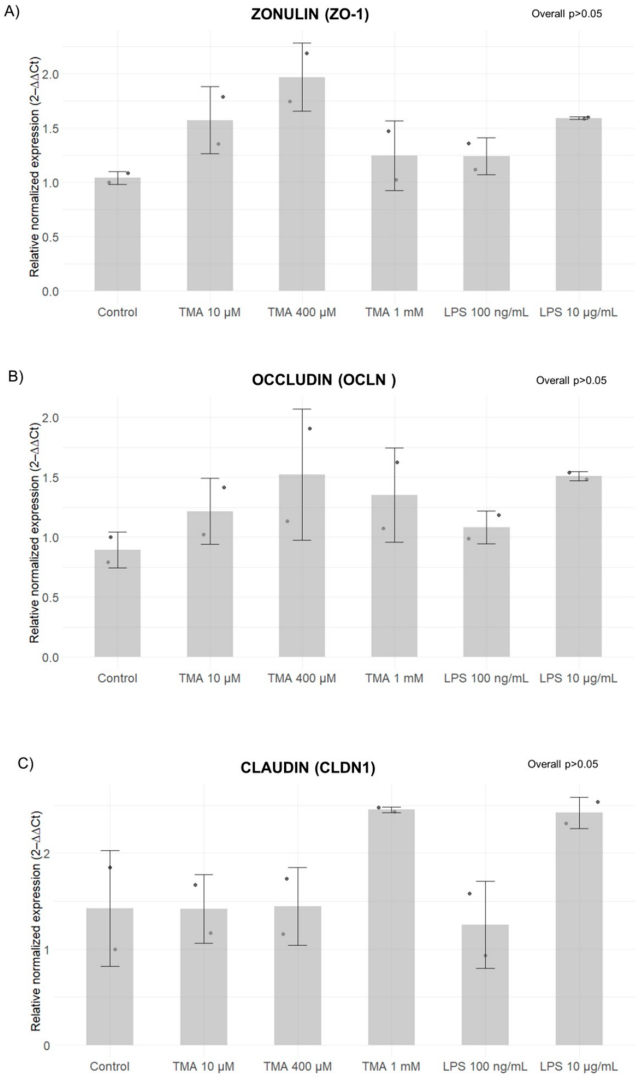
A)
ZONULIN (ZO-1)
Overall p>0.05
Relative normalized expression (2−ΔΔCt)
0.0
0.5
1.0
1.5
2.0
Control
TMA 10 µM
TMA 400 µM
TMA 1 mM
LPS 100 ng/mL
LPS 10 µg/mL
B)
OCCLUDIN (OCLN)
Overall p>0.05
Relative normalized expression (2−ΔΔCt)
0.0
0.5
1.0
1.5
2.0
Control
TMA 10 µM
TMA 400 µM
TMA 1 mM
LPS 100 ng/mL
LPS 10 µg/mL
C)
CLAUDIN (CLDN1)
Overall p>0.05
Relative normalized expression (2−ΔΔCt)
0
1
2
Control
TMA 10 µM
TMA 400 µM
TMA 1 mM
LPS 100 ng/mL
LPS 10 µg/mL

Abbreviations

AP: apical; ATP6: ATP synthase membrane 6; B2M: Beta 2 microglobulin; BL: basal; BSA: bovine serum albumin; Caco-2 cells: colon adenocarcinoma cells; Cf-DNA: cell-free DNA; Cf-mtDNA: cell-free mitochondrial DNA; Cf-mtDNAcn: cell-free mitochondrial DNA copy number; Cf-nDNA: cell-free nuclear DNA; CO1: cytochrome c oxidase 1; CVDs: cardiovascular diseases; CYTB: cytochrome B; D-loop: displacement loop; DMEM: Dulbecco's modified Eagle's medium; DNMT1: DNA methyltransferase 1; DNMT3A: DNA methyltransferase 3A; DNMT3B: DNA methyltransferase 3B; DNMTs: DNA methyltransferases; FBS: fetal bovine serum; fMLS: N-Formylmethionyl-leucylphenylalanine; FMOs: hepatic flavin monooxygenases; HSP: promoter of the heavy strand; IL-1β: Interleukin 1β; IL-6: Interleukin 6; LPS: lipopolysaccharide; LSP: promoter of the light strand; LY: Lucifer Yellow; MeSH: Metabolic Steatohepatitis; mtDNA: mitochondrial DNA; mtDNAcn: mitochondrial DNA copy number; MTT: 3-(4,5-Di-2-yl)-2,5-ditetrazolium bromide; ND6: NADH dehydrogenase 6; NEAAs: non-essential amino acids; NUMTs: nuclear insertions of mitochondrial origin; PBS: Phosphate-Buffered Saline; qPCR: quantitative real-time polymerase chain reaction;

SIRT1: Sirtuin 1; SIRT6: Sirtuin 6; SIRT7: Sirtuin 7; SIRTs: Sirtuins; SOCS 3: cytokine signaling 3;

TEER: transepithelial electrical resistance; TMA: trimethylamine; TMAO: Trimethylamine-N-Oxide; ΔΨm: mitochondrial membrane potential.

References

1. Andraos, S.; Lange, K.; Clifford, S.A.; Jones, B.; Thorstensen, E.B.; Kerr, J.A.; Wake, M.; Saffery, R.; Burgner, D.P.; O'Sullivan, J.M. Plasma Trimethylamine N-Oxide and Its Precursors: Population Epidemiology, Parent-Child Concordance, and Associations with Reported Dietary Intake in 11- to 12-Year-Old Children and Their Parents. Curr. Dev. Nutr. 2020, 4, nzaa103. [CrossRef] [PubMed]
2. Rath, S.; Heidrich, B.; Pieper, D.H.; Vital, M. Uncovering the Trimethylamine-Producing Bacteria of the Human Gut Microbiota. Microbiome 2017, 5, 54. [CrossRef] [PubMed]
3. Zeisel, S.H.; Warrier, M. Trimethylamine N-Oxide, the Microbiome, and Heart and Kidney Disease. Annu. Rev. Nutr. 2017, 37, 157–181. [CrossRef] [PubMed]
4. Coutinho-Wolino, K.S.; de F Cardozo, L.F.M.; de Oliveira Leal, V.; Mafra, D.; Stockler-Pinto, M.B. Can Diet Modulate Trimethylamine N-Oxide (TMAO) Production? What Do We Know so Far? Eur. J. Nutr. 2021, 60, 3567–3584. [CrossRef] [PubMed]
5. Jalandra, R.; Makharia, G.K.; Sharma, M.; Kumar, A. Inflammatory and Deleterious Role of Gut Microbiota-Derived Trimethylamine on Colon Cells. Front. Immunol. 2022, 13, 1101429. [CrossRef] [PubMed]
6. López-Armada, M.J.; Riveiro-Naveira, R.R.; Vaamonde-García, C.; Valcárcel-Ares, M.N. Mitochondrial Dysfunction and the Inflammatory Response. Mitochondrion 2013, 13, 106–118. [CrossRef]
7. Castellani, C.A.; Longchamps, R.J.; Sun, J.; Guallar, E.; Arking, D.E. Thinking Outside the Nucleus: Mitochondrial DNA Copy Number in Health and Disease. Mitochondrion 2020, 53, 214–223. [CrossRef]
8. Riley, J.S.; Tait, S.W. Mitochondrial DNA in Inflammation and Immunity. EMBO Rep. 2020, 21, e49799. [CrossRef]
9. Stoccoro, A.; Coppedè, F. Mitochondrial DNA Methylation and Human Diseases. Int. J. Mol. Sci. 2021, 22, 4594. [CrossRef]
10. Mposhi, A.; Cortés-Mancera, F.; Heegsma, J.; de Meijer, V.E.; van de Sluis, B.; Sydor, S.; Bechmann, L.P.; Theys, C.; de Rijk, P.; De Pooter, T.; et al.

Mitochondrial DNA Methylation in Metabolic Associated Fatty Liver Disease. Front. Nutr. 2023, 10, 964337.[CrossRef]

11. Mposhi, A.; Van der Wijst, M.G.; Faber, K.N.; Rots, M.G. Regulation of Mitochondrial Gene Expression, the Epigenetic Enigma. Front. Biosci. (Landmark Ed.) 2017, 22, 1099–1113. [CrossRef]
12. Bordoni, L.; Smerilli, V.; Nasuti, C.; Gabbianelli, R. Mitochondrial DNA Methylation and Copy Number Predict Body Composition in a Young Female Population. J. Transl. Med. 2019, 17, 399. [CrossRef] [PubMed]
13. Corsi, S.; Iodice, S.; Shannon, O.; Siervo, M.; Mathers, J.; Bollati, V.; Byun, H.-M. Mitochondrial DNA Methylation Is Associated with Mediterranean Diet Adherence in a Population of Older Adults with Overweight and Obesity. Proc. Nutr. Soc. 2020, 79, E95.4 [CrossRef]
14. Theys, C.; Ibrahim, J.; Mateiu, L.; Mposhi, A.; García-Pupo, L.; De Pooter, T.; De Rijk, P.; Strazisar, M.; Ince,˙ I.A.; Vintea, I.; et al.˙ Mitochondrial GpC and CpG DNA Hypermethylation Cause Metabolic Stress-Induced Mitophagy and Cholestophagy. Int. J. Mol. Sci. 2023, 24, 16412. [CrossRef]
15. Shock, L.S.; Thakkar, P.V.; Peterson, E.J.; Moran, R.G.; Taylor, S.M. DNA Methyltransferase 1, Cytosine Methylation, and Cytosine Hydroxymethylation in Mammalian Mitochondria. Proc. Natl. Acad. Sci. USA 2011, 108, 3630–3635. [CrossRef] [PubMed]
16. Bayarsaihan, D. Epigenetic Mechanisms in Inflammation. J. Dent. Res. 2011, 90, 9–17. [CrossRef]
17. Tan, S.Y.X.; Zhang, J.; Tee, W.-W. Epigenetic Regulation of Inflammatory Signaling and Inflammation-Induced Cancer. Front. Cell Dev. Biol. 2022, 10, 931493. [CrossRef] [PubMed]
18. Hartnett, L.; Egan, L.J. Inflammation, DNA Methylation and Colitis-Associated Cancer. Carcinogenesis 2012, 33, 723–731. [CrossRef]
19. Ligthart, S.; Marzi, C.; Aslibekyan, S.; Mendelson, M.M.; Conneely, K.N.; Tanaka, T.; Colicino, E.; Waite, L.L.; Joehanes, R.; Guan, W.; et al. DNA Methylation Signatures of Chronic Low-Grade Inflammation Are Associated with Complex Diseases. Genome Biol. 2016, 17, 255. [CrossRef]

20. Wielscher, M.; Mandaviya, P.R.; Kuehnel, B.; Joehanes, R.; Mustafa, R.; Robinson, O.; Zhang, Y.; Bodinier, B.; Walton, E.; Mishra, P.P.; et al. DNA Methylation Signature of Chronic Low-Grade Inflammation and Its Role in Cardio-Respiratory Diseases. Nat. Commun. 2022, 13, 2408. [CrossRef]
21. Das, D.; Karthik, N.; Taneja, R. Crosstalk between Inflammatory Signaling and Methylation in Cancer. Front. Cell Dev. Biol. 2021, 9, 756458. [CrossRef] [PubMed]
22. Pan, Z.; Dong, H.; Huang, N.; Fang, J. Oxidative Stress and Inflammation Regulation of Sirtuins: New Insights into Common Oral Diseases. Front. Physiol. 2022, 13, 953078. [CrossRef]
23. Xu, J.; Kitada, M.; Koya, D. The Impact of Mitochondrial Quality Control by Sirtuins on the Treatment of Type 2 Diabetes and Diabetic Kidney Disease. Biochim. Biophys. Acta. Mol. Basis Dis. 2020, 1866, 165756. [CrossRef] [PubMed]
24. Rovira-Llopis, S.; Apostolova, N.; Bañuls, C.; Muntané, J.; Rocha, M.; Victor, V.M. Mitochondria, the NLRP3 Inflammasome, and Sirtuins in Type 2 Diabetes: New Therapeutic Targets. Antioxid. Redox Signal. 2018, 29, 749–791. [CrossRef] [PubMed]
25. Cordone, V.; Pecorelli, A.; Valacchi, G. Sirtuins as Potential Therapeutic Targets for Mitigating OxInflammation in Typical Rett Syndrome: Plausible Mechanisms and Evidence. Redox Exp. Med. 2022, 2022, R26–R39. [CrossRef]
26. López-Armada, M.J.; Caramés, B.; Martín, M.A.; Cillero-Pastor, B.; Lires-Dean, M.; Fuentes-Boquete, I.; Arenas, J.; Blanco, F.J. Mitochondrial Activity Is Modulated by TNFalpha and IL-1beta in Normal Human Chondrocyte Cells. Osteoarthr. Cartil. 2006, 14, 1011–1022. [CrossRef] [PubMed]
27. Stadler, J.; Bentz, B.G.; Harbrecht, B.G.; Di Silvio, M.; Curran, R.D.; Billiar, T.R.; Hoffman, R.A.; Simmons, R.L. Tumor Necrosis Factor Alpha Inhibits Hepatocyte Mitochondrial Respiration. Ann. Surg. 1992, 216, 539–546. [CrossRef]
28. Zell, R.; Geck, P.; Werdan, K.; Boekstegers, P. TNF-Alpha and IL-1 Alpha Inhibit Both Pyruvate Dehydrogenase Activity and Mitochondrial Function in

Cardiomyocytes: Evidence for Primary Impairment of Mitochondrial Function. Mol. Cell. Biochem.1997, 177, 61–67. [CrossRef]

29. West, A.P.; Shadel, G.S. Mitochondrial DNA in Innate Immune Responses and Inflammatory Pathology. Nat. Rev. Immunol. 2017, 17, 363–375. [CrossRef] [PubMed]
30. Nakahira, K.; Kyung, S.-Y.; Rogers, A.J.; Gazourian, L.; Youn, S.; Massaro, A.F.; Quintana, C.; Osorio, J.C.; Wang, Z.; Zhao, Y.; et al. Circulating Mitochondrial DNA in Patients in the ICU as a Marker of Mortality: Derivation and Validation. PLoS Med. 2013, 10, e1001577. [CrossRef]
31. Rosa, H.S.; Ajaz, S.; Gnudi, L.; Malik, A.N. A Case for Measuring Both Cellular and Cell-Free Mitochondrial DNA as a Disease Biomarker in Human Blood. FASEB J. Off. Publ. Fed. Am. Soc. Exp. Biol. 2020, 34, 12278–12288. [CrossRef]
32. Kim, K.J.; Kim, Y.; Jin, S.G.; Kim, J.Y. Acai Berry Extract as a Regulator of Intestinal Inflammation Pathways in a Caco-2 and RAW 264.7 Co-Culture Model. J. Food Biochem. 2021, 45, e13848. [CrossRef] [PubMed]
33. Borrel, G.; McCann, A.; Deane, J.; Neto, M.C.; Lynch, D.B.; Brugère, J.-F.; O'Toole, P.W. Genomics and Metagenomics of Trimethylamine-Utilizing Archaea in the Human Gut Microbiome. ISME J. 2017, 11, 2059–2074. [CrossRef] [PubMed]
34. Fazzini, F.; Schöpf, B.; Blatzer, M.; Coassin, S.; Hicks, A.A.; Kronenberg, F.; Fendt, L. Plasmid-Normalized Quantification of Relative Mitochondrial DNA Copy Number. Sci. Rep. 2018, 8, 15347. [CrossRef]
35. Sun, X.; Vaghjiani, V.; Jayasekara, W.S.N.; Cain, J.E.; St John, J.C. The Degree of Mitochondrial DNA Methylation in Tumor Models of Glioblastoma and Osteosarcoma. Clin. Epigenetics 2018, 10, 157. [CrossRef]
36. Liu, Z.; Liu, M.; Meng, J.; Wang, L.; Chen, M. A Review of the Interaction between Diet Composition and Gut Microbiota and Its Impact on Associated Disease. J. Futur. Foods 2024, 4, 221–232. [CrossRef]
37. Duttaroy, A.K. Role of Gut Microbiota and Their Metabolites on Atherosclerosis, Hypertension and Human Blood Platelet Function: A Review. Nutrients 2021, 13, 144. [CrossRef] [PubMed]

38. Agus, A.; Clément, K.; Sokol, H. Gut Microbiota-Derived Metabolites as Central Regulators in Metabolic Disorders. Gut 2021, 70, 1174–1182. [CrossRef]
39. Cani, P.D. Microbiota and Metabolites in Metabolic Diseases. Nat. Rev. Endocrinol. 2019, 15, 69–70. [CrossRef]
40. Rahman, S.; O'Connor, A.L.; Becker, S.L.; Patel, R.K.; Martindale, R.G.; Tsikitis, V.L. Gut Microbial Metabolites and Its Impact on Human Health. Ann. Gastroenterol. 2023, 36, 360–368. [CrossRef]
41. Gatarek, P.; Kaluzna-Czaplinska, J. Trimethylamine N-Oxide (TMAO) in Human Health. EXCLI J. 2021, 20, 301–319. [CrossRef] [PubMed]
42. Jaworska, K.; Hering, D.; Mosieniak, G.; Bielak-Zmijewska, A.; Pilz, M.; Konwerski, M.; Gasecka, A.; Kapłon-Cies´licka, A.; Filipiak, K.; Sikora, E.; et al. TMA, A Forgotten Uremic Toxin, but Not TMAO, Is Involved in Cardiovascular Pathology. Toxins 2019, 11, 490. [CrossRef] [PubMed]
43. Bordoni, L.; Petracci, I.; Pelikant-Malecka, I.; Radulska, A.; Piangerelli, M.; Samulak, J.J.; Lewicki, L.; Kalinowski, L.; Gabbianelli,R.; Olek, R.A. Mitochondrial DNA Copy Number and Trimethylamine Levels in the Blood: New Insights on Cardiovascular Disease Biomarkers. FASEB J. 2021, 35, e21694. [CrossRef] [PubMed]
44. Foran, E.; Garrity-Park, M.M.; Mureau, C.; Newell, J.; Smyrk, T.C.; Limburg, P.J.; Egan, L.J. Upregulation of DNA Methyltransferase-Mediated Gene Silencing, Anchorage-Independent Growth, and Migration of Colon Cancer Cells by Interleukin-6. Mol. Cancer Res. 2010, 8, 471–481. [CrossRef] [PubMed]
45. Yang, Z.-H.; Dang, Y.-Q.; Ji, G. Role of Epigenetics in Transformation of Inflammation into Colorectal Cancer. World J. Gastroenterol. 2019, 25, 2863–2877. [CrossRef]
46. Kim, J.H.; Yoo, B.C.; Yang, W.S.; Kim, E.; Hong, S.; Cho, J.Y. The Role of Protein Arginine Methyltransferases in Inflammatory Responses. Mediators Inflamm. 2016, 2016, 4028353. [CrossRef]
47. Serrano-Marco, L.; Chacón, M.R.; Maymó-Masip, E.; Barroso, E.; Salvadó, L.; Wabitsch, M.; Garrido-Sánchez, L.; Tinahones, F.J.; Palomer, X.; Vendrell,

J.; et al. TNF-α Inhibits PPARβ/δ Activity and SIRT1 Expression through NF-KB in Human Adipocytes. Biochim. Biophys. Acta 2012, 1821, 1177–1185. [CrossRef]

48. Bai, X.; He, T.; Liu, Y.; Zhang, J.; Li, X.; Shi, J.; Wang, K.; Han, F.; Zhang, W.; Zhang, Y.; et al. Acetylation-Dependent Regulation of Notch Signaling in Macrophages by SIRT1 Affects Sepsis Development. Front. Immunol. 2018, 9, 762. [CrossRef]
49. Vachharajani, V.T.; Liu, T.; Wang, X.; Hoth, J.J.; Yoza, B.K.; McCall, C.E. Sirtuins Link Inflammation and Metabolism. J. Immunol. Res. 2016, 2016, 8167273. [CrossRef]
50. Covarrubias, A.J.; Kale, A.; Perrone, R.; Lopez-Dominguez, J.A.; Pisco, A.O.; Kasler, H.G.; Schmidt, M.S.; Heckenbach, I.; Kwok, R.; Wiley, C.D.; et al. Senescent Cells Promote Tissue NAD(+) Decline during Ageing via the Activation of CD38(+) Macrophages. Nat. Metab. 2020, 2, 1265–1283. [CrossRef]
51. Ke, Y.; Li, D.; Zhao, M.; Liu, C.; Liu, J.; Zeng, A.; Shi, X.; Cheng, S.; Pan, B.; Zheng, L.; et al. Gut Flora-Dependent Metabolite Trimethylamine-N-Oxide Accelerates Endothelial Cell Senescence and Vascular Aging through Oxidative Stress. Free Radic. Biol. Med. 2018, 116, 88–100. [CrossRef]
52. Luo, T.; Liu, D.; Guo, Z.; Chen, P.; Guo, Z.; Ou, C.; Chen, M. Deficiency of Proline/Serine-Rich Coiled-Coil Protein 1 (PSRC1) Accelerates Trimethylamine N-Oxide-Induced Atherosclerosis in ApoE(-/-) Mice. J. Mol. Cell. Cardiol. 2022, 170, 60–74. [CrossRef] [PubMed]
53. Makrecka-Kuka, M.; Volska, K.; Antone, U.; Vilskersts, R.; Grinberga, S.; Bandere, D.; Liepinsh, E.; Dambrova, M. Trimethylamine N-Oxide Impairs Pyruvate and Fatty Acid Oxidation in Cardiac Mitochondria. Toxicol. Lett. 2017, 267, 32–38. [CrossRef]
54. Yoshida, Y.; Shimizu, I.; Shimada, A.; Nakahara, K.; Yanagisawa, S.; Kubo, M.; Fukuda, S.; Ishii, C.; Yamamoto, H.; Ishikawa, T.; et al. Brown Adipose Tissue Dysfunction Promotes Heart Failure via a Trimethylamine N-Oxide-Dependent Mechanism. Sci. Rep. 2022, 12, 14883. [CrossRef] [PubMed]

55. Cao, K.; Lv, W.; Wang, X.; Dong, S.; Liu, X.; Yang, T.; Xu, J.; Zeng, M.; Zou, X.; Zhao, D.; et al. Hypermethylation of Hepatic Mitochondrial ND6 Provokes Systemic Insulin Resistance. Adv. Sci. 2021, 8, 2004507. [CrossRef]
56. Pirola, C.J.; Gianotti, T.F.; Burgueño, A.L.; Rey-Funes, M.; Loidl, C.F.; Mallardi, P.; Martino, J.S.; Castaño, G.O.; Sookoian, S. Epigenetic Modification of Liver Mitochondrial DNA Is Associated with Histological Severity of Nonalcoholic Fatty Liver Disease. Gut 2013, 62, 1356–1363. [CrossRef]
57. Trumpff, C.; Michelson, J.; Lagranha, C.J.; Taleon, V.; Karan, K.R.; Sturm, G.; Lindqvist, D.; Fernström, J.; Moser, D.; Kaufman, B.A.; et al. Stress and Circulating Cell-Free Mitochondrial DNA: A Systematic Review of Human Studies, Physiological Considerations, and Technical Recommendations. Mitochondrion 2021, 59, 225–245. [CrossRef] [PubMed]
58. De Gaetano, A.; Solodka, K.; Zanini, G.; Selleri, V.; Mattioli, A.V.; Nasi, M.; Pinti, M. Molecular Mechanisms of Mtdna-Mediated Inflammation. Cells 2021, 10, 2898. [CrossRef]
59. Newman, L.E.; Shadel, G.S. Mitochondrial DNA Release in Innate Immune Signaling. Annu. Rev. Biochem. 2023, 92, 299–332. [CrossRef]
60. Pinti, M.; Cevenini, E.; Nasi, M.; De Biasi, S.; Salvioli, S.; Monti, D.; Benatti, S.; Gibellini, L.; Cotichini, R.; Stazi, M.A.; et al. Circulating Mitochondrial DNA Increases with Age and Is a Familiar Trait: Implications for "Inflamm-Aging". Eur. J. Immunol. 2014, 44, 1552–1562. [CrossRef]
61. Zhang, Q.; Raoof, M.; Chen, Y.; Sumi, Y.; Sursal, T.; Junger, W.; Brohi, K.; Itagaki, K.; Hauser, C.J. Circulating Mitochondrial DAMPs Cause Inflammatory Responses to Injury. Nature 2010, 464, 104–107. [CrossRef] [PubMed]

3.3 Research Article n° 3

Exploring mitochondrial DNA copy number in circulating cell- free DNA and extracellular vesicles across cardiovascular health status: A prospective case–control pilot study

Chiara Rucci[1,2] , Gaia de Simone, Saniya Salathia[3] Cristina Casadidio[3] , Roberta Censi[3], Laura Bordoni[2]

[1] School of Advanced Studies, University of Camerino, Camerino, Italy

[2] Unit of Molecular Biology and Nutrigenomics, School of Pharmacy and Health Products, University of Camerino, Camerino, Italy

[3] School of Pharmacy, Drug Delivery Division, University of Camerino, ChIP Research Centre, Camerino, Italy

Published in the FASEB Journal

Published in: . FASEB J. 2024 May 31;38(10):e23672. doi: 10.1096/fj.202400463R. PMID: 38775929.

Abstract

Cardiovascular disease (CVD) is a leading global cause of mortality, difficult to predict in advance. Evidence indicates that the copy number of mitochondrial DNA (mtDNAcn) in blood is altered in individuals with CVD. MtDNA released into circulation may act as a mediator of inflammation, a recognized factor in the development of CVD, in the long distance. This pilot study aims to test if levels of mtDNAcn in buffy coat DNA (BC-mtDNA), in circulating cellfree DNA (cf-mtDNA), or in DNA extracted from plasma extracellular vesicles (EV-mtDNA) are altered in CVD patients and if they can predict heart attack in advance. A group of 144 people with different CVD statuses (50 that had CVD, 94 healthy) was selected from the LifeLines Biobank according to the incidence of new cardiovascular event monitored in 6 years (50 among controls had heart attack after the basal assessment). MtDNAcn was quantified in total cf- DNA and EV- DNA from plasma as well as in buffy coat. EVs have been characterized by their size, polydispersity index, count rate, and zeta potential, by Dynamic Light Scattering. BC- mtDNAcn and cf- mtDNAcn were not different between CVD patients and healthy subjects. EVs carried higher mtDNAcn in subject with a previous history of CVD than controls, also adjusting the analysis for the EVs derived count rate. Despite mtDNAcn was not able to predict CVD in advance, the detection of increased EV- mtDNAcn in CVD patients in this pilot study suggests the need for further investigations to determine its pathophysiological role in inflammation.

K E Y W O R D S

cell- free DNA, CVD, extracellular vesicles, heart attack, mitochondrial DNA

1 Introduction

Mitochondrial DNA (mtDNA) is a small circular multicopy genome located in the inner matrix of mitochondria. It consists of 16 569 base pairs, and it contains 37 genes: 13 encoding for oxidative phosphorylation mRNAs, 22 for tRNAs, and 2 for rRNAs.[1] MtDNA exists in cells in a different copy number (mtDNAcn) depending on the tissue type, health status of cells or environmental exposures.[2- 13] Also, increasing evidence demonstrated the presence of mtDNA in body fluids as circulating cell-free mtDNA (ccf- mtDNA).[14] Ccf- mtDNA can circulate in body fluids as naked or contained in lipid- based vesicles.[14] The mechanisms underlying the release of mitochondrial DNA from cells into the extracellular compartment have not been fully elucidated, prompting the formulation of various hypotheses to address this phenomenon. In passive mechanisms, mtDNA is believed to be released into the extracellular space following cellular apoptosis or necrosis, packaged within apoptotic bodies, intact mitochondria, or as ccf- mtDNA.[14,15] Ccf- mtDNA can also be released by cells through an actively regulated process, residing inside extracellular vesicles (EVs), such as exosomes, mitochondria-derived vesicles, or neutrophils/eosinophils extracellular traps.[15]

There is a growing body of evidence associating both mtDNAcn and ccf- mtDNA with human health status. In particular, mtDNAcn has been associated with metabolic and cardiovascular disease (CVD).[2,12,16,17] Measurement of mtDNAcn in human buffy coat/circulating leukocytes has revealed an inverse association with prevalent and incident CVD outcomes.[18] Also, mtDNAcn in whole blood has been correlated to all cause of mortality and cardiovascular disease in peripheral arterial disease patients with intermittent claudication.[19] A potential role of ccf- mtDNA in the etiology of some inflammatory diseases has also been hypothesized.[20] MtDNA has been suggested to be inflammogenic and immunostimulatory, acting as a damage-associated molecular pattern (DAMP). [20,21] The immune system may recognize mtDNA as “foreign” due to its bacterial- like sequences, a trait linked to mitochondria's endosymbiotic origins.[20] Several pathways have been suggested through which mtDNA triggers immune responses, including TLR9 and ZBP1 receptor activation, cGAS- STING pathway engagement, NLRP3 and AIM2 inflammasome

activation.[20,22] Despite the unclear mechanisms of cell-free mitochondrial DNA (cf-mtDNA) entry into cells and its binding to intracellular receptors, changes in ccf-mtDNA levels have been measured in inflammation-related conditions, including diabetes, coronary heart disease, Parkinson's disease, and Alzheimer's disease.[23- 28] A direct involvement of ccf- mtDNA in CVD pathogenesis has been proposed, where mtDNA-LL37 complexes may accumulate in atherosclerotic plaques, leading to the activation of inflammatory cytokines and recruitment of immune cells in vitro.[20,29]

EVs (and their cargoes) have also been implicated in the pathophysiology of CVD and have recently been proposed as potential biomarkers for these conditions.[30] For instance, exosomes derived from vascular smooth muscle cells have been shown to transfer miR-155 from smooth muscle to endothelial cells, resulting in endothelial cell damage and accelerated atherosclerosis.[31] Also, EVs released by endothelial cells may contribute to plaque formation by inducing a proliferative and migratory phenotype in vascular smooth muscle cells following arterial injury.[32,33] Among cargoes carried by EVs, DNA is also included. Extracellular vesicles DNA (EV-DNA), possibly both nuclear and mitochondrial, can be located on the surface or inside the vesicle.[34] The level of mtDNA carried by EVs, particularly exosomes, has been studied in different pathologies,[35- 38] with an observed increase in patients with chronic heart failure.[39]

Despite significant evidence supporting mtDNAcn as a biomarker for CVD, the translation of this evidence into clinical practice remains limited. Uncertainties persist regarding if mtDNAcn from the buffy coat or ccf-DNA or its fractions is associated to CVD, as well as whether the impact of blood composition on this biomarker affects its predictive capabilities. In the light of this evidence, this case–control pilot study aims at testing if levels of mtDNA in buffy coat (BC- mtDNAcn), ccf- mtDNA or extracellular vesicles mitochondrial DNA (EV-mtDNA) are altered in CVD patients, and if they can predict heart attack in advance, compared to other established CVD predictors (i.e., Systemic Coronary Risk Estimation 2 (SCORE2),[40] and triglycerides/high- density lipoprotein cholesterol ratio (TG/ HDL)[41,42]). Additionally, this research aims to characterize EVs in different cardiovascular health statuses, seeking to discern whether the properties of these particles can serve as predictive indicators of CVD outcomes or if they are associated with their mtDNA content.

2 | MATERIALS AND METHODS

2.1 | Participant recruitment and data collection

The study is in collaboration with the LifeLines Biobank. LifeLines[43,44] is a multi-disciplinary prospective population- based cohort study examining in a unique three-generation design the health and health- related behaviors of 167 729 persons living in the North of the Netherlands. It employs a broad range of investigative procedures in assessing the biomedical, socio-demographic, behavioral, physical, and psychological factors which contribute to the health and disease of the general population, with a special focus on multi-morbidity. The LifeLines study was approved by the ethics committee of the University Medical Centre Groningen, document number METC UMCG METc 2007/152. LifeLines operates in the highest ethical standards and strictly controls, and it takes into account rules regarding the irreversible pseudonymization of participants, encryption of data, use of trusted third parties (TTPs), and controlled data access. This will guarantee that both personal data and samples respect the EU Directive 2004/23 on standards for the donation, procurement, testing, processing, preservation, storage, and distribution of human tissues and cells and EU Regulation 2016/679 of the European Parliament and of the Council of April 27, 2016, on the protection of natural persons with regard to the processing of personal data and on the free movement of such data. All participants signed an informed consent (http:// wiki. lifelines . nl/ doku. php?i d= informed _ consent).

From 2007 to 2013, over 167 000 participants were included at baseline (1A), with the aim to follow up for at least 30 years.[44] Questionnaires completed during the study generated around 8000 variables and cover a broad range of topics (detailed information are available at LifeLines Wiki [http:// wiki-life l ines. web.rug .n l] or catalog [https:// data- catal ogue.life l ines. nl]). Subjects enrolled have been invited to complete two follow- up questionnaires within the following 6 years [from 2011 to 2013] (time 1B and 1C, about 1.5y and 2.5y after baseline assessment, respectively). A second assessment (2A) to collect health- related data, physical measurements, and additional biological samples was performed after 6y from baseline [from 2014 to 2017].

For the participants included in this study (according to the study design described in paragraph 2.3), SCORE2 was calculated. SCORE2 is as an established predictive biomarker for CVD, as detailed in the 2021 European Society of Cardiology Guidelines on cardiovascular disease prevention in clinical practice. SCORE2 algorithm estimates the 10- year risk of fatal and non-fatal CVD events in apparently healthy people aged 40–69 years.[45] SCORE2 estimates the risk of CVD events based on sex, systolic blood pressure (mmHg), total cholesterol (mmol/L) (tCHOL), HDL cholesterol (mmol/L) smoking habits (being or not being a smoker), and geographical origin. In this study, SCORE2 has been calculated according to the formulas contained in the supplementary materials of the paper published in 2021 by SCORE2 working group and ESC Cardiovascular risk collaboration.[40] We applied the formulas specific for low- risk CVD countries (as Netherlands is indexed).

2.2 | Sample collection, processing, and storage

Blood samples have been collected at LifeLines center using BD Vacutainer® 10.0 mL K2E (EDTA) 18.0 mg Plus blood collection tubes, immediately centrifuged for 15 min at 2500 RCF to isolate plasma and buffy coat, then stored at −80° upon shipment. Data about tCHOL, HDL, low- density lipoproteins cholesterol (LDL), triglycerides (TG), and blood composition (i.e., neutrophilic, basophilic, eosinophilic granulocytes, monocytes, leukocytes, lymphocytes, thrombocytes) were collected by LifeLines operators at the laboratory of the University Medical Centre Groningen (certified according to NEN- EN- ISO 9001:2008 and NEN- EN- ISO 15189:2012 standards). Genomic DNA (gDNA) was extracted from the buffy coat at LifeLines center using the Perkin- Elmer Chemagic 360 to perform magnetic bead DNA extraction. Both gDNA from buffy coat (BC-DNA) and plasma from selected samples were shipped to the University of Camerino for further analysis.

2.3 | Study design

In this pilot study, information about sex, gender, age, body mass index (BMI), blood pressure (measured automatically using the DinaMap PRO100 or DinaMap PRO100V2), dietary records, diet quality (according to the LifeLines Diet Score [LLDS]),[46] smoking, physical activity, cardiovascular health, and any other disease

onset was used to select a subcohort of 144 people according to the experimental design shown in Figure 1 and detailed as follows. Recruited participants were selected according to three different CVD statuses: 50 individuals reported a CVD event that previously occurred (within 2 years before baseline assessment) (γ group). 94 individuals were healthy at baseline assessment. Of them, 50 individuals reported a heart attack occurred after baseline assessment (within the following 1.5 years) (β group). The remaining 44 did not report any cardiovascular event for the following 6 years (α group), representing healthy controls (Figure 1). Individuals who were healthy at baseline but reported a heart attack during follow-up (β group) were selected among new cases of heart attack reported within the following 1.5y after baseline assessment. Healthy controls (groups α) were selected matching individuals from β group for age, sex, and BMI. Considering potential confounding factors able to affect mtDNAcn according to previous literature, we selected individuals so that groups did not show significant differences in age, ethnicity, country of origin, sex, body composition, dietary habits, and physical activity levels (see results section). To this aim, the selection was performed according to the following inclusion and exclusion criteria. Exclusion criteria were BMI <18 or ≥40; age <45 or >65; no fasting; missing info about LLDS; other ethnicities than Caucasian; other birthplaces than Netherlands; individuals who reported at baseline one or more of the following pathologies: cancer, stroke, diabetes, atherosclerosis, aneurism, or coagulopathy. Inclusion criteria were $18 \leq BMI < 40$, $45 \leq age \leq 65$, blood fasting samples available, available data about LLDS, Caucasian ethnicity, and Netherlands birthplace. This study design allowed comparison of matched cases and controls considering a significant number of new cases of heart attack over time in a restricted number of samples, controlling for numerous other confounding conditions.

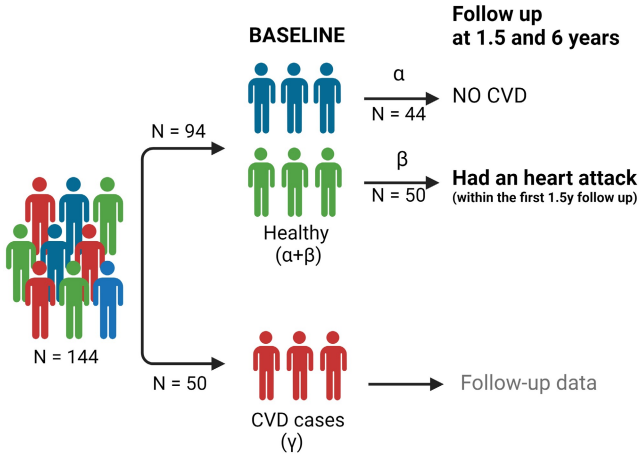

FIGURE 1 Study design: A total of 144 subjects were included in the study according to their cardiovascular health status. 50 individuals reported a CVD event that previously occurred within 2 years before baseline assessment (γ group). In all, 94 individuals were healthy at baseline assessment. Of them, 50 individuals reported a heart attack occurred after baseline assessment (within the following 1.5 years) (β group). The remaining 44 did not report any cardiovascular event for the following 6 years (α group). Individuals were recruited according to specific inclusion and exclusion criteria to control for confounding factors that has been associated to mtDNAcn by previous studies (see paragraph 2.3 for details). Individuals were matched so that the selected groups did not show significant differences in age, ethnicity, country of origin, sex, body composition, dietary habits, and physical activity levels. Figure created with BioRe nder. com.

2.4 | Relative quantification of buffy coat mtDNA copy number (BC-mtDNAcn)

Relative quantification of mtDNAcn (mtDNAcn/nuclear DNA copy number [nDNAcn]) has been assessed in gDNA extracted from buffy coat by qPCR using CFX96 (Biorad, Hercules, California, USA). The following genes have been amplified for the detection of mitochondrial and nuclear DNA, respectively, using the listed primers: mtDNA- tRNALeu (Fw: 5′- CACCCAAGAACAGGGTTTGT- 3′; Rv: 5′- TGGCCATGGGTATGTTGTTA- 3′) and beta- 2- microglobulin (B2M) (Fw: 5′- TGCTGTCTCCATGTTTGAT GTATCT- 3′; Rv: 5′- TCTCTGCTCCCCACCTCTAAGT- 3′). These primers have been validated by Fazzini and colleagues[47] and verified for their specificity (unique amplification of

mtDNA) and for the absence of co- amplified nuclear insertions of mitochondrial origin (NUMTs).

2.5 | Total cell- free DNA (tcf- DNA) extraction

Plasma samples were thawed at 37° for 5 min and mixed to avoid precipitation of insoluble particles that might reduce the yield of EVs isolation. According to Trumpff et al.,[14] plasma was further centrifuged at 5000 g for 10 min to remove potential residual platelets and large vesicular apoptotic bodies. Clean plasma was used for subsequent analyses. Total cell- free DNA (tcf- DNA) has been isolated from 480 µL of clear plasma using the Plasma/Serum Cell- Free Circulating DNA Purification Mini Kit (Cat. 55100, Norgen, Thorold, ON, Canada) according to manufacturer's instruction.

2.6 | EVs isolation, characterization and DNA extraction

Small EVs have been isolated from 850 µL of clear plasma using the Plasma/Serum Exosome Purification Mini Kit (Cat. 57400, Norgen, Thorold, ON, Canada). EVs quantification and characterization have been conducted using Dynamic Light Scattering (DLS) (Zetasizer Nano- S90, Malvern Panalytical, Malvern, UK) as previously described.[48- 55] For DLS analysis, 1000 µL of ultrapure water has been added to 5 µL of EVs extract and 1000 µL of the solution has been transferred in a polystyrene cuvette and equilibrated at 22°C. Z- Average size, Polydispersity Index (PDI), Derived Count Rate (DCR), and Zeta potential (ZP) have been measured. The Z- average size (nm) is defined as the intensity- weighted mean hydrodynamic size of the ensemble collection of particles measured by DLS. PDI is a dimensionless measure of the heterogeneity of a sample based on size.[56] The DCR (kpcs) indicates the number of photons collected by the light detector of the instrument in a second: higher DCR usually indicates higher concentrations, larger particles or higher concentration and larger particles. The ZP (mV), an indicator of colloidal stability, is influenced by the surface charge of extracellular vesicles.[57] The net surface charge of extracellular vesicles, indicated by the ZP, determines the stability of the particles or their tendency to aggregate.[57] After characterization, 100 µL of the solution containing EVs have been

used to extract EV-DNA by the Qiamp DNA mini kit (Cat. 51304, Qiagen, Hilden, Germany) according to manufacturer's instructions.

2.7 | Quantification of mtDNA in tcf- DNA and EV- DNA by digital PCR

Absolute quantification of total cell-free mitochondrial DNA (tcf- mtDNA), total cell-free nuclear DNA (tcf- nDNA), EV- mtDNA, and extracellular vesicles nuclear DNA (EV- nDNA) has been performed by QIAcuity digital PCR (Qiagen, Hilden, Germany) according to manufacturer's indication. The imaging profiling has performed setting the instrument on an exposure duration of 350 ms and a gain of 4. MtDNA-tRNALeu and B2M were amplified to detect mtDNA or nuclear DNA (nDNA), respectively. Poisson statistics have been applied to calculate the average amount of target DNA per well (QIAcuity Software Suite 2.1.8.23, Qiagen, Hilden, Germany). A number of copies of target DNA contained in 1 mL of plasma were calculated accordingly.

2.8 | Statistical analysis

Statistical analysis was performed using SPSS (IBM, version 25, USA) and R studio (2023.06.0 + 421 version). Data were tested for normality using the Shapiro–Wilk test and log- transformed prior to analysis where necessary to normalize distribution. Parametric tests were such as unpaired student *t*-test or one- way ANOVA. Tukey's mul- tiple comparison test was used as a post- hoc test to test significant difference between mean's groups. A receiver operating characteristic (ROC) analysis was performed, and the area under curve (AUC) was calculated to test predictiveness of the selected biomarkers. Significance was accepted with $p \leq .05$.

3 | RESULTS

3.1 | Descriptive statistics of the cohort and CVD risk biomarkers

Table 1 presents the descriptive statistics of the selected cohort. No differences between the three groups are measured for age (Kruskal–Wallis; $p = .907$), BMI (Kruskal–Wallis; $p = .680$), or sex distribution (Pearson's chi- square; $p = .970$), in accordance with the case–control design of the study. The three groups were exposed to current similar lifestyle habits among those that may impact cardiovascular risk

(smoking, diet, physical activity). In particular, current smokers were not differently distributed among groups (Pearson's chi- square; $p = .551$). Dietary habits (measured considering the LLDS[46] as an index of the overall diet quality) were not significantly different among groups (ANOVA; $p = .457$). Moderate- to- vigorous physical activity was not different between groups neither for hours per week (Kruskal– Wallis; $p = .801$) nor for the activity score (Kruskal– Wallis; $p = .932$).

3.1.1 | Blood composition in the CVD groups

Given that changes in blood composition have been previously observed in patients with CVD or at risk,[58] and it has been hypothesized that thrombocyte levels may influence ccf-mtDNA levels, [14] data on the blood composition of participants have been analyzed. Table 2 shows the differences in blood composition in the three groups. A p for trend difference was observed for leukocytes (ANOVA, $p = .082$), where lower levels were measured in α than in β group ($p = .026$). A significantly different distribution between groups was measured for mononuclear cells (ANOVA, $p = .020$), with higher levels in β than α group ($p = .005$). Levels of eosinophilic granulocytes were different in the three groups (ANOVA, $p = .038$), with higher values in γ than α group ($p = .016$). No significant differences between groups were observed for other parameters describing blood cell composition (Table 2).

Difference between the groups in platelets/leukocytes ratio (P/L), a factor believed to influence the quantification of mtDNAcn in blood cells,[59] exhibited a p for trend (ANOVA, $p = .059$). In particular, P/L was higher in α (P/L = 43.1 ± 12.6) than γ (P/L = 37.4 ± 8.4) ($p = .033$) or β (P/L = 38.7 ± 13.0) ($p = .042$). β P/L was not different to γ P/L ($p = .913$).

TABLE1 Generaldescriptivestatisticsoftheentirecohort($N=$ andofthegroups: $\alpha(N=44)$ $\beta(N=50)$ $\alpha+\beta(N=94)$ and $\gamma(N=50)$.

	α(*N* = 44)				β(*N* = 50)				α + β(*N* = 94)				γ(*N* = 50)				WholePopulation(*N* = 144)			
	Min	**Max**	**Mean**	***SD***	**Min**	**Max**	**Mean**	***SD***	**Min**	**Max**	**Mean**	***SD***	**Min**	**Max**	**Mean**	***SD***	**Min**	**Max**	**Mean**	***SD***
Age	45	65	55	6.0	45	65	55	6.1	45	65	55	6.1	45	65	55	6.9	45.0	65.0	55.1	6.3
BMI	22.3	38.6	28.0	4.0	22.3	37.8	27.4	3.6	22.2	38.6	27.7	3.8	22.3	35.0	27.7	2.9	22.3	38.6	27.7	3.5
	n		%		*n*		%		*n*		%		*n*		%		*n*		%	
Females	15		34		16		32		31		33		17		34		48		33	
Males	29		66		34		68		63		67		33		66		96		67	

Note: $N=$ numberofparticipantsinthegroup.

Abbreviations:Max,maximum;Min,minimum; N,number; SD,standarddeviation.

TABLE 2 Blood composition in the three groups (α, β, γ).

	α *(N = 44)*					β *(N = 50)*					γ *(N = 50)*					
	N	**Min**	**Max**	**Mean**	***SD***	***N***	**Min**	**Max**	**Mean**	***SD***	***N***	**Min**	**Max**	**Mean**	***SD***	***p***
Basophilic granulocytes (10^9/L)	43	0	0.08	0.030	0.016	49	0	0.07	0.033	0.016	49	0.01	0.15	0.032	0.022	.460
Eosinophilic granulocytes (10^9/L)	43	0.03	0.48	**0.173**	0.1	49	0.03	0.65	**0.235**	0.146	49	0.02	0.65	**0.233**	0.128	**.038**
Erythrocytes (10^{12}/L)	44	4.15	5.79	4.844	0.361	50	3.91	5.74	4.829	0.374	50	4.3	6	4.869	0.35	.856
Leukocytes (10^9/L)	44	2.4	10.2	**5.932**	1.50	50	2.7	13.7	**6.706**	2.187	50	4.1	9	**6.408**	1.111	**.082**
Lymphocytes (10^9/L)	43	0.79	4.07	2.034	0.601	49	1.02	3.01	2.172	0.558	49	1.21	3.95	2.165	0.568	.394
Mononuclear cells (10^9/L)	43	0.22	0.75	**0.470**	0.136	49	0.27	1.17	**0.574**	0.197	49	0.26	0.98	**0.518**	0.143	**.020**
Neutrophilic granulocytes (10^9/L)	43	1.9	7.38	3.284	1.068	49	1.05	7.34	3.547	1.479	49	2.06	5.88	3.416	0.802	.710
Thrombocytes (10^9/L)	44	163	363	242.6	53.184	50	118	358	242.28	61.217	50	160	378	234.62	45.991	.707

Abbreviations: Max, maximum; Min, minimum; *N*, number; *p*, overall *p*-value.; *SD*, standard deviation.

Significant results are in bold.

3.1.2 | Classical CVD risk biomarkers

TG/HDL ratio (considered a CVD risk biomarker[41,42]) was different between groups (Kruskal–Wallis; $p = .026$). γ group showed a TG/HDL ratio significantly higher than α ($p = .008$). No significant differences were measured between α and β ($p = .076$) or β and γ ($p = .355$). The three groups did not show significant differences for the SCORE2 profile (Kruskal–Wallis, $p = .060$), which is considered an established predictor of CVD.[40] Results are shown in Table 3.

TABLE 3 Classical biomarkers of CVD (TG/HDL and SCORE 2) in the three groups: α ($N = 44$), β ($N = 50$), and γ ($N = 50$).

	α ($N = 44$)				β ($N = 50$)				γ ($N = 50$)				
	Min	**Max**	**Mean**	***SD***	**Min**	**Max**	**Mean**	***SD***	**Min**	**Max**	**Mean**	***SD***	***p***
TG/HDL	0.21	7.49	**1.132**	1.250	0.152	5.100	**1.306**	1.024	0.367	3.664	**1.346**	0.802	**.026**
SCORE2	0.010	0.160	0.042	0.028	0.012	0.104	0.046	0.022	0.008	0.086	0.035	0.017	.060
SCORE2 (%)	0.949	16.014	4.190	2.770	1.181	10.426	4.566	2.192	0.826	8.606	3.458	1.686	.060

Abbreviations: Max, maximum; Min, minimum; *N*, number; $p = p$-value; *SD*, standard deviation.
Significant results are in bold

3.2 | mtDNAcn from buffy coat (BC- mtDNAcn) in different CVD statuses

Relative quantification of buffy coat mtDNAcn (mtDNAcn/nDNAcn) was not associated to age ($p = .703$), which was suggested to affect this parameter in previous studies.[59] This observation could potentially be attributed to the relatively narrow age range within the cohort (Table 1). BC-mtDNAcn was significantly correlated with blood composition. In particular, mtDNAcn was positively correlated with leukocyte levels (Pearson's correlation = .264, $p = .002$), especially mononuclear cells (Pearson's correlation = .232, $p = .006$). A nominal correlation was detected also with neutrophils (Pearson's correlation = .188; $p = .027$) and basophilic granulocytes (Pearson's correlation = .178; $p = .037$) but not with eosinophils ($p = .487$). No correlation with platelets, the other major cellular component of buffy coat, was measured ($p = .219$). Since P/L is considered a confounding factor for mtDNAcn assessments in blood,[59] we tested the association between BC-mtDNAcn and this parameter. Results showed a significant correlation between BC- mtDNAcn and P/L ratio (Pearson's correlation = −.177; $p = .036$).

No differences were observed for BC- mtDNAcn between individuals who were healthy at baseline (α + β) and CVD cases (γ) ($p = .558$). Given the previously

mentioned correlation with blood cells, we normalized BC- mtDNAcn for platelet/leukocyte ratio. Still, no significant differences were measured (p = .995) (Figure 2A). No significant differences were measured by distinguishing between healthy controls (α), individuals who reported a heart attack in 1.5y (β), and previous CVD cases (γ) (p = .442) (Figure 2B).

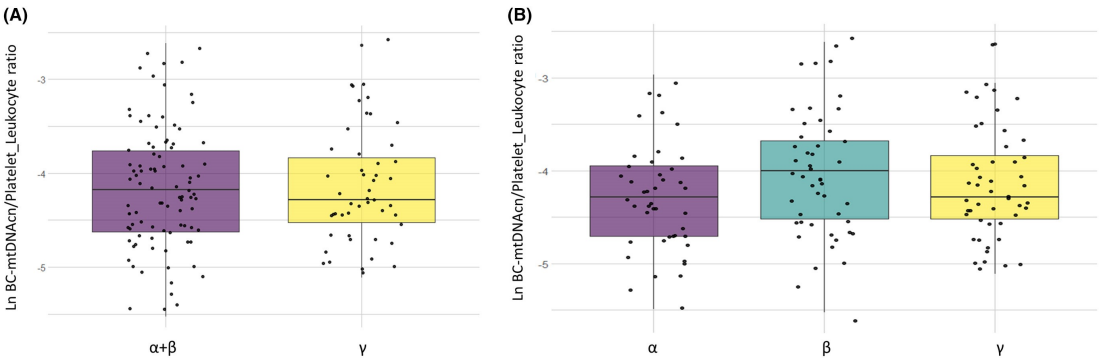

FIGURE 2 BC- mtDNAcn normalized for platelets/leukocytes ratio in (A) healthy individuals at baseline (α + β) and CVD cases (γ) or (B) in the three groups α, β, and γ.

3.3 | mtDNA from total cell- free DNA (tcf-mtDNA)

Mean levels of total cell-free mitochondrial DNA copy number (tcf- mtDNAcn) were 48068.72 ± 41744.96 copies/mL, while levels of total cell-free nuclear DNA copy number (tcf- nDNAcn) were 1407.52 ± 859.51 copies/mL of plasma. As expected, tcf- mtDNAcn was higher than tcf-nDNAcn detected in the same starting volume of plasma (1 mL). No differences in tcf-mtDNAcn (p = .510) (Figure 3A) or tcf-nDNAcn (Figure 3B) (p = .387) or tcf- mtDNAcn/tcf- nDNAcn ratio (p = .922) have been observed between subjects that were healthy at baseline (α + β) and CVD cases (γ). No differences in tcf- mtDNAcn (p = .796) (Figure 3C) or tcf- nDNAcn (p = .134) (Figure 3D) or tcf- mtDNAcn/nDNAcn (p = .296) amount have been measured between groups.

No correlations between tcf- DNAcn and blood composition (data not shown) were measured, except for tcf- mtDNAcn/nDNAcn ratio, which was significantly correlated with leukocyte abundance in blood (Pearson's correlation = .235; p = .005). No

correlations between the BC-mtDNAcn and tcf- mtDNAcn (p = .444) or tcf-mtDNAcn/nDNAcn (p = .450) were measured.

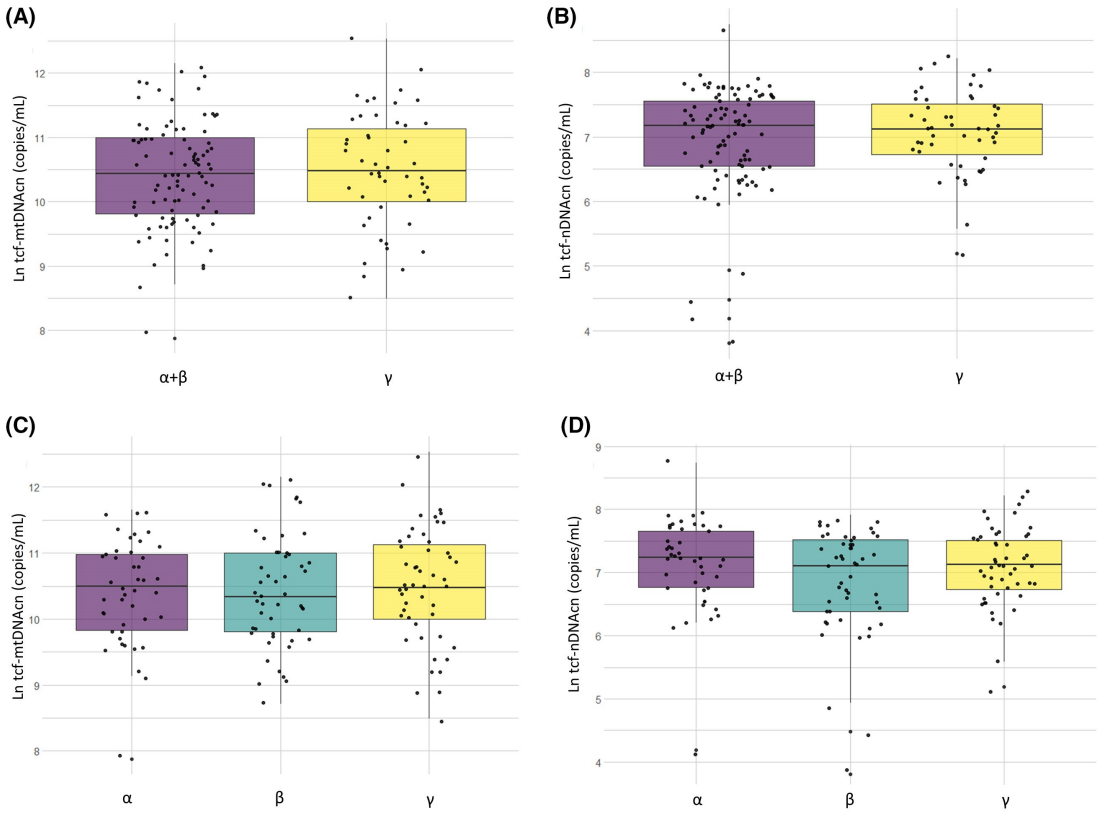

FIGURE 3 Tcf- mtDNAcn and tcf- nDNAcn measured in healthy subjects at baseline (α + β) versus CVD cases (γ) (A, B). Tcf- mtDNAcn and tcf- nDNAcn measured in the three groups α, β, and γ (C, D).

3.4 | Plasma EVs characterization and EV- DNA cargoes

3.4.1 | Plasma EVs characterization

DLS results show a homogeneous population of isolated extracellular vesicles (PDI: 0.29 ± 0.19). DCR, Z-average, and ZP for the overall group are shown in Table 4. No significant differences were measured in terms of DCR no significant differences among groups were observed and PDI (Table 4). Thus, no differences in DNA cargoes for EVs Z- average and ZP (Table 4), suggesting that no between CVD groups can be attributed to differential major differences in EVs dimension and charge can be

processing of the samples during EVs extraction. Also, measured in different cardiovascular health statuses.

TABLE 4 Characterization of plasma EVs by DLS in α (*N* = 44), β (*N* = 50), and γ (*N* = 50) groups.

	α (*N* = 44)				β (*N* = 50)				γ (*N* = 50)				
	Min	**Max**	**Mean**	***SD***	**Min**	**Max**	**Mean**	***SD***	**Min**	**Max**	**Mean**	***SD***	***p***
DCR (kcps)	182	5417	1640	1177	306	7413	1453	1316	343	7473	2001	1726	.22
Z-average (nm)	105	357	236	62	118	368	242	63	120	366	241	60	.87
PDI	0.03	0.69	0.27	0.18	0.39	0.77	0.31	0.19	0.04	0.68	0.30	0.20	.53
Z-potential (mV)	−25.6	−3.0	−11.3	4.8	−22.4	−2.4	−11.3	3.9	−25.6	−3.1	−10.6	4.9	.61

Note: Kruskal–Wallis test was applied.

Abbreviations: Max, maximum; Min, minimum; *N*, number; *p*, *p*-value; SD, standard deviation.

TABLE 4 Characterization of plasma EVs by DLS in α (*N* = 44), β (*N* = 50), and γ (*N* = 50) groups.

3.4.2 | Quantification of mtDNA and nDNA in plasma EVs

Both mtDNA and nDNA were detected by QIAcuity dPCR in the DNA extracted from EVs. In particular, EV- mtDNAcn plasma levels were 1840.0 ± 2663.5 copies/mL, while EV-nDNAcn was 126.4 ± 105.7 copies/mL of plasma. EV- mtDNAcn/EV-nDNAcn ratio was 51.00 ± 83.99 in the whole sample.

EV- mtDNAcn was significantly positively correlated with the DCR (Pearson's correlation = .294; $p = 3.5*10^{-4}$), proving that mtDNA is a cargo in the isolated EVs. Since the DCR depends on the number of particles and their average size, we also tested the correlation between the EV- mtDNAcn and the DCR adjusting for the average size. The correlation between mtDNAcn and DCR is confirmed (β = 0.328, *p* = .003), with no contribution of the average size (*p* = .766) to the model. This corroborates the hypothesis that EV- mtDNcn is correlated with the abundance of EVs, and even eventual nanoparticle aggregates are not responsible for differences observed between groups. EV- mtDNAcn was correlated with Z- average (*p* = .044) but not with the ZP (*p* = .574). Since ZP depends on the EVs surface charge, these results suggest that it is unlikely that mtDNA is passively carried on the surface of the EVs, while it is rather carried as expected within EVs.

On the contrary, EV-nDNA was not correlated to extra- cellular vesicles DCR (*p* = .315), Z- average (*p* = .626), or ZP (*p* = .284). This suggests that the low level of nDNA measured in EVs is likely a residual contamination rather than a real EVs cargo.

According to this hypothesis, the ratio EV- mtDNA/EV- nDNA was not associated to exosomes DCR (p = .725), Z- average (p = .427), or ZP (p = .445).

EV- mtDNA was not associated to the blood composition in the whole group (Additional file 1: Table S1). EV- nDNAcn was correlated to the levels of basophilic granulocytes (Pearson's correlation = 0.272; p = .001) and mononuclear cells (Pearson's correlation = .205; p = .017). EV- nDNA was also correlated with BC- mtDNAcn (Pearson's correlation = .223; p = .009), tcf- mtDNAcn (Pearson's correlation = .209; p = .013), and tcf- nDNAcn (Pearson's correlation = .226; p = .007). This evidence (EV- nDNA correlating to total levels of DNA circulating in plasma but not to the abundance of EVs) supports the hypothesis that EV- nDNA detected in these samples is rather a contamination than EV- DNA cargo. On the contrary, EV- mtDNAcn (which was associated to the abundance of EVs in the sample) was correlated neither with BC- mtDNAcn nor with the tcf- mtDNAcn or tcf- nDNAcn levels (Table 5). This supports the hypothesis that EV- mtDNAcn is due to a biological phenomenon independent of the total cell-free DNA levels.

-

TABLE5 Pearsoncorrelationcoefficient(r)and p-value($p$ofthecorrelationbetweenBC mtDNAcn,Tcf- mtDNAcn,Tcf- nDNAcn,Tcf- mtDNAcn/Tcf- nDNAcn,EV- mtDNAcn,EV- nDNAcn,andEV- mtDNAcn/EV- nDNAcn.

	BC-mtDNAcn		**Tcf-mtDNAcn**		**Tcf-nDNAcn**		**Tcf-mtDNAcn/ Tcf-nDNAcn**		**EV-mtDNAcn**		**EV-nDNAcn**		**EV-mtDNAcn/ EV-nDNAcn**	
	r	***p***	***r***	***p***	***r***	***p***	***r***	***p***	***r***	***p***	***r***	***p***	***r***	***p***
BC.- mtDNAcn	1		−0.065	.444	−0.154	.068	0.064	.450	0.163	.054	**0.223**	**.009**	0.064	.450
Tcf- mtDNAcn	−0.065	.444	1		**0.288**	**$4*10^{-4}$**	**0.658**	**$3*10^{-19}$**	−0.032	.699	**0.209**	**.013**	**0.658**	**$3*10^{-5}$**
Tcf- nDNAcn	−0.154	.068	**0.288**	**$4*10^{-4}$**	1		**−0.532**	**$6*10^{-12}$**	−0.057	.495	**0.226**	**.007**	**−0.532**	**$6*10^{-12}$**
Tcf- mtDNAcn/Tcf- nDNAcn	0.065	.450	**0.658**	**$3*10^{-19}$**	**−0.532**	**$6*10^{-12}$**	1		0.016	.845	0.016	.851	**1**	**0**
EV- mtDNAcn	0.163	.054	−0.032	.699	−0.057	.495	0.016	.845	1		0.187	.28	0.16	.845
EV- nDNAcn	**0.223**	**.009**	**0.209**	**.013**	**0.226**	**.007**	0.016	.851	0.187	.28	1		−0.016	.851
EV- mtDNAcn/EV- nDNAcn	0.064	.450	**0.658**	**$3*10^{-5}$**	**−0.532**	**$6*10^{-12}$**	**1**	**0**	0.016	.845	0.016	.851	1	

Significantresultsareinbold

3.4.3 | EVs DNA cargoes in CVD groups

Individuals who were healthy at baseline (α + β) had lower levels of EV- mtDNAcn than in CVD cases (γ) (p = .006) (Figure 4A). In particular, the γ group showed significantly higher levels of EV-mtDNAcn than the α group (p = .019) and the β group (p = .016), with no differences between α and β groups (p = .995) (Figure 4C). The association between EV- mtDNAcn and CVD status remained significant (β = 0.195; p = .022) also adjusting the analysis for the blood composition (that differed between CVD groups), suggesting that increased EV-mtDNAcn is not a direct consequence of blood cell composition differences.

EV- nDNAcn was significantly higher in CVD cases than in healthy subjects at baseline (p = .033) (Figure 4B). Also, EV- nDNAcn was significantly higher in γ than β group (p = .009), but it did not differ from α group (p = .167) (Figure 4D). However, a multivariate linear regression model adjusted for blood composition showed no significant association between EV- nDNAcn and CVD status (p = .477). Similarly, no significant associations were detected adjusting for DCR, Z- average, or ZP between EV- nDNA with the CVD status (p = .326). On the contrary, the association between EV- mtDNAcn and CVD status was significant (β = 0.180; p = .025) even adjusting the model for the DCR (that is per se associated to the EV- mtDNAcn; β = 0.294; p = .003), the Z-average, and the ZP (which do not contribute to this association). These results suggest that both the EVs abundance and their mtDNA cargoes contribute to explain the difference between the three groups.

To understand if the concentration of circulating EVs (DCR) and/or EV- mtDNAcn were able to distinguish between healthy subjects (α + β) and CVD patients (γ), we performed a multivariate logistic regression. The analysis showed that EV-mtDNAcn (β = 1.673; p = .019), but not the EVs DCR (p = .410), significantly contributed to the prediction model. This suggests the hypothesis that EV- mtDNAcn cargo (rather than the number of EVs) is the major driver of the association between EV-mtDNAcn and the cardiovascular health status.

Considering the possibility to distinguish in advance subjects that are going to develop CVD from really healthy subjects (i.e., comparing α with β group), neither EV-mtDNAcn (p = .994) nor EVs DCR (p = .396) were able to predict the onset of CVD in advance.

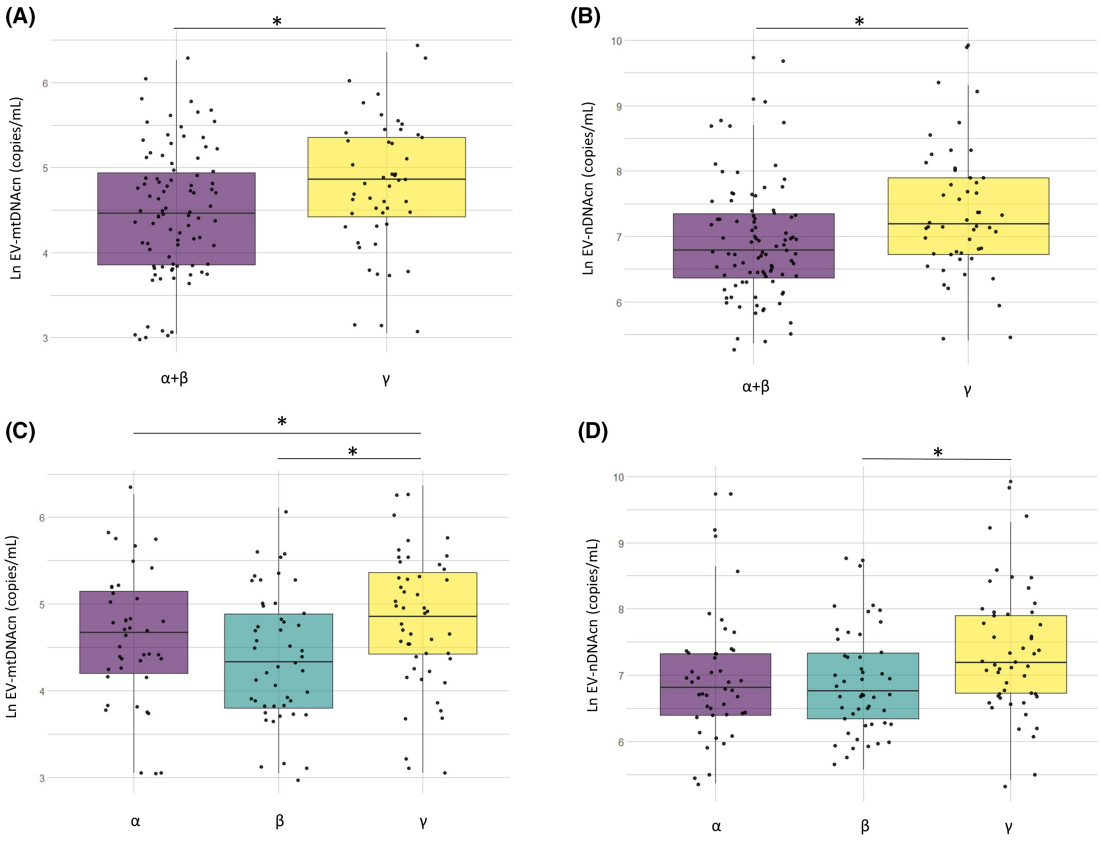

*FIGURE 4 EV- mtDNAcn and EV- nDNAcn measured in healthy subjects at baseline (α + β) and in CVD cases (γ) (A, B). EV- mtDNAcn and EV- nDNAcn measured in the three groups α, β, and γ (C, D). *p < .005.*

3.5 | CVD risk prediction

No significant correlations were measured between CVD risk biomarkers such as TG/HDL or SCORE2 and BC- mtDNAcn, tcf- mtDNAcn, or EV- mtDNAcn (Table 6). However, SCORE2 was correlated to the EVs DCR (total number of exosomes isolated from the same amount of plasma) (β = 0.171; p = .049), independently from the EV- mtDNAcn (β = 0.014; p = .875), and the CVD status (β = −0.152; p = .072). To assess the predictive power and compare the selected biomarkers for CVD, we conducted ROC analysis. Results showed that only EV-mtDNAcn (AUC = 0.648; p = .002) was predictive of CVD presence at baseline (α + β vs. γ). A p for trend was measured for TG/HDL (AUC = 0.595; p = .051). No significant results were obtained for SCORE2 (AUC = 0.411; p = .068), tcf- mtDNAcn (AUC = 0.544; p = .390), or

BC- mtDNAcn (AUC = 0.450; *p* = .337) (Figure 5A). Testing the predictiveness of heart attack in advance (α vs. β), none of the classifiers resulted to be significantly associated to the outcome [EV- mtDNAcn, AUC = 0.648; *p* = .002; TH/HDL, AUC = 0.595; *p* = .051; SCORE2, AUC = 0.570; *p* = .068; tcf- mtDNAcn, AUC = 0.544; *p* = .390; BC- mtDNAcn, AUC = 0.450; *p* = .337] (Figure 5B).

	BC- mtDNAcn	***p***	**Tcf- mtDNAcn**	***p***	**EV- mtDNAcn**	***p***
TG/HDL ratio	−0.032	.704	−0.035	.675	0.089	.289
SCORE2	0.075	.376	−0.064	.447	0.034	.686

TABLE 6 Pearson coefficient and p- value (p) of the correlation between BC- mtDNAcn, Tcf-mtDNAcn, EV- mtDNAcn, and TG/HDL ratio and SCORE2.

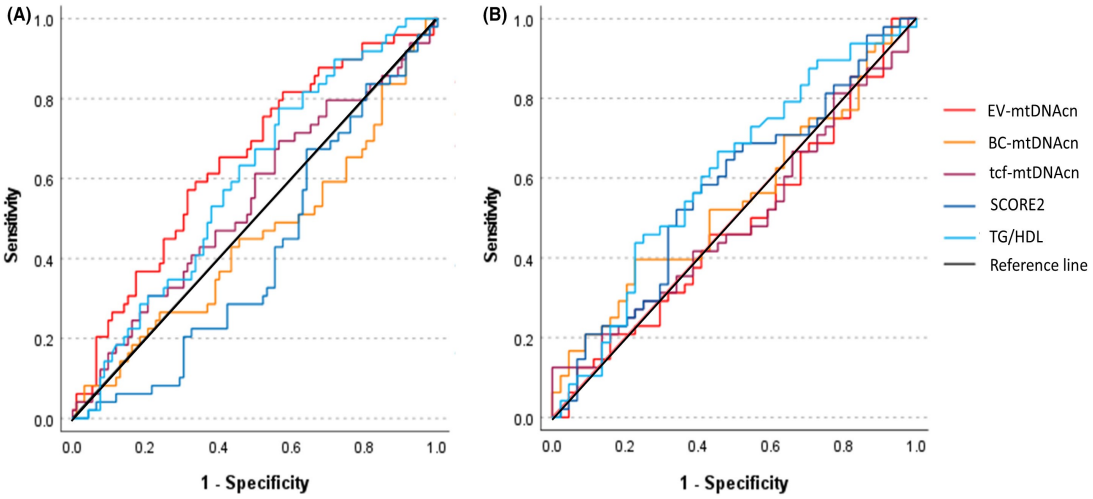

FIGURE 5 *ROC curve analysis evaluating the predictiveness of the selected biomarkers for CVD presence at baseline (A) or after 1.5 years from baseline (B).*

4 | DISCUSSION

A large body of literature describes the link between CVD and inflammation,[60] which in turn is connected to mitochondrial homeostasis.[61] Remarkably, Chen et al. recently showed that small EVs from young plasma reverse age- related functional declines by improving mitochondrial energy metabolism, suggesting a functional link between EVs and mitochondrial functions.[62] Intracellular mtDNAcn, initially proposed as a surrogate biomarker of mitochondrial functions, has been associated to metabolic and cardiovascular health in humans.[12] Also, ccf- mtDNA may be implicated in the pathogenesis of CVD, owing to its potential pro-inflammatory properties. [14,20,22] Thus, the hypothesis that mtDNAcn might be used as a predictive tool for CVD prevention and risk stratification has been postulated.[18] Previous studies have shown an inverse correlation between whole blood[63-65] or BC-mtDNAcn [18,66] (relative to nDNA) and both prevalent and incident CVD.[18] However, concerns about this measurement have been raised,[59] particularly considering that blood composition might influence this parameter. This concern arises from the varied abundance of mtDNAcn in different cell types, with platelets, in particular, contributing to the measurement with mtDNA but not nDNA. Therefore, mtDNAcn measured from whole blood or buffy coat may serve as an index of overall blood composition rather than specifically reflecting mitochondrial functions. In our study, BC- mtDNAcn was not different in subjects that were healthy at baseline ($\alpha + \beta$) than in CVD cases (γ). No significant difference has been seen neither in adjusting the analysis for platelet/leukocyte ratio. The BC-mtDNAcn was not associated to SCORE2 or TG/HDL. Despite platelets and leukocytes being major contributors to the release of ccf- mtDNA, no correlations between BC- mtDNAcn and tcf- mtDNAcn were observed. It is worth noting that platelets and leukocytes, while significant contributors, are not the sole contributors to this phenomenon.[14] In any case, BC- mtDNAcn was not informative of the cardiovascular health status in this cohort.

While numerous studies have tested the associations between CVD and mtDNAcn from whole blood, there is a scarcity of data from human cohorts concerning ccf-mtDNAcn in CVD. Berezina et al.[67] showed that heart failure patients ($N = 120$) have higher ccf- nDNAcn but lower ccf- mtDNAcn than controls ($N = 120$). In contrast, Liu et al.[24,68] measured an increase in mtDNA in diabetic patients with coronary heart

disease (CHD) (N = 50) compared to those without CHD (N = 44). Wiersma et al.[69] showed increased levels of ccf- mtDNAcn in paroxysmal atrial fibrillation (N = 100) but reduced levels in persistent atrial fibrillation (N = 116) and longstanding- persistent atrial fibrillation (N = 20) compared to controls (N = 84). Ueda et al.[70] measured higher levels of both ccf-mtDNAcn and ccf- nDNAcn in patients with atherosclerotic plaques (N = 62) than controls (N = 21). Only Ye et al.[39] selectively investigated the plasma exosomes- derived mtDNA (by droplet digital PCR), showing that both the plasma exosome particle numbers and the exosomal mtDNAcn were elevated in chronic heart failure patients (N = 20) compared to controls (N = 20). In our study, no significant differences were observed between healthy subjects (α + β) and CVD patients (γ) in terms of mtDNAcn measured in the total fraction of cell-free DNA (tcf-mtDNAcn). Tcf- mtDNAcn was not different neither between α and β groups. However, the specific fraction of mtDNAcn carried in EVs was higher in CVD patients (γ) than healthy subjects (α + β), while no difference was observed between individuals who reported a heart attack after 1.5 years (β) and those remaining healthy in the following 6 years (α). The association between EV- mtDNAcn and CVD status remained significant even after adjusting the analysis for both the abundance of EVs and blood composition. This observation suggests that variations in EV-mtDNAcn may offer more insights into cardiovascular health compared to tcf- mtDNAcn. This is significant because tcf-mtDNA includes both passively released mtDNA (resulting from necrosis or apoptosis) and actively released mtDNA, while EV- mtDNA specifically originates from an active and regulated process.[14] Little is known about the mechanistic explanation of the packaging of mtDNA in EVs but increasing attention has recently started to be addressed to this phenomenon. EVs containing mtDNA have been hypothesized to derive from mitochondria- derived vesicles,[22] given that they transport mitochondrial proteins.[71] However, a recent study denied the presence of mtDNA in mitochondria-derived vesicles [72] proposing the hypothesis that different mechanisms could be implicated in the translocation of mtDNA to EVs, or that other transporters of mtDNA from mitochondria to EVs may exist.[22] Our results lead us to speculate that cells may initiate an active response to CVD, resulting in the packaging of mtDNA inside EVs released into the bloodstream. Indeed, a positive correlation between the EV- mtDNAcn and EVs abundance was measured in our

cohort. The role of mtDNA transfer by EVs in CVD has been previously investigated,[73] especially in vitro.[74,75] While the molecular pathways activated by mtDNA in EVs are only partially defined, compelling evidence regarding the pro-inflammatory potential of ccf- mtDNA has been gathered.[20,22,76] Fan et al.[77] showed increased levels of inflammatory biomarker in chronic kidney disease patients with high mtDNAcn. Also, mtDNA released within exosomes has been recently shown to promote inflammation in Behçet's syndrome, a chronic systemic inflammatory disorder.[78] Indeed, exosomes, which represent a large part of EVs, play a crucial role in the process of intracellular and inter- organ communication transporting fundamental biological signals which can have paracrine or long-rage effects. [34] The uptake of exosomes by recipient cells involves the endosomal pathway.[79] As a DAMP, mtDNA may activate TLR9, cGAS- STING, and NLRP3.[22] Of note, previous studies have shown that the cGAS- STING- IRF3 or the STING–NF-kB pathway is activated when oxidized mtDNA leaks into the cytosol.[80] Also, the activation of the NLRP3 inflammasome requires the release of oxidized mtDNA.[81] These findings suggest that biochemical modifications of mtDNA (not limited to oxidation but potentially including other modifications, such as methylation or hydroxymethylation) might represent an additional layer of regulation of these mechanisms and modulate the pro-inflammatory potential of the mtDNA over long distances. This interesting hypothesis might represent an additional level of regulation of mtDNA pro-inflammatory effects, warranting further investiga- tions currently ongoing in our laboratories.

A role for exosomes per se has been suggested in the development of CVD,[30,33] with previous literature showing higher levels of plasma exosomes in chronic heart failure patients and acute ischemic stroke patients than controls.[39,82] In our study, EV-mtDNAcn remained associated with CVD even after adjusting for the characteristics of EVs and blood composition, suggesting that the cargo, rather than the number and size of EVs, may play a crucial role in the biological phenomena occurring after a heart attack. Nevertheless, we found a correlation between the abundance of EVs and SCORE2, an international index considered a predictor of CVD in the long range,[40] corroborating the importance of EVs in defining the risk for CVD.

In our study, EV-mtDNAcn was not associated with the EVs surface charge, suggesting that the DNA is contained within the vesicles rather than being externally

associated with the vesicle surface. This evidence aligns with our hypothesis, suggesting a cellular response in the context of CVD, leading to the active packaging of mtDNA as a cargo within EVs. The presence of double- stranded DNA on the surface of EVs has been previously reported.[83] Complexes constituted by double-stranded DNA and histones such as H2A, H2B, and H3 have been found on the surface of exosomes.[84] In line with this evidence, a few copies of nuclear DNA were also detected in EVs in our study, where EV- nDNAcn was higher in CVD patients than in subjects who were going to develop a heart attack. No differences have been seen in the EV-nDNAcn levels between CVD patients and controls. However, EV-nDNAcn was not as- sociated to the abundance of EVs (measured as DCR by DLS), while it was correlated with both mtDNAcn and nDNAcn from the overall cell-free fraction, as well as to the number of blood mononuclear cells and basophilic granulocytes. This hinted at the hypothesis that the few copies of nDNA detected in our EVs samples could potentially be passively carried on the surface of the vesicles rather than being a real EVs cargo. Also, nDNA detected in EVs might be a remnant of nDNA from the total cell- free DNA fraction. Indeed, despite some studies that reported nDNA in EVs,[85,86] the presence of genomic DNA in EVs is still a matter of debate. In particular, the mechanism by which nDNA, which is compartmentalized in the nucleus, is transported into EVs remains an open question.[87] A hypothesis posits that micronuclei, structural formations in the nuclear membrane that arise during cell division in the event of errors in chromosome distribution, may collapse, releasing their DNA content into the cytoplasm.[87] In turn, the nDNA released by micronuclei may be loaded into exosomes. Indeed, higher levels of DNA have been found in the exosomes produced by cancer cells or by cells exposed to genotoxic conditions which contains a higher number of micronuclei.[86- 88] Despite this intriguing hypothesis, our findings do not confirm that the low levels of nDNA detected in EVs, even with advanced and highly sensitive technologies like digital PCR, represent a reliable signal. Concerning the possibility to predict CVD, neither classical predictors (TG/HDL,[41] SCORE2[40]) nor levels of mtDNAcn (both in buffy coat or EVs) were able to predict heart attack 1.5y in advance (distinguishing α from β group). In contrast, SCORE2 was significantly able to predict CVD onset after 6y.

This study shows preliminary findings, and some drawbacks have to be acknowledged. The first limitation arises from the unavailability of blood samples from acute cases of heart attack for analysis. These samples would have been valuable as positive controls. Unfortunately, this constraint originates because the LifeLines cohort primarily focuses on studying healthy individuals. Consequently, we weren't able to identify a significant number of samples still matching cases and controls by adhering to the selection and matching criteria. The sample size of 144 individuals is a second limitation, potentially increasing the risk of false negative outcomes. However, this risk is mitigated by the study's robust case–control design, which is founded on stringent inclusion and exclusion criteria outlined earlier. These criteria consider not only information at basal assessment (i.e., age, smoking, diet, physical activity, other disease presence) but also prospective disease onset (i.e., we excluded individuals who developed any other diseases than heart attack in 1.5y). For this reason, this is a unique cohort, where differences between samples are likely attributed to the presence or onset of heart attack, controlling for numerous confounding factors, which are rarely used as selection criteria in bigger cohorts. Unfortunately, it was not possible to consider familial history for CVD and to compare predictiveness of mtDNAcn with other specific biomarkers of cardiovascular health in this cohort. Future studies addressing this research question in larger cohorts and including these information would enhance the potential for translating the evidence into clinical practice.

In conclusion, risk stratification and prediction of cardiovascular event remains a challenge, emphasizing the need for further research investments. This is particularly crucial given the substantial impact of these pathologies on the health system. Although several studies suggested the usage of mtDNAcn as a predictor of CVD,[2,18,19,89-91] applications of this evidence in clinical practice remain to be validated. Nevertheless, our preliminary findings suggest EVs and their cargoes (including mtDNA) as a promising and novel focus for a better understanding of CVD pathophysiology. Further research is warranted to investigate how mtDNA released in plasma exerts its biological effects, especially in the context of inflammation- driven pathologies.

SUPPLEMENTAL DATA

***Table S1**: Pearson coefficient (r) and P-value (p) of the correlation between EV-mtDNA or EVnDNA and components of blood.*

	EV-mtDNA		EVnDNA	
	r	p	r	p
Basophilic granulocytes (10^9/l)	0.089	0.293	**0.272**	**0.001**
Eosinophilic granulocytes (10^9/l)	0.064	0.454	0.113	0.189
Erythrocytes (10^{12}/l)	0.075	0.370	(-0.012)	0.893
Leukocytes (10^9/l)	0.093	0.269	(-0.013)	0.877
Lymphocytes (10^9/l)	0.150	0.076	0.056	0.520
Mononuclear cells (10^9/l)	0.016	0.850	**0.205**	**0.017**
Neutrophilic granulocytes (10^9/l)	0.027	0.754	(-0.006)	0.948
Thrombocytes (10^9/l)	0.118	0.158	0.109	0.200

REFERENCES

1. Taanman JW. The mitochondrial genome: structure, transcription, translation and replication. *Biochim Biophys Acta*. 1999;1410:103-123.
2. Bordoni L, Petracci I, Pelikant- Malecka I, et al. Mitochondrial DNA copy number and trimethylamine levels in the blood: new insights on cardiovascular disease biomarkers. *FASEB J*. 2021;35:e21694.
3. Hong YS, Battle SL, Puiu D, et al. Long- term air pollution exposure and mitochondrial DNA copy number: an analysis of UK biobank data. *Environ Health Perspect*. 2023;131:57703.
4. Gu S, Fu L, Wang J, et al. MtDNA copy number in oral epithelial cells serves as a potential biomarker of mitochondrial damage by neonicotinoid exposure: a cross-sectional study. *Environ Sci Technol*. 2023;57:15816-15824.
5. Zhao H, Shen J, Leung E, Zhang X, Chow W- H, Zhang K. Leukocyte mitochondrial DNA copy number and built environment in Mexican Americans: a cross- sectional study. *Sci Rep*. 2020;10:14988.
6. Bordoni L, Perugini J, Petracci I, et al. Mitochondrial DNA in visceral adipose tissue in severe obesity: From copy number to D- loop methylation. *Front Biosci (Landmark Ed)*. 2022;27:172.
7. Bordoni L, Smerilli V, Nasuti C, Gabbianelli R. Mitochondrial DNA methylation and copy number predict body composition in a young female population. *J Transl Med*. 2019;17:399.
8. Smith AR, Hinojosa Briseño A, Picard M, Cardenas A. The prenatal environment and its influence on maternal and child mitochondrial DNA copy number and methylation: a review of the literature. *Environ Res*. 2023;227:115798.
9. Fu M, Wang C, Hong S, et al. Multiple metals exposure and blood mitochondrial DNA copy number: a cross- sectional study from the Dongfeng- Tongji cohort. *Environ Res*. 2023;216:114509.
10. Wang X, Hart JE, Liu Q, Wu S, Nan H, Laden F. Association of particulate matter air pollution with leukocyte mitochondrial DNA copy number. *Environ Int*. 2020;141:105761.
11. Yang K, Forman MR, Monahan PO, et al. Insulinemic potential of lifestyle is inversely associated with leukocyte mitochondrial DNA copy number in US white adults. *J Nutr*. 2020;150:2156-2163.
12. Castellani CA, Longchamps RJ, Sun J, Guallar E, Arking DE. Thinking outside the nucleus: mitochondrial DNA copy number in health and disease. *Mitochondrion*. 2020;53:214-223.
13. Mengel-From J, Thinggaard M, Dalgård C, Kyvik KO, Christensen K, Christiansen L. Mitochondrial DNA copy number in peripheral blood cells

declines with age and is associated with general health among elderly. *Hum Genet*. 2014;133:1149-1159.
14. Trumpff C, Michelson J, Lagranha CJ, et al. Stress and circulating cell-free mitochondrial DNA: a systematic review of human studies, physiological considerations, and technical recommendations. *Mitochondrion*. 2021;59:225-245.
15. De Gaetano A, Solodka K, Zanini G, et al. Molecular mechanisms of mtDNA-mediated inflammation. *Cells*. 2021;10:1-21.
16. Kaaman M, Sparks LM, van Harmelen V, et al. Strong association between mitochondrial DNA copy number and lipogenesis in human white adipose tissue. *Diabetologia*. 2007;50:2526-2533.
17. Tin A, Grams ME, Ashar FN, et al. Association between mitochondrial DNA copy number in peripheral blood and incident CKD in the atherosclerosis risk in communities study. *J Am Soc Nephrol*. 2016;27:2467-2473.
18. Ashar FN, Zhang Y, Longchamps RJ, et al. Association of mitochondrial DNA copy number with cardiovascular disease.
JAMA Cardiol. 2017;2:1247-1255.
19. Koller A, Fazzini F, Lamina C, et al. Mitochondrial DNA copy number is associated with all- cause mortality and cardiovascular events in patients with peripheral arterial disease. *J Intern Med*. 2020;287:569-579.
20. West AP, Shadel GS. Mitochondrial DNA in innate immune responses and inflammatory pathology. *Nat Rev Immunol*. 2017;17:363-375.
21. Zanini G, Selleri V, Lopez Domenech S, et al. Mitochondrial DNA as inflammatory DAMP: a warning of an aging immune system? *Biochem Soc Trans*. 2023;51:735-745.
22. Newman LE, Shadel GS. Mitochondrial DNA release in innate immune signaling. *Annu Rev Biochem*. 2023;92:299-332.
23. Simmons JD, Lee Y- L, Mulekar S, et al. Elevated levels of plasma mitochondrial DNA DAMPs are linked to clinical outcome in severely injured human subjects. *Ann Surg*. 2013;258:591-598.
24. Liu J, Cai X, Xie L, et al. Circulating cell free mitochondrial DNA is a biomarker in the development of coronary heart disease in the patients with type 2 diabetes. *Clin Lab*. 2015;61:661-667.
25. Podlesniy P, Figueiro- Silva J, Llado A, et al. Low cerebrospinal fluid concentration of mitochondrial DNA in preclinical Alzheimer disease. *Ann Neurol*. 2013;74:655-668.
26. Pyle A, Brennan R, Kurzawa-Akanbi M, et al. Reduced cerebro- spinal fluid mitochondrial DNA is a biomarker for early-stage Parkinson's disease. *Ann Neurol*. 2015;78:1000-1004.
27. Alvarado-Vásquez N. Circulating cell- free mitochondrial DNA as the probable inducer of early endothelial dysfunction in the prediabetic patient. *Exp Gerontol*. 2015;69:70-78.

28. Bae JH, Jo SI, Kim SJ, et al. Circulating cell-free mtDNA con- tributes to AIM2 inflammasome- mediated chronic inflammation in patients with type 2 diabetes. *Cells*. 2019;8:328.
29. Zhang Z, Meng P, Han Y, et al. Mitochondrial DNA-LL- 37 complex promotes atherosclerosis by escaping from autophagic recognition. *Immunity*. 2015;43:1137-1147.
30. Neves KB, Rios FJ, Sevilla-Montero J, Montezano AC, Touyz RM. Exosomes and the cardiovascular system: role in cardiovascular health and disease. *J Physiol*. 2023;601:4923-4936.
31. Zheng B, Yin W-N, Suzuki T, et al. Exosome- mediated miR- 155 transfer from smooth muscle cells to endothelial cells induces endothelial injury and promotes atherosclerosis. *Mol Ther*. 2017;25:1279-1294.
32. Li B, Zang G, Zhong W, et al. Activation of CD137 signaling promotes neointimal formation by attenuating TET2 and transferrring from endothelial cell-derived exosomes to vascular smooth muscle cells. *Biomed Pharmacother*. 2020;121:109593.
33. Zarà M, Amadio P, Campodonico J, Sandrini L, Barbieri SS. Exosomes in cardiovascular diseases. *Diagnostics (Basel, Switzerland)*. 2020;10:1-24.
34. Isaac R, Reis FCG, Ying W, Olefsky JM. Exosomes as mediators of intercellular crosstalk in metabolism. *Cell Metab*. 2021;33:1744-1762.
35. Arance E, Ramírez V, Rubio-Roldan A, et al. Determination of exosome mitochondrial DNA as a biomarker of renal cancer aggressiveness. *Cancers (Basel)*. 2021;14:1-13.
36. Sansone P, Savini C, Kurelac I, et al. Packaging and transfer of mitochondrial DNA via exosomes regulate escape from dormancy in hormonal therapy- resistant breast cancer. *Proc Natl Acad Sci USA*. 2017;114:E9066-E9075.
37. Byappanahalli AM, Noren Hooten N, Vannoy M, et al. Mitochondrial DNA and inflammatory proteins are higher in extracellular vesicles from frail individuals. *Immun Ageing*. 2023;20:6.
38. Keserű JS, Soltész B, Lukács J, et al. Detection of cell- free, exosomal and whole blood mitochondrial DNA copy number in plasma or whole blood of patients with serous epithelial ovarian cancer. *J Biotechnol*. 2019;298:76-81.
39. Ye W, Tang X, Yang Z, et al. Plasma- derived exosomes contribute to inflammation via the TLR9- NF- κB pathway in chronic heart failure patients. *Mol Immunol*. 2017;87:114-121.
40. SCORE2 risk prediction algorithms: new models to estimate 10- year risk of cardiovascular disease in Europe. *Eur Heart J*. 2021;42:2439-2454.
41. Kosmas CE, Rodriguez Polanco S, Bousvarou MD, et al. The triglyceride/high-density lipoprotein cholesterol (TG/HDL- C) ratio as a risk marker for metabolic syndrome and cardiovascular disease. *Diagnostics (Basel, Switzerland)*. 2023;13:929.

42. Aimo A, Chiappino S, Clemente A, et al. The triglyceride/HDL cholesterol ratio and TyG index predict coronary atherosclerosis and outcome in the general population. *Eur J Prev Cardiol*. 2022;29:e203-e204.
43. Scholtens S, Smidt N, Swertz MA, et al. Cohort profile: Lifelines, a three-generation cohort study and biobank. *Int J Epidemiol*. 2015;44:1172-1180.
44. Sijtsma A, Rienks J, van der Harst P, Navis G, Rosmalen JGM, Dotinga A. Cohort profile update: lifelines, a three- generation cohort study and biobank. *Int J Epidemiol*. 2022;51:e295-e302.
45. Visseren FLJ, Mach F, Smulders YM, et al. 2021 ESC Guidelines on cardiovascular disease prevention in clinical practice. *Eur Heart J*. 2021;42:3227-3337.
46. Vinke PC, Corpeleijn E, Dekker LH, Jacobs DR, Navis G, Kromhout D. Development of the food-based lifelines diet score (LLDS) and its application in 129,369 lifelines participants. *Eur J Clin Nutr*. 2018;72:1111-1119.
47. Fazzini F, Schöpf B, Blatzer M, et al. Plasmid-normalized quan- tification of relative mitochondrial DNA copy number. *Sci Rep*. 2018;8:15347.
48. Tiwari S, Kumar V, Randhawa S, Verma SK. Preparation and characterization of extracellular vesicles. *Am J Reprod Immunol*. 2021;85:e13367.
49. Szatanek R, Baj-Krzyworzeka M, Zimoch J, Lekka M, Siedlar M, Baran J. The methods of choice for extracellular vesicles (EVs) characterization. *Int J Mol Sci*. 2017;18:1153.
50. Serrano- Pertierra E, Oliveira- Rodríguez M, Rivas M, et al. Characterization of plasma- derived extracellular vesicles isolated by different methods: a comparison study. *Bioeng (Basel, Switzerland)*. 2019;6:8.
51. Baranyai T, Herczeg K, Onódi Z, et al. Isolation of exosomes from blood plasma: qualitative and quantitative comparison of ultracentrifugation and size exclusion chromatography methods. *PLoS ONE*. 2015;10:e0145686.
52. Gurunathan S, Kang M- H, Jeyaraj M, Qasim M, Kim J- H. Review of the isolation, characterization, biological function, and multifarious therapeutic approaches of exosomes. *Cells*. 2019;8:307.
53. Lawrie AS, Albanyan A, Cardigan RA, Mackie IJ, Harrison P. Microparticle sizing by dynamic light scattering in fresh-frozen plasma. *Vox Sang*. 2009;96:206-212.
54. Gercel- Taylor C, Atay S, Tullis RH, Kesimer M, Taylor DD. Nanoparticle analysis of circulating cell- derived vesicles in ovarian cancer patients. *Anal Biochem*. 2012;428:44-53.
55. Kogej K, Božič D, Kobal B, Herzog M, Černe K. Application of dynamic and static light scattering for size and shape characterization of small extracellular nanoparticles in plasma and ascites of ovarian cancer patients. *Int J Mol Sci*. 2021;22:12946.
56. Mudalige T, Qu H, Van Haute D, Ansar SM, Paredes A, Ingle T. Chapter 11—characterization of nanomaterials: tools and challenges. In: López Rubio A, Fabra

Rovira MJ, Martínez Sanz M, L. G. B. T.-N. for F. A. Gómez- Mascaraque, eds. *Micro and Nano Technologies*. Elsevier; 2019:313-353.
57. Midekessa G, Godakumara K, Ord J, et al. Zeta potential of extracellular vesicles: toward understanding the attributes that determine colloidal stability. *ACS Omega*. 2020;5:16701-16710.
58. Lassale C, Curtis A, Abete I, et al. Elements of the complete blood count associated with cardiovascular disease incidence:
findings from the EPIC-NL cohort study. *Sci Rep*. 2018;8:3290.
59. Picard M. Blood mitochondrial DNA copy number: what are we counting? *Mitochondrion*. 2021;60:1-11.
60. Henein MY, Vancheri S, Longo G, Vancheri F. The Role of Inflammation in Cardiovascular Disease. *Int J Mol Sci*. 2022;23:12906.
61. López- Armada MJ, Riveiro- Naveira RR, Vaamonde- García C, Valcárcel- Ares MN. Mitochondrial dysfunction and the inflammatory response. *Mitochondrion*. 2013;13:106-118.
62. Chen X, Luo Y, Zhu Q, et al. Small extracellular vesicles from young plasma reverse age-related functional declines by im- proving mitochondrial energy metabolism. *Nat Aging*. 2024.
63. Liu X, Sun X, Zhang Y, et al. Association between whole blood- derived mitochondrial DNA copy number, low-density lipopro- tein cholesterol, and cardiovascular disease risk. *J Am Heart Assoc*. 2023;12:e029090.
64. Liu X, Longchamps RJ, Wiggins KL, et al. Association of mitochondrial DNA copy number with cardiometabolic diseases. *Cell Genomics*. 2021;1:100006.
65. Yue P, Jing S, Liu L, et al. Association between mitochondrial DNA copy number and cardiovascular disease: current evidence based on a systematic review and meta- analysis. *PLoS ONE*. 2018;13:e0206003.
66. Hong YS, Longchamps RJ, Zhao D, et al. Mitochondrial DNA copy number and incident heart failure: the atherosclerosis risk in communities (ARIC) study. *Circulation*. 2020;141:1823-1825.
67. Berezina TA, Kopytsya MP, Petyunina OV, et al. Lower circulating cell- free mitochondrial DNA is associated with heart failure in type 2 diabetes mellitus patients. *Cardiogenetics*. 2023;13:15-30.
68. Liu J, Zou Y, Tang Y, et al. Circulating cell- free mitochondrial deoxyribonucleic acid is increased in coronary heart disease patients with diabetes mellitus. *J Diabetes Investig*. 2016;7:109-114.
69. Wiersma M, van Marion DMS, Bouman EJ, et al. Cell-free cir- culating mitochondrial DNA: a potential blood-based marker for atrial fibrillation. *Cells*. 2020;9:1159.
70. Ueda K, Sakai C, Ishida T, et al. Cigarette smoke induces mitochondrial DNA damage and activates cGAS- STING pathway: application to a biomarker for atherosclerosis. *Clin Sci (Lond)*. 2023;137:163-180.

71. Todkar K, Chikhi L, Desjardins V, El-Mortada F, Pépin G, Germain M. Selective packaging of mitochondrial proteins into extracellular vesicles prevents the release of mitochondrial DAMPs. *Nat Commun*. 2021;12:1971.
72. König T, Nolte H, Aaltonen MJ, et al. MIROs and DRP1 drive mitochondrial-derived vesicle biogenesis and promote quality control. *Nat Cell Biol*. 2021;23:1271-1286.
73. Chen J, Zhong J, Wang L- L, Chen Y- Y. Mitochondrial transfer in cardiovascular disease: From mechanisms to therapeutic implications. *Front Cardiovasc Med*. 2021;8:771298.
74. Ikeda G, Santoso MR, Tada Y, et al. Mitochondria-rich extra- cellular vesicles from autologous stem cell- derived cardiomyocytes restore energetics of ischemic myocardium. *J Am Coll Cardiol*. 2021;77:1073-1088.
75. Puhm F, Afonyushkin T, Resch U, et al. Mitochondria are a subset of extracellular vesicles released by activated monocytes and induce type I IFN and TNF responses in endothelial cells. *Circ Res*. 2019;125:43-52.
76. Jeon H, Lee J, Lee S, et al. Extracellular vesicles From KSHV- infected cells stimulate antiviral immune response through mitochondrial DNA. *Front Immunol*. 2019;10:876.
77. Fan Z, Feng Y, Zang L, Guo Y, Zhong X- Y. Association of circulating MtDNA with CVD in hemodialysis patients and in vitro effect of exogenous MtDNA on cardiac microvascular inflammation. *BMC Cardiovasc Disord*. 2023;23:74.
78. Konaka H, Kato Y, Hirano T, et al. Secretion of mitochondrial DNA via exosomes promotes inflammation in Behçet's syndrome. *EMBO J*. 2023;42:e112573.
79. Gurung S, Perocheau D, Touramanidou L, Baruteau J. The exosome journey: from biogenesis to uptake and intracellular signalling. *Cell Commun Signal*. 2021;19:47.
80. Fang C, Mo F, Liu L, et al. Oxidized mitochondrial DNA sensing by STING signaling promotes the antitumor effect of an irradiated immunogenic cancer cell vaccine. *Cell Mol Immunol*. 2021;18:2211-2223.
81. Kim J, Kim H- S, Chung JH. Molecular mechanisms of mitochondrial DNA release and activation of the cGAS- STING pathway. *Exp Mol Med*. 2023;55:510-519.
82. Ji Q, Ji Y, Peng J, et al. Increased brain- specific MiR-9 and MiR- 124 in the serum exosomes of acute ischemic stroke patients. *PLoS ONE*. 2016;11:e0163645.
83. Thakur BK, Zhang H, Becker A, et al. Double- stranded DNA in exosomes: a novel biomarker in cancer detection. *Cell Res*. 2014;24:766-769.
84. Tutanov O, Shtam T, Grigor'eva A, Tupikin A, Tsentalovich Y, Tamkovich S. Blood plasma exosomes contain circulating DNA in their crown. *Diagnostics (Basel, Switzerland)*. 2022;12:854.
85. Lichá K, Pastorek M, Repiská G, Celec P, Konečná B. Investigation of the presence of DNA in human blood plasma small extracellular vesicles. *Int. J. Mol Sci*. 2023;24:5915.

86. Yokoi A, Villar- Prados A, Oliphint PA, et al. Mechanisms of nuclear content loading to exosomes. *Sci Adv*. 2019;5:eaax8849.
87. Elzanowska J, Semira C, Costa- Silva B. DNA in extracellular vesicles: biological and clinical aspects. *Mol Oncol*. 2021;15:1701-1714.
88. Fenech M, Kirsch- Volders M, Natarajan AT, et al. Molecular mechanisms of micronucleus, nucleoplasmic bridge and nuclear bud formation in mammalian and human cells. *Mutagenesis*. 2011;26:125-132.
89. Wei R, Ni Y, Bazeley P, et al. Mitochondrial DNA content is linked to cardiovascular disease patient phenotypes. *J Am Heart Assoc*. 2021;10:e018776.
90. Sundquist K, Sundquist J, Palmer K, Memon AA. Role of mitochondrial DNA copy number in incident cardiovascular diseases and the association between cardiovascular disease and type 2 diabetes: a follow- up study on middle- aged women. *Atherosclerosis*. 2022;341:58-62.
91. Nie S, Lu J, Wang L, Gao M. Pro- inflammatory role of cell- free mitochondrial DNA in cardiovascular diseases. *IUBMB Life*. 2020;72:1879-1890.

4. General Discussion and Conclusion

Increasing evidence suggests that inflammation represents a common biological mechanism linking aging, gut dysfunction and cardiometabolic pathologies [1]. It acts both as a driver and a consequence of these conditions, establishing a complex, bidirectional feedback loop that perpetuate itself over time leading to systemic, chronic low grade inflammatory states [2]. Epigenetic regulation, transcriptomic reprogramming and mitochondrial function play pivotal roles in controlling cellular homeostasis. Indeed, through the regulation of gene expression and metabolic homeostasis, these interconnected mechanisms are involved in the inflammatory responses [3], [4]. Also, diet play a key role in modulating inflammation as it influences gut health and provides bioactive molecules with potential anti-inflammatory effects [2].

Thus, the aim of this research was to investigate the epigenetic, transcriptional and mitochondrial mechanisms underlying inflammation, focusing on the responses to nutritional bioactive molecules, microbial metabolites, aging and cardiovascular disease.

The aging process is characterized by the establishment of a low-grade sterile inflammatory status which has a systemic impact [5]. Indeed, aged cells acquire the SASP phenotype producing inflammatory molecules that affect neighboring cells and contribute to tissues dysfunctions [6]. Aging is characterized by several conserved mechanisms (adaptation to stress, epigenetics alteration, macromolecular damage, metabolic dysregulation, impaired proteostasis and decline on stem cells and regeneration) which converge on inflammation [7]. Indeed, dysregulation of one of these mechanisms triggers inflammation which in turn affects all the others [7]. Since ageing is a strong risk factor for the development of age-related diseases and age-related diseases represent a major public health concern, identifying a natural product able to against aging process and counteract age-associated inflammation is a major challenge in the field of biomedical research.

Thus, our main research objective was the investigation of how MRME, a plant-derived compound with suggested anti-inflammatory properties, affects the epigenetic

and transcriptomic profile of an in vitro model of cellular senescence. According to our results MRME exerted anti-inflammatory and anti-aging effects throughout the modulation of the expression of inflammaging genes via mechanisms independent of DNA methylation. These findings highlighted MRME as a promising candidate for further in vivo studies aimed at exploring its clinical translational potential in counteracting inflammaging underling the role of dietary bioactive compounds in healthy aging.

Preserving the structural and functional integrity of the intestinal barrier is one of the defences mechanisms preventing the onset of chronic, systemic inflammation [8]. Unhealthy diets and lifestyles have been suggested to be associated to dysbiosis and gut dysfunction leading to increased intestinal permeability and inflammation [9]. Thus, our secondary research objective was the investigation of the effect of TMA, a metabolite produced by gut microbiota from dietary precursors, on the intestinal functionality, with a particular focus on its action on gene expression regulation and mitochondrial homeostasis. Interestingly, the exposure of an intestinal epithelium model to TMA led to an increased expression of IL-6, IL-1β, SIRT1, DNMT1 and ND6 genes. TMA reduced total ATP levels, intracellular mitochondrial DNA copy number and it increased the release of cf-mtDNA in the cell culture medium. Furthermore, TMA disrupted the intestinal epithelium permeability, and, in a cell-free assay, it induced a dose-dependent reduction in Sirtuin enzyme activity. Thus, taking together these preliminary results our speculation was that high levels of TMA might promote inflammation in intestinal epithelial cells disrupting the epigenetic and mitochondrial homeostasis.

The persistent inflammatory environment associated with gut dysfunction and aging is a risk factor for the development of CVD [1], [10]. Thus, our third research objective was to investigate the molecular mechanisms of inflammation in different CVD states. Since cell-free mitochondrial DNA has been suggested to be inflammogenic, we quantified mtDNAcn in circulating cell-free DNA and extracellular vesicles, comparing healthy subjects and patients with cardiovascular disease in order to assess whether it was altered in CVD patients and whether it may serve as a predictive biomarker of cardiovascular events. According to our results mtDNAcn in cell-free DNA could not predict CVD occurrence in advance, however mtDNAcn in

extracellular vesicles of CVD patients has been found increased compared to healthy control. This last result allows us to speculate the occurrence of an active packaging of mtDNA in extracellular vesicles after a CVD event suggesting the need for further investigations to determine its pathophysiological role.

All the studies described in this thesis have some limitations that need to be considered. The first and the second studies were conducted using in vitro models, thus their results require further validation in more complex biological system to enhance the clinical relevance and transability. The main limitation of the third study is the modest sample size (144 individuals) that may increase the risk of false negative results; however, this risk is mitigated by the case-control design of the study and the use of rigorous selection criteria.

Despite the limitations, the research studies presented in this thesis provide valuable preliminary insights into how inflammation can be modulated throughout diet or diet-derived compounds. Furthermore, we proposed a previously unrecognized molecular mechanism (packaging of DNA into exosomes in CVD patients) occurring across inflammation-driver pathologies, such as CVD.

Overall, the findings of this thesis contribute to a better understanding of the complex interplay between diet, inflammation, and cardiovascular disease, and it opens the way for future studies aimed at translating these observations into clinical applications.

Bibliography

[1] S. Liu *et al.*, "Targeting gut microbiota in aging-related cardiovascular dysfunction: focus on the mechanisms.," *Gut Microbes*, vol. 15, no. 2, p. 2290331, Dec. 2023, doi: 10.1080/19490976.2023.2290331.

[2] L. M. Beaver, P. E. Jamieson, C. P. Wong, M. Hosseinikia, J. F. Stevens, and E. Ho, "Promotion of Healthy Aging Through the Nexus of Gut Microbiota and Dietary Phytochemicals.," *Adv Nutr*, vol. 16, no. 3, p. 100376, Mar. 2025, doi: 10.1016/j.advnut.2025.100376.

[3] S. Zhang *et al.*, "Targeting epigenetic regulators for inflammation: Mechanisms and intervention therapy.," *MedComm (Beijing)*, vol. 3, no. 4, p. e173, Dec. 2022, doi: 10.1002/mco2.173.

[4] X. Xu, Y. Pang, and X. Fan, "Mitochondria in oxidative stress, inflammation and aging: from mechanisms to therapeutic advances.," *Signal Transduct Target Ther*, vol. 10, no. 1, p. 190, Jun. 2025, doi: 10.1038/s41392-025-02253-4.

[5] Li X, Li C, Zhang W, Wang Y, Qian P, Huang H. Inflammation and aging: signaling pathways and intervention therapies. Signal Transduct Target Ther. 2023 Jun 8;8(1):239. doi: 10.1038/s41392-023-01502-8. PMID: 37291105; PMCID: PMC10248351.

[6] Y. Li, X. Tian, J. Luo, T. Bao, S. Wang, and X. Wu, "Molecular mechanisms of aging and anti-aging strategies.," *Cell Commun Signal*, vol. 22, no. 1, p. 285, May 2024, doi: 10.1186/s12964-024-01663-1.

[7] C. Franceschi, P. Garagnani, P. Parini, C. Giuliani, and A. Santoro, "Inflammaging: a new immune–metabolic viewpoint for age-related diseases," *Nat Rev Endocrinol*, vol. 14, no. 10, pp. 576–590, 2018, doi: 10.1038/s41574-018-0059-4.

[8] F. Di Vincenzo, A. Del Gaudio, V. Petito, L. R. Lopetuso, and F. Scaldaferri, "Gut microbiota, intestinal permeability, and systemic inflammation: a narrative review.," *Intern Emerg Med*, vol. 19, no. 2, pp. 275–293, Mar. 2024, doi: 10.1007/s11739-023-03374-w.

[9] Y.-R. Chae, Y. R. Lee, Y.-S. Kim, and H.-Y. Park, “Diet-Induced Gut Dysbiosis and Leaky Gut Syndrome.,” *J Microbiol Biotechnol*, vol. 34, no. 4, pp. 747–756, Apr. 2024, doi: 10.4014/jmb.2312.12031.

[10] J. F. Aranda, C. M. Ramírez, and M. Mittelbrunn, “Inflammageing, a targetable pathway for preventing cardiovascular diseases.,” *Cardiovasc Res*, vol. 121, no. 10, pp. 1537–1550, Aug. 2025, doi: 10.1093/cvr/cvae240.

SCIENTIFIC PRODUCTION DURING THE THREE YEARS PHD

•Laura Bordoni, Fatemeh Mansouri; **Chiara Rucci**; João Agostinho de Sousa; Ferdinand von Meyenn; Impact of dietary habits on epigenetic age acceleration: evaluating the intermediary role of low-grade inflammation. Article submitted on Clinical Nutrition Journal

•**Rucci C**., Sordini E., Persico G., Ciurlia E., Pappagallo N., Matacchione G., Giorgio M., Fraternale D., Albertini M.C., Annear D., De Rijk P., De Pooter T., Strazisar M., Vanden Berghe W., Bordoni L., Amatori S., Gabbienelli R., THE NUTRIGENOMIC EFFECT OF MELA ROSA MARCHIGIANA CALLUS EXTRACT ON CELLULAR SENESCENCE: INSIGHT FROM A PRELIMINARY IN VITRO STUDY. Molecular Nutrition and Food Research. (Article in Press)

•Bordoni L, Petracci I, Feliziani G, de Simone G, **Rucci C**, Gabbianelli R. Gut Microbiota-Derived Trimethylamine Promotes Inflammation with a Potential Impact on Epigenetic and Mitochondrial Homeostasis in Caco-2 Cells. Antioxidants (Basel). 2024 Aug 30;13(9):1061. doi: 10.3390/antiox13091061. PMID: 39334721; PMCID: PMC11428692.

•**Rucci C**, de Simone G, Salathia S, Casadidio C, Censi R, Bordoni L. Exploring mitochondrial DNA copy number in circulating cell-free DNA and extracellular vesicles across cardiovascular health status: A prospective case-control pilot study. FASEB J. 2024 May 31;38(10):e23672. doi: 10.1096/fj.202400463R. PMID: 38775929.

•Gabbianelli R, Shahar E, de Simone G, **Rucci C**, Bordoni L, Feliziani G, Zhao F, Ferrati M, Maggi F, Spinozzi E, Mahajna J. Plant-Derived Epi-Nutraceuticals as Potential Broad-Spectrum Anti-Viral Agents. Nutrients. 2023 Nov 8;15(22):4719. doi: 10.3390/nu15224719. PMID: 38004113; PMCID: PMC10675658.

THE RESULTS OF THE PHD PROJECT WERE PRESENTED IN SEVERAL SCIENTIFIC CONGRESSES

12 June 2025: Clinical Epigenetics International Conference 2025

Poster Title: “The transcriptomic and epigenetic effect of Mela Rosa Marchigiana callus extract: insight from an in vitro model of cellular senescence”

Authors: Chiara Rucci, Laura Bordoni, Dale Annear, Enrica Sordini, Giuseppe Persico, Eugenia Ciurlia, Noemi Pappagallo, Giulia Matacchione, Marco Giorgio, Daniele Fraternale, Maria Cristina Albertini, Stefano Amatori, Peter De Rijk, Tim De Pooter,
Mojca Strazisar, Wim Vanden Berghe, Rosita Gabbianelli

Naples, Italy

09 June 2025: SIB-TUM 2025, congress of the Italian society of Biochemistry and Molecular Biology

Poster Title: “Exploring the transcriptomic and epigenetic impact of Mela Rosa Marchigiana callus extract on cellular aging: insight from an in vitro study”

Authors: Chiara Rucci, Laura Bordoni, Enrica Sordini, Giuseppe Persico, Eugenia Ciurlia, Noemi Pappagallo, Giulia Matacchione, Marco Giorgio, Daniele Fraternale, Maria Cristina Albertini, Stefano Amatori, Rosita Gabbianelli.

Florence, Italy

PRIZE AS BEST POSTER

07 September 2023: NuGo week conference

Poster Title: “Effects of trimethylamine on the mitochondrial DNA: evidence from an in vitro model of intestinal epithelial cells.”

Authors: Chiara Rucci, Elisa Veloni, Laura Bordoni e Rosita Gabbianelli

Senigallia, Italy

09 July 2023: FEBS Congress

Poster Title: “Absolute quantification of mitochondrial DNA copy number from circulating cell-free DNA and exosomes in different cardiovascular health status: a case-control study from Lifelines biobank”

Authors: Chiara Rucci, Gaia de Simone, Sanyia Salathia, Cristina Casadiddio, Roberta Censi and Laura Bordoni.

Tours, France

CURRICULUM

PERSONAL INFORMATION

Chiara Rucci

Via d'Ancaria 30 (AP)

3477457618

chiara.rucci@unicam.it

Date of birth 11/03/1996 | Nationality Italian

CURRENT POSTION

30 November 2022 – current

PhD student in Life and Health Sciences

Curriculum: Nutrition, food and health

Laboratory of Nutrigenomics and Molecular Biology

Supervisors Prof. Rosita Gabbianelli, Prof Laura Bordoni

University of Camerino, Italy

EDUCATION

December 2022

Licensing as senior Biologist

University of Camerino, Italy

July 2022

Master's degree in Biological Sciences

Curriculum: Nutrition and functional food

University of Camerino, Italy

Final grade: 110 with laude

Experimental thesis in Epigenetics "The impact of dietary patterns and physical activity on mitochondrial DNA: any intermediary role for trimethylamine metabolism?"

Supervisors: Dr. Laura Bordoni and Prof. Rosita Gabbianelli

December 2019

Licensing as Junior Biologist

University of Camerino, Italy

October 2019

Bachelor's degree in Biologia della Nutrizione

University of Camerino

Final grade: 110 with laude

Bachelor thesis in Biochimica della Nutrizione "Dieta chetogenica in pazienti con sindrome dell'ovaio policistico"

Tutor: Prof Valeria Polzonetti, Dott.ssa Anna Paola Scioletti

INTERNSHIPS

February 2025 – August 2025

Internship at the Cell Death Signaling – Epigenetic Laboratory

University of Antwerp, Belgium

Supervisor Prof Wim Vanden Berghe

Bioinformatic training in Nanopore epi-sequencing

Practical experience in methylation microarray data analysis

Practical experience in protein tyrosine kinase assay on PamChip arrays on the PamStation

17 February 2025 - 24 February 2025

Internship at VIB-UAntwerp Center for Molecular Neurology, Neuromics Support Facility

University of Antwerp, Belgium

Supervisors Dr. Mojca Strazisar and Dr. Tim de Pooter

Practical training in Nanopore sequencing

September 2020 – July 2021

Internship at the Nutrigenomics and Molecular Biology laboratory

University of Camerino, Italy

Supervisor Dr. Laura Bordoni, Prof Rosita Gabbianelli

May 2019 – September 2019

Internship at Dr. Anna Paola Scioletti (PhD, Specialist in Clinical Pathology) nutritional clinic

Ascoli Piceno, Italy

SCHOOL, COURSES and WORKSHOPS

30 June 2025 – 2 July 2025

Workshop “Data Visualization in R: From Data Wrangling to Interactive Plots”

Physalia courses

12 hours (1ECTs)

10 February 2025 - 14 February 2025

Workshop “DNA Methylation in Ecology and Evolution”

Physalia courses

25 hours (1ECTs)

21 October 2024 – 25 October 2024

Autumn School in Bioinformatics

Physalia courses

30 hours (1ECTs)

18 June 2024 – 21 June 2024

5th European Summer School on Nutrigenomics

University of Camerino

Senigallia, Italy

03 June 2024 – 07 June 2024

2nd Advanced school on biophysical methods for protein-protein and protein-ligand interaction analysis

Università degli Studi di Milano, Unversità del Piemonte Orientale, Gruppo San Donato

40 hours

17 November 2023 – 27 November 2023

Workshop: Analysis of RNAsequencing data with R/Bioconductor

Physalia courses

27 hours (1ECTs)

03 September 2023 – 05 September 2023

Post-graduate course: "Primers in omic data analysis: genomics and transcriptomics to boost your research in molecular nutrition"

NuGO Association and University of Camerino

Senigallia, Italy

21 June 2021 – 25 June 2021

4th European Summer School on Nutrigenomics

University of Camerino, Held Online

SCIENTIFIC PRODUCTION

- Laura Bordoni, Fatemeh Mansouri; **Chiara Rucci**; João Agostinho de Sousa; Ferdinand von Meyenn; Impact of dietary habits on epigenetic age acceleration: evaluating the intermediary role of low-grade inflammation. Article submitted on Clinical Nutrition Journal

- **Rucci C**., Sordini E., Persico G., Ciurlia E., Pappagallo N., Matacchione G., Giorgio M., Fraternale D., Albertini M.C., Annear D., De Rijk P., De Pooter T., Strazisar M., Vanden Berghe W., Bordoni L., Amatori S., Gabbienelli R., The nutrigenomic effect of Mela Rosa Marchigiana callus extract on cellular senescence: insight from a preliminary in vitro study. Molecular Nutrition and Food Research. (Article in Press)

- Bordoni L, Petracci I, Feliziani G, de Simone G, **Rucci C**, Gabbianelli R. Gut Microbiota-Derived Trimethylamine Promotes Inflammation with a Potential Impact on Epigenetic and Mitochondrial Homeostasis in Caco-2 Cells. Antioxidants (Basel). 2024 Aug 30;13(9):1061. doi: 10.3390/antiox13091061. PMID: 39334721; PMCID: PMC11428692.

- **Rucci C**, de Simone G, Salathia S, Casadidio C, Censi R, Bordoni L. Exploring mitochondrial DNA copy number in circulating cell-free DNA and extracellular vesicles across cardiovascular health status: A prospective case-control pilot study. FASEB J. 2024 May 31;38(10):e23672. doi: 10.1096/fj.202400463R. PMID: 38775929.

- Gabbianelli R, Shahar E, de Simone G, **Rucci C**, Bordoni L, Feliziani G, Zhao F, Ferrati M, Maggi F, Spinozzi E, Mahajna J. Plant-Derived Epi-Nutraceuticals as Potential Broad-Spectrum Anti-Viral Agents. Nutrients. 2023 Nov 8;15(22):4719. doi: 10.3390/nu15224719. PMID: 38004113; PMCID: PMC10675658.

CONFERENCES

11 June 2025 - 13 June 2025 — Clinical Epigenetics International Conference 2025
Organized by Prof. Lucia Altucci
Naples, Italy

09 June 2025 — SIB-TUM 2025, congress of the Italian society of Biochemistry and Molecular Biology
Florence, Italy

04 May 2025 — The future of biomedical research: Cloud conference
University of Antwerp
Antwerp, Belgium

12 April 2025 — Cancer Research Day
University of Antwerp
Antwerp, Belgium

05 September 2023 – 08 September 2023 — NuGO week conference: "Impact of nutrition during different life stages – tracing the impact of diet on human health"
Senigallia, Italy

8 July 2023 – 12 July 2023 — FEBS Congress
Tours, France

POSTER PRESENTATIONS

12 June 2025 — Clinical Epigenetics International Conference 2025
Poster Title: “The transcriptomic and epigenetic effect of Mela Rosa Marchigiana callus extract: insight from an in vitro model of cellular senescence”
Authors: **Chiara Rucci**, Laura Bordoni, Dale Annear, Enrica Sordini, Giuseppe Persico, Eugenia Ciurlia, Noemi Pappagallo, Giulia Matacchione, Marco Giorgio, Daniele Fraternale, Maria Cristina Albertini, Stefano Amatori, Peter De Rijk, Tim De Pooter, Mojca Strazisar, Wim Vanden Berghe, Rosita Gabbianelli
Naples, Italy

09 June 2025 **SIB-TUM 2025, congress of the Italian society of Biochemistry and Molecular Biology**

Poster Title: “Exploring the transcriptomic and epigenetic impact of Mela Rosa Marchigiana callus extract on cellular aging: insight from an in vitro study”

Authors: **Chiara Rucci**, Laura Bordoni, Enrica Sordini, Giuseppe Persico, Eugenia Ciurlia, Noemi Pappagallo, Giulia Matacchione, Marco Giorgio, Daniele Fraternale, Maria Cristina Albertini, Stefano Amatori, Rosita Gabbianelli.

Florence, Italy

PRIZE AS BEST POSTER

07 September 2023 **NuGo week conference**

Poster Title: “Effects of trimethylamine on the mitochondrial DNA: evidence from an in vitro model of intestinal epithelial cells.”

Authors: **Chiara Rucci**, Elisa Veloni, Laura Bordoni e Rosita Gabbianelli

Senigallia, Italy

09 July 2023 **FEBS Congress**

Poster Title: “Absolute quantification of mitochondrial DNA copy number from circulating cell-free DNA and exosomes in different cardiovascular health status: a case-control study from Lifelines biobank”

Authors: **Chiara Rucci**, Gaia de Simone, Sanyia Salathia, Cristina Casadiddio, Roberta Censi and Laura Bordoni.

Tours, France

ORAL PRESENTATIONS

22 May 2025 **Presentation titled “The nutrigenomic effect of Mela Rosa Marchigiana callus extract on cellular senescence: insight from a preliminary in vitro study”**

InnovOcean Meeting

Ostenda, Belgium

15 July 2025 **Presentation of the PhD project at the Lab retreat of the Cell Death Signaling - Epigenetics lab of Prof. Wim Vanden Berghe, Tom Vanden Berghe and Andy Wullaert**

Lier, Belgium

PRIZES AND AWARDS

09 June 2025

PRIZE as best poster at SIB-TUM 2025, congress of the Italian society of Biochemistry and Molecular Biology

Poster Title: “Exploring the transcriptomic and epigenetic impact of Mela Rosa Marchigiana callus extract on cellular aging: insight from an in vitro study”

Authors: **Chiara Rucci**, Laura Bordoni, Enrica Sordini, Giuseppe Persico, Eugenia Ciurlia, Noemi Pappagallo, Giulia Matacchione, Marco Giorgio, Daniele Fraternale, Maria Cristina Albertini, Stefano Amatori, Rosita Gabbianelli.

Florence, Italy

26 June 2025

Winner of “Biodiversity Gateway” Scholarship to attend an advanced training program (Corso di alta formazione) on bioinformatics

Awarded by the National Biodiversity Future Center (NBFC)

ACADEMIC ROLES

05 June 2024 – current

Cultore della materia in Biologia Molecolare 05/BIOS-07 – BIOCHIMICA (ex 05/E1-Biochimica generale)

University of Camerino

Camerino, Italy

05 June 2024 – current

Cultore delle Materia in Biochimica della Nutrizione e Nutrigenomica 05/BIOS-07 – BIOCHIMICA (ex 05/E1-Biochimica generale)

University of Camerino

Camerino, Italy

05 June 2024 – current

Cultore della Materia in Alimentazione del Fitness 05/BIOS-07 – BIOCHIMICA (ex 05/E1-Biochimica generale)

University of Camerino

Camerino, Italy

05 June 2024 – current

Cultore della Materia in Scienze dell'alimentazione e principi di nutrizione 05/BIOS-07 – BIOCHIMICA (ex 05/E1-Biochimica generale)

University of Camerino

Camerino, Italy

05 June 2024 – current

Cultore della materia Biochimica e Biologia molecolare

05/BIOS-07 – BIOCHIMICA (ex 05/E1-Biochimica generale)
University of Camerino
Camerino, Italy

TEACHING ACTIVITIES

17 April 2023 — Lecture on “Vitamines”
Duration: 2h
Topics: Vitamine liposolubili e idrosolubili. Ruoli biochimici e fonti alimentari.
Course: Scienze dell’Alimentazione
Degree programme: Pharmacy
School of Pharmacy and Health Products
University of Camerino
Camerino, Italy

18 April 2023 — Lecture on “Molecular Biology techniques”
Duration: 3h
Topics: Cell culture, RNA extraction, DNA extraction, reverse transcription, real-time PCR, Pyrosequencing, Digital PCR
Course: Molecular Biology
Degree programme: Chimica e Tecnologie Farmaceutiche
School of Pharmacy and Health Products
University of Camerino
Camerino, Italy

21 April 2023 — Lecture on “Molecular Biology techniques”
Duration: 3h
Topics: Cell culture, RNA extraction, DNA extraction, reverse transcription, real-time PCR, Pyrosequencing, Digital PCR
Course: Molecular Biology
Degree programme: Chimica e Tecnologie Farmaceutiche
School of Pharmacy and Health Products
University of Camerino
Camerino, Italy

30 May 2023 — Lecture on “Molecular Biology techniques”
Duration: 2h
Topics: Cell culture, RNA extraction, DNA extraction, reverse transcription, real-time PCR, Pyrosequencing, Digital PCR
Course: Scienze dell’Alimentazione
Degree programme: Pharmacy
School of Pharmacy and Health Products
University of Camerino
Camerino, Italy

9 April 2024

Lecture on “Vitamines”

Duration: 2h

Topics: Vitamine liposolubili e idrosolubili. Ruoli biochimici e fonti alimentari.

Course: Scienze dell’Alimentazione

Degree programme: Pharmacy

School of Pharmacy and Health Products

University of Camerino

Camerino, Italy

23 April 2024

Lecture on “Molecular Biology techniques”

Duration: 4h

Topics: Cell culture, RNA extraction, DNA extraction, reverse transcription, real-time PCR, Pyrosequencing, Digital PCR

Course: Molecular Biology

Degree programme: Chimica e Tecnologie Farmaceutiche

School of Pharmacy and Health Products

University of Camerino

Camerino, Italy

27 May 2024

Lecture on “Molecular Biology techniques”

Duration: 2h

Cell culture, RNA extraction, DNA extraction, reverse transcription, real-time PCR, Pyrosequencing, Digital PCR

Course: Scienze dell’Alimentazione

Degree programme: Pharmacy

School of Pharmacy and Health Products

University of Camerino

Camerino, Italy

17 December 2024

Lecture on “Molecular Biology techniques”

Duration: 2h

Course: Scienze dell’Alimentazione

Degree programme: Pharmacy

School of Pharmacy and Health Products

University of Camerino

Camerino, Italy

OTHER ACTIVITIES

September 2025 – November 2025

Supervision of the Master students’ activities in the Nutrigenomic and molecular biology lab

University of Camerino

Camerino, Italy

13 July 2025 – 15 July 2025

Participation at the Lab retreat of the Cell Death Signaling -

Epigenetics lab of Prof. Wim Vanden Berghe, Tom Vanden Berghe and Andy Wullaert

February 2025 – March 2025 — Revision of scientific paper published in the journal "Molecular Nutrion and Food research"

18 june 2024 – 21 June 2024 — Member of the organizing committee of the 5th European Summer School on Nutrigenomics
University of Camerino
Senigallia, Italy

05 September 2023 – 08 September 2023 — Member of the organizing committee of the NuGO week conference: "Impact of nutrition during different life stages – tracing the impact of diet on human health"
Senigallia, Italy

Academic year 2023/2024 — Exams of geology (Geologia I) 12 cfu (SBM006)

Academic year 2017/2018 — Exams for Teaching Expertise Improvement (pf24): Antropology (FIT003), Metodologie e tecnologie didattiche (FIT004), Processi cognitivi, di apprendimento e sviluppo (FIT002), Progettazione, valutazione ricercar educative (FIT001)
University of Camerino
Camerino, Italy

THIRD MISSION ACTIVITIES

September 2025 — NUTRIMENTE FESTIVAL: LABORATORI PER SCUOLA PRIMARIA E SECONDARIA DI I GRADO e ATTIVITA' APERTE AL PUBBLICO
Title "Alla scoperta della Nutrigenomica: Come studiare gli effetti molecolari dei cibi che mangiamo."
San Benedetto del Tronto, Italy

September 2024 — NUTRIMENTE FESTIVAL: LABORATORI PER SCUOLA PRIMARIA E SECONDARIA DI I GRADO e ATTIVITA' A PERTE AL PUBBLICO
Title "Alla scoperta della Nutrigenomica: Come studiare gli effetti molecolari dei cibi che mangiamo."
San Benedetto del Tronto, Italy

SEMINARS

19.01.23 — NuGO Webinar: Lifelines Biobank for diet and health research

Held online by NuGo organization

18.03.23 **Seminar: Insights and drawbacks of the publishing process**

University of Camerino

29.03.23 **Seminar: Physiological implications of ghrelin processing.Dr. Daniela Lufrano**

University of Camerino

April 2023 **Thematic course: Introduction to Nanopore Sequencing**

Held online by ONT

18.04.23 **Seminar: Cristallization in food**

Prof, Katrin Laos. Department of Chemistry and Biotechnology Tallinn, University of Technology (Taltech), Tallinn, Estonia

University of Camerino

02.05.23 **Seminar: Introduction to meat analogues**

Dr. Enrico Federici, Ph.D. Food Science, Innovation Scientist, Beyond Meat,

El Segundo,

CA, USA

University of Camerino

11.05.23 **Seminar: Nutrition and Cancer**

Prof. Jamal Mahajna. Head of the department of Nutrition and Natural products – The laboratory of Cancer Drug Discovery Program - Migal- Galilee Research Institute Kiryat Shmona – Israel.
University of Camerino, Camerino, Italy

25.05.23 **Seminar: Cancer targeted therapy**

Prof. Jamal Mahajna. Head of the department of Nutrition and Natural products –

The laboratory of Cancer Drug Discovery Program - Migal- Galilee Research

Institute Kiryat Shmona – Israel.

University of Camerino

08.06.23 **Seminar: Transcriptomics: leveraging RNA-Seq for functional genomics**

Prof. Ignazio S. Piras. Research Associate Professor, Translational Genomics Research
Institute (TGen), Phoenix, AZ, USA.

University of Camerino

22.06.2023 **Seminar: Nutrition and longevity**

Prof. Jamal Mahajna. Head of the department of Nutrition and Natural products –

The laboratory

of Cancer Drug Discovery Program - Migal- Galilee Research Institute

Kiryat Shmona - Israel

University of Camerino

22.06.23 **Seminar: Charting the genetics of Alzheimer's Disease across APOE, Age, Sex and Ancestry.**

Dr. Michael E. Belloy, Ph.D., Instructor of Neurology and Neurological Sciences

Stanford University School of Medicine Stanford, CA, USA
University of Camerino

27.09.23 **Seminar series: Implementing Circular Economy Solution For Sustainability: Case Studies**
Organized by the AlgaeBrew Consortium ERANET-SUSFOOD2-FOSC Joint Call 2021University of Camerino

07.11.23 **NuGO webinar: how to find analyse and share data**
Held online by NuGO association

15.11.23 **Seminar: Freedom of Research and Legal Protection**
University of Camerino

24.11.24 **Seminar: Open Science & Open Innovation**
Univerisity of Camerino

28.11.23 **Seminar: EU FUNDING: POLICIES & OPPORTUNITIES**
University of Camerino

13.12.23 **Seminar: Cancer as a matter of FAT: emerging roles of lipids in Ferroptosis and cancer cell death**
Caterina Bartolacci Ph.D., University of Cincinnati, Division of Hematology and Oncology
University of Camerino

09.05.2024 **Seminar: Cell cultured meat: overview of the ecosystem, science, promises, and challenges**
Dr. Franks Kamgang Nzekoue, Ph.D., Research Scientist, Gourmey, Paris
University of Camerino

21.05.24 **Seminar: Sustainable food innovation: Proteins, Carbohydrates and Lipids**
Dr. Luca Serventi, Team Leader of Food Chemistry and Functionality Plant & Food Research Lincoln, New Zealand
University of Camerino

28.05.24 **Sustainable Food Innovation: Omega-3 Fatty Acids, Iron and Vitamin B12**
Dr. Luca Serventi, Team Leader of Food Chemistry and Functionality Plant & Food Research Lincoln, New Zealand
University of Camerino

13.06.24 **NuGO seminar: How to use Artificial Intelligence in Nutrition Research**
Held online by NuGo organization

17.06.24 **Seminar: New trends in sample preparation**
Valentina Fernandes Domingues, REQUIMTE/LAQV, ISEP, Polytechnic of Porto, Portugal
University of Camerino

17.06.24 **Biomonitoring of lipophilic endocrine disruptors in women**
Valentina Fernandes Domingues, REQUIMTE/LAQV, ISEP, Polytechnic of Porto, Portugal
University of Camerino

17.06.24 **Seminar: Portuguese shrimps: nutritional added value and contaminants evaluation**
Valentina Fernandes Domingues, REQUIMTE/LAQV, ISEP, Polytechnic of Porto, Portugal
University of Camerino

24.06.24 **Seminar: The higher utilization of cereals and pseudo-cereals to obtain fortification food**
Prof. Marc (Vlaic) Romina Alina PhD Eng., University of Agricultural Sciences a nd Veterinary Medicine Cluj-Napoca, Faculty of Food Science and Technology, Cluj-Napoca, Romania
University of Camerino

24.06.24 **Seminar: Mespilus germanica L. (Medlar) chemical composition, biological activity, its applications (traditional, medicinal, commercial), and the utilization of plant waste**
Prof. Marc (Vlaic) Romina Alina PhD Eng., University of Agricultural Sciences a nd Veterinary Medicine Cluj-Napoca, Faculty of Food Science and Technology, Cluj-Napoca, Romania University of Camerino

26.06.24 **Seminar: The utilization of food waste in fortified food products**
Prof. Marc (Vlaic) Romina Alina PhD Eng., University of Agricultural Sciences and Veterinary Medicine Cluj-Napoca, Faculty of Food Science and Technology, Cluj-Napoca, Romania
University of Camerino

15.11.24 **NuGO Seminar: Opportunities and challenges with digital health data collection and usage**
NuGo Organization

21.11.24 **NuGO Seminar: Precision nutrition applied to female reproductive health**
Held online by NuGo organization

05.12.25 **The development of magnetic separation and its application in the detection of foodborne pathogens**
Dr. Juan Du Associate Professor Zhengzhou University of Light Industry
University of Camerino

08.01.25 **Effect of Processed Foods on Genome Stability**
Isabel Gaivao Department of Genetics and Biotechnology and CECAV, University of Trasos Montes and Alto Douro, Vila Real, Portugal
University of Camerino

05.03.25 Mitochondria: from Parkinson's disease to cancer
Dr. Elias Adriaenssens (Vienna BioCenter (VBC)
University of Antwerp

11.03.25 Seminar: A novel, radiotherapy actionable immunological mechanism of resistance to CDK4-6 inhibition in breast cancer
Professor Lorenzo Galluzzi, affiliated with Fox Chase Cancer Center (PA) and Yale University School of Medicine (NY), USA.
University of Antwerp

14.04.25 NuGO ECN Webinar: Analysing and preparing microbiome data for publication
Held online by NuGo organization

18.04.25 Biomina luch talk: Understanding and designing cis-regulatory elements using machine learning
Dr. Jacob Schreiber - Institute of Molecular Pathology (Vienna)
University of Antwerp

18.04.25 Seminar: DNA Methylation Profiling: Biomarkers and Beyond
Professor Joe Ibrahim - Center of Medical Genetics (University of Antwerp)
University of Antwerp

21.04.25 Biomina Lunch Talk: Decoding life: exploring applications of nanopore sequencing and bioinformatics
Paco Hulpiau - Bioinformatics Knowledge Center (Howest University of Applied Sciences)
University of Antwerp

21.04.25 BIomina lunch talk: Exploring genotype-phenotype relationships in a federated setup – WiNGS
Nishkala Sattanathan - Center of Medical Genetics (University of Antwerp)
University of Antwerp

01.05.25 NuGO ECN Webinar: The interplay between dietary and lifestyle factors, omics data, and cardiometabolic diseases
NuGO association

01.05.25 Seminar: Regulation of HBV/HCV Infection by N6-methyladenosine Modification
University of Antwerp

03.11.25 Chiara Ricci